# DEVELOPMENT OF A PSEUDOVIRUS-BASED ASSAY FOR ANALYSIS OF NEUTRALIZING ACTIVITY AGAINST SARS-CoV-2

by
CEVRİYE PAMUKCU

Submitted to the Graduate School of Engineering and Natural Sciences
in partial fulfilment of
the requirements for the degree of
Doctor of Philosophy

Sabanci University
December 2021

DEVELOPMENT OF A PSEUDOVIRUS-BASED ASSAY FOR ANALYSIS OF NEUTRALIZING ACTIVITY AGAINST SARS-CoV-2

APPROVED BY:

Prof. Dr. Selim Çetiner .....
(Thesis Supervisor)

Asst. Prof. Dr. Nur Mustafaoğlu Varol .....

Asst. Prof. Dr. Meral Yüce .....

Prof. Dr Batu Erman .....

Assoc. Prof. Dr. Ayça Sayı Yazgan .....

DATE OF APPROVAL: 16/12/2021

# ABSTRACT

DEVELOPMENT OF A PSEUDOVIRUS-BASED ASSAY FOR ANALYSIS OF NEUTRALIZING ACTIVITY AGAINST SARS-CoV-2

Cevriye Pamukcu

Biological Sciences and Bioengineering, PhD Thesis, 2021

Thesis Supervisor: Selim Çetiner

Co-supervisor: Tolga Sütlü

Keywords: SARS-CoV-2, COVID-19, Neutralizing Antibodies, Convalescent Plasma

As the COVID-19 pandemic caused by Severe Acute Respiratory Syndrome Coronavirus 2 (SARS-CoV-2) continues to spread around the globe, effective vaccination protocols are actively being implemented. The delayed deployment of effective vaccines, especially in the developing world and the lack of an effective antiviral treatment inadvertently increased the interest in approaches such as the use of convalescent plasma (CP) or monoclonal antibody products. Initial clinical evaluation revealed that critical factors determining the outcome of CP or antibody-based therapies need to be defined clearly if clinical efficacy is to be expected. Measurement of neutralizing activity against SARS-CoV-2 using wildtype virus presents a reliable functional assay but the availability of suitable BSL3 facilities for virus culture restricts its applicability. Instead, the use of pseudovirus particles containing elements from the SARS-CoV-2 virus is widely applied to determine the activity of CP or other neutralizing agents.

In this thesis, we present our approach to production of lentiviral particles pseudotyped with the SARS-CoV-2 Spike (S), Membrane (M), Envelope (E) and Nucleocapsid (N) proteins for use in neutralization. Furthermore, we evaluate different transgenes such as the Green Fluorescent Protein (GFP) or Secreted Alkaline Phosphatase (SEAP) as reporter genes in an attempt to develop faster and more practical analysis of multiple samples in a short time. Our findings show that the use of optimized SEAP-based methods can increase the availability of neutralizing assays by overcoming the need for advanced equipment and increase the processing speed of multiple samples in a given lab.

# ÖZET


SARS-CoV-2'YE KARŞI NÖTRALİZAN AKTİVİTENİN ANALİZİ İÇİN PSÖDOVİRUS TABANLI TEST GELİŞTİRİLMESİ

Cevriye Pamukcu

Biyoloji Bilimleri ve Biyomühendislik, Doktora Tezi, 2021

Tez Danışmanı: Selim Çetiner

Eş Danışman: Tolga Sütlü

Anahtar kelimeler: SARS-CoV-2, COVID-19, Neutralizan Antikor, Konvelasan Plazma

Şiddetli Akut Solunum Yolu Sendromu Koronavirüs 2'nin (SARS-CoV-2) neden olduğu COVID-19 pandemisi dünya çapında yayılmaya devam ederken, etkin aşı protokolleri aktif olarak uygulanmaya başlanmıştır. Aşıların özellikle gelişmekte olan ülkelere geç dağılması ve etkin bir antiviral tedavinin olmaması, konvelesan plazma (CP) veya monoklonal antikor gibi kullanımı gibi yaklaşımlara olan ilgiyi artırmıştır. İlk klinik değerlendirmeler, eğer tedaviden bir fayda bekleniyorsa, CP veya antikor bazlı yaklaşımlarda yanıtı belirleyen kritik faktörlerin net bir şekilde tanımlanması gerektiğini ortaya koydu. Vahşitip virüs kullanılarak SARS-CoV-2'ye karşı nötralizan aktivitenin ölçülmesi güvenilir bir fonksiyonel analiz sunmaktadır ancak virüs kültürü için uygun olan Biyogüvenlik Seviyesi 3 (BSL3) tesislerinin yaygın olmaması, bu yöntemin uygulanabilirliğini kısıtlamaktadır. Bunun yerine, SARS-CoV-2 virüsünden parçalar içeren Psödovirüslerin kullanımı, konvelasan plazma veya diğer nötralize edici ajanların aktivitesini belirlemek için yaygın olarak kullanılabilir.

Bu tezde, nötralizan aktivitenin ölçümünde kullanılmak üzere SARS-CoV-2 Spike (S), Membran (M), Zarf (E) ve Nükleokapsid (N) proteinleri ile psödotiplenmiş lentiviral partiküllerin üretimine yönelik yaklaşımımızı sunuyoruz. Buna ek olarak, kısa sürede çoklu numunelerin daha hızlı ve pratik analizini mümkün kulabilmek amacıyla Yeşil Floresan Protein (GFP) veya Salgılanmış Alkalin Fosfataz (SEAP) gibi farklı transgenleri, raportör genler olarak değerlendiriyoruz. Bulgularımız, optimize edilmiş SEAP tabanlı yöntemlerin kullanılmasının, gelişmiş ekipman ihtiyacını ortadan kaldırarak nötralizasyon testlerinin hızını ve dolayısıyla da yaygınlığını artırabileceğini göstermektedir.

*To my lovely family and my super grandmother…*

*Canım aileme ve super babanneme…*

## ACKNOWLEDGEMENTS

I would like to begin by expressing my gratitude and thanks to my supervisor, Asst. Prof. Tolga Sütlü, for helping me better understand what it means to be a good scientist and for welcoming me into his research group. I am thankful to have had the opportunity to study with him during an excellent PhD study time. In both my personal and academic life, I always feel his support. Because of his encouraging perspective, I began getting ready for the future. Thank you for everything especially for introducing me to immunotherapy.

I would also like to thank Prof. Dr. Batu Erman for his help and support for me and my research. As a result of his constant passion for science and education, I was always improving my skills.

I would also like to thank Prof. Dr. Selim Çetiner for accepting to be my supervisor and his support. I want to express my kindly appreciation to esteemed jury members, Assoc. Prof. Meral Yüce, Assoc. Prof. Ayça Sayı Yazgan and Asst. Prof. Nur Mustafaoğlu Varol for accepting to participate in my thesis jury and for their valuable feedback with great interest. I also want to thank my past jury member, Asst. Prof. Emre Deniz participated in my thesis jury helpful valuable feedback with great interest and friendship.

I am thankful to Prof. Dr. İhsan Gürsel and Prof. Dr. Mayda Gürsel for sharing their knowledge and plasmids with us, Prof. Dr. Nesrin Özören and Prof. Dr. Gizem Dinler Doğanay for having productive work with Covid-19 vaccine project at Boğaziçi University. I am also grateful to Prof. Dr. Günnur Deniz and Prof. Dr. Safa Barış for our collaborative study and their support during my thesis work. I would like to thank our collaborator Duru Lab members and Asst. Prof. Adil Doğanay Duru. He has always been supportive for Sutlu lab.

Excellent science needs excellent friendships, and I am happy to have the most excellent coworkers. I'd would like to express my gratitude to all of the past and present members

of Sutlulab for giving me with such amazing moments; Elif Çelik, Ebru Zeynep Ergün, Zeynep Sena Karahan, Mertkaya Aras, Gözde Özcan, Didem Özkazanç Ünsal, Canan Sayitoğlu, Alp Ertunga Eyüpoğlu, Ayhan Parlar, Pegah Zahedimaram, Aydan Saraç, Başak Özata, Lolai Ikromzoda, Serra Özarı, Ayşegül Durgun, Bahar Orhan, Eren Can Ekşi. Among these great people, special thanks go to to Elif and Zeyneps. They spent many hours trying to help me finish this thesis. I would also especially like to show my appreciation to Mertkaya and Ertunga for being with me every time I cry. I would like to thank Barış Can Mandacı for excellent microscope images and Beyza Cabri for helping me to draw wonderful figures.

Likewise, I would like to thank a very supportive and helpful group of people, Erman Lab past and present members; Melike Gezen, Hakan Taşkıran, Ronay Çetin, Sarah Barakat, Sinem Usluer, Sofia Piepoli for their collaboration of all time. Also, thank you very much to the Akil Lab and Doganay Lab members that we have worked with heart and soul during the difficult times at the beginning of the pandemic.

I would like to thank my best friend Pınar Akçakaya who has been my friend for 16 years. She has always been with me in my worst and most depressive times and, of course, most beautiful memories. Thank you for enduring me.

This PhD could not have been possible without my dearest family, providing me with the most prominent love and support one can ever wish for. I want to express my heartfelt gratitude to my mother İlknur and father Erol Pamukcu, my ever-loving sister Ceren, and my namesake super-grandma Cevriye. I would also like to thank my boyfriend Yiğit Süvari to be my brilliant companion. Their unconditional love and endless support encouraged me to complete my achievements. Hopefully, I will make them proud of me with their inspiration. I thank you for always believing in me.

* This thesis was supported by Bogazici University BAP grant “Development of Pseudovirus-based Neutralization Test to Determine Antibody Activity in COVID-19 Convalescent Plasma Donors” Grant Number 20B01SUP8; TUBITAK 1004 grant “Production of SARS-CoV-2 Vaccine with ASC Particle Technology” Grant Number 18AG020. Cevriye Pamukcu’s scholarship has been supported by TUBITAK 1007 grant “Development and Production of Bio-Similar Product with Bevacizumab Active Substance” Grant Number 115G074.

* The Results in this thesis have been partially published on biorxiv (Pamukcu et al., 2020).

*All experiments in this thesis were performed at Boğaziçi University Department of Molecular Biology and Genetics.

## TABLE OF CONTENTS

## LIST OF FIGURES

## LIST OF TABLES

## LIST OF SYMBOLS AND ABBREVIATIONS

| | |
|---|---|
| 2019-nCoV | 2019 novel Coronavirus |
| 3CLpro | Chymotrypsin-like protease |
| AAV | Adeno-Associated Virus |
| ACE2 | Angiotensin-Converting Enzyme 2 |
| Ad26 | Adenovirus 26 |
| Ad5 | Adenovirus 5 |
| ADAP | Agglutination Polymerase Chain Reaction |
| ADE | Antibody-Dependent Enhancement |
| AGS | Gastric Adenocarcinoma |
| ARDS | Acute Respiratory Distress Syndrome |
| BCoV | Bovine Coronavirus |
| BSA | Bovine Serum Albumin |
| $CaCl_2$ | Calcium Chloride |
| CCID50 | Cell Culture Infectious Dose |
| CFR | Case-Fatality Rate |
| cGAS | cyclic GMP-AMP synthase |
| cGAS-STING | Cyclic GMP–AMP synthase/stimulator of IFN genes |
| ChAd | Chimpanzee Adenovirus vector |
| CK | Creatine Kinase |
| CLRS | C-lectin-like Receptors |
| COVID -19 | Coronavirus Disease -2019 |
| CoVs | Coronaviruses |
| CP | Convalescent Plasma |
| CPE | Cytopathic Effect |
| CRNT | Chemiluminescence Reduction Neutralization Test |
| CSG | Coronaviridae Study Group |
| CTD | C-terminal Domain |
| DAMPs | Damage-Associated Molecular Patterns |
| E | Envelope |
| ER | Endoplasmic Reticulum |
| ERGIC | Endoplasmic Reticulum-Golgi Intermediate Compartment |
| ERRS | Endoplasmic Reticulum Retention Signal |
| F | Phenylalanine |
| FDA | Food and Drug Administration |
| FIPV | Feline Infectious Peritonitis Virus |

| | |
|---|---|
| FP | Fusion Peptide |
| FRNT | Focus Neutralization Reduction Test |
| GCE | Genome Code Expansion |
| GFP | Green Fluorescent Protein |
| H | Histidine |
| H1N1 | Influenza A |
| HAT | Human Airway Trypsin-like Protease |
| HEK | Human Embryo Kidney |
| HEK293 | Human Embryonic Kidney 293 |
| IBV | Infectious Bronchitis Virus |
| IC50 | Half-maximal Inhibitory Concentration |
| ICTV | International Committee on Taxonomy of Viruses |
| IFN | Interferon |
| IL-6 | Interleukin-6 |
| ISG15 | IFN-stimulated Gene 15 protein |
| IVIg | Intravenous Immunoglobulins |
| LB | Luria Broth |
| LNPs | Lipid Nanoparticles |
| M | Membrane |
| mAbs | Monoclonal Antibodies |
| MERS | Middle-Eastern Respiratory Syndrome |
| MHRA | Medicines and Healthcare Products Regulatory Agency |
| MMLV | Moloney Murine Leukaemia Virus |
| MN | Microneutralization |
| MPER | Membrane-proximal External Region |
| Mpro | 3C-like protease |
| mRNA | messenger RNA |
| N | Asparagine |
| N | Nucleocapsid |
| NAbs | Neutralizing Antibodies |
| NaBut | Sodium Butyrate |
| NETs | Neutrophil Extracellular Traps |
| nsps | Non-structural proteins |
| NT50 | Neutralizing Titer 50 |
| NTD | N-Terminal Domain |
| PAMPs | Pathogen-Associated Molecular Patterns |
| PBM | PDZ-Binding Motif |
| PBMCs | Peripheral Blood Mononuclear Cells |
| PBS | Phosphate-Buffered Saline |
| PCR | Polymerase Chain Reaction |
| PEG | Polyethylene Glycol |
| PFA | Paraformaldehyde |
| PFU | Plaque-Forming Units |
| PLpro | Papain-like protease |
| pMN | Pseudotype MN |
| ppNT | Pseudoparticle Neutralization Test |
| PRNT | Plaque Reduction Neutralization Test |
| PRRs | Pattern Recognition Receptors |
| PsVNA | Pseudovirion Neutralization Assay |
| qRT-PCR | Quantitative Real-Time Polymerase Chain Reaction |

| | |
|---|---|
| R | Purine |
| RBD | Receptor Binding Domain |
| RCCL | Replication-Competent Cell Line |
| RdRp | RNA-dependent RNA Polymerase |
| RLRs | RIG-1-like Receptors |
| RNP | Ribonucleoprotein |
| RT-PCR | Reverse Transcription-Polymerase Chain Reaction |
| RTC | Replication-Transcriptase Complex |
| rVSV-dG | Recombinant Vesicular Stomatitis Virus with Protein G |
| S | Spike |
| SARS-CoV-2 | Severe Acute Respiratory Syndrome Coronavirus 2 |
| SEAP | Secreted Alkaline Phosphatase |
| SNPs | Single Nucleotide Polymorphisms |
| sgRNA | Subgenomic RNA |
| ss-RNA | Single-stranded RNA |
| T | Threonine |
| TBE | Tris-Borate-EDTA |
| TCID50 | Tissue Culture Infectious Dose |
| TGEV | Transmissible Gastroenteritis Virus |
| Th1 | T helper1 |
| Th2 | T helper2 |
| TLRs | Toll-like receptors |
| TMD | Transmembrane Domain |
| TMPRSS-2 | Transmembrane Serine Protease-2 |
| TRSs | Transcription-Regulating Sequences |
| USA | United States of America |
| UTRs | Untranslated Regions |
| VEGF | Vascular Endothelial Growth Factor |
| VLP | Virus-like Particles |
| VOC | Variants of Concern |
| VOI | Variants of Interest |
| WHO | World Health Organization |
| Y | Tyrosine |

# 1. INTRODUCTION

## 1.1 SARS-CoV-2 and COVID-19 Pandemic

### 1.1.1 Current State of SARS-COV-2 Pandemic

In December 2019, several unexplained pneumonia cases of unidentified etiology were reported in Wuhan, Hubei Province, China. On January 12, 2020, the World Health Organization (WHO) named this new virus the 2019 novel coronavirus (2019-nCoV). On January 30, 2020, the WHO proclaimed the COVID-19 pandemic an international public health emergency. On February 11, 2020, the WHO officially named this new coronavirus disease caused by 2019-nCoV as Coronavirus Disease -2019 (COVID -19) and the International Committee on Taxonomy of Viruses (ICTV) called 2019-nCoV as Severe Acute Respiratory Syndrome Coronavirus 2 (SARS-CoV-2) (M. Y. Wang et al., 2020a). On February 23, 2020, 77 041 confirmed cases of SARS-CoV-2 infection were reported in China (P. Sun et al., 2020). The virus quite rapidly spread across the world via travellers, and the number of cases has now passed 264,618,498 with 5,253,394 deaths globally (as of December 03 2021) (Worldometer, COVID-19 Coronavirus Pandemic, 2020, Accessed on December 03, 2021, <https://www.worldometers.info/coronavirus/>).

### 1.1.2 The Epidemiological Characteristics of COVID-19

Wuhan, Hubei Province in China had its first case of COVID-19 and a cluster of COVID-19 patients linked to an animal wholesale market at the end of December 2019 (Rothan & Byrareddy, 2020). Other nations and provinces were quickly being affected by COVID-19 as it moved throughout Asia. Consequently, Asia was the first breakout continent, and China had the most confirmed cases and deaths worldwide. Other continents, such as Europe and America, have followed various transmission channels, including international transportation by cruise ship and airline and local and community broadcast.

Virion samples from five patients were used to identify and characterize SARS-CoV-2 in Wuhan, China, the source of the pandemic. 79.6% similarity was identified to SARS-CoV, which caused the 2002 epidemic of SARS (P. Zhou et al., 2020). A 50% similarity to the MERS-CoV sequences responsible for the Middle Eastern Respiratory Syndrome (MERS) pandemic in the Middle East between 2012 and 2013 has also been found (Sommer & Roberto Bakker, 2020). However, at the whole-genome level, a genetic study of SARS-CoV-2 revealed a 96.2% resemblance to a CoV from bats, BatCoVRaTG13.7. This resemblance has led to the idea that the transmission of bat CoV to humans may have been facilitated by the presence of an intermediary host capable of acting as a reservoir for CoVs. Zhang et al. showed that pangolins might be acting naturally as a reservoir for SARS-CoV-2. An analysis of pangolin-CoV at the whole-genome level revealed that it is 91.02 percent identical to SARS-CoV-2. This makes it the second closest relation of human SARS-CoV-2, after only BatCoV RaTG13 in terms of genetic similarity. Pulmonary fibrosis and frothy liquid in the lungs of two deceased Malayan pangolins were used to identify CoV with an 80.24–88.93% genetic similarity to known SARS-CoVs on October, 2019. (Liu et al., 2019). In this study, the researchers found that the timing of the outbreaks matched up with a SARS epidemic in Wuhan, China. They also found that the SARS-CoV-2 in humans was genetically closer to Pangolin-CoV than other SARS-CoVs. Their findings support the hypothesis that pangolins act as an intermediate host. Dogs, ducks, pigs and chickens are the only animals in close proximity to people that do not allow for infection to occur. As with humans, cats and ferrets are ideal hosts for the SARS-CoV-2 virus.(J. Shi et al., 2020) It is also capable of spreading in golden hamsters (Sia et al., 2020).

SARS-CoV-2 is spread by spores and droplets when infected and uninfected people come into close, unprotected contact. The primary source of infection is symptomatic and asymptomatic individuals. Indirect touch transmission is another way for the virus to spread. Hands get contaminated with virus-containing droplets, and individuals subsequently come into touch with the mucous membranes of the nose, eyes and mouth resulting in infection. SARS-CoV-2 aerosol transmission has been established in several investigations. SARS-CoV-2 can spread via aerosols, according to a research conducted during the epidemic of COVID-19 that measured viral RNA in two Wuhan hospitals. Aerosols created by medical operations may provide a risk of airborne transmission in healthcare facilities. Therefore, aerial transmission is the primary mode of COVID-19 transmission (Meselson, 2020; Chan, Yuan, et al., 2020).

SARS-CoV-2 is capable of infecting human intestine organoids and epithelial cells, according to recent investigations. Consequently, SARS-CoV-2 can spread via the digestive system. The bat's intestines can be exposed to SARS-CoV-2. (Lamers et al., 2020). In COVID-19 patients, viral RNA was identified in numerous organs. Infectious SARS-CoV-2 was isolated not only from respiratory specimens but also the urine of some COVID-19 patients (J. Sun et al., 2020). In one study, nine pregnant women who had been infected with SARS-CoV-2 were studied. The result showed no evidence that the virus could be transmitted to an infant by being in contact with a pregnant woman during pregnancy. However, several investigations have also shown that SARS-CoV-2 may be transmitted vertically when the infection occurs in the third trimester of pregnancy. (T. Chen et al., 2020). When a woman was diagnosed with SARS-CoV-2 in the last three months of pregnancy, her baby was infected with SARS-CoV-2, resulting in neurological impairment. In another example, the neonate's cytokine and anti-SARS-CoV-2 IgM antibodies were elevated, despite no physical contact, indicating transplacental transmission (L. Dong et al., 2020). The probability of perinatal SARS-CoV-2 transmission is minimal. The current reports say that perinatal transmission is possible, but rare. It is also unknown whether a pregnant woman was exposed to the virus during her first or second trimester of pregnancy. (Egloff et al., 2020).

Everyone is considered at risk, and the median age is about 50 years old, according to current epidemiological data (Guan et al., 2020). Clinical symptoms vary with age. An older patient population was shown to have greater amounts of urea nitrogen in the blood, more inflammatory markers, and more lung damage in one investigation. Patients above

the age of 60 have a higher risk of respiratory failure and a prolonged illness course. The disease is less severe among individuals under 60 (Y. Liu et al., 2020). According to one research, there have been 72,314 confirmed cases in China, with most patients (87%) between the ages of 30 and 79. There were no deaths among the children under the age of nine. However, the case-fatality rate (CFR) in the group aged 70-79 is 8.0%, while the CFR in those aged 80 and above is 14.8%. The CFR is 10.5, 7.3, 6.3, 6.0, and 5.6% for individuals with various concomitant diseases such as diabetes, hypertension, cardiovascular disease, chronic pulmonary disease and cancer, respectively. COVID-19 patients are more likely to death from comorbid disorders than those without them, according to these findings (Z. Wu & McGoogan, 2020). 1099 individuals of COVID-19 infection were verified, with individuals with severe illness being seven years older than those with non-severe infection (Guan et al., 2020). Patients with severe illness were seven years older than those with non-severe disease among the 1,099 cases with COVID-19. More than 1,000 children under the age of six were infected, with the median age being 6.7 years and the majority showing symptoms that are less severe (X. Lu et al., 2020). Patients higher the age of 65 who are infected with COVID-19 are at a greater risk of death, particularly those who have acute respiratory distress syndrome (ARDS) and comorbid (R.-H. Du et al., 2020).

### 1.1.3. Clinical Characteristics and Pathogenesis of COVID-19

According to the WHO-China Joint Mission on COVID-19 study, 80% of infections are mild to moderate, including pneumonia and non-pneumonia cases, 13.1% develop severe illness, and 6.1% suffer critically dangerous disease needing intensive care (*Report of the WHO-China Joint Mission on Coronavirus Disease 2019 (COVID-19)*, n.d.). Fever, cough, and exhaustion are common symptoms of symptomatic COVID-19, although other less common and abnormal symptoms have also been reported. According to the severity of symptoms, COVID-19 is classified into three levels: mild, severe, and critical. The majority of individuals experience minor symptoms and eventually recover (B. Hu et al., 2020). Asymptomatic infection cases were also recorded, although most asymptomatic individuals developed the illness after collecting the data (Huang et al., 2020). Table 1.1 summarizes the symptoms of COVID-19 and the three different severity levels of COVID-19 (Wang et al., 2020).

| | | |
|---|---|---|
| **Clinical Symptoms** | **The symptoms of pneumonia include muscle ache, headache, fever, shortness of breath, dry cough, confusion, sore throat, rhinorrhea, chest pain, diarrhea, vomiting, chills, sputum production, haemoptysis, dyspnea, bilateral pneumonia anorexia and chest pain. Higher levels of plasma cytokines (IL2, IL7, IL10, GSCF, IP10, MCP1, MIP1A, and TNFa) are seen in ICU patients.** | |
| **Three different levels of COVID-19** | Mild | fever, fatigue, cough, non-pneumonia and mild pneumonia |
| | Severe | Dyspnea, blood oxygen saturation less than 93%, respiratory frequency <30/min, partial pressure of arterial oxygen to fraction of inspired oxygen ratio <300, and/or lung infiltrates >50% within 24 to48 h, are all potentially indicative of a patient needing ICU. |
| | Critical | ARDS, respiratory failure, multiple organ dysfunction or failure, septic shock, coagulation dysfunction |

**Table 1.1.** Clinical symptoms and three different levels of COVID-19.

Severe COVID-19 is defined as tachypnea (hyperventilation, less than 30 breaths per minute), oxygen saturation <93% at rest. In contrast, critical disease is characterized as respiratory failure necessitating mechanical ventilation, septic shock, or other organ dysfunction or failure needing intensive care support (Adil et al., 2021). The elderly (over the age of 60) and those suffering from diabetes, hypertension, obesity, cancer, chronic respiratory disease, cardiovascular disease, and liver disease are at the highest risk of severe and critical disease (Guan et al., 2020). According to one study, children of all ages can become infected. While most infections in children are asymptomatic or moderate, results in young children, particularly newborns, can be severe, with a 7–10% frequency of severe and critical illness (Y. Dong et al., 2020).

The pathogenesis of severe and critical COVID-19 is complicated, and several hypotheses have been suggested. The most common explanation is that SARS-CoV-2 infects cells through the angiotensin-converting enzyme 2 (ACE2) receptors in the lungs, triggering intracellular viral replication until the cell bursts, releasing numerous virus particles that infect other cells. This also activates innate and adaptive immunity, potentially triggering a cytokine storm and resulting in tissue damage both locally and systemically. Patients with severe COVID-19 show dysregulated immunological response, with significantly lower CD4+T cells, CD8+T cells, B cells, natural killer cells,

monocytes, eosinophils, and basophils, as well as a higher neutrophil count (X. Cao, 2020). The cytokine storm is characterized by elevated pro-inflammatory cytokines such as IL-8, IL-6, IL-2, IL-17, IL-1beta, G-CSF, GM-CSF and TNF (Z et al., 2020). Massive neutrophil and macrophage infiltration occur in the lungs, causing hyaline membrane deposition and widespread alveolar destruction, which leads to respiratory failure and ARDS. The systemic inflammatory response causes pan-systemic damage to the heart, liver, and kidney, resulting in multi-organ dysfunction and immune-mediated damage. Even though the elderly have worse results, no one is immune to severe disease at any age (Y. Dong et al., 2020).

Furthermore, among patients younger than 60 years of age, obesity is the most significant risk factor for hospitalization and poor critical care outcomes (Lighter et al., 2020). Alternative theories for the pathophysiology of severe and vital COVID-19 have been presented in the literature, but these need to be validated with more study. According to one study, the ACE2 receptor is expressed at high levels in the heart, which might explain symptoms such as chest tightness and palpitations (Y.-Y. Zheng et al., 2020). A rise in cardiac-specific troponins during hospitalization in 11.8% of patients without pre-existing cardiac chronic conditions who eventually died has been shown to be a possible cause of death in severe COVID-19 disease as evidenced by an excess of myocardial damage, myocarditis and consequent cardiac failure. (Y.-Y. Zheng et al., 2020). Another study implicated thrombotic events, diffuse intravascular coagulation and temporary rises of anti-phospholipid antibodies in critically sick individuals due to SARS-CoV-2 viraemia (Yan Zhang et al., 2020). Severe respiratory failure could be caused by ability of SARS- CoV-2 to infect peripheral nerve terminals, which subsequently allows it to enter the brain stem through a synapse-connected pathway. This neuroinvasive potential has been proposed to play a role in respiratory failure in severe COVID-19 patients (Y.-C. Li et al., 2020). Another study claims that SARS-CoV-2 targets the 1-beta chain of haemoglobin and grabs the porphyrin, inhibiting human heme metabolism. However, this idea has been widely criticized for its poor approach to interpreting the data (Wenzhong and Hualan 2020).

### 1.1.4. Classification of SARS-COV-2

Human Covs (HCoVs) are enveloped viruses with a single-stranded, non-segmented, positive-sense RNA genome that infect vertebrates (Masters, 2006). The current classification includes 39 CoV species into 27 subgenera, five genera, and two subfamilies within the family Corona viridae (Siddell et al., 2019). The International Committee for Taxonomy of Viruses (ICTV) has divided HCoVs into four primary genera: AlphaCoV, BetaCoV, GammaCoV, and DeltaCoV, and placed them under the Coronavirinae subfamily of the Coronaviridae family for genotypic and serological evaluation (F. Wu, Zhao, et al., 2020).

Only mammals are infected by alphacoronaviruses and betacoronaviruses. These viruses, known as gammacoronaviruses and deltacoronaviruses, infect birds, but they may also infect mammals in rare cases (Woo et al., 2012). Human respiratory sickness is often brought on by alpha- and betacoronaviruses, whereas gastroenteritis in animal. SARS-CoV and MERS-CoV, two highly pathogenic viruses, cause severe respiratory syndrome in humans, whereas the other four human coronaviruses . (The first four CoVs: HCoV-NL63, HCoV-229E, HCoV-OC43, and HKU1) only cause milder infections of the upper respiratory tract (Su et al., 2016).

As a taxonomic group, the HCoV-229E and HCoV-NL63 are classed as AlphaCoV, whereas the HCoV-HKU1, the HCoV-OC43 , SARS- and MERS-Cov are identified as BetaCov. The SARS-CoV and MERS-CoV are subgroups of subgenera Sarbecovirus and Merbecovirus (van Boheemen et al., 2012). Notably, newly emerged SARS-CoV-2 is distinct from SARS-CoV and MERS-CoV so the taxonomic classification of SARS-CoV-2 under the subgenus Sarbeco virus is temporary and subject to change depending on additional evidence (Gorbalenya et al., 2020) (Figure 1.1a ).

An 88% similarity between SARS-CoV-2 and two bat-derived SARS-like CoVs was found, as well as a distant resemblance of roughly 79% and 50% to SARS and MERS-CoV sequences in a sequence study of SARS-CoV-2. (Figure 1.1b) (H. Lu, 2020).

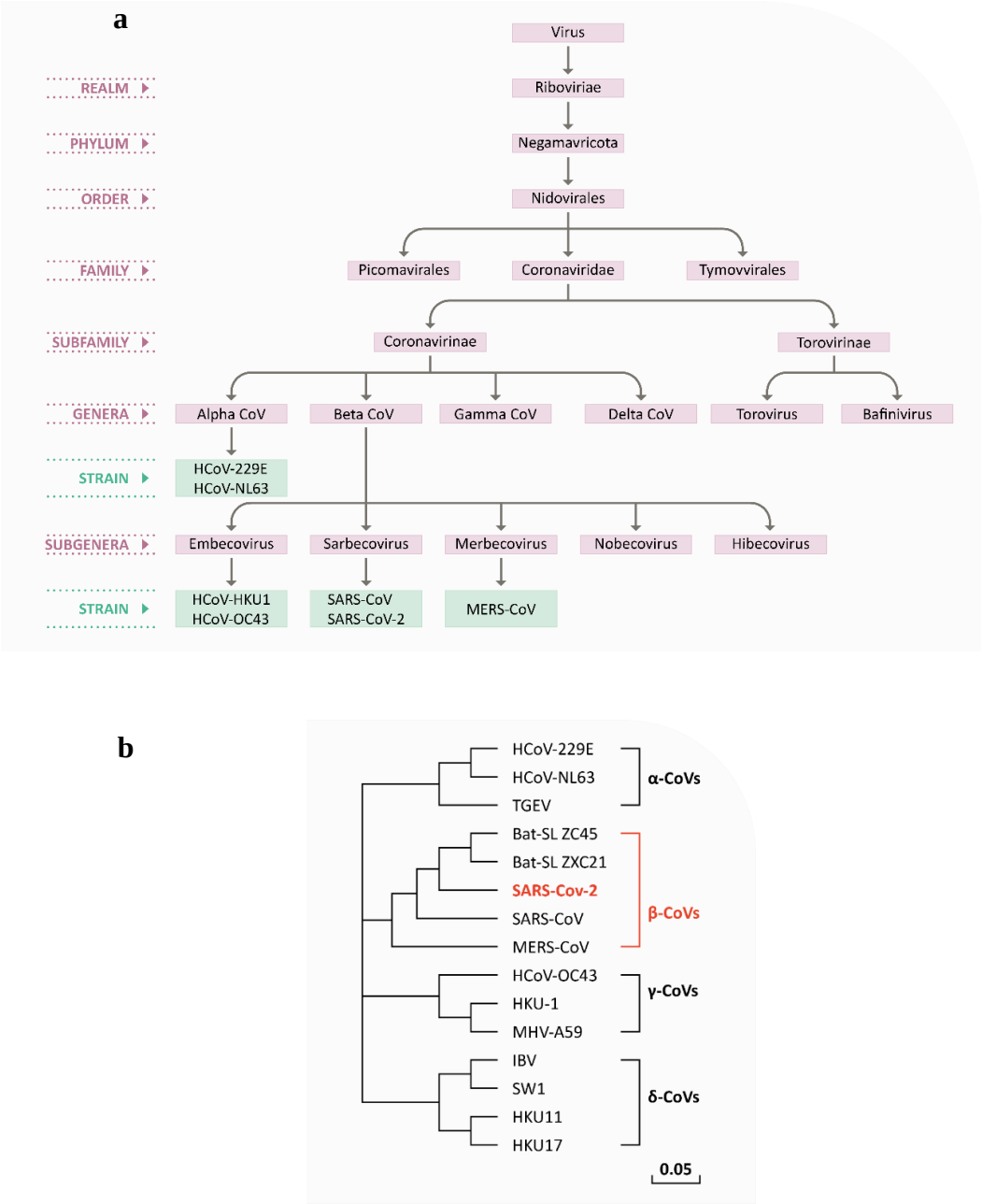


**Figure 1.1. The classification of Coronavirus.** (a) The taxonomic classification of the known seven HCoVs. (b) phylogenetic tree analysis of based on S gene sequences. (Figure adapted from (Kirtipal et al., 2020))

### 1.1.5. Origin of the coronaviruses that infect humans

Recent research has related the development of HCoVs to accelerated urbanization, and animal farming since these activities enable frequent species exchange and simplified species barrier crossing as well as genomic recombination in these viruses (Jones et al., 2013). Bats were known as host of varios CoVs. Although direct transmission of CoVs

from bats to people has not been established conclusively, transfer via intermediary hosts to humans by direct contact has been extensively hypothesized as a possible transmission mechanism.

In November 2002, the first recorded case of SARS-CoV was discovered in Foshan, China (Ge et al., 2015). It spread to 28 countries, resulting in 8,090 cases and 772 deaths (Ge et al., 2015). The first evidence of the SARS-CoV's origins was identified in masked palm civets and raccoon dogs. Detection of SARS-CoV-specific antibodies in Chinese ferret badgers in an animal market in Shenzhen lead researchers to think that this animal was the source of human transmission (Drexler et al., 2014). However, further research suggested that these animals were only accidental hosts, given the absence of evidence supporting the spread of SARS-CoV-like viruses among palm civets that could be found in the wild or in artificial breeding facilities (Figure 1.2) (L. F. Wang et al., 2006). Further investigation revealed that genetically distinct CoVs associated to SARS-CoV were also detected in Chinese horseshoe bats, indicating that these species may serve as a reservoir for this unique HCoV (Lau et al., 2005). Together with an explanation for the Ebola virus in African flying foxes (Pteropus spp.), these discoveries attracted attention to bats as hosts of new viral infections (Leroy et al., 2005). Among the several criteria supporting bats as animal reservoirs of mammalian viruses, their high-density colonies, lifespan, intimate social contact, and capacity to fly are also considered (Calisher et al., 2006).

Similarly, in June 2012, the first case of MERS-CoV was identified in Jeddah, Saudi Arabia (Ge et al., 2015) . Until November 2019, there were 2,492 recorded cases of MERS-CoV in 28 countries that resulted in 859 deaths. It was predicted more than 30 years ago that the ancestor virus would pass into dromedary camels from bats, and this prediction has been confirmed by serological data ever since. Dromedary camels are a significant reservoir for MERS-CoV (Müller et al., 2014). (Figure 1.2).

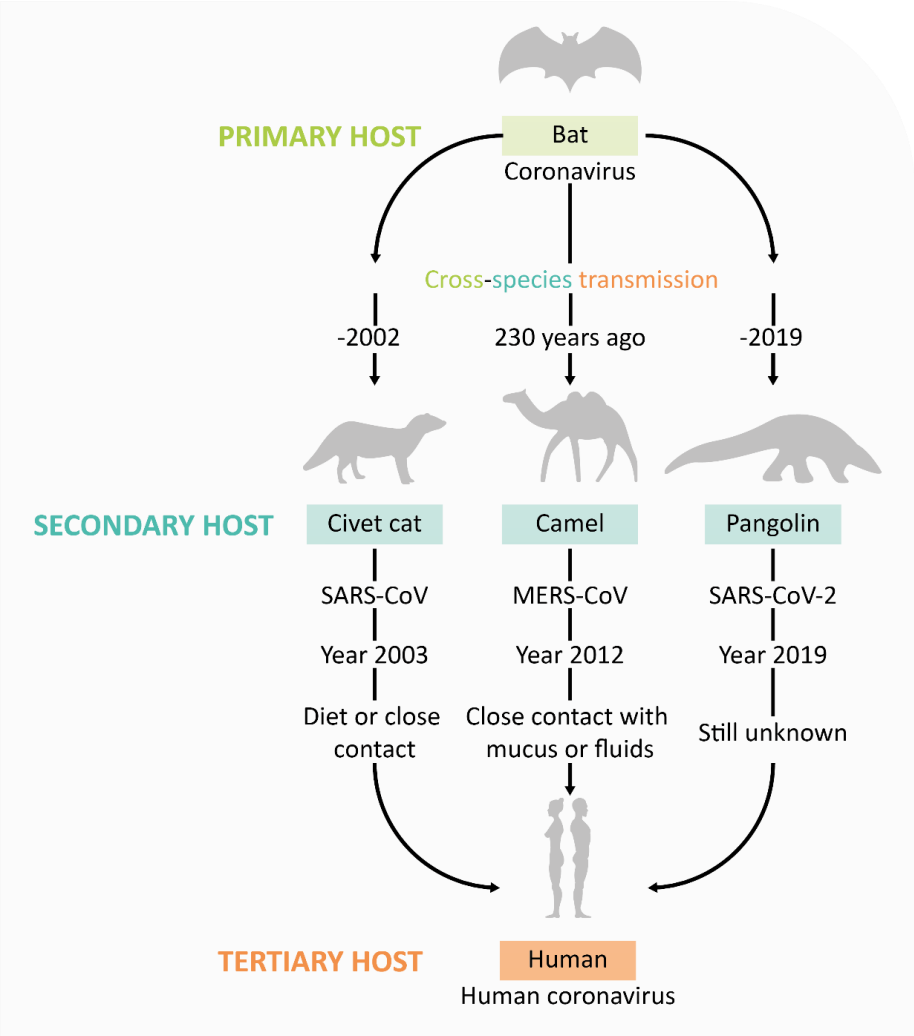


**Figure 1.2. Schematic representation of HCoVs transmission.** Transmission from bats to humans of SARS-CoV, MERS-CoV, and SARS-CoV-2 through intermediate hosts (Figure taken from (Kirtipal et al., 2020)).

The recent SARS-CoV-2 pandemic put forward the existence of an undiscovered wild zoonotic reservoir of lethal viruses (Malik et al., 2020). A live animal market in Wuhan, China, was related to the SARS-CoV-2 epidemic in 2019. Bat-SL-CoVZX45 and bat-SL-CoVZX2, two SARS-like CoVs that shared 96% of their genome with SARS-CoV-2, bats were shown to be the natural hosts of SARS-CoV-2 by genetic study (Z. Xu et al., 2020). However, the intermediary host and the path via which the virus was transmitted to humans was unknown. Transmission of SARS-CoV-2 from bats to humans was first hypothesized by Ji et al. to occur by homologous recombination within the S protein in snakes (Ji et al., 2020). Pangolins (Manis spp.) was later identified as a possible intermediate host for SARS-CoV-2 due to their 99% genetic similarity to pangolin CoVs (Figure 1.2).

### 1.1.6 Structure of SARS-COV-2

CoVs are RNA viruses with envelopes that range in size from 80 to 220 nanometers. Under electron microscopy, the envelope has 20 nm crown-like spikes that resemble the sun's corona, hence the name coronavirus (Figure 1.3) (S. E. Park, 2020). They also have the largest genomes of any RNA virus currently known, with a size between 27 and 34 kB. Specifically, SARS-CoV-2 particles were found to be spherical in shape with a diameter of 60-140 nanometers with spikes of 9-12 nanometers (N. Zhu et al., 2020a).

SARS-CoV-2's main structure is built by four major structural proteins: spike (S), membrane (M), nucleocapsid (N), and envelope (E). All four of these proteins are encoded within the 3' end of the SARS-CoV-2 genome. The transmembrane S glycoprotein with a molecular weight of 150 kDa extends from the virus's surface. S protein forms homotrimers, which help the virus attach to the ACE2 receptor on the host cell (Hwang et al., 2020). A host cell protease splits this glycoprotein into two subunits, S1 and S2. The host viral range and cellular tropism are determined by the S1 subunit, which is characterized by the C-terminal domain (CTD) that contains the receptor-binding domain (RBD) and the N-terminal domain (NTD). Membrane fusion is mediated by the S2 subunit, which includes an internal membrane fusion peptide (FP), two 7-peptide repeats (HR), a membrane-proximal external region (MPER), and a transmembrane domain (TM) (Guo et al., 2020; F. Li, 2016).

Molecular weight of M glycoprotein, the most abundant surface structural protein, has an important role in viral assembly (Neuman et al., 2011). SARS-E CoV-2's protein, the smallest one, is involved in viral generation and maturation. The virus's nucleic acid is attached to the N protein, which means it is engaged in the viral genome and replication cycle (Schoeman & Fielding, 2019).

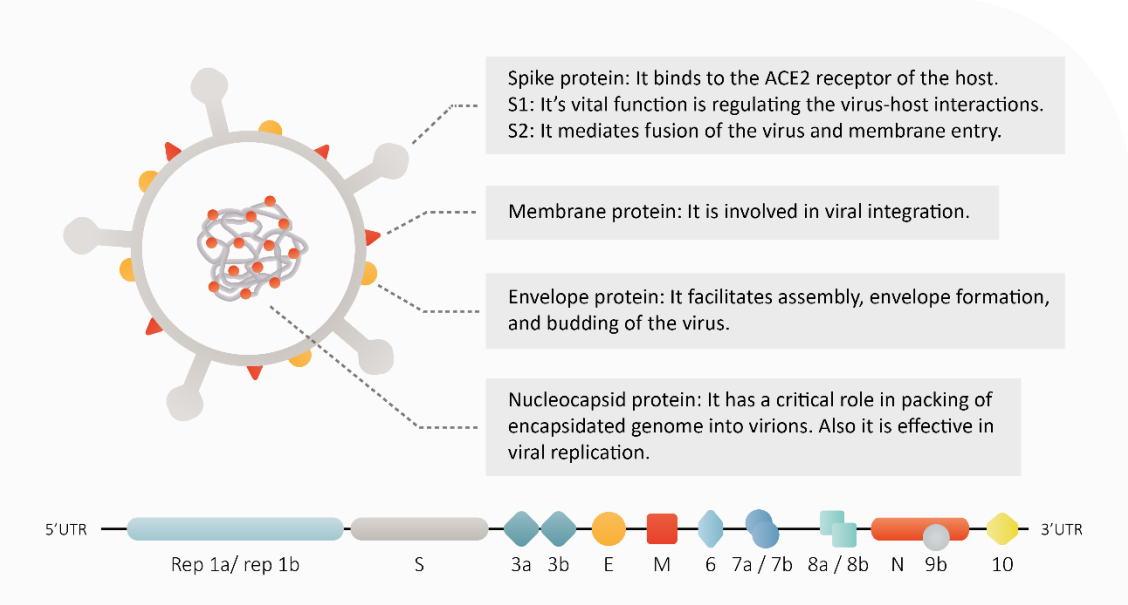


**Figure 1.3. Coronavirus schematic illustration.** The four structural genes, which include the spike, envelope, membrane, and nucleocapsid genes, encode structural proteins, as well as genome organization and the encoded proteins of pp1ab and pp1a, as well as accessory proteins (3a, 3b, 6, 7a, 7b,8a, 8b, 9b, and ORF10). ORFs are initials for open reading frames.

### 1.1.7 Genome Organization of SARS-CoV-2

There are 13–15 (12 functional) open reading frames (ORFs) inside the SARS-CoV-2 genome, which is between ~29.9 kilobytes in size. Sixteen nonstructural proteins (nsps) are encoded by the first ORF, which makes up around 67% of the genome, whereas structural and accessory proteins are encoded by the remaining ORFs. It has two untranslated regions (UTRs) at the 5′ and 3′ positions..(J. F. W. Chan et al., 2020; A. Wu et al., 2020). SARS-genome CoV-2's initiates viral genome replication and transcription by translating two polyproteins from the ORF1a and ORF1b region into sixteen nsps (nsp1-16). Additionally, the SARS-CoV-2 genome contains four structural and up to six accessory proteins (3a, 6, 7a, 7b, 8, 9b and 10), however the subgenomic RNAs (sgRNAs) are required for the translation of these proteins in infected cells that have been newly generated.. (Figure 1.4). The viral genome, which is ready to be translated into proteins due to the virus's positive sense RNA nature, is released after entrance into the host cell (Naqvi et al., 2020).

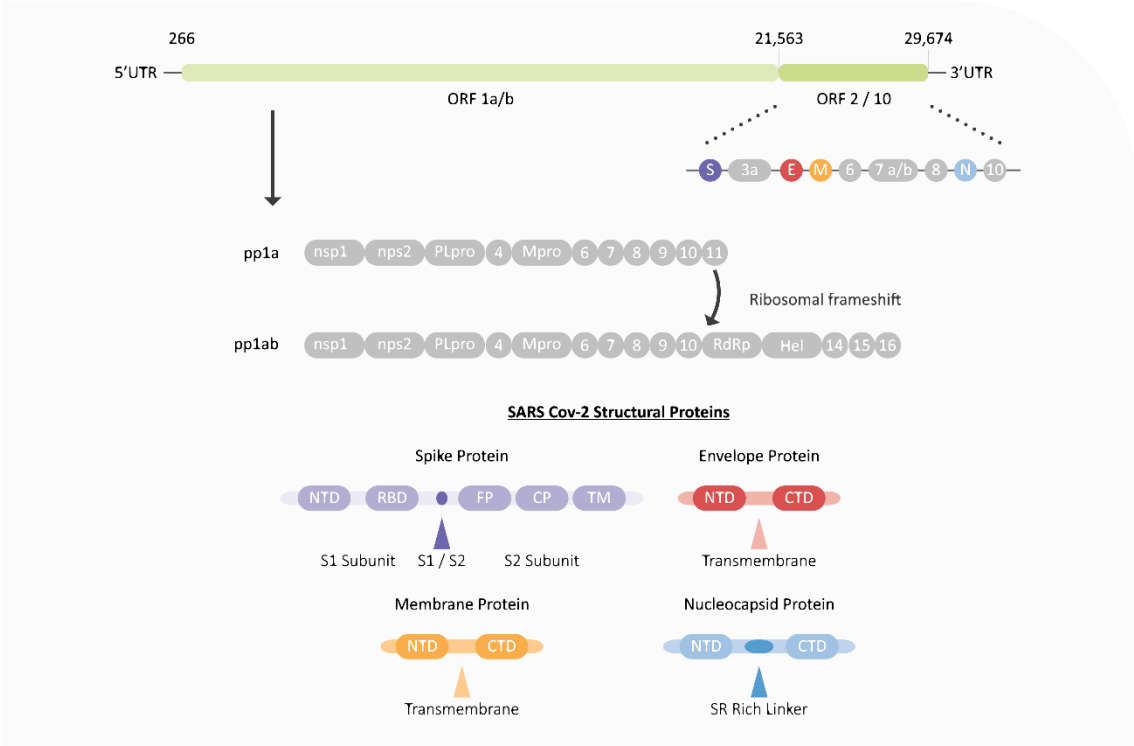


**Figure 1.4. The arrangement of the SARS-CoV-2 genome is shown schematically.** The genome comprises a single long open reading frame flanked by two untranslated sections (UTRs). The genome is ordered by 5′ UTRs-orf1a-orfS-orf3a-orfE-orfM-orf6-orf7a-orf7b-orf8-orf9b-orfN-orf10-3′UTR. ORF1ab is responsible for producing two big polypeptides, pp1a and pp1ab. These two polyproteins are expressed by ribosomal frameshifting. The genome is composed of four structural proteins: spike protein (S), envelope protein (E), membrane protein (M), and nucleocapsid protein (N), as well as six accessory proteins: 3a, 6, 7a, 7b, 8, 9b and 10. The four structural proteins' primary domains are shown.

## ORF1ab

### *Non-structural polyproteins (nsps)*

Once ORF1ab is translated, it produces two large non-structural polyproteins. The two big pp1ab and pp1a ,replicase polyproteins, are produced by ribosomal frameshifting during translation. These polyproteins are processed to produce 16 different nsps. Two proteases are involved in polyprotein cleavage: First is the papain-like protease (PLpro), which is encoded by nsp3. The second is serine-type Mpro (3CLpro) which is the major protease encoded by nsp5 (Tu et al., 2020). The functions of these nsps are reviewed in Table 1.2.

| nsp | aa length and position | Function | Ref |
|---|---|---|---|
| nsp1 | 180 aa (1-180) | Innate immunological responses are suppressed. It inhibits IFN-type 1 production in infected cells. The translational machinery is blocked, and the host mRNA is destroyed. | (J. F. W. Chan et al., 2020) |
| nsp2 | 638 aa (181-818) | Participates in a variety of cellular functions via interactions with the host factors prohibitin 1 and 2. | (Cornillez-Ty et al., 2009) |
| nsp3 | 1945 aa (A819-G2763) | It is the largest protein in the coronavirus genome. It is a papain-like protease (PLpro), a large transmembrane protein that degrades viral polyproteins derived from genomic RNA into their component proteins. Additionally, it was shown to be antagonistic against the host's innate immunity. | (Oostra et al., 2008) |
| nsp4 | 500 aa (K2764-Q3263) | It is responsible for membrane rearrangement. It interacts with nsp3 and 6 to create double membrane vesicles, which are essential for cell survival. This contact is critical for the development of the viral replication complex. | (Sakai et al., 2017) |
| nsp5 | 306 aa (S3264-Q3569) | Mpro, chymotrypsin-like protease (3CLpro), the major viral protease, is a critical enzyme that digests viral polyproteins at 11 conserved sites, including autolytic cleavage from polyproteins pp1a and pp1ab. | (Snijder et al., 2016) |
| nsp6 | 290 aa (S3570-Q3859) | With nsp4 and nsp3, it forms a double membrane vesicles protein. | (Fehr & Perlman, 2015) |
| nsp7 | 83 aa (S3860-Q3942) | For RNA polymerase and primase, a cofactor forms a hexadecameric complex with nsp8 and acts as a processivity clamp. | (Snijder et al., 2016) |
| nsp8 | 198 aa ( A3943-Q4140) | For RNA polymerase and primase, a cofactor forms a hexadecameric complex with nsp7 and acts as a processivity clamp. | (J. F. W. Chan et al., 2020) |
| nsp9 | 113 aa ( N4141-Q4253) | A protein that binds to single-stranded RNA (ss-RNA). By stabilizing nascent nucleic acid during replication or transcription, it protects it from nucleases. | (Shanker et al., 2020) |
| nsp10 | 139 aa ( A4254-Q4392) | A tiny protein that is hypothesized to have several roles. It interacts with nsp14 and nsp16, which are both required for replication fidelity. It interacts with nsp14 and 16 to enhance exonuclease and O-methyl transferase activity.. | (Snijder et al., 2016) |
| nsp11 | 11-23 aa (S4393-V4405) | It's a short peptide that works as a frameshift barrier and is found near the end of ORF1a. It's the outcome of a pp1a cleavage that hasn't been determined yet. | (Fehr & Perlman, 2015) |
| nsp12 | 932 aa (S4393-Q5324) | This RNA-dependent RNA polymerase replicates and transcribes the viral genome (RdRp). The RdRp-mediated synthesis of new viral RNA is an important step in the viral life cycle. | (Posthuma et al., 2017) |
| nsp13 | 601 aa (A5325-Q5925) | A helicase contains a metal-binding domain at the N-terminus and a conserved helicase domain. It is necessary for viral replication because it can unwind duplex RNA and DNA. | (Jang et al., 2020) |
| nsp14 | 527 aa (A5926-Q6452) | As a 3'-5' exoribonuclease and N-7-Guanine methyl transferase, it plays a vital role in proofreading and in mRNA capping. | (Totura & Baric, 2012) |
| nsp15 | 346 aa (S6453-Q6798) | It's a poly(U)-specific endoribonuclease that cleaves RNA at the uridylates' 3′ end. It has been | (Snijder et al., 2016) |

| | | | |
|---|---|---|---|
| | | shown that the lack of nsp15 impairs viral replication and pathogenicity. | |
| nsp16 | 298 aa (S6799-N7096) | It has 2-O methyltransferase activity, which is needed to cap viral mRNA and keep it from being detected by the host. | (J. F. W. Chan et al., 2020) |

**Table 1.2.** Non-structural polyproteins of SARS-CoV-2

**ORF 2-10**

It has sequences that code for the four structural and six accessory proteins. In the Golgi apparatus, some of these proteins are glycosylated (Sakr et al., 2021).

***Structural Proteins***

**S protein**

S protein is 150 kDa and contains 1300 amino acids. It is found on the viral surface and forms the corona. It functions as a homotrimer and contains 20 asparagine-linked glycan signal sequences (Fehr & Perlman, 2015). The protein includes two main subunits responsible for receptor-binding (S1) and membrane-fusion (S2). The S1 subunit includes a receptor-binding domain (RBD) (Heald-Sargent & Gallagher, 2012).

At the time of host-virus integration in all CoVs, host proteases like TMPRSS2 and lysosomal proteases like cathepsins cleave S proteins (Shang et al., 2020). SARS-CoV-2 S protein has 33 unique amino acids (2.59%), with the most significant variants being 439-449 and 482-505 (C. Li et al., 2020). Furthermore, different studies have discovered that SARS-CoV-2 has a unique peptide (PRRA) insertion that influences protease cleaving (Qiong Wang et al., 2020). Because this protease plays such a critical role in viral entry into the host cell, inhibiting compounds and nafamostat mesylate can be applied to treat SARS-CoV-2.

Inhibiting protein S activity, which can prevent the virus, is a major strategy to treat people infected with SARS-CoV-2 (Bestle et al., 2020). One of the medicines used to treat infected people is Griffithsin. It's a lectin drug used to treat by binding glycoproteins to regulate S protein (C. Lee, 2019). S protein is frequently the target of antibody-based treatments.

**M protein**

M protein, a type III transmembrane glycoprotein (Arndt et al., 2010) is the most abundant protein on the virus's surface, providing a main scaffold for the virus shape. M protein has 230 amino acids and a mass of 25-35 kDa, the smallest of the structural proteins (Arndt et al., 2010).

This protein is involved in entry into the host cell and virus maturation (Thomas, 2020). It has been suggested that viral infectivity is linked to the M protein's ability to connect to the viral S protein and the surface receptors of the host, which would facilitate membrane fusion. It seems to have a role in the antigenicity that is indicated by the host immune responses elicited by viruses. Because of its importance in coronavirus virion assembly and morphogenesis, the M protein may play an important role in viral replication control and viral particle packing of genomic RNA (Y. Hu et al., 2003).

**N protein**

This protein has a molecular weight of 43–50 kD can bind to RNA and interact with it through the aminoacid sequences arginine and lysine (Chang et al., 2006). It is known that this protein is known to be phosphorylated at multiple positions in various CoVs, which may affect functions such as the ability to distinguish between non-viral and viral RNA and affect virus maturation and assembly (Y. Chen et al., 2019). The essential mechanism for phosphorylation, on the other hand, has remained unclear. The N protein can also be involved in viral transcription control and genomic RNA replication (Cong et al., 2020).

On a molecular level, N's primary role is to package virus genome RNA into long-helical RNPs and engage in virion assembly via interactions with the viral genome and membrane protein M. It has been established that the CoV N protein regulates viral life cycles by interfering with interferons, inhibiting RNA interference, or inducing cell death in the host. As a diagnostic and immunogenic antigen, the N protein is also an immunodominant antigen in the host immune response (Bai et al., 2021).

**E protein**

E protein is a small hydrophobic protein with a length of ~74–109 amino acids and a molecular weight of 8.4–10.9 kDa. It is required for ion channel function, viroporin activity, and viral assembly in budding viruses (Schoeman & Fielding, 2019).

The E protein is the smallest and least known of the main structural proteins. Viral subtypes share an abundance of this protein. It's still not clear exactly what the E protein does during viral replication. The viral particle envelope's E protein interacts with other structural proteins to perform its function. The viral particle's shape is maintained and its release is facilitated by its interaction with the E and M proteins. Coexpression of E and M causes the S protein to move to the ER-Golgi intermediate site or the Golgi region in host cells. Apoptosis is induced by a mutation in the E protein gene (Schoeman & Fielding, 2019).

Even while each infected cell produces a high quantity of E protein throughout the CoV replication cycle, only a tiny portion of this produced E protein gets inserted into the viral membrane. The endoplasmic reticulum (ER), Golgi, and ER-Golgi intermediate compartment (ERGIC), which are involved in CoV assembly and budding, contain most of the protein. The fact that recombinant CoVs missing the E protein have lower viral titers and maturation or generate incompetent progeny suggests the relevance of the E protein in virus generation and maturation, which is supported by the data. Additionally, the E protein may bind to PALS1, which results in accelerated epithelial barrier degradation, an increased inflammatory response, and the stimulation of tissue remodelling, indicating that the E protein plays a significant role in viral infection (Nieto-Torres et al., 2011).

***Accessory Proteins***

ORF 3a codes for the 3a accessory protein and is 828 nucleotides long (Changtai Wang et al., 2020). It's also worth noting that accessory protein 3b was discovered in several early investigations on SARS-CoV-2 (A. Wu et al., 2020). One research was characterized as a four-helix short new putative protein (J. F. W. Chan et al., 2020). ORF 6 is a 186-nucleotide gene that codes for the Orf6 accessory protein, with 61 amino acids (Changtai Wang et al., 2020). ORF 7a and ORF 7b, respectively, comprise 366 and 132 nucleotides (Changtai Wang et al., 2020). Protein 7a is thought to have a role in viral

pathogenesis by inducing apoptosis and arresting the cell cycle in infected cells, and stimulating the production of pro-inflammatory cytokines (Schoeman & Fielding, 2019). ORF8 is a 366-nucleotide protein-coding gene. It has been shown to activate inflammasomes and initiate intracellular stress pathways (C. S. Shi et al., 2019). When an infection occurs, the host cell secretes ORF9b, a 97-amino acid protein. By targeting mitochondria, it connects with the flexible adaptor TOM70, which is important in the immunological evasion process. ORF 10 is a 117-nucleotide coding sequence (Changtai Wang et al., 2020). Except for ORF8 and ORF 10, other ORFs were shown to be preserved for SARS-CoV-2 in other related viruses in research by Tang et al. (Tang et al., 2020). As a result, it's expected that ORF10 protein might be used to identify SARS-CoV-2 infection faster than PCR-based methods (Khailany et al., 2020).

### 1.1.8 The Lifecycle of SARS-COV-2 and Cell Entry of Coronaviruses

There are three basic processes by which the SARS-CoV-2 virus can enter a host cell: binding to the receptor; proteolysis; and triggering of membrane fusion in endosomes (Figure1.6) (Boopathi et al., 2020). Both endosomes and plasma membrane fusion are the entry mechanisms for SARS-CoV-2. S glycoprotein interaction to the ACE2 receptor requires conformational changes in both moieties. In the case of SARS-CoV-2, the protease TMPRSS2 and lysosomes cleave the S protein into two fragments: S1 and S2 (Qihui Wang et al., 2020). The S1 segment comprises the RBD, which binds to ACE2, while the S2 component is crucial for membrane fusion (Brielle et al., 2020).

Following attachment, the virus undergoes fusion via an endocytic route, releasing viral RNA into the cytoplasm (H. Wang et al., 2008). The inside of endosomes has an acidic pH due to the existence of a proton pump (Gerasimenko et al., 1998). Additionally, cysteine proteases, most likely cathepsin, enable the virus to be released from the cytoplasm in a pH-dependent manner (Figure1.5) (M Hoffmann et al., 2020). Non-endosomal-independent entrance is the alternative entry mechanism. The cell membrane-associated serine protease, TMPRSS2, activates/cleaves the S protein into S1 and S2 domains.

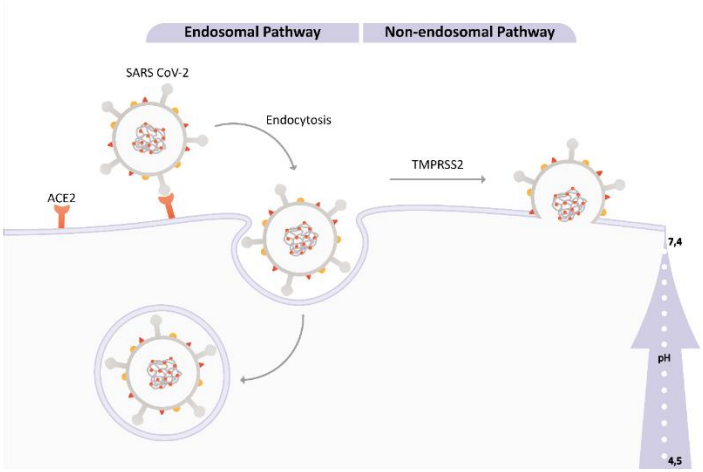


**Figure 1.5. SARS-CoV-2 entry model into the host cell.** When the S1 domain of the S protein interacts with the ACE2 receptor on the host cell surface, conformational changes in the S2 domain cause internalization and subsequent membrane fusion. A low pH and the pH-dependent cysteine protease cathepsin L promotes the endosomal process. The other entry mechanism is non-endosomal/clathrin-independent mechanism. It is mediated by the cleavage of the S protein into S1 and S2 domains by TMPRSS2.

After being released into the cell's cytoplasm, the virus' genome is translated as an mRNA by the host cell's machinery, resulting in the production of essential enzymes for RNA synthesis (Nsp12, an RNA dependent RNA polymerase, RdRp; and Nsp13, a zinc-binding helicase, HEL), proofreading (Nsp14), and capping (Nsp16 complex) (Nsp14-Nsp16 complex).

The first gene is translated into the replicase enzyme, which begins replication. PLpro and Mpro, two viral proteases that convert this enzyme into 16 nsps. The process of synthesising RNA from RNA templates is done RdRp. As part of the replication process, negative strand RNA is synthesized and used as a template for genomic RNA. (Pachetti et al., 2020).

sgRNAs serve as mRNAs for structural and accessory genes that are located downstream of the replicase polyproteins. Transcription-regulating sequences (TRSs) found at the 3′ end of the leader sequence (TRS-L) act to control the transcription through RdRp that terminates transcription at each TRS sequence. Therefore, the transcription process is discontinuous and the resulting sgRNA is translated into structural, non-structural, and accessory proteins, resulting in the formation of new viruses (Sakr et al., 2021).

Following replication, transcription, and translation, the endoplasmic reticulum and Golgi apparatus assemble virion particles (Masters, 2006). The SARS-CoV-2 virus's assembly process is still a mystery. Coronavirus-infected cells release virions through two different processes: helical nucleocapsids and viral envelope construction.

Helical nucleocapsids are assembled in the cytoplasm (de Haan et al., 2000). N protein and RNA constitute the nucleocapsid. Occasionally, the M protein is also detected (de Haan & Rottier, 2005). N protein is a glycoprotein with several functions. It primarily attaches to leader RNA to facilitate replication and transcription. It interacts with the viral genome and encapsulates it in a helical structure named the ribonucleoprotein (RNP) complex (McBride et al., 2014). Additionally, the N protein interacts with the nsp3 and M proteins, forming the replication-transcriptase complex (RTC) to assemble package the genome (Hsieh et al., 2005).

In the second step, the viral envelope is assembled in the intracellular membranes of the cells. Normally, the viral nucleocapsid budding through the cellular membranes provides the membranes for enveloped viruses. ERGIC is where SARS-CoVs form at intracellular membranes. They then budding takes place inside the lumen and particles are released by exocytosis (Gupta et al., 2021). The viral membrane proteins are crucial in the development of the viral envelope. M and E proteins are essential for virion assembly and release however, E protein is only detectable in trace levels. As a result, the assembly is mostly dependent on interactions between M proteins (de Haan et al., 2000). M protein also acts as a matrix for nucleocapsid attachment, allowing budding to occur.

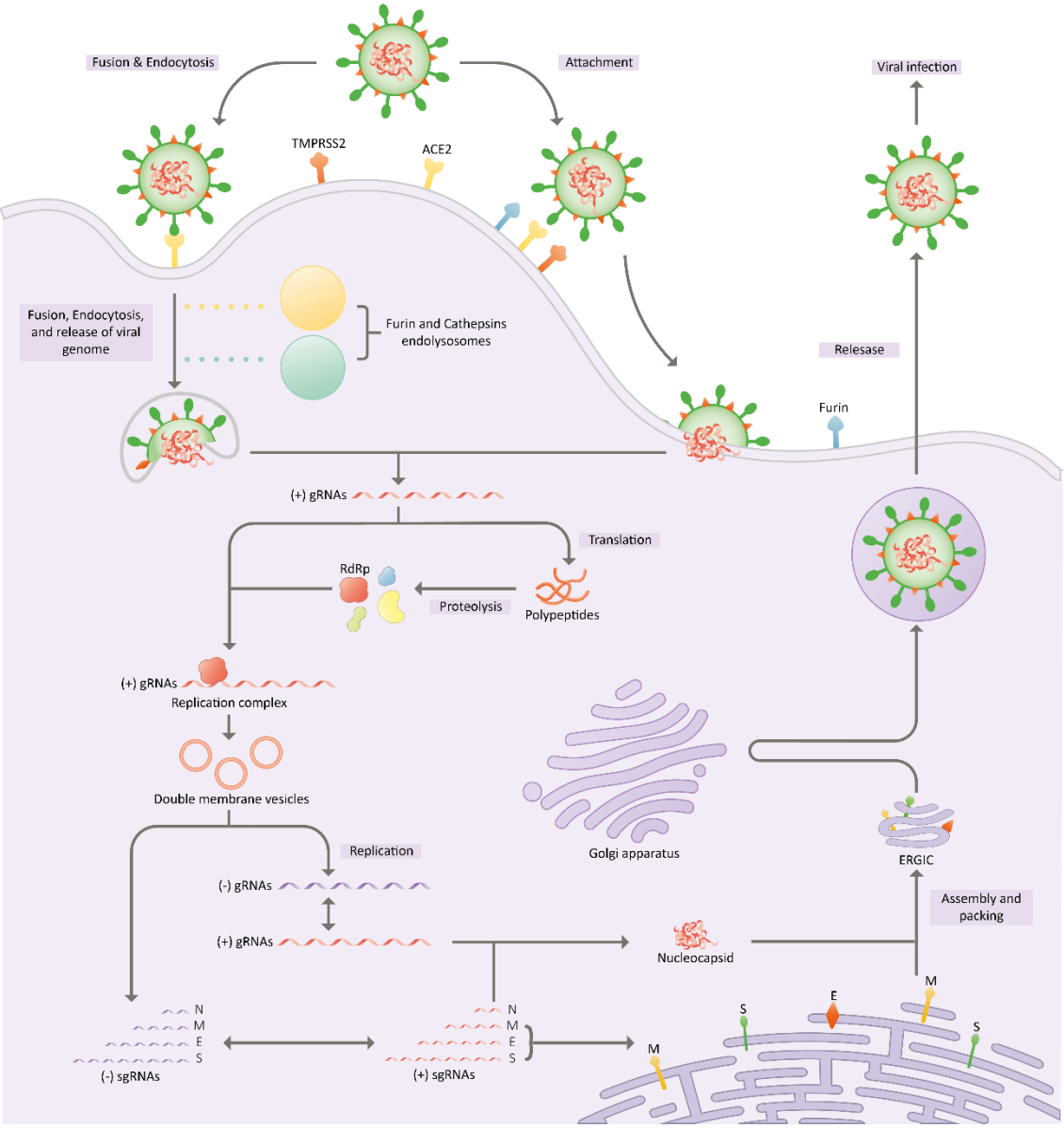


**Figure 1.6. The Lifecycle of SARS-COV-2**. The NSPs domain is produced as two polypeptides once the viral RNA genome is released into the host cell environment, ultimately producing PLpro, Mpro (also known as 3CLpro), and RdRp. The two polypeptides are first processed by host proteases and then spread by PLpro and Mpro. The viral RdRp is also in charge of the viral genome's replication and amplification. The viral RNA and structural protein N are produced in the cytoplasm of the host cell, whereas viral structural proteins S, M, and E are produced in the endoplasmic reticulum and transferred to the Golgi apparatus. ERGIC assembles the viral RNA–N complex, as well as the S, M, and E proteins. The budding process produces the mature virus. Exocytosis then releases the virus. Note: The virus enters by membrane fusion in endo/lysosomes, which needs cathepsin's proteolytic activation, or through fusion at the cell membrane, which requires TMPRSS2's proteolytic activation. (Figure adapted from (Al-Horani & Kar, 2020))

### 1.1.9 Mutations of SARS-COV-2

SARS-CoV-2 variations are described as viruses that accumulate changes, such as single nucleotide polymorphisms (SNPs), that provide a selective advantage on them, such as increased infectivity within the host and transmissibility across hosts (Smith & Denison, 2013). Concerning variants are viruses that have acquired antigenic alterations that impair the immune response and/or the effectiveness of drugs. Sequencing the virus's genome enables observation of the virus's continuing evolution. While changes across the SARS-CoV-2 genome have been observed, the most worrying ones have occurred in the Spike encoding gene.

At the viral membrane, SARS-COV-2 spike protein is organized into a clove-shaped trimer. The S1 segment, composed of the NTD, the RBD, and the CTD is involved in viral attachment to the target cell. NTD and RBD are two antigenic areas with mutations affecting both infectivity and immunity. The S2 segment comprises components necessary for viral genome transport into the target cytosol, such as the fusion peptide (FP). So far, mutations in the S2 subunit have not been associated with viral transmission or immunity escape.

**Spike RBD and S1-CTD mutations**

***D614G:*** According to structural analyses, the D614G mutation enhances the capacity of the RBD to be shifted into the "up" position necessary for ACE2 receptor binding (Yurkovetskiy et al., 2020). D614G has been shown to increase SARS-CoV-2 infection and transmissibility, consistent with this hypothesis (Plante et al., 2020). This mutation is present in all currently recognized variations.

***N501Y:*** The S protein's position 501 contains one of the six amino acid (a.a.) residues that come into interaction with ACE2. The N501Y change has been found to increase SARS-affinity CoV-2's for ACE2 (Starr et al., 2020). SARS-CoV-2 adaptation tests with the N501Y mutation demonstrate that the virus may replicate in animals whose ACE2 does not easily engage the S protein (Gu et al., 2020). This change has a negligible antigenic effect, with no discernible influence on the *in vitro* neutralizing activity of

convalescent plasma or sera from vaccinated individuals (P. Wang et al., 2021). N501Y is prevalent in the majority of contemporary variations of concern.

***K417N/T:*** The replacement of an N (Asparagine) for K417 in S.A variations or a T (Threonine) for K417 in the BRA variant converts a polar amino acid to a neutral amino acid. According to a mouse adaption study, the K417N mutation enhances the Spike interaction with ACE2 (S. Sun et al., 2021).

***E484K:*** S.A variations and the BRA variant both carry the E484K mutation. This amino acid substitution may contribute to SARS-CoV-2 escape from monoclonal antibodies and convalescent COVID-19 patient sera (Greaney et al., 2021). It has been suggested that the K (Lysine) substitution at position 484 breaks hydrogen bonding with clinical monoclonal antibodies (mAbs) directed against the Spike RBM or polyclonal antibodies from vaccinee sera (P. Wang et al., 2021).

***P681H:*** The U.K variant's P681 alteration for a H (Histidine) occurs next to the SARS-CoV-2 furin cleavage site (also known as the S1/S2 cleavage site) (Frampton et al., 2021).

***L452R:*** The CAL (USA) variant's L452 to R (Purine) mutation is found inside the SARS-CoV-2 RBD (Garcia-Beltran et al., 2021). While the L452 residue does not directly contact the ACE2 receptor, the L452R mutation may result in structural alterations that favour the Spike-Ace2 interaction (X. Deng et al., 2021). Additionally, this conformational shift has been claimed to affect neutralizing antibody binding (Garcia-Beltran et al., 2021).

**Spike S1-NTD mutations**

The least conserved domain on the SARS-CoV-2 Spike protein is the NTD (Plante et al., 2021). This area has several substitutions and deletions. Notably, 90% of Spike deletions occur in four regions of the NTD termed "recurrent deletion regions" (RDR1–RDR4) (McCarthy et al., 2021). These RDRs bind outer surfaces bearing antibody epitopes, contributing to the resistance of SARS-CoV-2 to neutralizing antibodies (McCarthy et al., 2021).

***L18F:*** The substitution of L18 for F (Phenylalanine) is an SNP seen in both the BRA and S.A. B.1.351 v2 variants (Garcia-Beltran et al., 2021). Based on structural studies, it has

been anticipated that the L18F mutation affects mAb binding (McCallum et al., 2021). Additional functional investigations are now needed to evaluate this concept.

***Del69-70:*** The most often occurring RDR1 deletion is the loss of two residues at positions 69 and 70 (Garcia-Beltran et al., 2021). Del69-70 has been identified in both the UK version and a variation that arose in Danish mink farms in April 2020 (Munnink et al., 2021). While this deletion is located in a conspicuous outer loop of the Spike, it has not been linked with resistance to NTD antibodies in vitro neutralization studies employing convalescent patients or vaccinee sera (Meng et al., 2021). Del69-70 increases Spike incorporation into virions by a factor of two but does not promote cell-cell fusion (Xuping Xie et al., 2021). Additional research is necessary to ascertain the mutation's overall effect.

**Del144/5:** The deletion of one of two adjacent Y (Tyrosine) residues at position 144/145 in RDR2 is the United Kingdom version (Frampton et al., 2021). This mutation is located near glycosylation sites, which may aid in the attachment of SARS-CoV-2 to target cells or in the evasion of neutralizing antibodies (Plante et al., 2021).

***Del242-4:*** Another popular Spike variant is the deletion of a.a. in the 242-244 region of RDR4. It is one of the SNP signatures for S.A variations and the only one not exposed to the surface (Tegally et al., 2020). There is little evidence of its effect on SARS-CoV-2 infectivity and immunological escape. This mutation is targeted by antibodies isolated from convalescent patients against the Spike NTD antigenic supersite (Meng et al., 2021). With the R246I mutation, del242-4 plays a significant role in the resistance of S.A variants to most NTD mAbs (P. Wang et al., 2021).

***R246I:*** This alteration is located near del242-4 and is another SNP marker for one of the three S.A. variants described, B.1.351 v3 (Tegally et al., 2020). Additionally, it is a Spike NTD antigenic supersite member and is anticipated to enhance antibody neutralization (McCallum et al., 2021). Along with the 242-4 deletion, R246I has a significant role in the B.1.351 v3 S.A. variant's resistance to the majority of NTD mAbs (P. Wang et al., 2021).

**Variants of concern (VOCs)**

The Wuhan-Hu D614 isolate/strain was reported as the first of the pandemic's strains in December 2019 (N. Zhu et al., 2020b). The original variety was taken out in April 2020, favouring the D614G version (Korber et al., 2020). Since then, the D614G variation has accumulated several mutations, allowing for enhanced viral spread. The WHO classifies SARS-CoV-2 variations into two categories: variants of concern (VOC) and variants of interest (VOI). Since the outbreak started in December 2019, many VOCs have developed from the initial wild-type strain discovered in Wuhan. VOCs have enhanced transmissibility, virulence, vaccine resistance, or acquired immunity from prior infection, and the capacity to evade diagnostic identification.

***D614G variant:*** Beginning in April 2020, the D614G variation began to outcompete the original Wuhan-Hu-1 virus, gradually establishing itself as the worldwide dominant form (Korber et al., 2020). It is identified by the Spike protein's distinctive D614G substitution, which allows for a more fusion-competent confirmation (Yurkovetskiy et al., 2020). Antibody escape has not been connected with the D614G variant. Nevertheless, it collected more mutations, resulting in new variations of concern in diverse geographical locations.

***Alpha Variant (B.1.1.7) variant-United Kingdom:*** The B.1.1.7 variation first appeared in the United Kingdom in October 2020 (Frampton et al., 2021) before spreading to several other nations. Apart from the D614G mutation, B.1.1.7 has the following eight Spike mutations: del69/70, del144/5, N501Y, A570D, P681H, T716I, S982A, and D1118H (Frampton et al., 2021). Among them, del69/70, del144/5, N501Y, and P681H are the most concerning mutations retained in future versions (see above). Additionally, mutations in ORF1ab (T1001I, A1708D, I2230T, del3675-77), Orf8 (Q27stop, R25I, Y73C), and Nucleocapsid (D3L and S235F) occur outside of Spike (Frampton et al., 2021).

The United Kingdom variation is expected to be 30%-60% more infectious than ancestral strains (Xuping Xie et al., 2021). In vitro neutralization experiments employing VSV-based SARS-CoV-2 pseudoviruses bearing all eight Spike mutations in the U.K. variety demonstrated that B.1.1.7 is resistant to most NTD monoclonal antibodies and somewhat resistant to several RBD monoclonal antibodies (P. Wang et al., 2021). Additionally,

neutralization titers against B.1.1.7 are lowered somewhat (2 fold) but remain strong in convalescent and Moderna or Pfizer vaccinee sera (X. Shen et al., 2021).

***Beta Variant (B.1.351) - South Africa:*** In October 2020, the B.1.351 variation was discovered in South Africa (Tegally et al., 2020) and had since spread to all continents. Three S.A strains have been identified (B.1.351 v1, B.1.351 v2, and B.1.351 v3). They all have the same RBD mutations: K417N, E484K, and N501Y. The three S.A variants also share the Spike mutations D614G and N501Y with the U.K version. As a result, it is believed to have a high transmission potential. Each B.1.351 variation has its collection of Spike mutations: D80A, D215G, and A701V for B.1.351 v1, L18F, D80A, D215G, and A701V for B.1.351 v2, and D80A, R246I, and A701V for B.1.351 v3 (Garcia-Beltran et al., 2021). Certain of these changes have been related to a reduction in the in vitro neutralization potency of convalescent plasma (tenfold) and sera from Moderna and Pfizer vaccinees (five to sixfold) (Garcia-Beltran et al., 2021). P71L in the Envelope protein, T205I in the Nucleocapsid protein, and K1655N in ORF1a are additional SNPs in the B.1.351 lineage (Tegally et al., 2020).

***Gamma Variant (B.1.1.28.1) - Brazil:*** The B.1.1.28.1 variety was discovered in December 2020 in the Amazonas state of northern Brazil (Sabino et al., 2021), and quickly expanded to Japan, North America, Europe, and Australia. The BRA variation shares the D614G and N501Y Spike mutations with the variants from the United Kingdom and South Africa. As a result, it is believed to have a high transmission potential. Additionally, it shares two of the most concerning RBD alterations, K417N/T and E484K, with the S.A. variations (Sabino et al., 2021). Notably, in vitro studies have linked K417N/T and E484K alterations to enhanced ACE2 binding (S. Sun et al., 2021) and SARS-CoV-2 escape from monoclonal antibodies and convalescent COVID-19 patient sera (Weisblum et al., 2020). Additionally, SNPs in the P.1 lineage have been identified in ORF1ab (S1188L, K1798Q, del3675-7, E5666D), Spike (L18F, T20N, P26S, D138Y, R190S, H655Y, T107I, V1116F), Orf8 (E92K, ins28269-28273), and Nucleocapsid (P80R) (Sabino et al., 2021).

***Delta (B.1.617.2) – India***: B.1.617.2, known as the Delta variant, was originally found in December 2020 in India. This variation was discovered for the first time in the United States in March 2021.The B.1.617.2 variation has 10 spike protein mutations which

are T19R, 156del, 157del, R158G, L452R, T478K, D614G, P681R, and D950N (Cascella et al., 2021).

Changes in the RBD (L452R) and furin cleavage site (P681R) amino acid sequences are thought to be responsible for the increased transmission. The P681R mutation, which is also present in the Alpha version, was shown to enhance fusion activity, implying an increase in infectivity. Research on the Delta strain's transmissibility suggests that it's a more risky strain than the other varieties. Hospitalization risk was also shown to be twice that of the Alpha variant, with a recent research revealing that Delta-infected patients had more severe illness and a greater likelihood of death (Mistry et al., 2022).

***Omicron (B.1.1.529) – South Africa:*** Variant Omicron (B.1.1.529), newly recognized VOC by the WHO, was initially discovered in November 2021 in South Africa and has since been discovered in a number of other nations. Many researchers are examining epidemiological data to see how the Omicron variation affects transmission and pathogenicity. Omicron has 30 mutations, 15 of which occur in the RBD, as well as 3 deletions and 1 insertion. (Kumar et al., 2021) and this might affect how rapidly it spreads or how severe the disease it develops.

It is still uncertain how rapidly the Omicron variant could spread. The replacement of Delta by Omicron as the prevalent variety in South Africa indicates a higher transmissibility of the Omicron variant compared to Delta. The differences in the spike protein suggest that the Omicron variety is more prone to spread than the original SARS-CoV-2 virus (National Center for Immunization and Respiratory Diseases (NCIRD), 2021). The spike mutations of SARS-COV-2 variants are shown in Figure 1.7.

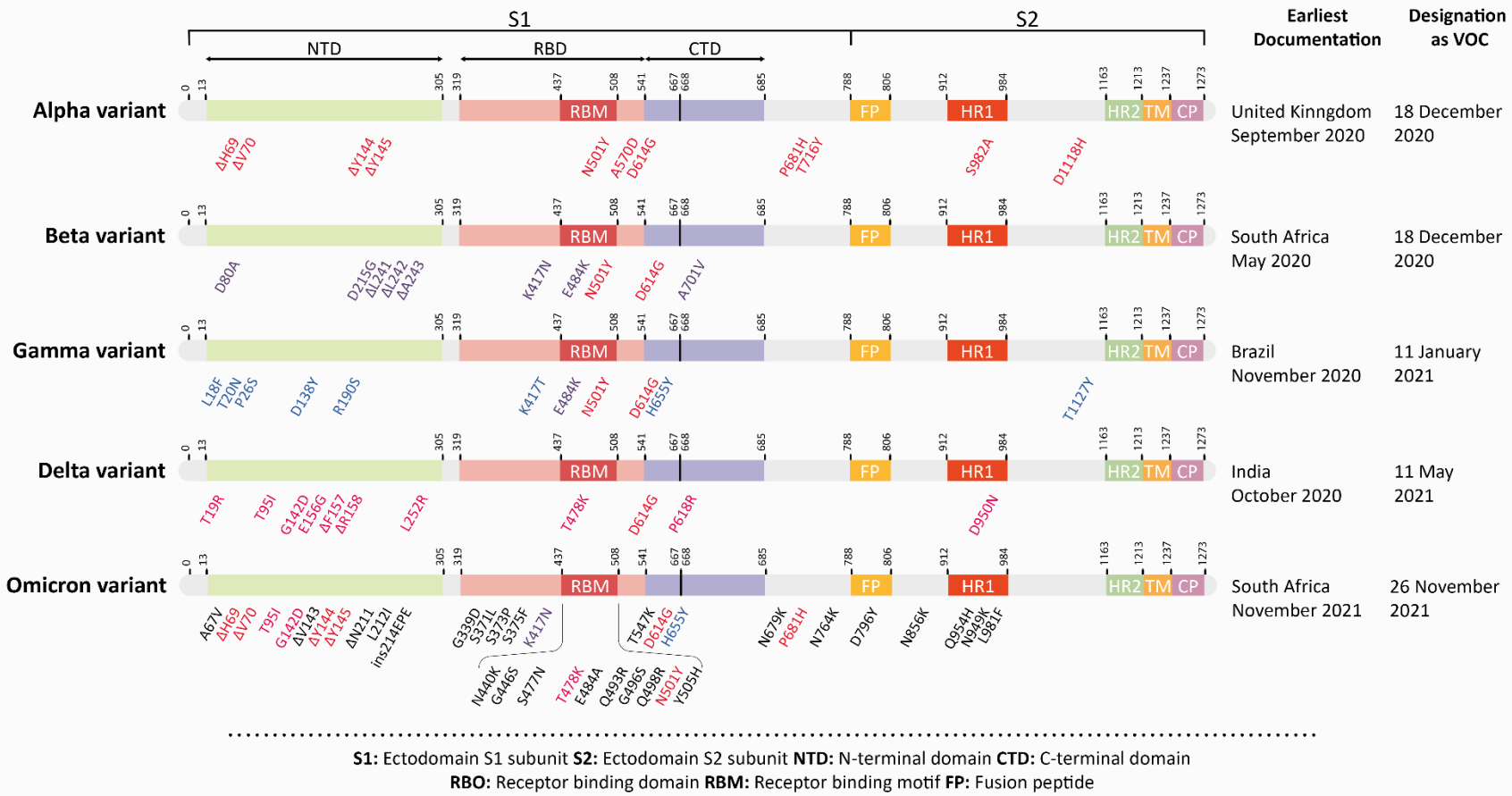


**Figure 1.7.** Spike mutations of SARS-Cov-2 variants (Figure adapted from (Sarkar et al., 2021)

## 1.2 Immune Response to SARS-CoV-2

The initial line of defense against viral infections is the host innate immune system (Braciale & Hahn, 2013). Pattern recognition receptors (PRRs) in innate immune cells recognize viral pathogen-associated molecular patterns (PAMPs) and damage-associated molecular patterns (DAMPs) (M. R. Thompson et al., 2011). As a consequence, antiviral interferon responses and other innate mediators are activated to limit virus reproduction and dissemination. Consequently, antigen-presenting cells take up and deliver viral antigens to induce adaptive immune responses (Freer & Matteucci, 2009). To prevent the propagation of the virus, neutralizing antibodies secreted and cytotoxic T-cells are activated. Viral NsPs have been associated in insufficient immunological responses, despite the fact that the immune response normally clears the infection.(Beachboard & Horner, 2016). Coronavirus-mediated lung injury and systemic disease are exacerbated by an immune response that is dysregulated and hyperactive, resulting in excessive inflammation. Viral binding may downregulate ACE2 and direct immunological dysregulation produced by the virus (Channappanavar & Perlman, 2017). The protective antiviral innate and adaptive immune responses, for SARS-CoV-2 are reviewed in Figure 1.8.

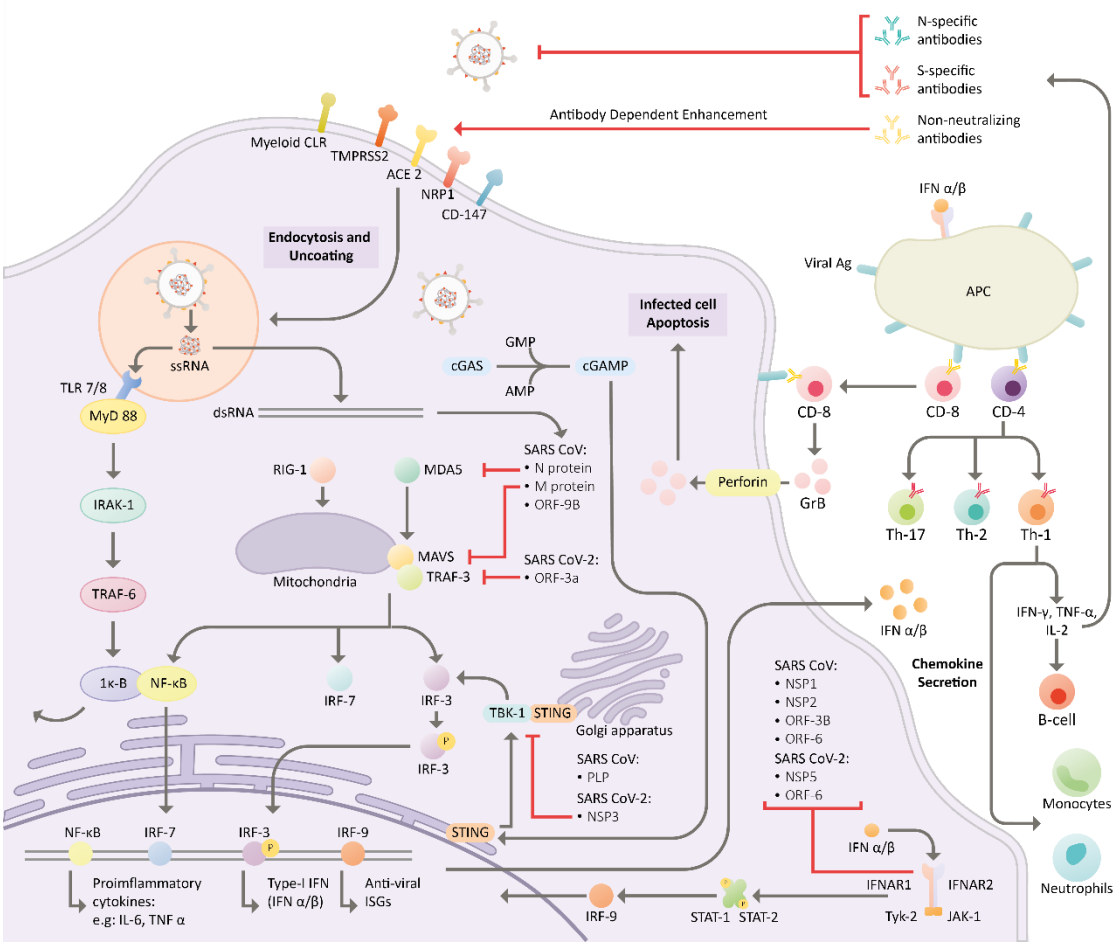


**Figure 1.8. The infection process of the Severe Acute Respiratory Syndrome Coronavirus-2 (SARS-CoV-2) and the human immune response after infection.** The viral attachment and entrance, as well as post-infection and viral replication, are mediated by TMPRSS2, ACE2, and CD147. The beginning of PRR signaling (TLRs, RLRs, CLRs, and cGAS-STING), which leads to the activation of type I IFN and proinflammatory cytokines, kicks off host immune response sooner. Toll-like receptors (TLRs); RIG-1-like receptors (RLRs); C-lectin-like receptors (CLRS); cGAS-STING (cyclic GMP-AMP synthase-Stimulator of Interferon Genes); interferon (IFN). (Figure adapted from (McGill et al., 2021)).

### 1.2.1 Innate Immune Responses

Lung cells undergo pyroptosis , represents a type of cell death caused by proinflammatory signals and related to inflammation, when SARS-CoV-2 enters and replicates, resulting in inflammation, the production of IL-1, and the recruitment of immune cells to the infection site (Yap et al., 2020). SARS-CoV-2 engages inflammasome and triggers pyroptosis in human monocytes. In human primary monocytes, pyroptosis was related

with caspase-1 activation, IL-1ß production, gasdermin D cleavage, and increased pro-inflammatory cytokine levels.

PRRs bind PAMPs and DAMPs to start a signalling cascade that promotes type I IFN-/and proinflammatory cytokine production. TLRs, RLRs, C-type lectin like receptors (CLRs), and cGAS-STING (cyclic GMP-AMP synthase-Stimulator of Interferon Genes) are four types of PRRs implicated in the immune response to Coronaviruses (L. Sun et al., 2012). Cytosolic RNA sensors like RIG-I and MDA-5 activate the cyclic GMP–AMP synthase/stimulator of IFN genes (cGAS-STING) pathway. In vitro infection with SARS-CoV-2 activated MDA-5 in primary human epithelia and cell lines and elevated RIG-I signaling in Huh7 cells (liver cell line) (Appelberg et al., 2020), eliciting a strong type I and type III IFN response, however this activation failed to inhibit viral replication (Antoine et al., 2020). SARS-CoV-2 also activates NF-kB through cGAS-STING in inflammatory immunological responses (Neufeldt et al., 2020), and STING polymorphisms have been linked to a delayed over-secretion of IFN-b in SARSCoV-2 infection (Berthelot & Lioté, 2020). Previous research has shown that PRR signalling is necessary for the clearance of SARS-CoV and MERS infections (Fehr et al., 2016).

TLRs 1-6 are present on the plasma membrane, whereas TLRs 7-9 are found inside endosomes in mice and humans (Kawasaki & Kawai, 2014). *In vivo* investigations have shown that animals lacking MyD88, TRIF, TLR3, and TLR4 have severe lung pathology and are more susceptible to SARS-CoV infection (Totura & Baric, 2012). Furthermore, SARS-CoV nsp3 was found to directly block the TLR7 pathway, to decrease viral recognition and interferon activation (S. W. Li et al., 2016). Interestingly, inhibition of NF-kB was demonstrated to improve lifespan in SARS-CoV infected mice. This shows how immunological dysregulation may lead to abnormal inflammation, with viral proteins possibly inhibiting and inducing TLRs (DeDiego et al., 2014).

The SARS-CoV-2 N protein is shown to dampen type I IFN response by inhibiting STAT1 and STAT2 phosphorylation and nuclear translocation (Mu et al., 2020). Similarly, the M protein is shown to additionally inhibit IFN responses by physically interacting with RIG-I/MDA-5 (Yi Zheng et al., 2020). Furthermore, IFN responses were reported to be inhibited by the ORF-9b protein of SARS-CoV-2 (C.-S. Shi et al., 2014). which directly binds to TOM-70 (a RIG-I/MAVS signalling complex adaptor). This

suppression could experimentally be restored by increased expression of TOM-70 (H. wei Jiang et al., 2020).

HCoVs often target the cytoplasmic DNA sensing cGAS-STING system. When a cell is infected, monomeric cGAS attached to the cell membrane synthesizes cGAMP using GMP and AMP (G. Ni et al., 2018). STING is then bound by cGAMP, causing it to translocate from the ER to the Golgi apparatus. STING, TBK1, and IRF3 form a complex during translocation, in which TBK1 phosphorylates IRF3, causing activation of the type-I IFN response. STING was shown to be activated by RNA virus infection and its deficiency was shown to promote RNA virus replication (Holm et al., 2016). Sun et al. demonstrated the importance of cGAS-STING signalling in SARS-CoV infection by reducing STING dimerization in infected cells (L. Sun et al., 2012). STING-mediated IRF3 activation is inhibited when either virus's membrane-anchored PLP domain is expressed. Even though SARS-CoV-2 PLpro shares 83% of its sequence with SARS-CoV PLP, it selectively binds the ubiquitin-like IFN-stimulated gene 15 protein (ISG15) with high affinity, causing the IFN response to be abrogated (Shin et al., 2020). As a result, a SARS-CoV-2 PLPro inhibitor (e.g., GRL-0617) has been suggested as a treatment method that inhibits viral multiplication, cytopathic impact, and IFN signalling.

Understanding the innate immune response to SARS-CoV-2 might aid in developing therapeutics that could prevent viral infection by boosting the innate immune system. More research into the innate processes addressed in this section is needed since they may help define variations in the acute response to the virus, which varies greatly from patient to patient.

### 1.2.2 Adaptive Immune Responses

Antigen presenting cells (APCs) which are mainyly Dendritic Cells (DCs) and macrophages link the innate and adaptive immune systems (Rossi & Young, 2005). Antigen presentation, DC maturation, or the following T-cell response may be altered by coronaviruses in order to avoid being eliminated by the immune system (Freer & Matteucci, 2009). *In vitro* infection of DCs and macrophages with SARS-CoV and SARS-CoV-2 results in an increase of proinflammatory cytokines (TNF-α, MCP-1, IL-6, MIP-1, IL-8,), and a reduction in IFN response (Law et al., 2005). It has also been

reported in post-mortem analysis of COVID-19 patients that SARS-CoV-2 infects CD169+, ACE2+ tissue-resident macrophages to stimulate IL-6 production (Z. Feng et al., 2020). Importantly, IL-6, like TNF-α, has been linked to severe COVID-19 illness and higher mortality risk (Del Valle et al., 2020). In the absence of adequate antiviral immunity, the increased cytokine response promotes inflammatory disease development. Activated macrophages, especially alveolar macrophages, are thought to be responsible for this cytokine storm, leading to lung injury (Otsuka & Seino, 2020).

T cells and alveolar macrophages, but not neutrophils are found abundantly in the alveolar space as observed by the analysis bronchoalveolar lavage fluid isolated from severe COVID-19 patients (Grant et al., 2020). Despite the absence of ACE-2, SARS-CoV-2 transcripts were found in alveolar macrophages, suggesting that the virus may infect these cells and cause chemokine production and T-cell recruitment. Activated T-cells release IFN, which activates alveolar macrophages, resulting in an inflammatory positive feedback loop. It has also been observed that around 10% of severe COVID-19 cases produced neutralizing autoantibodies against especially for IFN-α, IFN-ω, and other type 1 IFNs (Bastard et al., 2020). These autoantibodies, that were not found in mild or asymptomatic cases are thught to limit IFNs' capacity to stop SARS-CoV-2 replication.

Neutralizing antibodies (nAbs) against SARS-CoV-2 were found in the plasma of COVID-19 patients 10–15 days after the beginning of symptoms and these did not seem to cross-react with SARS-CoV (F. Wu, Wang, et al., 2020). Convalescent sera were effectively used to treat select severe instances of SARS-CoV and SARS-CoV-2, demonstrating the protective nature of these nAbs in limiting viral entry (Kai Duan et al., 2020a).

Antibodies against RBD and N protein were found in follow-up patients and further observations lead to the conclusion that the sera's neutralizing potential was associated with anti-RBD IgG levels rather than with anti-N IgG levels. nAb titers were shown to positively correlate with C-reactive protein levels and an inverse correlation with lymphocyte numbers was observed (Wuertz et al., 2019).

CD4 and CD8 T-cell responses are also critical for antiviral immune protection (Hoepel et al., 2020). CD4 T cells could develop into TH1 cells after activation, which assists to activate cytotoxic CD8 T cells (Swain et al., 2012). However, in many viral infections, the TH2 response, which is marked by a distinct cytokine profile (dominant with IL-4),

produces immunopathology. To cause apoptosis in virally infected cells, activated CD8 T lymphocytes produce cytotoxic granules, including perforin, granzymes, and granulysin. In severe cases of SARS-CoV, CD4 and CD8 T cells that produce IFN-γ and TNF-α were shown to be considerably higher than in mild-moderate cases (C. K. Li et al., 2008).

Pathogenic TH1 cells that secrete GM-CSF and CD14+CD16+ inflammatory monocytes with IL-6 secretion may enter the lungs of COVID-19 patients, resulting in serious pulmonary harm. (Yonggang Zhou et al., 2020). This shows that anti-GM-CSF or anti-IL-6 antibodies might help reduce inflammation and cytokine storms. N, RBD, and major protease specific T-cell responses arise in recovering SARS-CoV-2 patients, which seem to decrease in nearly all follow-up patients (L. Ni et al., 2020).

The numbers of N-specific T-cells were shown to be highly associated with the levels of NAbs, indicating that effective humoral and cellular responses may be necessary for viral clearance (Franz et al., 2018). SARS-CoV-2-specific CD4 T cells were detected in 83% of SARS-CoV-2 patients and 34% of healthy donors who were seronegative (Braun et al., 2020). In fatal instances of COVID-19, pathologic immune cell infiltration was discovered. CD16 and CD107A NK cells ,CD4 T-cells, CD11b and CD16 neutrophils and CD68 macrophages are seen in post-mortem lung autopsy images (Yulin Zhang et al., 2020).

Hyperinflammation-related neutrophils and neutrophil extracellular traps (NETs) (Borges et al., 2020) have previously been identified as essential components in tissue damage caused by inflammatory disorders and as a means of trapping invading microorganisms. The neutrophil-to-lymphocyte ratio in COVID-19 patients showed an increased inflammatory response, leading to ARDS (Qin et al., 2020). The large quantities of NETs seen in plasma from patients with severe COVID-19 (Veras et al., 2020). Treatments that target neutrophil NET production might minimize the collateral damage caused by neutrophil-driven hyper inflammation considerably. This method might help to reduce the severity of the illness and avoid the need for artificial ventilation. Inhibitors of the precursor molecules required for NET synthesis, such as gasdermin D (J. J. Hu et al., 2020) and PAD4 (Yost et al., 2016), are examples of medicines that target NET creation.

The connection between S protein and CD4 has recently been hypothesized as a mechanism by which SARS-CoV-2 may infect TH cells (Davanzo et al., 2020). Infected TH cells with SARS-CoV-2 release more IL-10 and less pro-inflammatory cytokines, including IFN-γ and IL-17. This observation is more prominent in severe cases of COVID-19 in comparison to moderate cases. *Ex vivo* stimulation of peripheral blood mononuclear cells (PBMCs) taken from convalescent individuals with SARS-CoV-2 peptides resulted in virus-specific CD8 T-cell proliferation that were shown to target the spike protein (269-277) and Orf1ab3183–3191 (Habel et al., 2020) in an HLA-restricted manner.

## 1.3 Diagnosis and Potential Therapeutics

### 1.3.1 Diagnosis

Molecular techniques, serology, and viral culture are the most common diagnostic tools in COVID-19. A complete blood count, coagulation testing, and serum biochemistry tests such as creatine kinase (CK), lactate dehydrogenase, procalcitonin, and electrolyte testing are routinely performed on hospitalized patients (G. Li et al., 2020). According to laboratory testing, most patients' total number of lymphocytes decreases significantly. Virus particles travel across the respiratory system and infect nearby uninfected cells during a COVID infection. As a result, a cytokine storm develops, triggering a cascade of severe immunological reactions. This process causes alterations in immune cells, especially lymphocytes, and eventually leads to immune system dysfunction (G. Li et al., 2020). As a result, a reduction in the number of circulating lymphocytes might be used to diagnose SARS-CoV-2 infection and its severity (N. Chen et al., 2020). Previous studies have associated increased levels of pro-inflammatory cytokines such IL1B, IL6, IL12, IFN, IP10, and MCP1, as well as cytokines like IFNγ, TNFα, IL15, and IL17, to pulmonary inflammation and lung damage in SARS-CoV and MERS-CoV infections, respectively. The high levels of cytokines such as IL1B, IFNγ, IP10, and MCP1 may, for example, stimulate T helper1 cells (Th1) response. On the other hand, SARS-CoV infection increased T helper 2 (Th2) production, and cytokines like IL4 and IL10 reduced peripheral white blood cells and immune cells like lymphocytes. It is likely to inhibit the inflammatory reaction and immune system function, followed by significant respiratory failure (Moxley et al., 2002). These findings indicate that a severe and unregulated inflammatory response is more destructive to COVID-19-induced lung damage than viral pathogenicity. Thus, in SARS-CoV-2 pneumonia, it is crucial to monitor cytokines and

chemokines to identify the effect of the SARS-CoV-2 at the disease's critical phase (Li et al., 2020; (Moxley et al., 2002).

The following steps in confirming COVID-19 infection include RT-PCR (reverse transcription-polymerase chain reaction), as well as genome sequencing from respiratory or blood specimens. The gold standard for detecting SARS-CoV-2 nucleic acid is to use RT-PCR. Many commercially available viral nucleic acid detection assays target ORF1b (including RdRp), N, E, or S genes (Bordi et al., 2020; Chan, CC et al., 2020). Although SARS-CoV-2 RNA has been found in throat swabs, posterior oropharyngeal saliva, nasopharyngeal swabs, sputum, and bronchial fluid, the virus load is more significant in lower respiratory tract samples (Pan et al., 2020; Wang et al., 2020). Even when respiratory samples were negative, viral nucleic acid was detected in samples from the gastrointestinal tract or blood (W. Zhang et al., 2020). Finally, the viral load may have already decreased since the start of the disease (Zou et al., 2020). As a result, when oral swabs are used, false negatives are possible, and several detection techniques should be employed to verify a COVID-19 diagnosis (Xuelei Xie, Z, W, et al., 2020). Therefore, other detecting methods were utilized to solve the problem. When the capacity of molecular detection in Wuhan was saturated, chest CT was applied to identify a patient rapidly. On initial CT, COVID-19 patients had typical symptoms, such as bilateral multilobar ground-glass opacities with a peripheral or posterior distribution (Kanne, 2020). For people with a strong clinical suspicion of COVID-19 but who test negative in first nucleic acid screening, it has been proposed that CT scanning along with repeated swab testing be performed (Xuelei Xie, Z, W, et al., 2020). Finally, serological assays for SARS-CoV-2 that identify antibodies to the N or S protein might be used to support molecular diagnosis, especially in the late stages of the disease or for retrospective investigations (To et al., 2020). However, the intensity and duration of immune responses remain unclear, and current serological tests range in their sensitivity and specificity, all of which must be considered when selecting and interpreting serological assays, as well as when testing for T cell responses.

Feng Zhang and his colleagues at the Broad Institute of MIT and Harvard have created the SHERLOCK system, which uses CRISPR-Cas13 to diagnose COVID-19. The This system is based on the CRISPR-Cas13 system, consisting of two RNA guides coupled with a Cas13 protein to produce a SHERLOCK system that detects the presence of COVID-19 viral RNA. Initially, the scientists employed synthetic segments of SARS-

CoV-2 RNA as a template for creating two RNA guides that can bind to COVID-19 RNA's complementary sequences. They used a paper strip (similar to a pregnancy test) to dipping into a prepared sample to get a visual readout. The presence of the virus in the sample is then indicated by the formation of a line on the paper strip (Kellner et al., 2019; Joung et al., 2020).

### 1.3.2 Therapeutics

For the treatment and prevention of COVID-19, there are no particular anti-viral therapeutic drugs yet. The COVID-19 pandemic is being managed with supportive therapy, which simply targets the symptoms. Oxygenation, ventilation, and hydration control are examples of supportive care. Because there is no evidence to support the effectiveness of current anti-viral medicines as a stand-alone treatment for SARS-CoV-2, a combination of low-dose systemic corticosteroids, anti-virals, and supportive respiratory care is being used (Shanmugaraj et al., 2020; Cunningham et al., 2020). As of October 14, 2021, around 506 COVID-19 medicinal medicines were in development, with almost 419 human clinical trials (COVID-19 vaccine and therapeutics tracker https://biorender.com/covid-vaccine-tracker/). Due to their quick availability in the clinic, repurposing licensed or under investigation antiviral medicines for other viral illnesses has been a common approach. The FDA recently authorized veklury (remdesivir) for the treatment of COVID-19, followed by the EUA of monoclonal antibodies bamlanivimab and casirimab/imdev (Table 1.3). Based on published clinical data and experience, possible treatments against SARS-CoV-2 are described in the sections below.

#### 1.3.2.1 Inhibition of virus entry

SARS-CoV-2 binds to ACE2 and utilizes human proteases as entrance activators, which enables it to bind to the viral membrane and invade cells. As a result, medicines that block entrance might be a possible therapy for COVID-19. Umifenovir (Arbidol) is authorized to treat influenza and other respiratory viral infections in Russia and China. It can inhibit membrane fusion by targeting the connection between the S protein and ACE2 (Figure 1.9). It exhibits activity against SARS-CoV-2 *in vitro*, and current clinical evidence suggests it may be more effective than lopinavir and ritonavir in treating COVID-19 (Z. Zhu et al., 2020). However, other clinical trials indicated that umifenovir might not

enhance the prognosis or increase the clearance of SARS-CoV-2 in individuals with mild to moderate COVID-19 (Lian et al., 2020). Nonetheless, several ongoing clinical trials are investigating its effectiveness in the treatment of COVID-19.

In Japan, camostat mesylate is allowed to treat pancreatitis and postoperative reflux oesophagitis. Previously published research demonstrated that it could inhibit SARS-CoV entry into cells by inhibiting TMPRSS2 activity and protect animals from fatal infection with SARS-CoV in a pathogenic mouse model (Y Zhou et al., 2015). As a result, it might be a possible anti-viral drug for SARS-CoV-2 infection; however, there is currently sufficient clinical evidence to confirm its effectiveness.

| **Category** | Drugs | Mechanism | Status of clinical use |
|---|---|---|---|
| **Anti-viral** | Remdesivir | Vviral replication is inhibited | Approved by the FDA |
| | Favipiravir | Viral-RNA dependent RNA polymerase is inhibited | Under clinical trials |
| | Lopinavir-Ritonavir | Protease enzymes are inhibited | Under clinical trials |
| | Umifenovir | Viral and cellular membrane fusion is inhibited | Under clinical trials |
| | Camostat (TMPRSS2 inhibitor) | Viral maturation and entrance into host cells are prevented. | Under clinical trials |
| | Hydroxychloroquine | ACE2 glycosylation is inhibited, endosomal pH is raised, and viral entry is prevented. | Emergency use terminated by the FDA |
| **Anti-inflammatory** | Azithromycin | Indirect immunomodulatory effects | Under clinical trials |
| | Tocilizumab | Blockade of IL-6 receptors and its downstream signalling pathways | Under clinical trials |
| | Anakinra | IL-1 receptor blockade and inhibition of downstream signaling pathways | Under clinical trials |
| | Ruxolitinib | JAK signalling inhibition, Immune suppression | Under clinical trials |
| | Baricitinib | Inhibition of viral invasion and JAK signalling, Immune suppression | Under clinical trials |
| | Thalidomide | Cytokine storm and inflammatory cell infiltration are reduced | Under clinical trials |
| | Glucocorticoids | Immunity and inflammation are suppressed. | Dexamethasone authorized use in critically ill patients |
| **Monoclonal antibody** | Bamlanivimab | Inhibition the virus entering into the host cells | Emergency Use Authorization |
| | Casirivimab and Imdevimab | Inhibition the virus entering into the host cells | Emergency Use Authorization |
| **Plasma therapy** | Convalescent plasma | Elimination of viruses by antibodies are for virus | Under clinical trials |
| **Cell-based therapy** | Mesenchymal stem cell | Regeneration and immunosuppression of tissue is promoted. | Under clinical trials |
| | NK cell | Strengthen immune response | Under clinical trials |

**Table 1.3.** Treatments against SARS-CoV-2

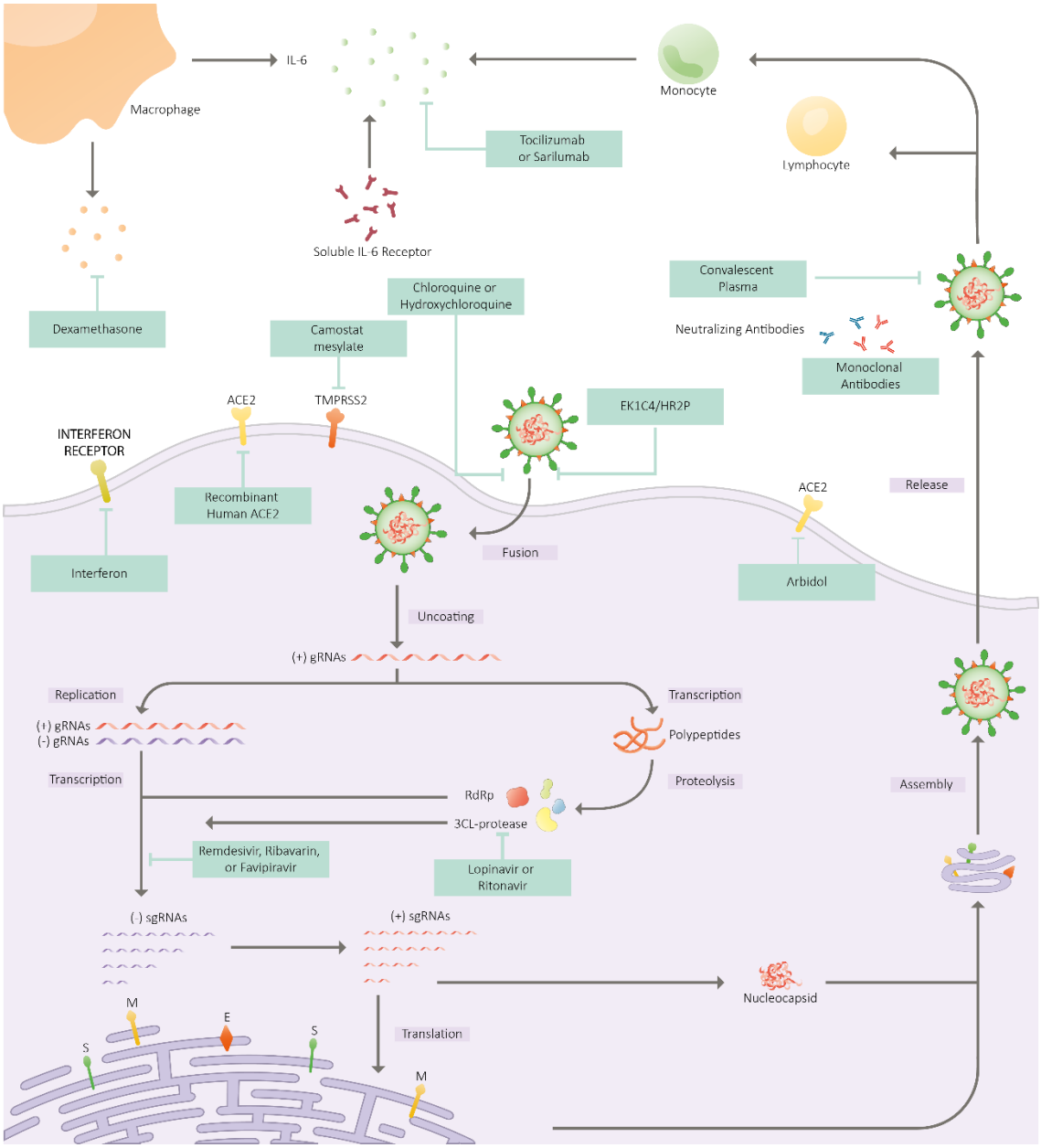


**Figure 1.9. Replication of SARS-CoV-2 and possible therapeutic targets.** Antiviral agents may target many stages of SARS-CoV-2 including receptor binding, entry and fusion, as well as replication. Additionally, immunoglobulin-based and immunomodulatory drugs are possible treatments. (Figure adapted from (B. Hu et al., 2020).

Other possible, although questionable drugs that block SARS-CoV-2 entrance include chloroquine and hydroxychloroquine. They have been used to prevent and treat malaria and autoimmune disorders such as rheumatoid arthritis and systemic lupus erythematosus. They can prevent cellular receptors from being glycosylated, interfere with virus-host receptor interaction, elevate endosomal pH, and prevent membrane

fusion. There is currently no scientific evidence on their efficacy in the treatment of COVID-19. *In vitro* analyses have shown that they can suppress SARS-CoV-2 infection, but clinical evidence is very limited (M. Wang et al., 2020). Two clinical trials showed no difference in mortality rates between patients who received chloroquine or hydroxychloroquine and those who did not and even indicated that it might increase the risk of death since the treated patients had a greater risk of cardiac arrest (Ranard et al., 2020). The US Food and Drug Administration (FDA) removed the emergency use permission for chloroquine and hydroxychloroquine to treat COVID-19 on June 15, 2020, due to adverse effects seen in clinical trials.

Another potential treatment approach is to block the S protein's binding to ACE2 by using soluble proteinst such as recombinant hACE2 or S protein-specific antibodies as well as fusion inhibitors targetin the S protein (Monteil et al., 2020) (Figure 1.10). The FDA has approved REGEN-COV™ (casirivimab and imdevimab) with emergency use authorization for the treatment of mild to moderate COVID-19 in adults and children above 12 years of age who test positive for SARS-CoV-2 and considered as high risk for progression to severe COVID-19 (The U.S. Food and Drug Administration, 2021).

#### 1.3.2.2 Inhibition of virus replication

Remdesivir (GS-5734), favipiravir (T-705), ribavirin, lopinavir, and ritonavir are all replication inhibitors. RdRp is inhibited by remdesivir, favipiravin, and ribavirin, whereas 3CLpro is inhibited by Lopinavir and Ritonavir (Tahir Ul Qamar et al., 2020) (Figure 1.10). It has been reported that remdesivir can shorten recovery time in hospitalized COVID-19 patients by a few days compared to placebo. However, on further analysis the difference in mortality rate was not statistically significant (Beigel et al., 2020). The FDA has approved remdesivir for emergency use authorization (EUA) in hospitalized patients. It is also the first European Union-approved therapy option for adults and adolescents with pneumonia who require supplementary oxygen. Several global phase III clinical studies (NCT04292730, NCT04280705) are still ongoing to evaluate remdesivir's safety and effectiveness in the treatment of COVID-19.

Favipiravir (T-705) has been licensed to treat COVID-19 in China, Russia, and India. It was reported to dramatically decrease the symptoms, improve sickness signs on chest imaging and shortened the time to viral clearance (Cai et al., 2020). A preliminary report

in Japan also reported clinical improvement of symptoms with favipiravir us in patients with mild and severe COVID-19. Other clinical trials in various stages are still ongoing.

Paxlovid™, Pfizer's investigational oral antiviral candidate, displayed an 89 percent reduction in COVID-19 risks in Phase II/III study (NCT04960202). It is designed to block the activity of the SARS-CoV-2-3CL protease and inhibits viral replication at a stage known as proteolysis.

#### 1.3.2.3 Immunomodulatory agents

SARS-CoV-2 causes a robust immunological response leading to cytokine storm syndrome (Mehta et al., 2020). As a result, immunomodulatory drugs that suppress an excessive inflammatory response might be a promising COVID-19 supplementary treatment. Dexamethasone is an anti-inflammatory and immunosuppressive corticosteroid that is commonly used to treat inflammation. According to the RECOVERY study, dexamethasone decreased mortality by roughly one third in hospitalized COVID-19 patients who had invasive mechanical ventilation and by one fifth in patients who received oxygen. On the other hand, patients who did not get respiratory assistance displayed no advantage (RECOVERY, 2020).

One of the essential innate immune defences against viral invasion is the interferon response. Interferons cause the production of various interferon-stimulated genes, which can disrupt viral replication at any stage. In previous investigations, type I interferons have been found as a potential treatment option for SARS (Stockman et al., 2006). SARS-CoV-2 is considerably more susceptible to type I interferons in vitro than SARS-CoV, indicating that type I interferons might be helpful in the early treatment of COVID-19 (Mantlo et al., 2020). The COVID-19 treatment guideline in China includes vapour inhalation of interferon (Sallard et al., 2020). Clinical efforts are underway worldwide to assess the efficacy of various interferon treatments, either alone or in combination with other medicines (A. Park & A, 2020).

#### 1.3.2.4 Immunoglobulin therapy

Another possible COVID-19 supplementary therapy is convalescent plasma treatment. Preliminary data show that the therapy improved clinical status (K Duan et al., 2020).

Under an emergency investigational new drug application, the FDA has provided guidelines for using COVID-19 convalescent plasma. This therapy, however, may have side effects such as antibody-mediated infection enhancement, transfusion-associated acute lung damage, and allergic transfusion responses.

In specific individuals, monoclonal antibody therapy is successful immunotherapy for the treatment of viral infections. In vitro and in vivo investigations have shown that particular monoclonal antibodies can neutralize SARS-CoV-2 infection (Chunyan Wang et al., 2020). Monoclonal antibodies can be produced in higher quantities to fulfil clinical requirements than convalescent plasma, which has limited availability. However, the expensive cost and limited production capacity, as well as the issue of escape variants, may limit this therapy's widespread use.

### 1.3.3 COVID-19 Prevention: Vaccine Development

Previous research on SARS-CoV and MERS-CoV supported the identification of potential antigens for activating neutralizing antibodies against SARS-CoV-2 (Zost et al., 2020). SARS and MERS vaccines, including the S1, RBD, and S2 subunits of the Spike protein, produced significant neutralizing antibody titers (Dai et al., 2020). Adjuvants, industrial processes, and delivery mechanisms must be chosen once the desired antigen is found for effective and safe immunization. Besides the rapid availability of SARS-CoV-2's genomic and structural information (R. Lu et al., 2020), advanced novel vaccination platform technologies have also helped with vaccine development and clinical translation (Lurie et al., 2020). SARS-CoV-2 proteins and subunits, live-attenuated and inactivated viruses, nucleic acids encoding a viral antigen, replicating and non-replicating viral vectors, virus-like particles are all being developed as COVID-19 vaccines (Table 1.4). The immunological parameters of the COVID-19 vaccine formulations and delivery platforms are reviewed elsewhere (Chung et al., 2021).

| Vaccine form | Antigen | Production | Advantages | Disadvantages |
|---|---|---|---|---|
| **Inactivated Virus** | Whole virion | Heat, chemicals, or radiation all work to render virus particles inactive. | Antibodies with high neutralizing titers that are safe and simple to make | Hypersensitivity may be a possible reason. |
| **Live-attenuated virus** | Whole virion | It was able to live since the virulence had been reduced. | There are fewer side effects, and the immune system is activated at a high level. | Reversion, whether phenotypic or genotypic, is not appropriate for all age groups (safety testing) |
| **RNA** | S Protein | RNA that has been genetically modified to produce an antigen. | Simple to construct, with a greater degree of adaptability, and capable of inducing a powerful immune response | High instability, as well as safety concerns |
| **DNA** | S Protein | DNA that has been genetically modified to produce an antigen. | High-titer neutralizing antibodies that are easy to develop and produce are safe and effective. | There is a need for a certain delivery tool, Reduced immune responses and toxicity from repeated usage |
| **Recombinant Protein** | S Protein | Whole or subunit antigenic components are produced | High safety, constant production, and the ability to elicit a cellular and humoral immunological response | High cost, decreased immunogenicity, and the need for repeated doses and adjuvants |
| **Viral vector-based vaccine** | S Protein | The target gene has been genetically modified. | Induces high levels of cellular and humoral immune responses and it is safe | Presenting various immunological responses as an option |

**Table 1.4.** Development of different types of COVID-19 vaccines

### 1.3.3.1 Nucleic Acid Vaccines

Numerous clinical experiments have employed nucleic acids for vaccinations against various illnesses, including infectious diseases and cancers, since the discovery of the potential to trigger an immune response following injection. (Lopes et al., 2019). Vaccines based on nucleic acids are promising because they are easy to make, safe, and highly immunogenic. (Hasson et al., 2015).

DNA vaccines, which are generally plasmid vectors encoding a target antigen, are easily made in massive quantities. Unlike typical protein/peptide or entire virus vaccinations, cold storage isn't necessary for DNA since it's quite stable. (Kutzler & Weiner, 2008). DNA has a longer half-life than mRNA but it require to reach the nucleus of a cell for transcription, which brings out many questions about delivery (M. Liu, 2019). T-cell activation is triggered by the transgene expression, which causes APCs to display antigenic peptides on their MHC I and II. Naked plasmid DNA vaccines do not generate

a sufficient immunological response, needing several injections or the inclusion of an adjuvant to boost the adaptive immune response (Hobernik & Bros, 2018).

The COVID-19 pandemic has witnessed a paradigm shift in terms of nucleic acid vaccines where many have looked at the immunization with mRNA expressing the S antigen as opposed to prior studies that used DNA (Jackson et al., 2020). mRNA does not enter the nucleus of a cell and it is enough for it to be be delivered to the host cell's cytoplasm for translation into antigenic proteins. Immune responses may be stimulated in a safe, efficient, and low-cost manner by using mRNA vaccines instead of traditional protein or entire virus vaccinations (Pardi et al., 2018). Instability and ineffective *in vivo* delivery, on the other hand, are limitations that had to be overcome, and numerous modifications and delivery strategies have been used to enhance *in vivo* half-life and antigen translation (Karikó et al., 2008; Kauffman et al., 2016).

The *in vivo* delivery of DNA and mRNA molecules into APCs has been a major challenge. The ability of nucleic acid vaccines to boost immunogenicity has risen as nucleic acid delivery technology has improved (Suschak et al., 2017). Physical approaches (Wells et al., 2000), cationic peptide delivery (Chunxi Zeng et al., 2020), lipid, and polymer-based delivery (Espeseth et al., 2020) have all been used to penetrate the lipid membrane successfully.

An ionizable cationic lipid, cholesterol, polyethylene glycol (PEG) and naturally occurring phospholipids (LNPs) have become one of the most used instruments for the transport of mRNAs. The preliminary results of phase III clinical investigations of mRNA vaccines indicated the effectiveness of 95 per cent (Polack et al., 2020) and 94.5 per cent in preventing COVID-19. Pfizer/BioNTech's BNT162b2 was approved for emergency use in the United Kingdom on Dec 2, 2020, and in the United States on Dec 11, 2020, and is now being widely administered all around the world. Additional mRNA vaccination platforms have been created and validated for immunogenicity and effectiveness extraordinary (Petsch et al., 2012). Furthermore, for mRNA-1273 (Moderna), messenger RNA (mRNA)-based vaccinations for the prevention of symptomatic COVID19 are 94% effective. Comparative efficacy of the BNT162b2 and mRNA-1273 vaccines was examined by Dickerman et al. They found that recipients of the mRNA-1273 vaccination had a higher SARS-CoV-2-binding antibody response than recipients of the BNT162b2 vaccine. The mRNA content of the vaccines (100μg for

mRNA-1273 vs. 30μg for BNT162b2), the interval between priming and boosting doses (4 weeks for mRNA-1273 vs. 3 weeks for BNT162b2), or other factors, such as the lipid composition of the nanoparticles used to package the mRNA content, could explain the difference in effectiveness between the two vaccines (Dickerman et al., 2021). Despite the challenges of cold chain distribution, the COVID-19 mRNA vaccines have the potential to assist reduce the global health crisis and give hope for the future of mRNA in the prevention of infectious illnesses.

#### 1.3.3.2 Protein Subunit Vaccines

Studies on the antigenicity of the S protein and its structure revealed that the S2 subunit domain induced neutralizing antibodies against both SARS-CoV and SARS-CoV-2. Additionally, earlier investigations utilizing the full-length S proteins on SARS-CoV and MERS-CoV patients was shown to induce the production of non-neutralizing antibodies that contributed to antibody-dependent enhancement of disease (ADE) and elevated systemic inflammation (Qidi Wang et al., 2020). There have been efforts to develop alternative protein vaccines that prevent the production of non-neutralizing antibodies by using S1, RBD and S2 domains. (L. Liu et al., 2020). However, the immunogenicity of protein subunits is restricted, and immune response must be triggered with the help of adjuvants.

Epitopes of the other structural proteins of SARS-CoV-2 have also been thoroughly examined as vaccine candidates (Ahmed et al., 2020). Especially, the N protein which is highly immunogenic and abundantly produced, has been regarded as a potential vaccine target (Dutta et al., 2020). It has been observed that T cell responses against the structural subunit proteins is dominant and long-lasting, and subunit vaccines are now being tested in clinical trials (Grifoni et al., 2020).

#### 1.3.3.3 Live-attenuated and whole inactivated viruses

Since the best immunogenic vaccine formulations employ the complete virus, which has been chemically or physically altered to make it less potent, traditional vaccinations against viral infections has produced many clinically beneficial vaccines (Plotkin, 2014). Coronaviruses have non-structural proteins that are not essential for replication and can

be modified in vivo, resulting in attenuation. Deletion of E proteins, for example, has been applied to attenuate several zoonotic coronaviruses (Y. Hou et al., 2018). Preclinical trials are underway for several live-attenuated viral vaccines and COVI-VAC from Codagenix is a Live Attenuated Vaccine Against COVID-19 in phaseI (NCT04619628 ).

Polio, hepatitis A, and influenza have all been effectively treated using inactivated viruses (Nunnally et al., 2015). Inactivated virus vaccines can be produced by propagating viruses in cell culture and then inactivating them with formaldehyde or beta-propiolactone depurination (Qiang et al., 2020). They are considered to be safer than live-attenuated viruses since their RNA has been destroyed, while they still contain intact viral epitopes which can activate immune responses (Watanabe et al., 2020). The immunogenicity of inactivated viruses is reduced by their inability to replicate, and long-term immunization needs several injections with adjuvants (Lauring et al., 2010).

Sinovac COVID-19 vaccine, CoronaVac, is an inactivated viral COVID-19 vaccine produced by Sinovac Biotech. It was tested in Phase III clinical trials in Brazil, Chile, Indonesia, the Philippines, and Turkey and uses classic technology, like other inactivated COVID-19 vaccines like Sinopharm BIBP and Covaxin. Turkey's Phase III findings revealed 83.5% effectiveness. based on 10,218 study participants. The findings from Brazil's phase III study were published in Lancet and revealed 50.7 percent symptomatic infection prevention and 83.7 percent mild case prevention (Palacios et al., 2021; Tanriover et al., 2021). The WHO validated the Sinovac-CoronaVac COVID-19 vaccine for emergency use on 1 June 2021.

#### 1.3.3.4 Recombinant viral vectors

Recombinant viral vectors are very adaptable vaccination platforms used to express antigens of target diseases (Ura et al., 2014). Viral vectors are used to deliver the genes for the target antigen(s), and the possibility to deliver a reasonably large genome suggests that a wide range of vaccines may be developed using this approach (Waehler et al., 2007). The use of recombinant viral vectors for delivery provides robust antigens that mimic natural infection and stimulate significant T cell responses without the need for an adjuvant (Humphreys & Sebastian, 2018). Recombinant viral vectors are also attractive for vaccine administration due to their efficient production (Choi & Chang, 2013). Adenovirus type 5 (Ad5) is typically used to make non-replicating viral vectors, and most

of these vaccines express the S protein or the RBD component of SARS-CoV-2 (F. C. Zhu et al., 2020).

Previous phase II clinical studies using the Ad5 platform to develop an Ebola vaccine demonstrated high initial nAbs but rapidly falling titers (Ledgerwood et al., 2010). Most participants had pre-existing immunity to Ad5, which reduced the vaccine's immunogenicity (L. Feng et al., 2018). Intramuscular delivery of the Ad5 vector encoding for the SARS-CoV-2 S protein, was assessed in Phase II clinical trials (F. C. Zhu, Li et al., 2020). Ad26 expressing S protein exhibited high neutralizing antibody titers despite having less pre-existing immunity than Ad5 (Mercado et al., 2020). This vaccine method has been proven efficacious in non-human primates and humans for HIV and Ebola immunization, respectively (Barouch et al., 2018).

ChAd expressing S protein has been one of the front runners during the race of COVID-19 vaccine development. Individuals in the general population have a low level of pre-existing immunity to the ChAd viral backbone (Barouch et al., 2018), and prior research on MERS (Folegatti et al., 2020) and the tuberculosis (Wilkie et al., 2020) verified the development of high-titer neutralizing antibodies.

The full-length codon-optimized S in the the Astra Zeneca – Oxford University AZD1222 vaccine candidate contains a tissue plasminogen activator leader sequence cloned in the replication-deficient simian adenovirus vector ChAdOx1. In the United States, phase III investigations are ongoing with subjects getting two vaccines with AZD1222 or placebo (NCT04516746). The UK has approved AZD1222 for emergency supply for active immunization of people 18 years and older with a recommended interval of four to 12 weeks (Chakraborty et al., 2021).

Denis Logunov and colleagues published intermediate findings from a phase 3 study of the Sputnik V COVID-19 vaccine (Logunov et al., 2021). This vaccine employs a heterologous recombinant adenovirus method to produce SARS-CoV-2 S by using adenovirus 26 (Ad26) and adenovirus 5 (Ad5) (Barouch et al., 2011). The findings of the study demonstrate a robust protective impact across all age categories of participants.

#### 1.3.3.5 Virus-like particles

Recombinant overexpression of structural proteins in a cell line results in the production of virus-like particles (VLPs). Hepatitis B and human HPV vaccines have successfully employed this platform (J. Wang & Zhang, 2013). VLPs are safe, simple to scale up for production and highly stable (Donaldson et al., 2018). While VLPs are physically very reminiscent of viruses, they lack viral DNA or RNA inside and are thus not infectious. The S protein is present on the surface of the particles which enables particle fusion with through the ACE2 receptor along with priming via TMPRSS2. (F. Deng, 2018). SARS-CoV-2 VLPs generated by overexpression of targeted genes in mammalian cells retained the virus's structural and morphological characteristics, making VLPs an attractive vaccine candidate and a potent tool for investigation into the virus's pathogenesis (Fang et al., 2020). In phase I clinical studies, SARS-CoV-2 VLPs derived from genetically modified plants have shown effectiveness in the production of neutralizing antibodies (NCT04450004) (Prasad et al., 2020). Phase I clinical studies for VLPs derived from hepatitis B surface antigen and modified to carry the SARS-CoV-2 S protein are also underway. (ACTRN12620000817943). Other VLP vaccine candidates, incorporating not on the S protein but also M, N and E proteins are also being tested in Phase-II clinical trials (NCT04962893).

### 1.3.4 Convalescent Plasma Therapy in COVID-19

As early as 1880, scientists discovered that diphtheria immunity was dependent on antibodies in the blood of animals that had been inoculated with non-lethal levels of toxins that could be passed to animals with active diseases. (Shahani et al., 2012). Besides neutralizing antibodies, immune plasma was shown to have passive immunomodulatory capabilities, allowing the receiver to moderate the excessive inflammatory cascade generated by numerous pathogenic pathogens or sepsis (Garraud et al., 2016). To treat major infectious illnesses as well as autoimmune problems such as allergies and immunodeficiencies, isolation and amplification of immunoglobulins from healthy donors or recovered patients was developed in the early 1950s. (Sherer et al., 2005).

Many convalescent blood products have been produced to treat infectious diseases, including immunoglobulins and polyclonal or monoclonal antibodies (Marano et al., 2016). However, they are difficult and costly to make in an emergency, and they may not provide enough infection control. Yet, CP has been frequently employed as first-line therapy in many epidemics due to a lack of efficient drugs or vaccinations (Garraud et al., 2016).

From the Spanish influenza pandemic to the present SARS-Cov-2 pandemic, it has been demonstrated that the use of CP decreases case fatality rates considerably. Furthermore, in other coronaviruses, such as SARS-CoV, the administration of CP decreased the number of days spent in the hospital in severely sick patients (Wong & Yuen, 2008). In addition, the use of CP in SARS-CoV and avian influenza A (H5N1) has been shown to reduce viral load in the respiratory tract (Hung et al., 2011). CP has been shown to lower viral load and improve the clinical condition in individuals with COVID-19 (C. Shen et al., 2020). However, randomized controlled studies are needed to validate the effectiveness of this strategy in both hospitalized patients with mild/severe symptoms and those in the intensive care unit. Yet, it is still a taunting task to optimize the therapy by choosing high-activity CP and applying it at the right time.

#### 1.3.4.1 Plasma composition and acquisition

Convalescent donors must undertake a routine pre-donation examination to comply with current plasma donation standards (Tiberghien et al., 2020). Convalescent donors between 18 and 65 are now recognized as healthy donors with no infectious symptoms and a negative COVID-19 test after 14 days of recovery. Apheresis is the preferred method of obtaining plasma. This process uses repeated centrifugation of blood from a donor to extract plasma selectively. From a single apheresis donation, this procedure yields roughly 400-800 mL. This quantity of plasma might be stored in 200 or 250 mL units and frozen within 24 hours after collection for future transfusions (Rojas et al., 2020).

Because CP manufacturing must meet high-quality requirements, it must be free of infection (Dodd et al., 2020). A nucleic acid test for HIV and hepatitis viruses is required to ensure the recipients' safety (Niazi et al., 2015). To increase the safety of CP, several

procedures recommend inactivating microorganisms using riboflavin or psoralen and then exposing them to UV radiation (Bello-López et al., 2018)

A standard CP transfusion dosage does not exist. The administration of CP in single or double scheme doses varies between 200 and 500 mL in various trials for coronaviruses. The current recommendation is to give 3 mL/kg each dosage over two days (Bloch et al., 2020). This technique makes plasma units (250 mL each) easier to distribute and provides a standard delivery option in public health efforts.

The composition of CP varies, and it contains a broad range of blood-derived components. Plasma comprises a complex combination of inorganic ions, organic chemicals, water, and over 1000 proteins (Benjamin & McLaughlin, 2012) (Figure 1.10A). These variables may have an impact on the immunomodulatory effect of CP in COVID-19 patients.

#### 1.3.4.2 Anti-viral mechanism of CP

One of the most critical roles of neutralizing antibodies (nAbs) is virus elimination and protection against viral infections. These nAbs may be provided via CP-induced passive immunity that restrict the infection. The concentration of nAbs in plasma from recovered donors has been linked to the success of this therapy (Rajendran et al., 2020). NAbs bind to the RBD, S1-N-terminal domain, and S2 in SARS-CoV and MERS, blocking their entrance and reducing viral proliferation (L. Du et al., 2009). Antibody-dependent cellular cytotoxicity, complement activity and phagocytosis may all have a role in improving the efficacy of CP.

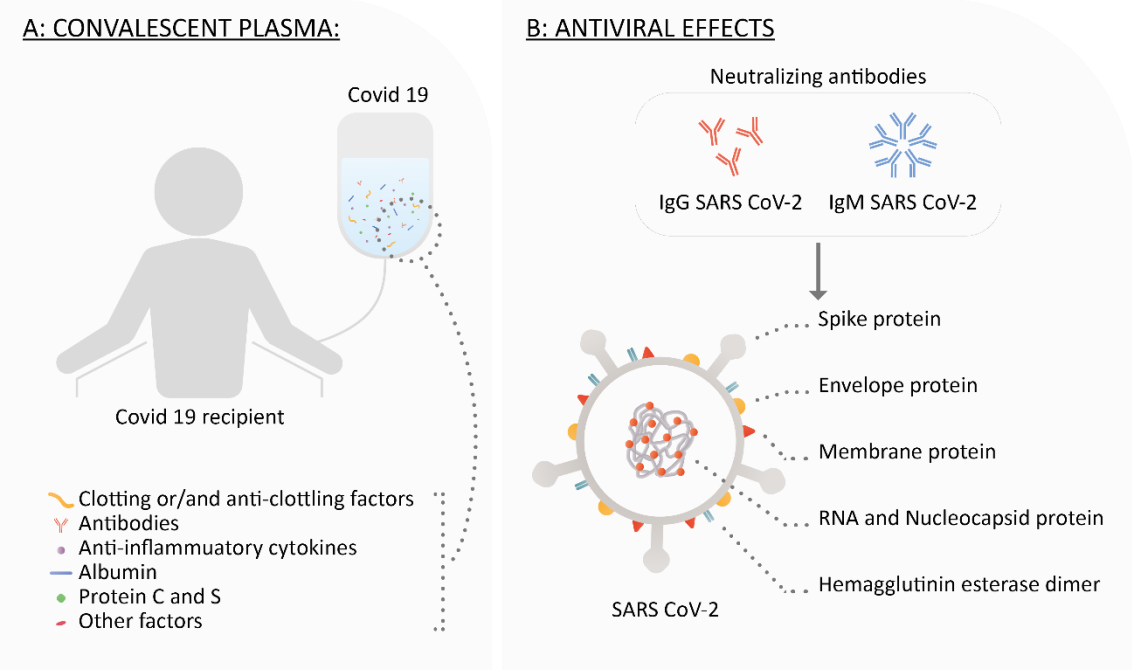


**Figure 1.10. A schematic illustration of the components of convalescent plasma and their modes of action.** A. Major components of convalescent plasma. B. The antiviral properties of NAbs. Although IgG and IgM are the predominant isotypes, IgA may also be significant, especially in mucosal viral infections.

Scientists developed a way to measure neutralizing antibodies in COVID-19 patients. This involved using pseudotyped-lentiviral-vector-based neutralization assay of plasma samples from recovered patients with SARS-CoV-2 infections. They found that 30% of the patients did not develop high neutralizing (F. Wu, Wang, et al., 2020).

Shen et al. discovered that donors who had recovered from COVID-19 infection had SARS-CoV-2–specific antibody levels ranging between 1.800 and 16.200, and that their levels of NAbs were between 80 and 480.(C. Shen et al., 2020). The viral load was reduced when plasma was collected from donors and transfused into recipients on the same day. The recipient's IgG and IgM titers elevated in a time-dependent way after receiving CP. Furthermore, the presence of NAbs in the recipients was critical in limiting viral infection. Another research looked at how SARS-CoV-2-specific NAbs developed over time as the disease progressed. NAb titers in SARS-CoV-2 infected individuals were low until day ten post-disease start, then rose, peaking 10 to 15 days after disease onset, and subsequently remained constant in all patients after that (F. Wu, Wang, et al., 2020).

### 1.3.4.3. Methods in Characterization of Convalescent Plasma Activity

The amount of SARS-CoV-2 neutralizing antibody responses varies greatly, and many convalescents have undetectable plasma nAb levels (Robbiani et al., 2020b). Studies on duration of immunity (natural or vaccinated) and selection of convalescent plasma donors (CP) are all impacted by exact nAb measurement (Focosi et al., 2020). In fact, individuals who recovered from infection had higher neutralizing potency sera than those who died from COVID-19, (Tighe et al., 2020), and CP treatment is more effective in patients receiving units with the highest nAb titres (Focosi et al., 2020).

These nAbs target the RBD, although some also target the S2 subunit or the S1/S2 proteolytic cleavage site (S. Jiang, Hillyer, et al., 2020). Steffen et al. found that a majority of the nAb in human target epitopes inside RBD (Steffen et al., 2020). These authors divided nAbs into three types. hNAbs with short CDRH3s that inhibit ACE2 with binding up RBDs, hNAbs that bind both up and down RBDs and may interact with neighbouring RBD, hNAbs that bind outside the ACE2 site and identify up and down RBDs (Barnes et al., 2020).

Convalescent patients should be examined for nAb levels, and only those with high nAb titres should be donated. Several regulatory agencies suggest threshold values for Covid19, but none include nAb assay details. The FDA recommends nAb titres of at least 1:160 when available. If no other matching unit is available, a titre of 1:80 may be appropriate (FDA, 2020). The ECDC recommends that immunocompromised patients get CP units with a titre of 1:320 or higher (ECDC, 2021). However, these criteria are meaningless without specifics, making study outcomes incomparable.

Historically, neutralizing antibody testing was performed manually, which was time-consuming and unsafe. Traditional techniques remain the gold standard for precise nAb measurement, even though high throughput platforms with quicker turnaround times and strong correlations with nAb are being studied. The COVID-19 pandemic has accelerated research on nAb testing advancements. The conventional nAb testing approach is examined by analyzing each major component (Focosi et al., 2021) (Figure1.11).

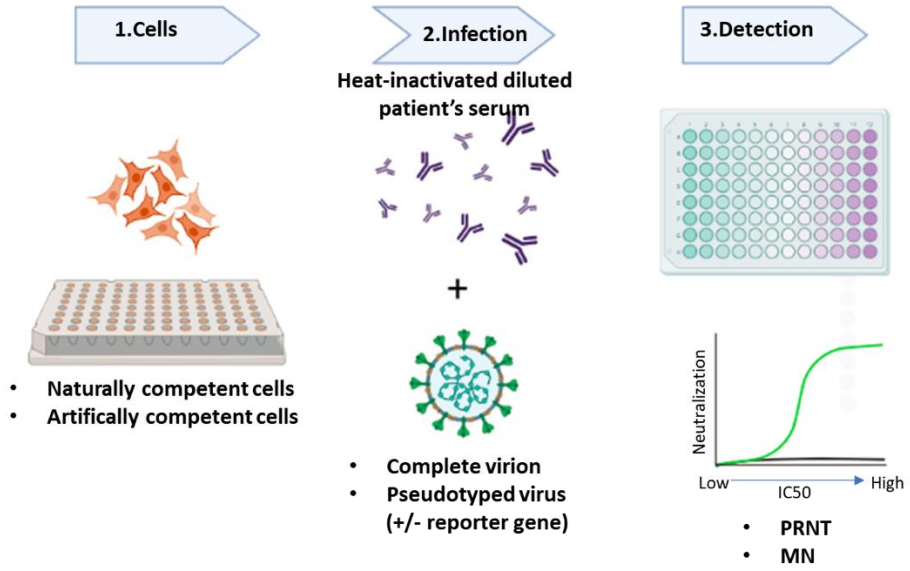


**Figure 1.11. The key components of a viral neutralization assay.**

### The competent cell line

The virus-serum combination is usually applied to a confluent monolayer of cells that express the receptor ACE2 and or the protease TMPRSS2. Many cell lines spontaneously express high amounts of ACE2 such as; Vero E6, HUVEC, HepG2 and HaCaT. Human ACE2 may also be transduced or plasmid transfected into mammalian cell lines (e.g., human lung epithelial cells A549 (Xuping Xie, Muruato, Zhang, et al., 2020), human embryo kidney [HEK] 293T (Tandon et al., 2020), or 293FT, or BHK21 (Xiong et al., 2020), or human connective tissue HT1080 (Schmidt et al., 2020) ). Moreover, it has been reported that the stable transfection? of TMPRSS2 increases infection susceptibility by 5–10 fold (Brochot et al., 2020; Johnson et al., 2020).

### Infection

#### *Intact virion*

The challenging dosage contains varying concentrations of viruses. Protein assays or plaque assays can be used to determine virus quantity which is generally reported as median tissue culture infectious dose [TCID50] or cell culture infectious dose [CCID50]. This number represents the amount of virus that is required to kill to produce a cytopathic effect [CPE] in 50% of inoculated cells in tissue culture. (Focosi et al., 2021).

Quantitative PCR, flow cytometry, transmission electron microscopy, ELISA are more recent techniques of viral quantification; but they do not offer information regarding virus vitality. As a result, it's simple to prove that TCID is often used to define the challenging dosage (Mendoza et al., 2020), and that the challenging value is typically 100 TCID50 of input virus per well, (Rowe et al., 1999), causing a problem for viruses that reproduce to low titer in cell culture.

***Pseudotyped virus***

Because pseudotyped viruses cannot create infectious offspring, they serve as a safe viral entrance model. As part of the pseudoparticle neutralization test a replication-defective virus (such as replication-defective HIV-1 or G protein-deficient VSV) is pseudotyped with the target antigen from the virus against which nAb should be measured. (Schmidt et al., 2020). BSL2 facilities can enable this activity. Codon optimization or deletion of the last C-terminal 19 to 26 amino acids of the cytoplasmic tail increased the production of S protein by nearly 10-fold in SARS-CoV-2.(C. P. Thompson et al., 2020). Previously, this approach was utilized to create pseudotyped viruses for SARS-CoV1 (Temperton et al., 2005) and MERS-CoV (Grehan et al., 2015). All of the increasing components together resulted in a titre of pseudotyped particles that was about $10^6$ infectious particles per ml.(Johnson et al., 2020).

***VSV pseudotypes***

The vesicular stomatitis virus (VSV) is assembled at the plasma membrane, and virions obtain an envelope that is composed of a lipid bilayer produced from the plasma membrane and trimers of the VSV-glycoprotein (VSV-G). Recently, VSVdG-luc carrying S chimaeras were employed to investigate SARS-CoV-2 and other lineage B betacoronavirus entrance and receptor utilization (Letko et al., 2020a). The approach relies on pseudotyped VSV expressing the full-length S protein of SARS-CoV-2 and Huh7 cells (Nie et al., 2020a). Interestingly, the lack of proof-reading activity in VSV-L polymerase has been used to develop viral stocks with a higher degree of variety (particularly in the S protein) than actual SARS-CoV-2 (Weisblum et al., 2020).

***Lentiviral pseudotypes***

A lentiviral pseudotype containing the shortened spike protein of SARS-CoV-2 was developed and employed to investigate virus entrance and immunological cross-reactivity

with SARS-CoV. In one investigation, Moloney murine leukaemia virus (MMLV) successfully pseudotyped the VSV-G glycoprotein but not the SARS-CoV-2 Spike protein (Tandon et al., 2020). However, MMLV could pseudotype the SARS-CoV-2 Spike protein in a separate investigation (Rowe et al., 1999). These variations might be explained by the expression constructs utilized in the two studies, with the former producing a full-length Spike protein and the latter expressing a Spike protein with a 19 amino acid (aa) deletion in the C terminus, which may help in expression as previously mentioned (Yue Zheng et al., 2021). In comparison, pLV effectively pseudotyped both glycoproteins; nevertheless, much greater titres of pLV-G particles were generated. HEK 293Ts expressing human ACE2 were transduced most effectively using the pLV-S method among all mammalian cells studied (Tandon et al., 2020). Both CP and human monoclonal antibodies showed a quantifiable correlation with nAb assessed utilizing an authentic SARS-CoV-2 neutralization test. The test produces findings in around 48 hours.

***Engineered viruses***

Numerous research groups have generated genetically modified viruses that include a reporter gene that is used to detect the virus: examples include luciferases (firefly, Renillareniformis, or nanoluciferase (Xuping Xie, Muruato, Zhang, et al., 2020)), green fluorescent protein (Noval et al., 2020), or mNeonGreen insertion into ORF7 (Xuping Xie, Muruato, Lokugamage, et al., 2020). *Gaussia princeps* luciferase, the smallest known luciferase, is spontaneously released into mammalian cell culture conditions, removing the need for cell lysis (Cong Zeng et al., 2020). The test is easy and has high throughput since the findings are acquired by automatically counting positive cells 5–12 hours after infection. Neutralization test in Vero CC81 cells demonstrated a strong correlation with the test employing intact virions in the instance of mNeonGreen (Muruato et al., 2020). The assay is called the chemiluminescence reduction neutralization test when a chemiluminescent reporter is utilized (Tani et al., 2021).

***Non-viral systems***

Another novel approach involves the development of a SARS-CoV-2 spike trimer coupled to a fluorescent protein, which serves as a flexible tool for high-throughput detection and phenotypic analysis of SARS-CoV-2 entrance inhibitors (Yali Zhang et al., 2020).

The Promega HiBiT/LgBiT® method may be used to generate HiBiT-tagged neutralization test: genomeless virus-like particles are combined with a short luciferase peptide (HiBiT), and their entrance into target cells expressing LgBiT reconstitutes NanoLuc luciferase within 3 hours (Miyakawa et al., 2020).

**The detection methods**

Neutralizing antibodies may be detected and measured using a "gold standard" technique known as the plaque reduction neutralization test (PRNT). Placing a virus-serum combination on virus-susceptible cells allows us to observe the antibody's impact on viral infectivity. In order to prevent the propagation of the progeny virus, the cells are covered with a semisolid medium. There are several approaches to identify a plaque, which is the result of a virally generated productive infection. The decrease in viral infectiousness relative to the antibody-free combination is measured by counting the plaques. Both positive and negative controls are included in each test. A microscope detects cytopathic effect plaques on the replication-competent cell line monolayer (X. Wang et al., 2020). Antibody titres are defined as the most significant serum dilution that resulted in >90% ($PRNT_{90}$) or >50% ($PRNT_{50}$) plaque reduction.

It was developed to create focus neutralization reduction test (FRNT) which uses immunostaining to visualize “plaques” referred to as foci, because certain viruses fail to produce cytolytic plaques because they do not destroy cells. The formation of visible spots in alternative FRNT cells is based on the time required for viral protein synthesis and infectious virus transmission to neighbouring susceptible cells. The number of infected cells per well can be counted using an ELISpot analyser. (J. G. Park et al., 2021). Again, antibody titers are defined as the reciprocal of the serum dilution at which the number of foci was reduced by >90% (FRNT90) or >50% (FRNT50).

As previously indicated, after inserting the firefly luciferase reporter gene into the viral construct, cells are lysed, and luciferase expression is quantified by a luminometer. (Garcia et al., 2014).

If fluorescent reporter gene (such as; green fluorescent protein, GFP) is inserted into viral construct, population of the individual infected cells are analyzed by Flow Cytometry. But it is time-consuming because of requiring trypsinization of host cells analysis of each sample individually in a flow cytometer.

## 2. AIM OF THIS STUDY

The functional measurement of neutralizing activity against SARS-CoV-2 using serum or plasma samples stands out as a critical tool in the management of the pandemic. Such assays can be utilized to identify better convalescent plasma donors and to follow-up immune response in COVID-19 patients or vaccinated individuals. Moreover, as novel variants of SARS-CoV-2 continue to emerge, neutralization assays provide an initial look at the levels of protection against novel variants in priorly infected or vaccinated individuals.

This study aims to develop a lentiviral pseudovirus-based neutralization assay against SARS-CoV-2 using 293FT cells overexpressing ACE2 and TMPRSS2 as targets. While developing the assay, we put special emphasis on the constitution of pseudovirus particles that include not only the Spike protein but also other structural proteins of SARS-CoV-2 in an attempt to better mimic the natural virus infection *in vitro.* Furthermore, we aim to utilize the SEAP gene along with a fast enzymatic assay that enables more practical and high-throughput analysis of neutralizing activity in different types of samples such as convalescent plasma or monoclonal antibodies. More specifically, our step-by-step optimization of the pseudovirus based neutralization assays aims the following:

I. Optimization of conditions for the production of lentiviral particles pseudotyped with the SARS-CoV-2 Spike, Membrane, Nucleocapsid and Envelope proteins.

II. Genetic modification of 293FT cells to overexpress the ACE2 receptor and the TMPRSS2 protease, to be used as a target cell for the assay.

III. Evaluation of GFP and SEAP transgenes for detection of infection rate.

IV. Application of the neutralization assay to analyze neutralizing activity in samples from convalescent plasma donors, COVID-19 patients and vaccinated individuals.

# 3. MATERIALS AND METHODS

## 3.1 Materials

### 3.1.1 Chemicals

There is a list of all the chemicals that were used in this thesis in the Appendix A section.

### 3.1.2 Equipments

There is a list of all the equipments that were used in this thesis in the Appendix B section.

### 3.1.3 Buffers and solutions

Agarose Gel: 1 gram of agarose powder was dissolved in 100 ml 0.5X TBE buffer by boiling to get 100 ml of 1% w/v gel. Ethidium bromide at a concentration of 0.01% (v/v) was added to the solution.

Calcium Chloride ($CaCl_2$) Solution: Glycerol (15%), 10mM PIPES (pH 7.00), and 60mM CaCl2 (diluted from 1M stock) were mixed and sterilized in an autoclave at 121$^{o}$C for 15 minutes and kept at 4$^{o}$C.

Tris-Borate-EDTA (TBE) Buffer: To prepare 1 liter of 5X stock solution, 54 grams of Tris-base, 27.5 grams of boric acid, and 20 milliliters of 0.5 molar EDTA has pH 8.00 were dissolved in 1 liter of ddH2O. Dilutions of 1 to 10 are used to prepare workable solutions of 0.5% TBE at room temperature (RT).

HBS solution (2X): 50 mM HEPES, 280 mM NaCl, and 1.5 mM Na2HPO4 are added to 10 M NaOH to adjust the pH to between 7.05 to 7.2, and the solution is sterilized by passing through a 0.22 m filter. Store at a temperature of -20$^{o}$C.

Phosphate-buffered saline (PBS): Filter-sterilized 1L 1X solution made from 100 milliliters of 10X DPBS mixed to 900 milliliters of ddH2O.

### 3.1.4 Growth media

Complete DMEM: 10% heat-inactivated fetal bovine serum, 1mM of Sodium Pyruvate, 2mM L-Glutamine, and 25mM HEPES, 0.1mM MEM Non-essential amino acid solution were added to the culture medium to sustain the viability of HEK 293FT cells.

Luria Broth (LB): An autoclave was used for 15 min at 121°C to sterilize the media, which was made up of 1 L of water and 20 grams of LB powder. Ampicillin, at a final concentration of 100 g/ml, was added to the liquid medium soon before use for ampicillin selection.

LB-Agar: Add 16 g LB powder and 12 g bacterial agar powder to 800 ml of ddH2O and autoclave at 121°C for 15 minutes to make 1X agar medium in a 1 L glass bottle. The antibiotic of interest is then added to a specified ratio of autoclaved LB agar on sterile Petri plates. Ampicillin, at a final concentration of 100 g/ml, was added to the liquid medium just before transferring to sterilized petri dishes. At a constant temperature of 4°C, sterile agar plates were maintained.

Freezing medium: The heat-inactivated fetal bovine serum used to freeze the cell lines included DMSO (v/v) at a concentration of 6%.

### 3.1.5 Commercial kits used in this study

| Commercial Kit | Company |
|---|---|
| QUANTI-Blue™ Solution | InvivoGen, USA |
| RNA isolation kit | Zymo Research, USA |
| Nucleo Spin® Plasmid Midiprep Kit | Macherey-Nagel, USA |
| Nucleo Spin® Plasmid Miniprep Kit | Macherey-Nagel, USA |
| Nucleo Spin® Gel and PCR Clean-up Kit | Macherey-Nagel, USA |
| RealQ Plus 2x Master Mix Green | Ampliqon, Denmark |
| RevertAid First Strand cDNA Synthesis Kit | Thermo Fisher, USA |

**Table 3.1.** List of Commercial Kits

### 3.1.6 Enzymes

| Enzyme | Company |
|---|---|
| NotI-HF | New England Biolabs (NEB), USA |
| BamHI-HF | New England Biolabs (NEB), USA |
| BglII | New England Biolabs (NEB), USA |
| DpnI | New England Biolabs (NEB), USA |
| CIAP | New England Biolabs, USA |
| EcoRI-HF | New England Biolabs, USA |
| T4 Ligase | New England Biolabs, USA |

**Table 3.2.** List of Enzymes

### 3.1.7 Antibodies

| Antibody | Company |
|---|---|
| Rabbit polyclonal Antihuman-ACE2 antibody (#4355) | Cell Signaling Technology (CST), USA. |
| HRP-conjugated anti-rabbit IgG (#7074) | Cell Signaling Technology (CST), USA. |
| SARS-CoV-2 Spike Antibody (clone:B3476M) | Novus Biologicals, USA |

**Table 3.3** List of Antibodies

### 3.1.8 Bacterial strains

General plasmid amplification and lentiviral vector amplifications are performed using *Escherichia coli* (*E. coli*) Top10.

### 3.1.9 Mammalian cell lines

293FT: Fast-growing and highly transfectable, the human embryonic kidney 293 (HEK293) cell line is a clonal isolation of human embryonic kidney cells transformed with the SV40 big T antigen.

### 3.1.10 Plasmids and oligonucleotides

The plasmids and the oligonucleotides are listed in Table 3.4 and Table 3.5.

| PLASMID NAME | PURPOSE OF USE | SOURCE |
|---|---|---|
| **pMDLg/pRRE** | 3rd generation lentiviral packaging plasmid (*Gag/Pol*) | Kind gift from Didier Trono Addgene (#12251) |
| **pRSV-REV** | 3rd generation lentiviral packaging plasmid (*Rev*) | Kind gift from Didier Trono Addgene (#12253) |
| **pCMV-VSV-g** | 3rd generation lentiviral packaging plasmid (*Env*) | Kind gift from Bob Weinberg Addgene (#8454) |
| **LeGO-G2** | Lentiviral construct for GFP expression | Kind gift from Prof. Boris Fehse of University Medical Center Hamburg-Eppendorf, Hamburg, Germany |

| | | |
|---|---|---|
| **LeGO-iG2** | Lentiviral construct for IRES and GFP expression | Kind gift from Prof. Boris Fehse of University Medical Center Hamburg-Eppendorf, Hamburg, Germany |
| **LeGO-iT2** | Lentiviral construct for tomato expression | Kind gift from Prof. Boris Fehse of University Medical Center Hamburg-Eppendorf, Hamburg, Germany |
| **LeGo-iT2puro** | Lentiviral construct for tomato expression with Puromycin resistance gene | Kind gift from Prof. Boris Fehse of University Medical Center Hamburg-Eppendorf, Hamburg, Germany |
| **pcDNA3.1+_C-(K)DYK-ACE2** | Expression of Homo sapiens angiotensin I converting enzyme 2 (hACE2) | NM_021804.2, OHu20260 |
| **pTwist EF1 Alpha-SARS-Cov-2-S-2xStrep** | Expression of the SARS-CoV-2 Spike protein | Kind gift gift from Nevan Krogan (Addgene plasmid #141382) |
| **pcDNA3-sACE2(WT)-Fc(IgG1)** | Mammalian expression plasmid for soluble ACE2-Fc fusion (IgG1) | Kind gift from Erik Procko Addgene ( #145163) |
| **pcDNA3-SARS-CoV-2-S-RBD-sfGFP** | Mammalian expression plasmid for RBD of SARS-CoV-2 protein S (spike) fused with sfGFP | Kind gift from Erik Procko Addgene (#141184) |
| **pGBW-m4134096** | Mammalian expression plasmid for SARS-CoV-2 M (membrane) | Kind gift from Ginkgo Bioworks (Addgene #152039) |
| **pLV-EF1a-IRES-Puro** | Empty lentiviral construct for cloning purposes | Addgene (#85132) |
| **TMPRSS2** | Expression of TMPRSS2 | Addgene (#53887) |
| **pLVX-EF1alpha-SARS-CoV-2-E-2xStrep-IRES-Puro** | Lentiviral expression of SARS-CoV-2 envelope (E) protein; transient expression and generate lentivirus | Kind gift gift from Nevan Krogan Addgene (#141385) |
| **pLVX-EF1alpha-SARS-CoV-2-N-2xStrep-IRES-Puro** | Lentiviral expression of SARS-CoV-2 nucleocapsid (N) protein; transient expression and generate lentivirus | Kind gift gift from Nevan Krogan Addgene (#141391) |
| **pNiFty3-N-SEAP** | Expression of SEAP (Secreted alkaline phosphatase) reporter gene. | Invivogen (cat no:pnf-sp2) |
| **LeGo-ACE2-iT2** | Lentiviral construct for hACE2 expression with IRES and tomoto | Lab construct |
| **LeGo-ACE2-iT2puro** | Lentiviral construct for hACE2 expression with IRES, tomoto and puromycin resistance genes | Lab construct |
| **pLV-EF1a-TMPRSS2iPuro** | Expression of TMPRSS2 with IRES and puromycin resistance genes | Lab construct |
| **pCMV-Spike** | Expression of the SARS-CoV-2 Spike protein | Lab construct |

| | | |
|---|---|---|
| **pCMV-SpikeΔ19** | Expression of the SARS-CoV-2 Spike protein | Lab construct |
| **pCMV-Spike(D614G)** | Expression of the SARS-CoV-2 Spike protein with point mutation on D614 | Lab construct |
| **pCMV-SpikeΔ19(D614G),** | Expression of the SARS-CoV-2 Spike protein 19 aminoacid truncated version without the endoplasmic reticulum retention signal (ERRS) regions with point mutation on D614 | Lab construct |
| **pCMV-SpikeΔ19(N501Y)** | Expression of the SARS-CoV-2 Spike protein 19 aminoacid truncated version without the endoplasmic reticulum retention signal (ERRS) regions and point mutation on N501 | Lab construct |
| **pCMV-SpikeΔ19(D614G/N501Y)** | Expression of the SARS-CoV-2 Spike protein 19 aminoacid truncated version without the endoplasmic reticulum retention signal (ERRS) regions and point mutation on both D614 and N501 | Lab construct |
| **pCMV-SARS-CoV-2-N-2xStrep** | Expression of SARS-CoV-2 nucleocapsid (N) protein | Lab construct |
| **pCMV-SARS-CoV-2-E-2xStrep** | Expression of SARS-CoV-2 envelope (E) protein | Lab construct |
| **LeGo-SEAP-iG2** | Lentiviral construct forSEAP expression with IRES and GFP | Lab construct |

**Table 3.4.** Complete list of plasmids used in this study.

| OLIGO NAME | SEQUENCE (5' to 3') | PURPOSE OF USE |
|---|---|---|
| **ACE2_NotI_forward** | AAT GCG GCC GCC ACC ATG TCA AG | PCR for isolation hACE2 with using forward primer containing NotI Cut site from pcDNA3.1+_C-(K)DYK-ACE2 plasmid |
| **ACE2_NotI_reverse** | TAT GCG GCC GCT TAA AAG GAG GTC TGA A | PCR for isolation hACE2 with using reverse primer containing NotI Cut site from pcDNA3.1+_C-(K)DYK-ACE2 plasmid |
| **BamHI_forward** | TTA TGG ATC CGC CGC CAC CAT GTT TGT T | PCR for isolation Spike region with using forward primer containing BamHI Cut site from pTwist EF1 Alpha-SARS-Cov-2-S-2xStrep |

| | | |
|---|---|---|
| **BamHI_reverse** | GGC GCG GAT CCT TAC GTG TAG TGC AAT T | PCR for isolation Spike region with using reverse primer containing BamHI Cut site from pTwist EF1 Alpha-SARS-Cov-2-S-2xStrep |
| **BamHI_reverse** | GTG TGG GAT CCT TAG CAG CAA CTA CCG C | PCR for isolation SpikeΔ19 region with using reverse primer containing BamHI Cut site from pTwist EF1 Alpha-SARS-Cov-2-S-2xStrep |
| **D614G SDM_forward** | CAG TTC TTT ATC AGG GCG TGA ATT GTA CAG AG | For point mutation on D614, pCMV-Spike and pCMV- SpikeΔ19 plasmids were PCR amplified with using this forward primer |
| **D614G SDM_reverse** | TCT GTA CAA TTC ACG CCC TGA TAA AGA ACT GC | For point mutation on D614, pCMV-Spike and pCMV- SpikeΔ19 plasmids were PCR amplified with using this reverse primer |
| **N501Y SDM_forward** | GTT TTC AAC CGA CGT ATG GGG TGG GAT AC | For point mutation on N501, pCMV-Spike and pCMV- SpikeΔ19 plasmids were PCR amplified with using this forward primer |
| **N501Y SDM_reverse** | GTA TCC CAC CCC ATA CGT CGG TTG AAA AC | For point mutation on N501, pCMV-Spike and pCMV- SpikeΔ19 plasmids were PCR amplified with using this reverse primer |
| **TMPRSS2_BglII_forward** | CAA GAG ATC TGG CAC CAT GGC TTT GAA CTC | PCR amplified TMPRSS2 region from TMPRSS2 plasmid with using forward primer containing BglII cut site |
| **TMPRSS2_EcoRI_reverse** | ACA TAG AAT TCC TAG CCG TCT GCC CTC ATT TG | PCR amplified TMPRSS2 region from TMPRSS2 plasmid with using reverse primer containing EcoRI cut site |
| **SEAP_BglII_forward** | CATGAGACTTGCCACCATGATTCTG | |
| **SEAP_EcoRI_reverse** | GCTAGGAATTCTCAATCCAGACGCT | |

**Table 3.5.** Complete list of primers and oligonucleotides used in this study.

### 3.1.11 DNA sequencing

Sequencing service was commercially provided by Macrogen (https://dna.macrogen-europe.com/eng/), Amsterdam, the Netherlands, Europe.

### 3.1.12 Software, computer-based programs, and websites

| Software/Company | Purpose of Use |
|---|---|
| CLC Main Workbench v7.7 /CLC Bio | Vector maps construction, Analysis of restriction and DNA sequencing |
| Flow Jo V10/Tree Star Inc. | Analyzing flow cytometer data |
| http://www.ensembl.org/index.html | Human genome sequence information |
| https://www.addgene.org/ | Plasmid map and sequence information |
| GraphPad Prism v8/ Inc., San Diego, CA, USA | Analyzing data statistically |
| https://primer3plus.com/ | Oligonucleotides design |
| PrimerX/https://www.bioinformatics.org/primerx/ | Designing a primer pair based on a mutation in my template DNA sequence(site-directed mutagenesis) |

**Table 3.6.** Complete list of software and programs.

## 3.2 Methods

### 3.2.1 Bacterial cell culture

Bacterial culture growth: In LB medium, *E. coli* cells were cultivated at 37ºC with 220 rpm shaking while being supplemented with the necessary antibiotics. Single-colony picking requires the use of glass beads to disperse cells on petri plates and incubate overnight at 37ºC without shaking. Single colonies formed overnight in liquid culture were then diluted 1:3 and cultivated for additional 3 hours at 37oC with 220 rpm shaking for long-term preservation of bacteria. Glycerol was added to 1 ml of bacteria at a final 10% (w/v) concentration and stored in cryotubes at -80oC.

Preparation of competent bacteria: In a 250ml-flask, competent *E.coli* cells were cultivated overnight (about 16 hours) at 37ºC with 220 rpm shaking in 50 ml LB without any antibiotics. Overnight-grown culture was added to 400ml of LB without antibiotics and cultured at 37ºC with a 220rpm shaker until the OD590 was about 0.375 the next day. It is incubated on ice for 5 to 10 minutes before being divided into eight 50ml containers. Centrifugation was performed at 1600g for 10 minutes at 4ºC every time. Once the supernatant was removed, each pellet was resuspended in 10 ml of ice-cold $CaCl_2$ solution and centrifuged at 1100g for 5 minutes at 4ºC. Before being resuspended again in 2 ml of $CaCl_2$ solution, the supernatant was removed from each pellet. We froze the cells for 30 minutes on ice before dividing them into 200 μl aliquots and snap-freezing them in liquid nitrogen and stored at -80°C.

Transformation of competent bacteria: Aliquots of 200 μl of competent *E. coli* cells were stored at -80ºC. Plasmid DNA and competent *E. coli* cells were thawed on ice for each transformation. For 30 minutes, competent cells were incubated on ice with the necessary quantity of plasmid DNA. They then placed into a pre-set 42ºC heat block and were

heated for 90 seconds before being cooled for a further 1 minute. Each tube contained 800 µl of LB and competent cells were cultured at 37°C for 45 minutes in a water bath. At 13,200 RPM, the cells were spun down for one minute and resuspended in 100 µl to be dispersed over the petri plates. A 100 µl bacterial cell solution was dispersed evenly over petri plates prepared with LB agar and a suitable antibiotic, then glass beads were added. Plates were incubated at 37°C for a further night without shaking.

Plasmid DNA isolation: The manufacturer's guidelines of Macherey-Nagel Mini-Midiprep Kits were used. A NanoDrop spectrophotometer was used to measure the final DNA concentration and purity.

### 3.2.2 Mammalian cell culture

Maintenance of cell lines: In sterile tissue culture flasks and at 37°C with 5% $CO_2$ incubators, 293FT cells were cultured in complete DMEM media. When the cells achieved a maximum of 90% confluency, they were divided. Trypsin was added to cell culture flasks after cells had been rinsed with PBS, and the flasks were then incubated for 5-6 minutes at 37°C with 5% $CO_2$. To avoid allowing the cells reach full confluence, they were divided every two days and resuspended in complete DMEM before being split 1:3 to 1:8.

Cell freezing: One day before to freezing, cells were divided at a 30%-40% confluency. At least $3x10^6$ cells were frozen in each vial on the next day. After centrifugation at 300g for 5 minutes, the supernatant was discarded and the pellet was resuspended in 0.5ml FBS before being incubated on ice for 15-20 minutes on each vial. Meanwhile, 0.5 ml of freshly manufactured FBS in 12 percent DMSO was made and incubated on ice for the next step. 1 ml of this solution contained 6% DMSO after it had been incubated for five minutes. For long-term storage, cells were initially kept in cryotubes at -80°C, and later in liquid nitrogen.

Cell thawing: On ice, cells in cryotubes were gently warmed to room temperature. Each cell was given a 15 ml tube containing 5 ml FBS. In order to prevent damaging cells and diluting DMSO residues, 1 ml of frozen material was gently pipetted into FBS, requiring 2-3 minutes in total. The supernatant was then discarded after the cells were centrifuged

at 300g for 5 minutes. After thawing, the cells were resuspended in full medium and monitored daily.

### 3.2.3 Cloning

For the overexpression of hACE2 and TMPRSS2 proteins on 293FT cells, LeGo-ACE2-iT2, LeGo-ACE2-iT2puro and pLV-EF1a-TMPRSS2iPuro vectors were constructed. hACE2 region from pcDNA3.1+_C-(K) DYK-ACE2 was Polymerase Chain Reaction (PCR) amplified using forward primer containing NotI Cut site, 5'- AAT GCG GCC GCC ACC ATG TCA AG-3' and the reverse primer containing NotI Cut Site 5'- TAT GCG GCC GCT TAA AAG GAG GTC TGA A-3' (restriction sites underlined). For preparation of the vector, LeGO-iT2 and LeGO-iT2puro plasmids were cut by NotI-HF and ligation with the NotI digested PCR products was performed for 1 hour at room temperature with T4 DNA ligase. TMPRSS2 region from TMPRSS2 plasmid was Polymerase Chain Reaction (PCR) amplified using forward primer containing BglII Cut site, 5'- CAA GAG ATC TGG CAC CAT GGC TTT GAA CTC -3' and the reverse primer containing EcoRI Cut Site 5'- ACA TAG AAT TCC TAG CCG TCT GCC CTC ATT TG -3' (restriction sites underlined). For preparation of the vector, pLV-EF1a-TMPRSS2iPuro plasmid was cut by BamHI-HF and EcoRI ligation with the BglII and EcoRI digested PCR products was performed for 1 hour at room temperature with T4 DNA ligase. Colonies were screened by restriction digestion for the directional insertion of PCR products and the resulting lentiviral vectors were validated by Sanger sequencing.

Full-length SARS-CoV-2 Spike gene and the 19 aminoacid truncated version without the endoplasmic reticulum retention signal (ERRS) (SpikeΔ19) regions from pTwist-EF1-Alpha-SARS-Cov-2-S-2xStrep were PCR amplified using the same forward primer containing BamHI cut site, 5'-TTA TGG ATC CGC CGC CAC CAT GTT TGT T-3' and different reverse primers containing BamHI cut sites 5'- GGC GCG GAT CCT TAC GTG TAG TGC AAT T-3' and 5'- GTG TGG GAT CCT TAG CAG CAA CTA CCG C-3'. pCMV-VSV-G was cut by BamHI-HF for removing the VSV-G coding region and the digested PCR products were cloned into this site. Ligations were performed with T4 DNA ligase for 15 minutes at room temperature followed by 1 hour at 16$^{o}$C. The

generated vectors were named pCMV-Spike and pCMV-SpikeΔ19 and constructs were validated by Sanger sequencing.

The D614G variants on both pCMV-Spike and pCMV-SpikeΔ19 plasmids and the N501Y variants on only pCMV-SpikeΔ19 plasmids were generated by site-directed mutagenesis. For point mutation on D614, pCMV-Spike and pCMV- SpikeΔ19 plasmids were PCR amplified using a forward primer 5'- CAG TTC TTT ATC AGG GCG TGA ATT GTA CAG AG-3' and a reverse primer 5'- TCT GTA CAA TTC ACG CCC TGA TAA AGA ACT GC-3. For point mutation on N501, pCMV- SpikeΔ19 and pCMV-SpikeΔ19(D614G) plasmids were PCR amplified using a forward primer 5'- GTT TTC AAC CGA CGT ATG GGG TGG GAT AC-3' and a reverse primer 5'- GTA TCC CAC CCC ATA CGT CGG TTG AAA AC-3. DpnI restriction enzyme was used to remove unmodified plasmids and the PCR products were transformed into Top10 E.coli for amplification. The generated vectors were named pCMV-Spike(D614G), pCMV-SpikeΔ19(D614G), pCMV-SpikeΔ19(N501Y), pCMV-SpikeΔ19(D614G/N501Y) and the mutagenesis was validated by Sanger sequencing.

For the expression of SARS-COV-2 envelope and nucleocapcid proteins pCMV-SARS-CoV-2-E-2xStrep and pCMV-SARS-CoV-2-N-2xStrep vectors were constructed. Nucleocapcid region from pLVX-EF1alpha-SARS-CoV-2-N-2xStrep-IRES-Puro and envelope region from pLVX-EF1alpha-SARS-CoV-2-E-2xStrep-IRES-Puro vectors were cut by BamHI-HF and EcoRI-HF enzymes. pCMV-VSV-G was first cut by BglII and second cut by EcoRI-HF for removing the VSV-G coding region. BglII and BamHI generate compatible ends. Digested E and N regions were cloned into this site. Ligations were performed with T4 DNA ligase for 15 minutes at room temperature followed by 1 hour at 16$^{o}$C. The constructs were validated by Sanger sequencing.

For the lentiviral expression of secreted alkaline phosphatase (SEAP) LeGo-SEAP-iG2 vector were constructed. SEAP region from pNiFty3-N-SEAP plasmid was PCR amplified using the forward primer containing BglII cut site, 5'- CAT GAG ACT TGC CAC CAT GAT TCT G -3' and the reverse primer containing EcoRI cut sites 5'- GCT AGG AAT TCT CAA TCC AGA CGC T-3'. LeGo-iG2 vector was double digested with BamHI-HF and EcoRI-HF. BglII and BamHI generate compatible ends. BglII-EcoRI digested PCR products were cloned into digested LeGo-iG2 vector before the IRES site. Ligations were performed with T4 DNA ligase for 15 minutes at room temperature

followed by 1 hour at 16$^{o}$C. The generated vector were named LeGo-SEAP-iG2 and construct was validated by Sanger sequencing.

### 3.2.4 Production of recombinant soluble proteins

For production of soluble proteins (RBD-GFP and ACE2-IgG1), 293FT cells (6x106) were seeded in poly-L-lysine (Sigma, USA) coated 100mm tissue culture dishes (Corning, USA). When cells reached 70% confluency on the following day, they were transfected with the 15 μg of the plasmids (either pcDNA3-SARS-CoV-2-S-RBD-sfGFP or pcDNA3-sACE2(WT)-Fc) using calcium phosphate precipitation in the presence of 25 μM chloroquine. After 8-10 h incubation, medium was changed with complete DMEM containing 5 mM sodium butyrate (NaBut). The supernatants were collected at 48-60 h after medium change and centrifuged at 300g for 5 mins to remove cell debris. After centrifugation, the supernatants were filtered through 0.45μm filters. Filtered supernatants of RBD-GFP were aliquoted and stored at -20°C as required.

Filtered supernatant of ACE2-IgG1 was diluted 1:3 with Buffer A (20 mM Sodium Phosphate, pH 7.4, 150 mM NaCl) and captured by HiTrap MabSelectSure (Cytiva) 1mL column using ÄKTA Avant 25 (GE Healthcare). The column was then washed with 7.5 CV Buffer A. Captured ACE2-IgG1 was eluted with 10 CV Buffer B (100 mM Glycine, pH 3.0) and fractionated in tubes already containing 15 μL Buffer C (1M Tris pH 8.5). Collected proteins were buffer exchanged into PBS via multiple rounds of centrifugation in 10 kDA ultrafiltration tubes. The purified protein content was measured by Bradford assay (B6916, Sigma-Aldrich) and analyzed under reducing conditions with 12% SDS-PAGE, followed by wet transfer on PVDF Membrane (Merck). The membrane was blocked with 5% skimmed milk in TBS-T and incubated overnight at 4°C with polyclonal rabbit anti human-ACE2 antibody. The dilution was prepared as 1:1000 in 5% Bovine Serum Albumin (BSA) in TBS-T. After washing with TBS-T, membrane was treated with HRP-conjugated anti-rabbit IgG and incubated 1h at room temperature. The band was visualized using ECL (Advansta, USA) on a gel documentation system (Syngene, G BOX) for validation of the purity and size of the produced ACE2-IgG protein.

### 3.2.5 Generation human ACE2 and TMPRSS2 overexpressing cells

For production the LeGo-hACE2-iT2puro and pLV-EF1a-TMPRSS2iPuro vectors, 293FT cells (5x106) were seeded in a poly-L-lysine coated 100mm tissue culture dish and when cells reached %70 confluency on the following day, they were transfected with the following mixture of plasmids; 7.5µg of LeGo-hACE2-iT2puro or pLV-EF1a-TMPRSS2iPuro, 3.75µg of pMDLg/pRRE, 2.25µg of pRSV-Rev and 1.5µg of phCMV-VSV-G using Calcium Phosphate transfection in the presence of 25 µM chloroquine. After 8-10h medium was changed and the supernatants were collected at 24h after medium change, filtered with 0.45µm filters, mixed at a 1:5 (v/v) ratio with 50% PEG8000 solution and stored at 4°C overnight. Next day, lentiviral particles were concentrated by centrifugation at 3000g for 30 minutes. Supernatants were removed and pellets resuspended in 500 µl serum-free DMEM.

For generation of 293FT-hACE2, 293FT-TMPRSS2 and 293FT-hACE2-TMPRSS2 cells, $1x10^6$ 293FT cells were seeded into a T25 flask one day prior to viral transduction. Cells were transduced with the concentrated LeGo-ACE2-iT2puro or pLV-EF1a-TMPRSS2iPuro or both (MOI=1) vector in the presence of 8 µg/ml protamine sulfate overnight. Virus containing supernatant was completely removed the next day and cells were cultured in their regular growth media for 72 hours before tdTomato expression was assessed by flow cytometry. After puromycin selection, 293FT cells stably expressing wild type ACE2 protein and TMPRSS2 were confirmed with flow cytometry.

### 3.2.6 Flow Cytometry

For surface staining of 293FT-hACE2 cells, $2.5x10^5$ cells were washed once with PBS and incubated at RT for 1 hour with 300 µl of RBD-GFP supernatant collected as described above. The stained cells were washed with PBS and data acquisition was performed on BD Accuri C6 (Becton, Dickinson and Company, USA).

For data acquisition of neutralization assays, 25µl of Trypsin-EDTA (0.05%) with phenol red (HyClone) was added for each well on the 96-well plate and incubated at 37°C for 5 min. Cells were collected from wells by pipetting with PBS (containing 2%FBS and 2mM

EDTA) and data acquisition was performed on a BD Accuri C6 (Becton, Dickinson and Company, USA). All flow cytometry data were analyzed with FlowJo v10.1 (BD Biosciences).

### 3.2.7 Microscopy

For microscopy, 105 293FT-hACE2 cells were seeded in a poly-L-lysine coated coverslip placed in a 24-well plate and incubated overnight. The following day, coverslips were washed once with PBS, fixed with 250 µl of 4% Paraformaldehyde (PFA) for 10 minutes at 37°C and were washed two more times with PBS. 250 µl of filtered permeabilization buffer (0.2%(w/v) Saponin, 2%(w/v) BSA) was added on the cover slips and incubated at RT for 1 hour. The permeabilized cells were washed once with PBS followed by incubation with 300 µl of RBD-GFP supernatant at RT for 1 hour. Finally, coverslips were washed twice with PBS and mounted on slides for imaging. Images acquisition was performed on a Leica TCS SP5 confocal microscope (Leica Microsystems GmbH, Wetzlar, Germany). All samples were captured with 2048*2048-pixel resolution, 40X magnification, and z-stack images of 0.6 µm. Laser power, gain, and offset were kept constant for all images. Analysis of the captured images was made by Fiji distribution of Image J software 1.52p (38). Colocalization was documented by merging the three channels.

### 3.2.8 RNA isolation and Quantitative Real-Time PCR (qRT-PCR)

For analyze the TMPRSS2 expression levels of genetically modified 293FT cell lines, 3-4 x$10^6$ 293FT cells expressing TMPRSS2 were used for RNA isolation as suggested by manufacturer's protocol (Zymo Research Quick-RNA™ Miniprep Kit #R1054). For synthesis of first strand cDNA from the RNA templates, RevertAid First Strand cDNA Synthesis Kit (Thermo Scientific Cat. No. K1622) was used. qRT-PCR was performed using a forward primer 5'- GCA GTG GTT TCT TTA CGC TGT-3' and a reverse primer 5'- CCG CAA ATG CCG TCC AAT G-3 with RealQ Plus 2x Master Mix Green Without ROX™ (Ampliqon Cat.No. A323402) in Thermo Scientific™ PikoReal™according to manufacturer's protocol.

### 3.2.9 Pseudovirus production and titration

Basic pseudovirus production: For production of Spike-pseudotyped lentiviral particles, 293FT cells ($5x10^6$) were seeded in a poly-L-lysine coated 100mm tissue culture dish and when cells reached %70 confluency on the following day, 7.5 μg vector plasmid containing GFP reporter gene (LeGo-G2) was co-transfected using Calcium-Phosphate precipitation as described above along with 3.75 μg of pMDLg/pRRE, 2.25 μg of pRSV-Rev and indicated amounts of one of the envelope plasmids encoding the SARS-CoV-2 Spike protein (pCMV-Spike for full length wildtype Spike protein, pCMV-SpikeΔ19 for wildtype Spike protein lacking 19 aminoacids in its C terminal tail, pCMV-SpikeΔ19(D614G) for Spike protein carrying the D614G mutation, pCMV-SpikeΔ19(N501Y) for Spike protein carrying the N501Y mutation or pCMV-SpikeΔ19(D614G/N501Y) for Spike protein carrying the both D614G and N501Y mutations and lacking the 19 amino acids in its C terminal tail). In indicated experiments 1 μg of the pGBW-m4134357 plasmid encoding for the SARS-CoV-2 M protein was included in this mixture. After 8-10h medium was changed with fresh medium containing 0.2mM NaBut and the supernatants containing pseudovirus particles were collected at 40-48 hours after chaning medium and filtered through a 0.45 μm syringe filter, divided into aliquots and stored at -80°C.

Production of enhanced SEAP-based pseudovirus: For production of SEAP-based spike-pseudotyped lentiviral particles, 293FT cells ($5x10^6$) were seeded in a poly-L-lysine coated 100mm tissue culture dish and when cells reached %70 confluency on the following day, 7.5 μg vector plasmid containing SEAP reporter gene (LeGo-SEAP-iG2) was co-transfected using Calcium-Phosphate precipitation as described above along with 3.75 μg of pMDLg/pRRE, 2.25 μg of pRSV-Rev and 0.5 μg of one of the envelope plasmids encoding the SARS-CoV-2 Spike protein (pCMV-SpikeΔ19 for wildtype Spike protein lacking 19 aminoacids in its C terminal tail, pCMV-SpikeΔ19(D614G) for Spike protein carrying the D614G mutation, pCMV-SpikeΔ19(N501Y) for Spike protein carrying the N501Y mutation or pCMV-SpikeΔ19(D614G/N501Y) for Spike protein carrying the both D614G and N501Y mutations and lacking the 19 amino acids in its C terminal tail). In indicated experiments 0.25 μg of the each plasmids encoding for the SARS-CoV-2 M, N and E protein was included in this mixture. After 8-10h medium was

changed with fresh medium containing 0.2mM NaBut and the supernatants containing pseudovirus particles were collected at 40-48 hours after chaning medium and filtered through a 0.45 μm syringe filter, divided into aliquots and stored at −80°C.

Virus titer was estimated by transducing $5x10^5$ 293FT-hACE2 cells per well in a 24-well plate with 250 μl viral supernatant for 16 hours in the presence of 8 μg/ml Protamine Sulfate. The transduced cells were cultured for 72 hours before GFP expression was analyzed by flow cytometry and the percentage of cells transduced was used to calculate as infectious units/per ml for the pseudovirus supernatant. We also did SEAP analysis to examine the correlation between SEAP and GFP. For SEAP analysis the supernatants from the transduced cells were collected and mixed with QuantiBlue substrate (10μl supertanant+ 90μl substrate). After incubation at 37ºC samples were acquired on a plate reader.

### 3.2.10 Pseudovirus-based neutralization assay

Sixteen hours prior to infection, $1x10^4$ 293FT-hACE2 and 293FT-hACE2-TMPRSS2 cells were seeded in 100 μl full growth media into flat bottom 96-well plates. Plasma samples were heat-inactivated in microcentrifuge tubes by heating to 56°C for 30 minutes, starting approximately 1 hour before infection of cells. At the end of heat inactivation, tubes were centrifuged in a tabletop microcentrifuge for 10 seconds at top speed to get rid of any precipitates and the supernatant was used. We used an initial plasma dilution of 1:20 and did 2-fold serial dilutions in serum-free DMEM up to 1:20480. For ACE2-IgG we used an initial concentration of 20μg/ml and did 2-fold serial dilutions in serum-free DMEM up to 19ng/ml. The plasma and/or ACE2-IgG1 dilutions were mixed with pseudovirus supernatants in triplicates in the wells of a fresh 96-well plate and incubated at 37 °C for 1 hour. At the end of the incubation these mixtures were transferred to wells with seeded cells and incubated overnight in the presence of 8 μg/ml Protamine Sulfate. Next day (24h post transduction), medium was changed and cells were cultured for 72 hours before GFP expression was analyzed by flow cytometry or SEAP analysis was done by plate reader.

Results of neutralization assays were plotted by normalization to samples where no plasma was used and the half-maximal inhibitory concentration (IC50) was calculated

using 4-parameter non-linear regression. The results of regression analysis were only deemed acceptable when the R2 value was above 0.9 and the dilution factor corresponding to the calculated IC50 was used as Neutralizing Titer 50 (NT50) values.

### 3.2.11 Donors and convalescent plasma samples

This study was approved by The Turkish Ministry of Health's Scientific Research Platform (05.05.2020) and by Boğaziçi University Institutional Review Board for Research with Human Subjects (FMINAREK) (04.08.2020-2020/07). Samples taken from clinical centers were also approved by their respective authorities (by Marmara University Clinical Research Ethics Committee (08.05.2020/554) and by Istanbul Faculty of Medicine Clinical Research Ethics Committee (11/05/2020-81367). All convelascent plasma donors applied voluntarily to the blood bank of Marmara University Pendik Education and Research Hospital for donation. They were screened and fulfilled the criteria for convalescent plasma donation set forth in the Turkish Ministry of Health's Handbook on COVID-19 Immune Plasma Procurement and Use. All donors signed informed consent for the study. Demographic information, comorbidities, symptoms, signs, imaging and PCR results were retrospectively collected from electronic health records. Severity of the patients at the time of diagnosis was defined using the World Health Organization (WHO) ordinal scale for clinical improvement. The overall characteristics of donors are given in Table 4.1.

Criteria to become a convalescent plasma donor involved: COVID-19 infection confirmed with a positive PCR result, 14 days past after recovery with two negative PCR results or 28 days past after recovery, and a positive SARS-CoV-2 IgG antibody result. A total of 430 mL convalescent plasma was collected using apheresis method in a Haemonetics MCS+ system. Plasma were cryopreserved as 200 ml per bag, while 30 ml was spared for experimental analysis.

### 3.2.12 Data analysis and statistics

Flow Cytometry data was analyzed using FlowJo v10.1 software (BD Biosciences). For the preparation of graphs and for statistical analysis, Prism v8.4.3 software (GraphPad

Software) was used. Additional information regarding the applied statistical tests are provided in relevant figure legends.

For the analysis of neutralizing activity, results of neutralization assays were plotted by normalization to samples where no plasma was used and the half-maximal inhibitory concentration (IC50) was calculated using 4-parameter non-linear regression. The dilution factor corresponding to the calculated IC50, that is the 1/IC50 value was used as Neutralizing Titer values.

# 4. RESULTS

## 4.1 Overexpression of hACE2 and TMPRSS2 in 293FT cells

To make 293FT cells susceptible to infection with Spike-pseudotyped lentiviral vectors, they were genetically engineered to overexpress the hACE2 and TMPRSS2 receptors. The hACE2 gene was cloned into the LeGO-iT2puro vector, which encodes a bicistronic transcript with an IRES sequence followed by a tdTomato fluorescent protein fused to a puromycin resistance gene under the control of an SFFV promoter (Figure 4.1A and 4.1B). The TMPRSS2 gene was cloned into pLV-EF1a-iPuro, which encodes a bicistronic transcript including an IRES sequence followed by a puromycin resistance gene under the control of the EF1a promoter. (Figure 4.1D). Flow cytometry was used to confirm the enrichment of tdTomato expressing hACE2+ cells after genetic modification and puromycin selection. Additionally, we used flow cytometry and confocal microscopy to examine the surface expression of hACE2 using an RBD-GFP fusion protein. Flow cytometry labeling with RBD-GFP demonstrated that 293FT cells modified with the LeGO-ACE2-iT2puro vector produced abundant hACE2 receptors on their cell surface, but control cells changed with an empty LeGO-iT2puro vector lacked RBD-GFP fluorescence (Figure 4.1A and 4.1B). This was corroborated further by microscopy examination, which revealed that the RBD-GFP labeling on the cell surface of transformed 293FT cells guaranteed appropriate hACE2 receptor expression and membrane trafficking (Figure 4.1C). The pLV-EF1a-TMPRSS2iPuro vector was employed to modify 293FT-ACE2 cells genetically (Figure 4.1D). By using qRT-PCR, we demonstrated that TMPRSS2 expression was very high in TMPRSS2+ 293FT cells (about 4000 times higher than in WT 293FT cells and hACE+ 293FT cells) (Figure 4.1E).

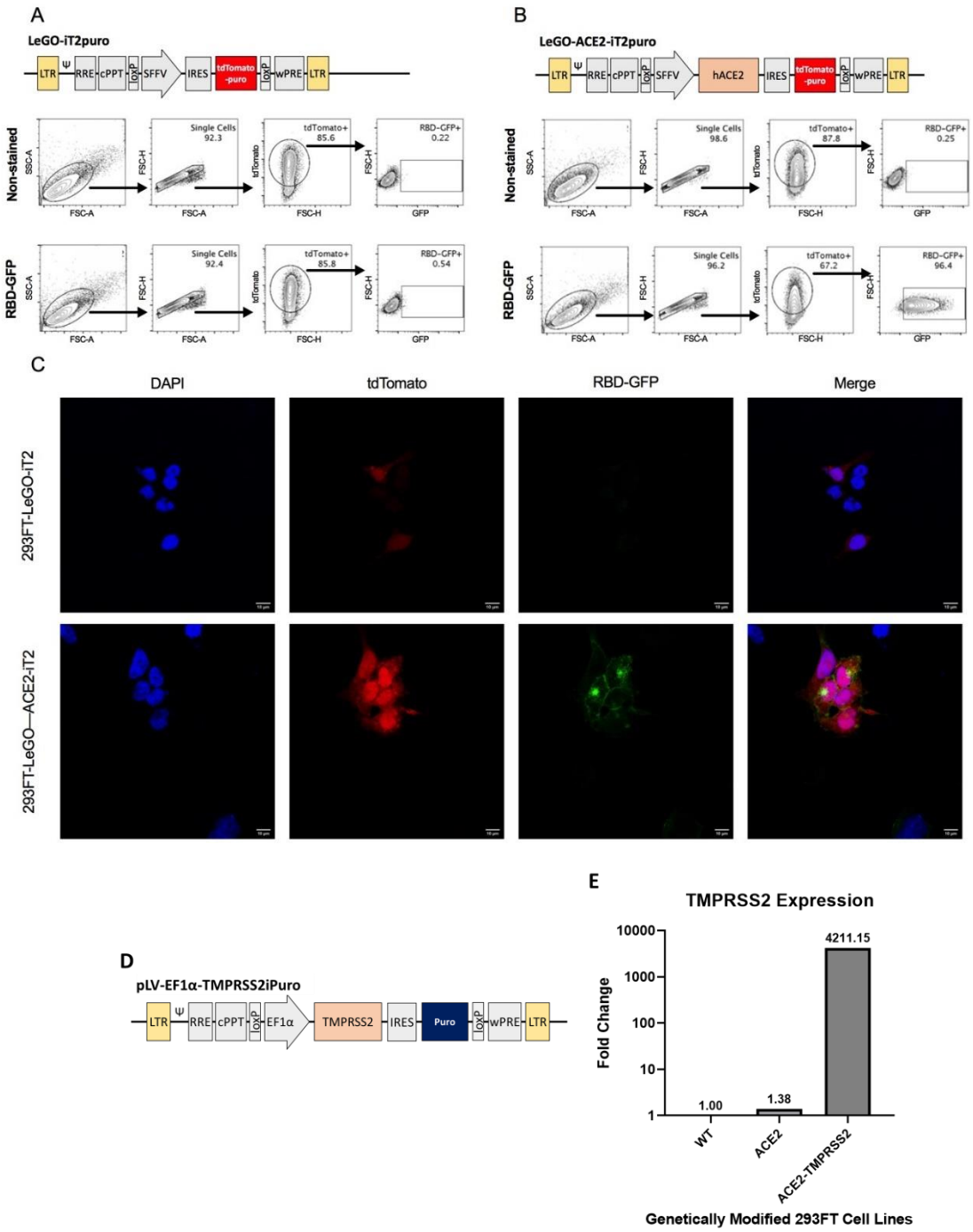


**Figure 4.1. Overexpression of hACE2 and TMPRSS2 in 293FT cells.** Upper panels in **(A)** and **(B)** represent the maps for the empty LeGO-iT2puro vector backbone and LeGO-hACE2-iT2puro vector used to genetically modify 293FT cells. Lower panels show representative flow cytometry analysis of RBD-GFP fusion protein staining on tdTomato or hACE2-tdTomato expressing 293FT cells. **(C)** Representative confocal microscopy images generated from RBD-GFP fusion protein stained tdTomato and hACE2-tdTomato expressing HEK293FT cells. **(D)** Plasmid map of pLV-EF1a-TMPRSS2iPuro vector used to genetically modify 293FT-ACE2 cells. **(E)** qPCR results of TMPRSS2 expression levels of genetically modified hACE2-293FT and hACE2-TMPRSS2-293FT cell lines. Data normalized to wild type 293FT cell line.

## 4.2 Optimization of conditions for basic pseudovirus production and transduction

To construct Spike-pseudotyped lentiviral vectors, the SARS-CoV-2 Spike gene was cloned into the pCMV backbone, which was also routinely used to produce the VSV-G envelope protein. The constructs used for pseudotyping included pCMV-Spike, which encodes the wildtype Spike protein, and pCMV-SpikeΔ19, which encodes the wildtype Spike protein but lacks the last 19 amino acids that function as an endoplasmic reticulum retention signal (ERRS). Additionally, site-directed mutagenesis was used on these two constructs to introduce the D614G mutation, resulting in the creation of two additional plasmids: pCMV-Spike(D614G) and pCMV-SpikeΔ19(D614G), and it was used on both pCMV-SpikeΔ19 and pCMV-SpikeΔ19(D614G) constructs to introduce the N501Y mutation (Figure 4.2). Pseudovirus production was carried out as described in Figure 4.3A, using calcium-phosphate precipitation to co-transfect one of the Spike-encoding plasmids into 293FT cells along with the LeGO-G2 lentiviral transfer vector encoding the green fluorescent protein (GFP) and the packaging plasmids encoding for Rev and Gag/Pol. The supernatants containing pseudovirus particles were collected 48 hours after transfection and their infectious ability was determined using 293FT-hACE2 cells. Flow cytometry analysis was used to determine the GFP gene delivery by the pseudovirus into 293FT-hACE2 cells three days after transduction (Figure 4.3 E).

Additionally, in an attempt to maximize pseudovirus particle generation, several conditions during transfection and supernatant collection were evaluated (Figure 4.3). First, the amount of envelope plasmid encoding the Spike protein included inside the transfection mixture was carefully titrated from 0.25 to 4μg. (Figure 4.3B). While small amounts of pCMV-Spike plasmid were insufficient for effective pseudovirus generation, concentrations more than 1 μg produced significantly lower titers owing to the possible toxic effects of Spike overexpression in 293FT cells. Our results demonstrated that using

0.5 µg pCMV-Spike19 was optimum for producing Spike-pseudotyped lentiviral vector particles under these conditions.

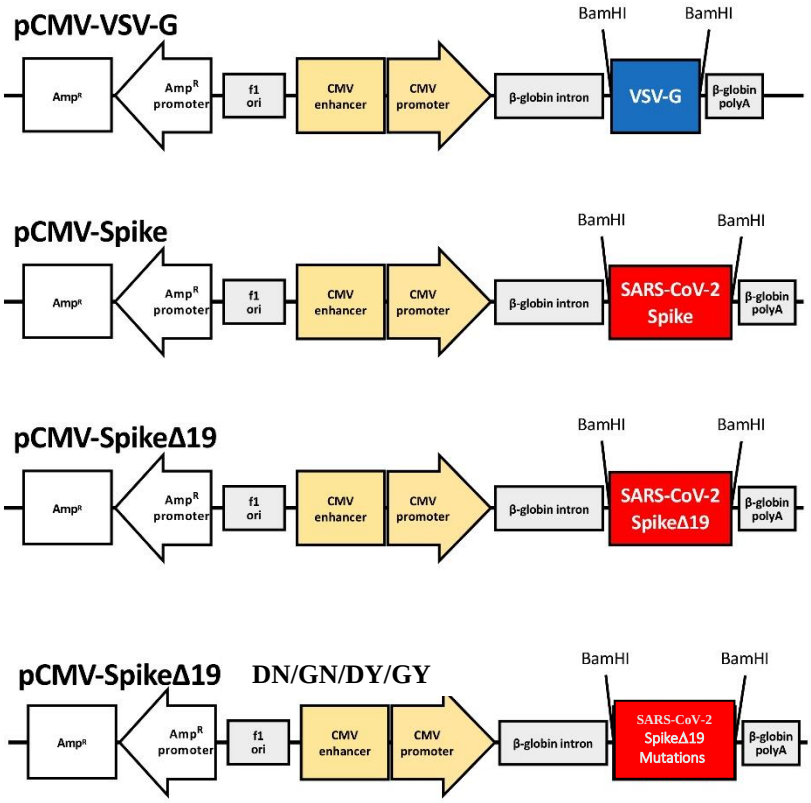


**Figure 4.2. Maps of plasmids used for expression of SARS-CoV-2 Spike protein.** pCMV-VSV-G backbone was used to clone different Spike sequences to be used for pseudotyping. Spike: Full length Spike protein. SpikeΔ19: Spike protein lacking 19 amino acids at the C terminal. SpikeΔ19(DN/GN/DY/GY): 4 different Spike proteins (DN: Wild Type Spike protein, GN: D614G mutated Spike protein, DY: N501Y mutated Spike protein, GY: Both N501Y and D614G mutated Spike protein) lacking 19 amino acids at the C terminal.

Following that, we evaluated the use of Sodium Butyrate (NaBut) to boost pseudovirus titers, as has been routinely reported in the literature for a variety of different pseudotypes. Indeed, post-transfection use of NaBut significantly increased the number of Spike-pseudotyped lentiviral particles produced (Figure 4.3C). While NaBut seemed to be harmful to producer cells at higher concentrations, we showed that a 2 mM concentration was acceptable and significantly boosted pseudovirus production.

We performed a series of experiments to determine whether the quantity of FBS in the collection medium or the temperature at which the cells were incubated influenced pseudovirus generation (Figure 4.3D). During production, no significant difference in pseudovirus titers was seen when varied FBS concentrations (2.5-10%) or incubation temperatures (35$^{o}$C vs 37$^{o}$C) were used. As a consequence of these findings, we chose to maintain the traditional approach of using 10% FBS and incubating at 37$^{o}$C for pseudovirus production.

Finally, we tried to improve pseudovirus transduction settings by determining if spinoculation or prolonged incubation durations significantly impacted the efficacy of gene transfer to 293FT-hACE2 cells. Our data demonstrated that spinning at 1000xg for 60 minutes during transduction resulted in a considerable increase in the number of GFP+ cells, especially in experiments using lower titer supernatants (Figure 4.3F). Additionally, we discovered that prolonged co-incubation of 293FT-hACE2 cells with pseudovirus particles increased gene delivery efficiency up to the 24h timepoint, at which point the number of GFP+ cells remained unchanged (Figure 4.3G). We chose not to use spinoculation for the development of neutralization tests due to practical concerns and the unnecessary risk of aerosol creation during spinoculation. Instead, we opted to use 24h co-incubation of the pseudovirus with 293FT-hACE2 cells.

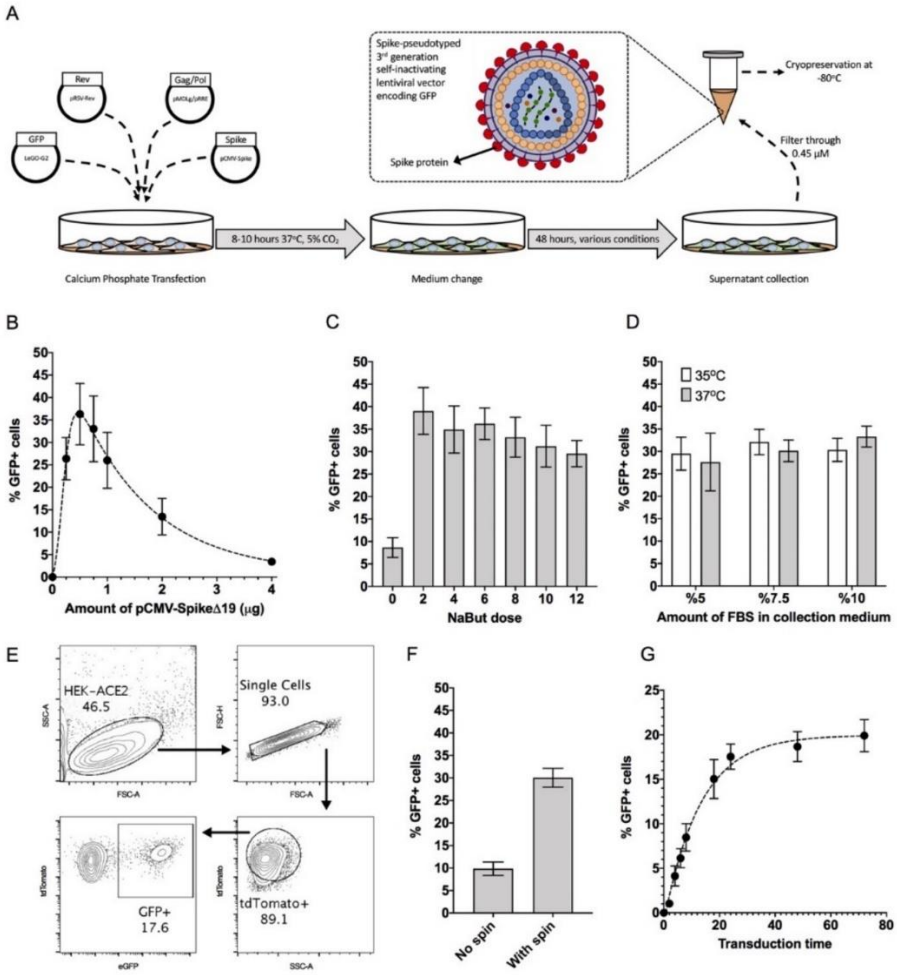


**Figure 4.3. Optimization of conditions for basic pseudovirus production and transduction. (A)** Representative protocol for the production of Spike-pseudotyped lentiviral vectors encoding GFP. **(B)** Percentage of GFP+ 293FT-hACE2 cells after transduction with pseudovirus containing supernatants prepared with varying levels of the plasmid pCMV-SpikeΔ19 during transfection. (Data from one representative experiment runt in triplicates, Mean +/- SEM plotted) **(C)** Percentage of GFP+ 293FT-hACE2 cells after transduction with pseudovirus containing supernatants collected in cell growth medium containing different concentrations of Sodium Butyrate (Data from one representative experiment runt in triplicates. **p<0.005, n.s. not significant, One-way ANOVA, Tukey's test) **(D)** Percentage of GFP+ 293FT-hACE2 cells after transduction with pseudovirus containing supernatants collected under different concentrations of FBS and temperatures. (Data from one representative experiment runt in triplicates. n.s. not significant) **(E)** Representative flow cytometry analysis of GFP expression 3 days after pseudovirus treatment of 293FT-hACE2 cells. Effects of **(F)** spinoculation and **(G)** exposure time to pseudovirus during transduction of 293FT-hACE2 cells. (Data from two experiments with two different batches of pseudovirus run in triplicates, **** p<0.001, paired t-test, two-tailed)

### 4.3 Production of enhanced pseudovirus by the addition of SARS-CoV-2 M, N and E proteins into the pseudovirus

We further tried to develop the pseudovirus particles by incorporating the M, N and E proteins of the SARS-CoV-2 virus. For this purpose, we included plasmids encoding the M, N, and E proteins during the transfection of 293FT cells for pseudovirus production (Figure 4.4A). After using produced supernatants on ACE2-expressing or ACE2 and TMPRSS2 expressing 293FT cells, we identified that the inclusion of M, N and E proteins increases the production efficiency 3-4 fold for SpikeΔ19-pseudotyped viruses. On the other hand, production efficiency with M, N and E proteins increased 2-3 fold for SpikeΔ19-D614G-pseudotyped viruses (Figure 4.4B).

Next, we examined the production of pseudovirus particles by using changing amounts of (0.25 μg, 1 μg) M, N and E expressing plasmids during transfection. Our data demonstrated that using 0.25 μg plasmids for relevant proteins during transfection showed the highest pseudovirus titer (approximately $1{,}7x10^5$infectious particles per ml) (Figure 4.4C).

We also tried to determine the impact of D614G mutation on pseudovirus production, and stability. To do this, pseudovirus particles with the D614G mutation and/or the M protein were used to infect 293FT-hACE2 cells immediately after supernatant collection and during a freeze/thaw cycle at -80$^o$C or incubation at 37$^o$C.

Our results demonstrate that the D614G mutation significantly increases pseudovirus production efficiency (Figure 4.5A), which can be attributed, at least in part, to the considerably increased stability of viral particles carrying the D614G mutation, which was most noticeable at 37$^o$C, where the half-life of pseudovirus particles was increased to 12 hours, compared to the 5 hours observed with the wildtype Spike protein (Figure 4.5B). These findings indicated that the D614G mutant exhibits higher stability and in

vitro infectivity. Additionally, we noticed that the insertion of M protein alone into the particles has no effect on production efficiency but may somewhat decrease the pseudovirus's stability. (Figure 4.5A and 4.5B).

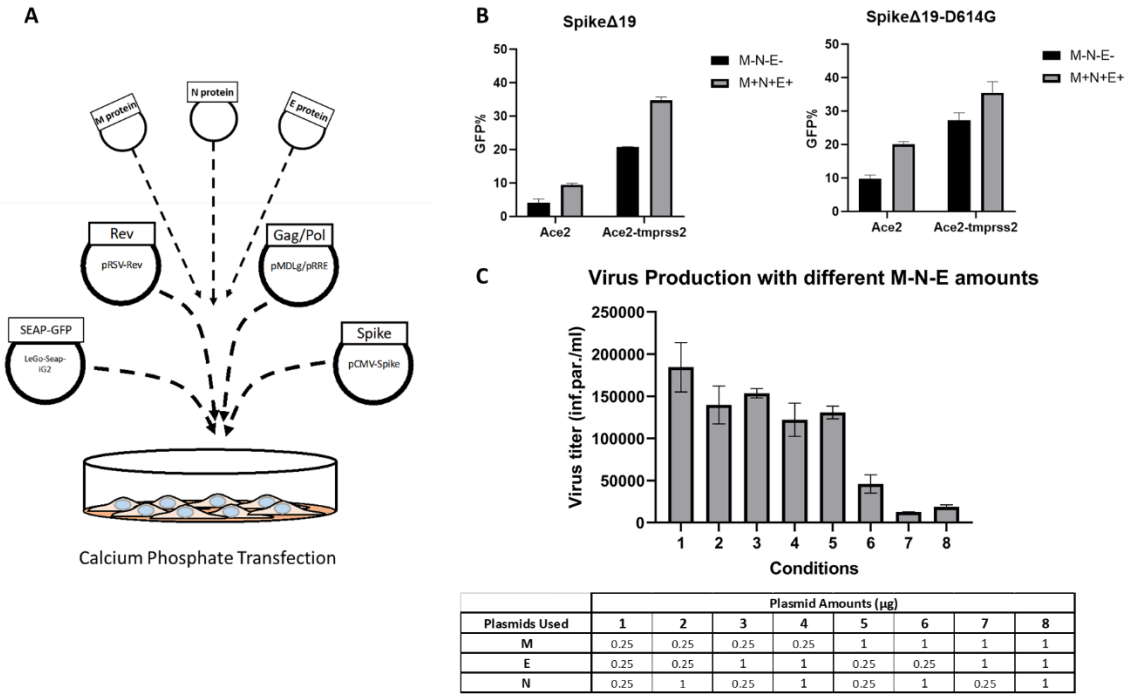


| | Plasmid Amounts (µg) | | | | | | | |
|---|---|---|---|---|---|---|---|---|
| Plasmids Used | 1 | 2 | 3 | 4 | 5 | 6 | 7 | 8 |
| M | 0.25 | 0.25 | 0.25 | 0.25 | 1 | 1 | 1 | 1 |
| E | 0.25 | 0.25 | 1 | 1 | 0.25 | 0.25 | 1 | 1 |
| N | 0.25 | 1 | 0.25 | 1 | 0.25 | 1 | 0.25 | 1 |

**Figure 4.4. Production of enhanced pseudovirus. (A)** Representative protocol for the production of Spike-pseudotyped lentiviral vectors encoding SEAP-GFP with M, N and E proteins. Lego-SEAP-iG2 lentiviral plasmid was co-transfected into 293FT cells, packaging constructs, the plasmid for Spike expression and M, N and E plasmids. Collected supernatants containing pseudovirus particles were used to infect 293FT-hACE2 and 293FT-hACE2-TMPRSS2 cells. **(B)** Percentage of GFP+ 293FT-hACE2 and 293FT-hACE2-TMPRSS2 cells after transduction with pseudoviruses with or without M, N and E proteins. **(C)** The virus titer (infectious particles/ml) of pseudoviruses produced with different amount of M, N and E plasmids (0.25µg-1µg/per transfection).

### 4.4 Development of neutralization assay using Spike-pseudotyped lentiviral vectors

After generating four different forms of pseudovirus particles, we aimed to examine if these modifications affected their neutralization by soluble ACE2-IgG. To analyze this, serial dilutions of pure ACE2-IgG were added to the medium during co-incubation of 293FT-hACE2 cells with pseudovirus particles. The percentage of GFP+ cells in each type of pseudovirus was normalized to samples without ACE2-IgG. As predicted, ACE2-IgG seemed to be exclusively inhibiting Spike-hACE2 interaction on the target cell surface, as no neutralizing effect was found when VSV-G pseudotyped particles were used. There was no noticeable difference in the susceptibility of pseudo-viral particles to neutralization by soluble ACE2-IgG, and the IC50 values calculated using these curves ranged between 4 and 8 g/ml. The supplementary sum-of-squares F test revealed no statistically significant difference between the various pseudotypes when the curves were compared (Figure 4.5C and 4.5D).

Taken together, our data demonstrate that, although the titer and stability of the pseudovirus can differ depending on the components used, they remain equally susceptible to neutralization by ACE2-IgG.

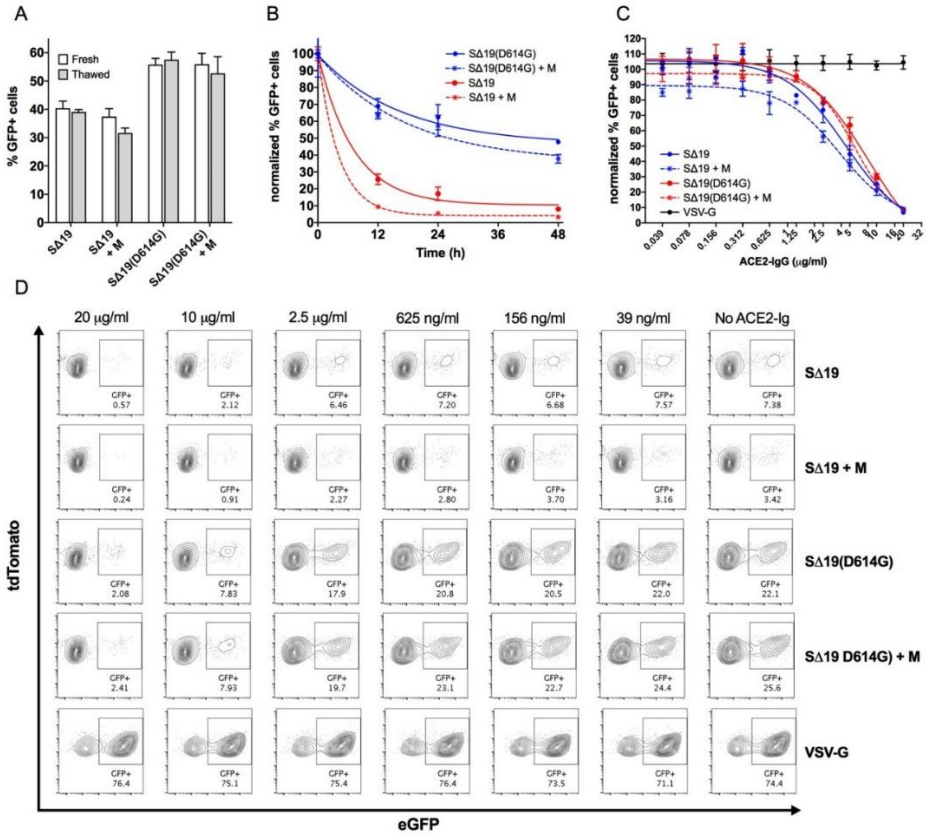


**Figure 4.5. Development of neutralization assay using Spike-pseudoyped lentiviral vectors. (A)** Percentage of GFP+ 293FT-hACE2 cells after transduction with pseudovirus containing supernatants using the WT or D614G SpikeΔ19 plasmids with or without the M protein plasmid. Transductions are done with either fresh or frozen and thawed viruses. (Results from three different batches of pseudovirus each run in triplicates, ** p<0.005, two-way ANOVA, Sidak's test) **(B)** Stability of SpikeΔ19 and SpikeΔ19(D614G) pseudoviruses with or without the M protein. Pseudovirus supernatants were incubated at 37ºC for up to 48 hours followed by transduction to tdTomato-hACE2 expressing HEK293FT cells. Data normalized to transduction results of freshly thawed supernatant. (Analyzed with one-phase decay model with least squares fit, R2>0.9 for all curves) **(C)** ACE2-IgG mediated neutralization of SpikeΔ19 and SpikeΔ19(D614G) lentiviruses with or without M protein. Spike-pseudotype and VSV-g enveloped lentiviruses were pre-incubated with various concentrations (20μg/ml – 39ng/ml) of ACE2-IgG for 1 hour at 37ºC followed by transduction of tdTomato-hACE2 expressing 293FT cells. VSV-G pseudotyped particles incubated with hACE2-IgG were used as control. Graph shows the percentage of GFP expressing cells as normalized to transduced without any ACE2-IgG pre-incubation. (Curve fitting was done by 4-parameter non-linear regression using variable slope, R2 values for all curves except VSV-G were above 0.9) **(D)** Results of flow-based analysis of neutralization by ACE2-IgG from one representative experiment.

### 4.5 Analysis of neutralizing activity in convalescent plasma samples

After demonstrating the effective neutralization of a variety of pseudovirus particles using soluble ACE2-IgG, we examined the neutralizing activity of plasma samples from recovered seropositive COVID-19 patients who volunteered to become convalescent plasma donors. Supernatants carrying pseudovirus were co-incubated at 37ºC for 1 hour with donor plasma at different dilutions ranging from 1/20 to 1/20480 before being applied in triplicate to 293FT-hACE2 cells in 96-well plates. Each donor's plasma was tested against the four different pseudotypes mentioned in Figure 4.5, as well as the control VSV-g pseudotype (Figure 4.6A). As negative controls, plasma samples from seronegative healthy donors were used and they had no neutralizing effect on any pseudotype (Figure 4.6B).

Using this technique, we examined the neutralizing activity of CP samples from 16 donors who had recovered from COVID-19 and were selected in accordance with the guidelines of the Turkish Ministry of Health. We found significant neutralizing activity in a subset of donors (Figure 4.6C), but little to no neutralization of the pseudovirus particles in others (Figure 4.6D). Our study found that 7/16 donors (44%) fell into this category of donors with very low neutralizing activity, for whom we were unable to determine NT50 values since even the lowest dilution of plasma used in the experiment was unable to neutralize half of the pseudovirus employed in the assay. Curve fitting was successful ($R^2$>0.9) for the remaining 9/16 donors (56%), and NT50 values were calculated. These findings suggest that the level of neutralizing activity in convalescent plasma samples varies considerably, and that identifying donors simply on the basis of IgG positivity may not be the most accurate method for predicting the efficacy of convalescent plasma treatment.

Consistent with this observation, we find that none of the donors presenting with low-activity plasma had been hospitalized due to COVID-19 and the extent of symptoms at diagnosis was generally higher in the group with high-activity CP (Table 4.1).

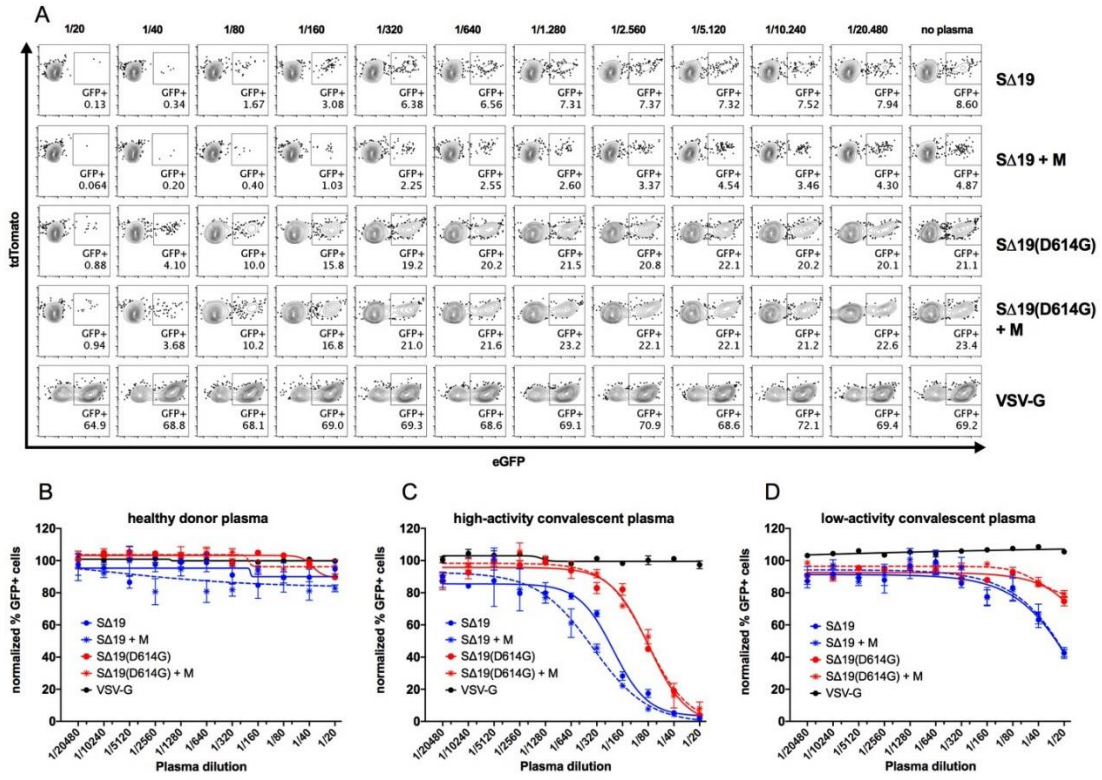


**Figure 4.6. The use of Spike pseudovirus for analysis of neutralizing activity in convalescent plasma samples**. Spike or VSV-G pseudotyped particles were incubated with serial dilutions (1:20 – 1:20480) of CP samples for 1 hour at $37^0$C followed by transduction to 293FT-hACE2 cells. VSV-G enveloped lentiviruses incubated with CP samples were used as negative controls. **(A)** Representative flow cytometry analysis of CP dependent neutralization assay from one donor. Plasma samples from healthy donors and 16 patients that recovered from COVID-19 were analyzed **(B)** Healthy donors are used as a control group and their plasma showed no neutralization effect. (Results from one representative healthy donor) **(C)** 9/16 of CP samples showed high neutralization activity. (Results from one representative high-activity CP) **(D)** 7/16 of CP samples showed no or low neutralization. (Results from one representative low-activity CP) Curve fitting was done by 4-parameter non-linear regression using variable slope.

***** World Health Organization (WHO) ordinal scale for clinical improvement available at https://www.who.int/publications/i/item/covid-19-therapeutic-trial-synopsis

| | All donors (n=16) | High Activity (n=9) | Low Activity (n=7) |
|---|---|---|---|
| Median Age (Range) | 40 (25-51) | 43 (35-50) | 36 (25-51) |
| Male / Female | 15 / 1 | 9 / 0 | 6 / 1 |
| CT positive (%) | 62,5 | 77,8 | 42,9 |
| Hospitalized (WHO scale ≥ 3)* (%) | 31,3 | 55,6 | 0,0 |
| Mean days from PCR+ to PCR – (Range) | 18,0 (2-33) | 14,5 (2-28) | 22,4 (12-33) |
| Symptoms at diagnosis (%) | | | |
| Fever | 50,0 | 66,7 | 28,6 |
| Cough | 68,8 | 88,9 | 42,9 |
| Shortness of breath | 31,3 | 44,4 | 14,3 |
| Headache | 33,3 | 37,5 | 28,6 |
| Muscle pain | 57,1 | 57,1 | 57,1 |
| Nausea | 7,1 | 14,3 | 0,0 |
| Diarrhea | 7,1 | 14,3 | 0,0 |
| Throat ache | 26,7 | 25,0 | 28,6 |
| Loss of smell | 14,3 | 0,0 | 28,6 |

**Table 4.1.** Characteristics and COVID-19 history of CP donors used in the study.

### 4.6 Analysis of neutralizing activity in high-activity convalescent plasma samples

Apart from determining the NT50 values via the pseudovirus-based neutralization test, we performed a semi-quantitative analysis of anti-SARS-CoV-2 antibodies in CP samples using WIZ Biotech's colloidal-gold-based fast detection kit in conjunction with the WIZ-A101 Portable Immunoanalyzer.

Despite the fact that IgG and IgM concentrations varied significantly across all plasma samples, high level of this positivity did not always correspond with high neutralizing activity (Figure 4.7A and 4.7B). While some plasma samples with high SARS-CoV-2 specific IgG titers demonstrated significant neutralization activity, our results also revealed the presence of donors with high IgG positivity who exhibit no detectable neutralizing activity, as well as donors with relatively low IgG positivity who perform better than expected. This absence of a direct association shows that the neutralizing activity of plasma is more dependent on the quality than on the quantity of the humoral immune response.

Additionally, our findings indicated that donor-dependent variations in the neutralizing activity of plasma samples against various viral pseudotypes (Figure 4.7C). Although the degree of neutralizing activity against the other pseudotypes remained constant, a trend toward decreased neutralization of the D614G mutant was noted. While these data suggest a distinct humoral response to the D614G mutant, the fact that we do not know the genotype of the virus that initially infected the donor prevents us from speculating more on this subject. The reaction to pseudovirus particles containing the M protein likewise varied donor-dependently and had no significant influence on the measured NT50 values.

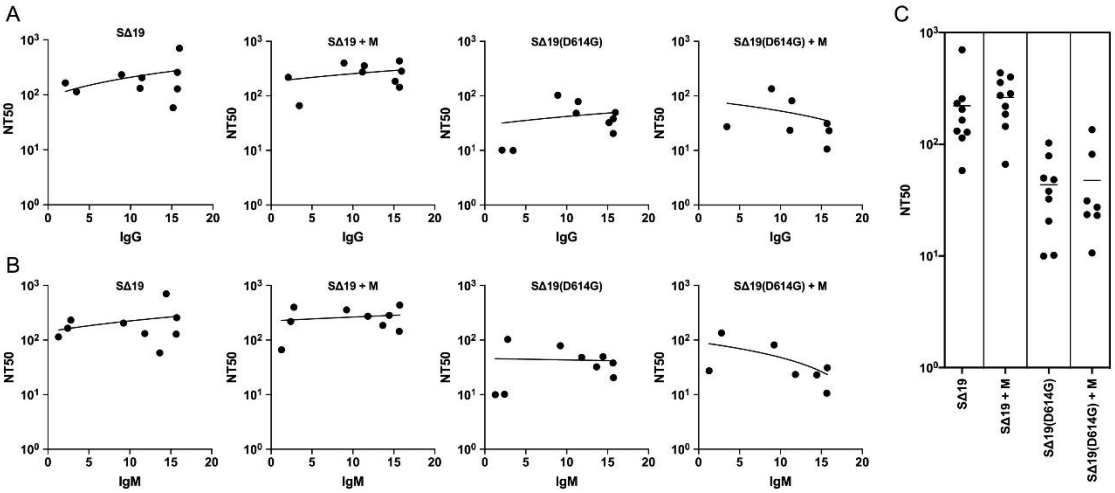


**Figure 4.7. Analysis of neutralizing activity in high-activity convalescent plasma samples.** The dilution factor corresponding to the calculated IC50 was used as Neutralizing Titer 50 (NT50) value. **(A)** NT50 values against the various pseudotypes used in this study plotted against IgG positivity measured a semi-quantitative colloidal-gold based rapid detection kit. (Lines show simple linear regression. Deviation from 0: not significant) **(B)** NT50 values against the various pseudotypes used in this study plotted against IgM positivity measured a semi-quantitative colloidal-gold based rapid detection kit. (Lines show simple linear regression. Deviation from 0: not significant) **(C)** NT50 values of high-activity convalescent plasma samples measured against the different pseudotypes used in this study.

## 4.7 Analysis of stability and transduction efficacy of Spike-pseudoviruses with different mutations

We also analyzed the stability and transduction efficacy of Spike-pseudoviruses with different mutations. Pseudovirus supernatants were incubated at $37^0$C for up to 48 hours followed by transduction to hACE2 or hACE2 and TMPRSS2 expressing cells, and the data were normalized to transduction results of freshly thawed supernatant. We observed that the D614G mutation of spike increases the transduction efficiency and the stability, especially on ACE2 positive cells, while the N501Y mutation does not seem to have this effect (Figure 4.8A-C).

As it is known, an essential factor for Spike-ACE2 interaction is the activation of Spike protein through cleavage by the TMPRSS2 enzyme on the cell surface. In order to mimic this detail of SARS-CoV-2 infection, we also transferred TMPRSS2 lentivirally to 293FT cells expressing ACE2 and observed that it had a significant effect on pseudovirus infection, as expected (Figure 4.8B). Also, the overexpression of TMPRSS2 seems to increase infection by the N501Y mutation dramatically but seems to affect the D614G variant minimally (Figure 4.8C).

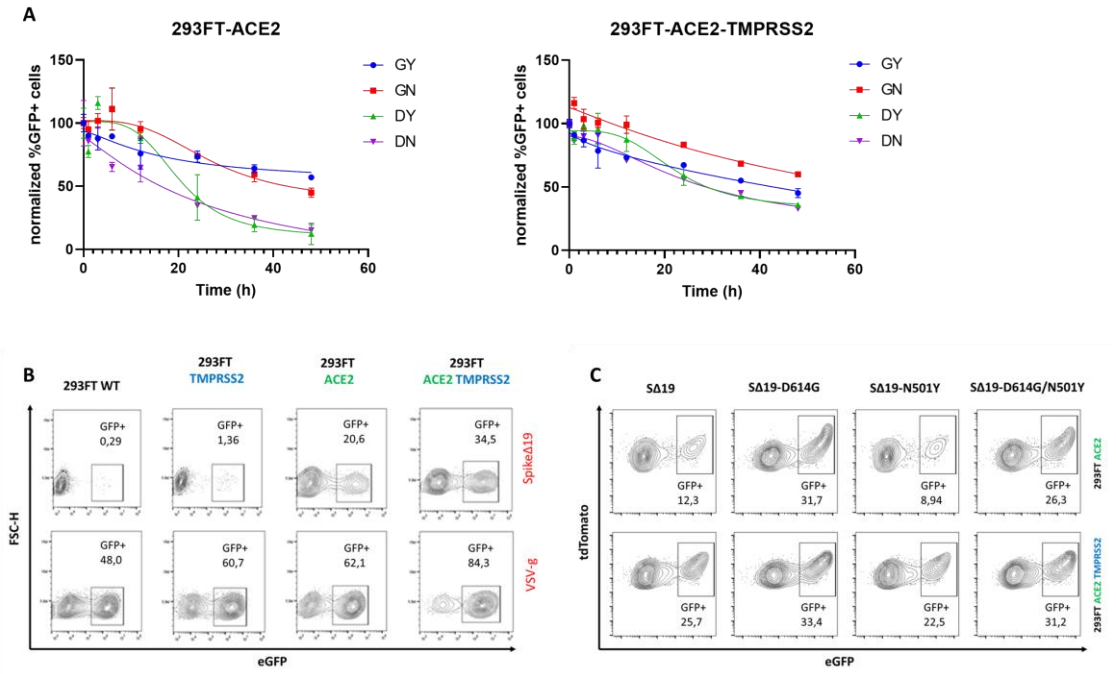


**Figure 4.8. Analysis of stability and transduction efficacy of different variants of Spike-pseudoviruses. (A)** Stability of lentiviral pseudoviruses. Pseudovirus supernatants were incubated at 37°C for up to 48 hours followed by transduction to hACE2 or hACE2 and TMPRSS2 expressing HEK293FT cells. Data normalized to transduction results of freshly thawed supernatant. **(B)** Flow cytometry analysis of transduction using Spike or VSV-G pseudotyped particles on hACE2 or TMPRSS2 or hACE2 and TMPRSS2 expressing HEK293FT cells. VSV-G enveloped lentiviruses were used as negative controls. **(C)** Flow cytometry analysis of transduction using lentiviral pseudoviruses produced with different mutations of spike protein (WT – D614G – N501Y – D614G/N501Y) on hACE2 or hACE2 and TMPRSS2 expressing HEK293FT cells.

## 4.8 The use of SEAP-based methods

For a standart neutralization test so far, we used each donor plasma at dilutions ranging from 1:20 to 1:20,000 against four different pseudovirus samples and the VSV-g pseudotype as a control. Considering that the experiment is run in triplicates, this adds up to hundreds of samples being run on a flow cytometer for each single plasma sample and seriously limits the number of samples that can be analyzed each day.

Therefore, we aimed to increase the throughput of this method with colorimetric measurements using simple Optical Density readings. For this purpose, we produced lentiviral vector-based SARS-Cov-2 pseudovirus particles encoding Secreted Embryonic Alkaline Phosphatase (SEAP). Detection of SEAP activity in cell culture supernatants proved faster and easier than Flow Cytometry based analysis of GFP expressing cells.

In this approach, we seeded target cells in full growth media into flat bottom 96-well plates six hours before infection. A lentiviral vector that encodes for both the GFP and SEAP transgenes (LeGO-SEAP-iG2) was used to make both modes of data acquisition possible. Plasma samples were heat-inactivated, and the plasma dilutions were mixed with pseudovirus supernatants for 1 hour prior to transduction. At the end of the incubation, these mixtures were transferred to wells with seeded cells and incubated overnight in the presence of 8 μg/ml Protamine Sulfate. After 24h, the first medium change was done for getting rid of viral particles. After another 24h, a second medium change was done for getting rid of uneven SEAP accumulation. At 72h, cells are ready for GFP and SEAP analysis. For SEAP analysis, the supernatants were collected and added to the SEAP substrate. After 30min to 240min of incubation at 37$^{o}$C, the samples were acquired on a plate reader (Figure 4.9).

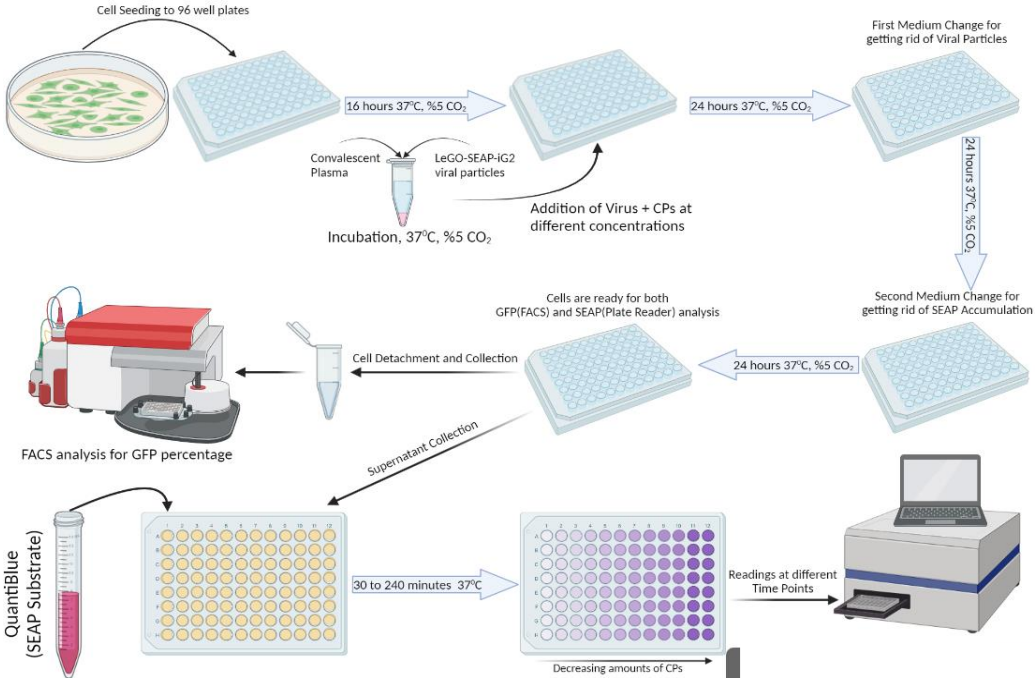


**Figure 4.9.** The use of SEAP-based methods. Representative work flow of SEAP-based neutralization assay.

We first optimized the incubation time after SEAP containing supernatants were mixed with the QuantiBlue substrate. To evaluate the sensitivity of the results, a vector encoding for both SEAP and GFP (LeGO-SEAP-iG2) was used and the same cells were acquired for GFP in flow cytometry, and the correlation of SEAP and GFP signals were analyzed. Using different convalescent plasma samples, optimized SEAP-based assays showed the best correlation ($R^2$>0.95) to GFP-based pseudovirus at 90 minutes of incubation time with supernatants from ACE2 expressing 293FT cells with the QuantiBlue substrate (Figure 4.10).

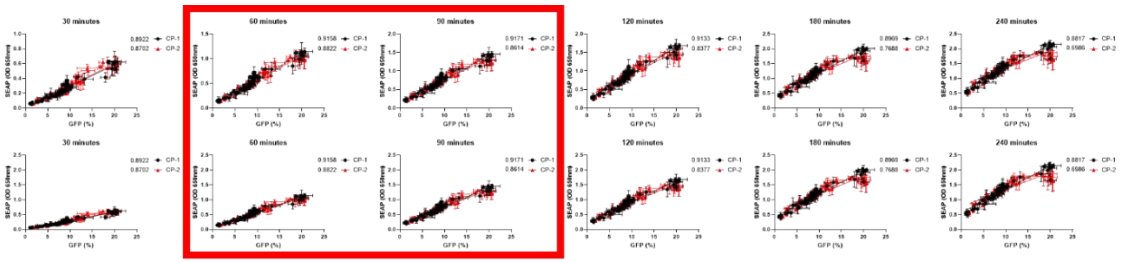

Supernatants collected at 48h

| $R^2$ Values | 30 Min | 60 Min | 90 Min | 120 Min | 180 Min | 240 Min |
|---|---|---|---|---|---|---|
| CP-1 | 0.8922 | 0.9158 | 0.9171 | 0.9133 | 0.8969 | 0.8817 |
| CP-2 | 0.8702 | 0.8822 | 0.8614 | 0.8377 | 0.7688 | 0.6986 |

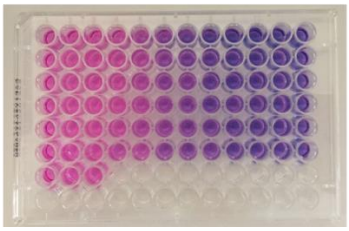

**Figure 4.10. The optimization of the SEAP-substrate incubation time for best correlation with GFP.** SEAP containing supernatants were incubated with the Quanti Blue substrate for varying amounts of time. The results from each timepoint were used to pinpoint the incubation time that gives the best correlation with the results acquired by GFP analysis in flow cytometry.

Next, we optimized the time of supernatant collection from the pseudovirus infected cells. We tested collecting supernatants 24 hour and 48 hours after the infection. Since we suspected that the uneven accumulation of SEAP during the early phases of pseudovirus infection might skew the results, we also tested changing medium at 24 hours and then collecting at 48 hours. Our results showed that the best correlation with GFP signals were seen when we did a medium change at 24h and collected supernatants at 48h, followed by 90 minutes of incubations with the QuantiBlue substrate (Figure 4.11).

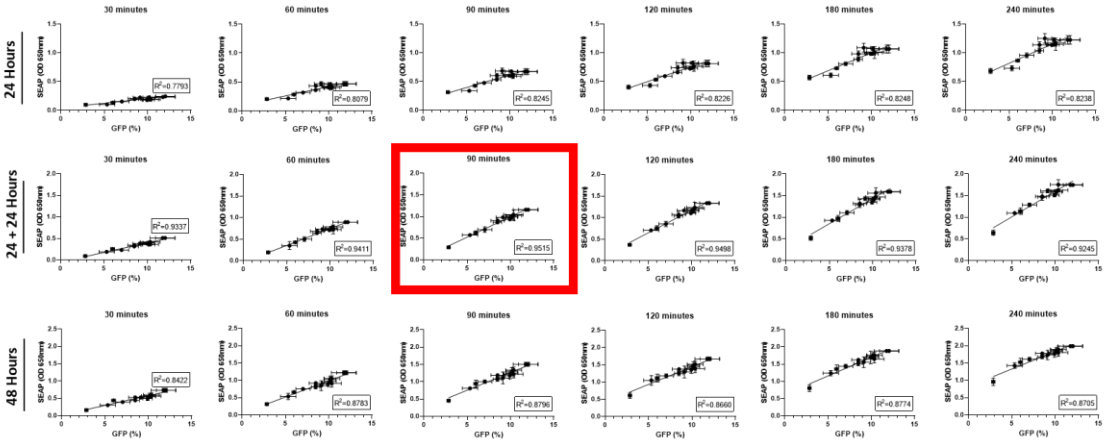


| $R^2$ Values | 30 Min | 60 Min | 90 Min | 120 Min | 180 Min | 240 Min |
|---|---|---|---|---|---|---|
| 24 Hours | 0.7793 | 0.8079 | 0.8245 | 0.8226 | 0.8248 | 0.8238 |
| 24 + 24 Hours | 0.9337 | 0.9411 | 0.9515 | 0.9498 | 0.9378 | 0.9245 |
| 48 hours | 0.8422 | 0.8783 | 0.8796 | 0.8660 | 0.8774 | 0.8795 |

**Figure 4.11. The optimization of the time of supernatant collection from the pseudovirus infected cells.** Supernatants were collected at different timepoints (24h, 24+24h, 48h) and SEAP activity was analyzed to pinpoint the incubation time that gives the best correlation with the results acquired by GFP analysis in flow cytometry.

### 4.9 SEAP-based Neutralization tests with different types of samples

We used the SEAP-encoding pseudovirus to analyze the neutralizing activity from a variety of sample types including soluble ACE2-IgG and anti-Spike antibody as well as serum samples taken from vaccinated individuals (Figure 4.12). As expected, our analysis showed higher activity of the monoclonal anti-spike antibody with an NC50 of 0.25µg/ml while the soluble ACE2-IgG showed an NC50 of 5.755µg/ml on ACE2 expressing cells (Figure 4.12A). We also tested the assay by using plasma samples from individuals receiving the Pfizer/Biontech vaccine and determining the variation in NC50 values between individuals (Figure 4.12B). We used the assay successfully on plasma samples from convalescent individuals and determined the different responses against viruses carrying different variants of the Spike protein (Figure 4.12C).

Our results showed the inter-individual variations between responses to different variants. Having optimized faster and cheaper analysis of cell-based neutralization assays, we intend to utilize this approach to analyze different cohorts of samples from patients and vaccinated individuals.

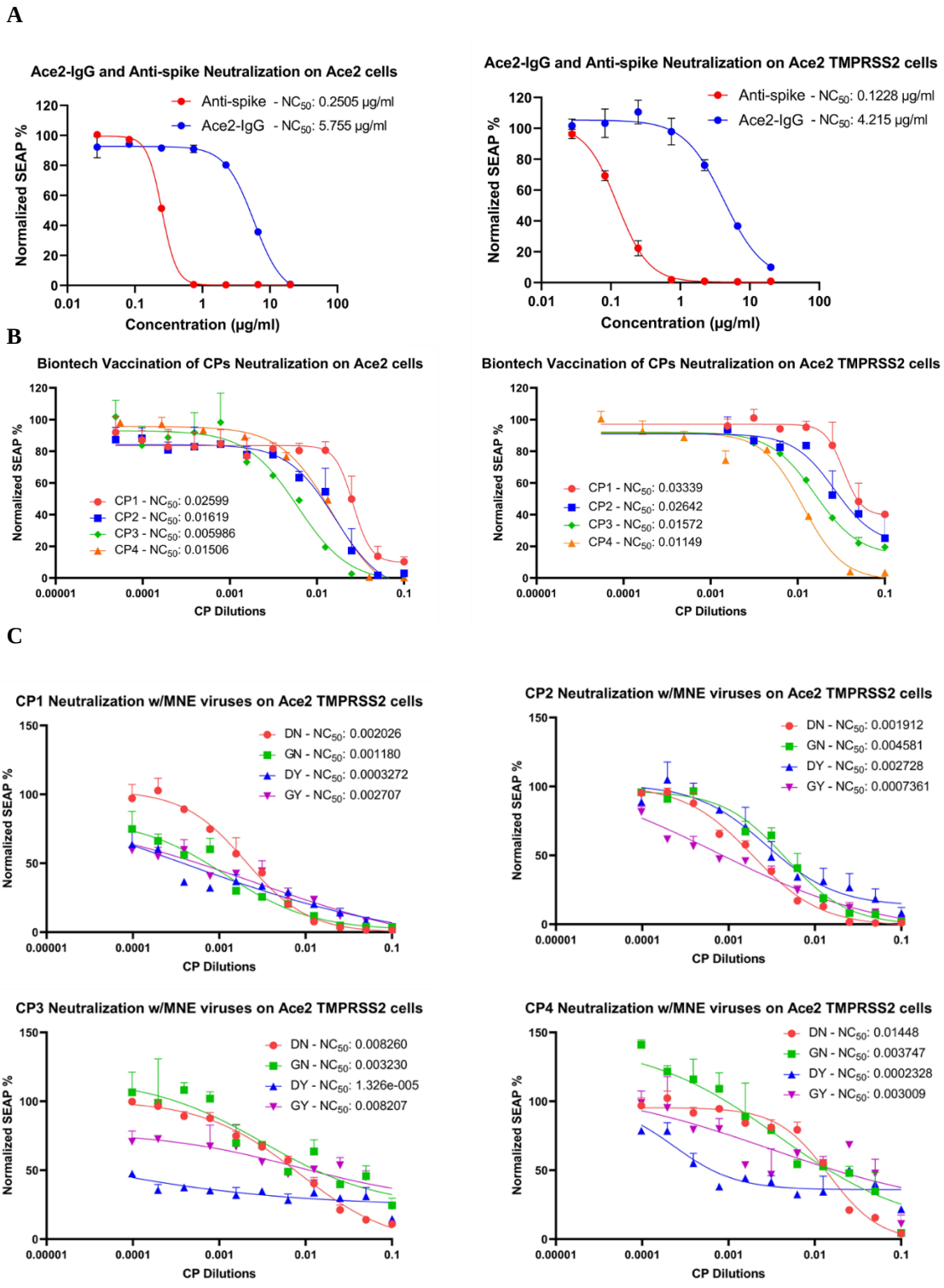


**Figure 4.12. SEAP-based neutralization tests with different types of samples. (A)** Neutralizing activity from a variety of sample types with soluble ACE2-IgG and anti-Spike antibody **(B)** with serum samples from Biontech-vaccinated individuals **(C)** with various serum samples and different variants of pseudotypes viruses on hACE2- and hACE2-TMPRSS2-293FT cells.

### 4.10 Analysis of neutralizing activity in vaccinated individuals

The kinetics of SARS-CoV-2 specific antibodies after COVID-19 infection are crucial for determining the duration of antibody-mediated protection against the virus and the optimum period for post-infection immunization. Our objective in this analysis was to examine the kinetics of SARS-CoV-2 specific antibody levels after COVID-19 infection and to evaluate the efficacy of vaccination on SARS-CoV-2 specific antibody levels and neutralizing activity.

We analyzed serum samples collected by our collaborators at Istanbul University Aziz Sancar Institute of Experimental Medicine, from a healthy two-dose Coronavac-vaccinated group (n=10), a COVID-baseline group (1 month after symptom onset of infection with SARS-COV-2) (n=19), a COVID-6 months group (non-vaccinated patients with COVID-19 at 6 months follow-up) (n=18) and a COVID-Coronavac group (individuals who have had the disease and have been vaccinated) (n=21).

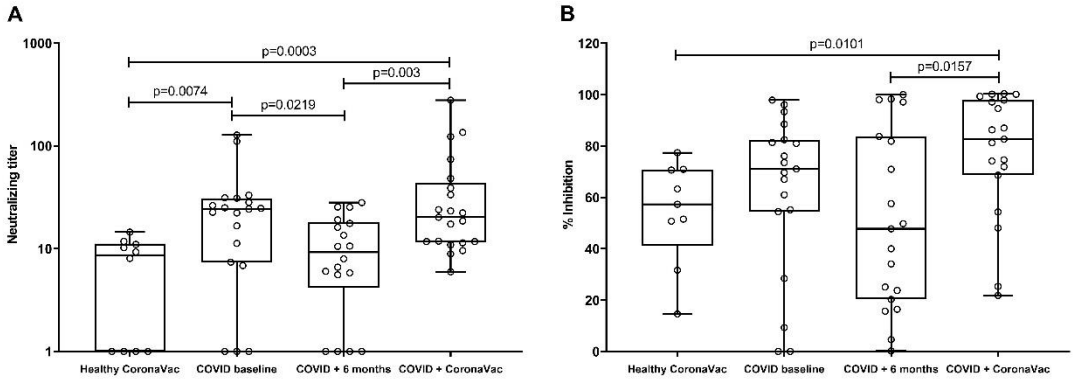


**Figure 4.13. Neutralizing activity against SARS-CoV-2. (A)** Neutralizing titer measured by a cellular experiment using lentiviral vectors pseudotyped with SARS-CoV-2 S, M, N and E proteins. **(B)** Inhibiton of ACE2 binding measured by an ELISA-based test. P values were calculated using unpaired Mann-Whitney U-test.

Analysis of neutralizing activity against a lentiviral vector pseudotyped with SARS-CoV-2 S, M, N and E proteins showed that healthy individuals vaccinated with Coronavac displayed moderate levels of neutralizing activity that was slightly lower than individuals recovering from natural SARS-CoV-2 infection. It was also observed that convalescent individuals had a significant drop in neutralizing activity as shown 6 months after the initial infection when no further vaccination was carried out. Corroborating the results from serum Ig measurements, vaccination following natural infection effectively boosted the humoral immune responses and these individuals showed the highest neutralizing activity within this cohort. Similar results were observed using the ELISA-based neutralization assay.

# 5. DISCUSSION

The COVID-19 pandemic began in late 2019 in China and quickly spread to infect millions of individuals around the worlds with SARS-CoV-2 (Dhama et al., 2020; N. Zhu et al., 2020a). While the evaluation for a long-lasting SARS-CoV-2 vaccine continues, there is yet no effective antiviral treatment for COVID-19. Passive immunotherapy techniques such as intravenous immunoglobulins (Y. Xie, Cao, Dong, et al., 2020), convalescent plasma transfer (Ju et al., 2020), and recombinant monoclonal antibodies (mAbs) as well as mAb combinations (Y. Cao et al., 2020; Tian et al., 2020; Chunyan Wang et al., 2020) are actively being studied in the clinic.

Convalescent Plasma (CP) is a passive immunotherapy approach that relies on the transfer of antibodies existing in the serum of someone who has recently recovered from the same infection (Mcguire & Redden, 1919; J. S. Zhang et al., 2005). In addition to blocking receptor contact, CP may help target complement reactions towards SARS-CoV-2 particles, thereby reducing viral multiplication (Ahn et al., 2020; Cunningham et al., 2020; S. Jiang, Zhang, et al., 2020). In the absence of better options, especially in the earlier days of the pandemic, CP therapy has often been used to treat COVID-19 patients (Kai Duan et al., 2020a; Yongchen et al., 2020).

The concentration of neutralizing antibodies (nAbs) in CP is likely to correlate with treatment efficacy (Barone & DeSimone, 2020; Kai Duan et al., 2020b). Since not all antibodies against SARS-CoV-2 antigens are neutralizing, measuring CP's neutralization activity is crucial to optimizing therapeutic benefit to the recipient. Neutralizing activity

can be measured using the wildtype SARS-CoV-2 virus in a BSL3 facility(Nie et al., 2020c) or alternatively a pseudovirus-based system in a BSL2 facility can be employed (Crawford et al., 2020). In this thesis, we have aimed at developing a pseudovirus-based neutralization test that can be used in regular BSL2 cell culture facilities in order to widen the applicability of neutralization tests.

The SARS-CoV-2 Spike protein binds to angiotensin-converting enzyme 2 (ACE2) on the plasma membrane of host cells, facilitating viral entrance (Markus Hoffmann et al., 2020a). Especially, the RBD of Spike protein is identified as a frequent target for neutralizing antibodies (Tai et al., 2020). Since the outbreak, the SARS-CoV-2 genome has accumulated several genetic variations in the Spike protein. The D614G mutation outside the Spike protein's Receptor Binding Domain (RBD) increased SARS-CoV-2 replication and infectivity (Korber et al., 2020). In neutralization tests, pseudovirions expressing full-length S protein (Amanat et al., 2020) or RBD are employed (L. Ni et al., 2020) along with the incorporation of these possible mutations that could help the virus escape nAbs. In this way, neutralization tests also provide valuable information regarding the susceptibility of novel mutants to neutralization by individuals that have recovered from the disease or got vaccinated prior to the rise of the new variant.

Pseudovirions are often generated using VSV or HIV-1 vector systems (Ou et al., 2020; Pinto et al., 2020) to include the S protein. Additionally, SARS-CoV-2 membrane (M), nucleocapsid (N), and envelope (E) proteins have also been utilized for better virus-like particle (VLP) production (Boson et al., 2021; Siu et al., 2008). Moreover, the M and E proteins were shown to be necessary for effective pseudovirus production, according to Xu et al. (R. Xu et al., 2020).

This thesis describes our attempts to create a lentiviral vector-based SARS-CoV-2 neutralization test that incorporates all structural proteins of the virus (S, M, N and E). Because the SARS-CoV-2 Spike protein binds to angiotensin-converting enzyme 2 (ACE2) on the plasma membrane of host cells, we firstly needed to appropriate target cells that express this receptor. ACE2 is abundant in many cell lines, including Vero E6 and human kidney epithelial cells. The CCL-81.4 subline of Vero was shown to generate about twice as many foci per well in plaque-forming assays (Stone et al., 2020). Caulu3, Hepatoma (Huh7.5 and Huh7), and Gastric Adenocarcinoma (AGS) have also shown effectiveness as Vero cells (Stone et al., 2020).

Human ACE2 can also be transduced or plasmid transfected into mammalian cell lines (e.g., human lung epithelial cells A549 (Xuping Xie, Muruato, Zhang, et al., 2020), human embryo kidney [HEK] 293T (Tandon et al., 2020), or 293FT, or BHK21 (Xiong et al., 2020), or human connective tissue HT1080 (Schmidt et al., 2020)) to create target cell lines for pseudovirion infection. Additionally, previous studies showed that the stable expression of TMPRSS2 increased infection susceptibility by 5–10 fold (Brochot et al., 2020; Johnson et al., 2020). In our study, we chose to genetically engineer 293FT cells to overexpress the hACE2 receptor and the TMPRSS2 protease. After genetic modification and puromycin selection, flow cytometry was utilized to confirm the enrichment of tdTomato expressing hACE2+ cells. Additionally, we examined the surface expression of hACE2 using an RBD-GFP fusion protein using flow cytometry and confocal imaging. Microscopy analysis confirmed this, demonstrating that the RBD-GFP labeling on the cell surface of transformed 293FT cells ensured proper hACE2 receptor expression and membrane trafficking. We also confirmed that TMPRSS2 expression was very high in TMPRSS2+ 293FT cells (about 4000 times more than in WT 293FT cells and hACE+ 293FT cells) using qRT-PCR.

Because pseudotyped viruses are incapable of producing infectious progeny, they provide a safe viral entry model. The test involves pseudotyping a single cycle, replication-defective viral vector with the surface protein of the virus against which nAb should be measured. Numerous coronaviruses' spike protein can be pseudotyped onto safer non-replicating viral particles in place of their natural envelope protein, hence requiring Spike-ACE2 interaction for entry into cells (Fukushi et al., 2005; Grehan et al., 2015; Letko et al., 2020b; Millet & Whittaker, 2016). Pseudotyping of SARS-CoV-2 has been described recently employed to produce HIV-based lentiviral particles (X. Chen et al., 2020; Ou et al., 2020), MLV-based retroviral particles (Pinto et al., 2020; Quinlan et al., 2020), and VSV (Markus Hoffmann et al., 2020b; Nie et al., 2020b; Xiong et al., 2020).

In this thesis, we used a 3rd generation lentiviral packaging system to produce viral particles pseudotyped with Spike protein. For pseudotyping, we used the pCMV-VSV-G backbone to remove the VSV-g envelope protein and instead clone in different variants of SARS-CoV-2 Spike protein. It has previously been reported that production of full-length SARS-CoV-2 S protein was increased more than ten-fold by removing the final C-terminal 18 or 19 amino acids, the cytoplasmic tails 26 amino acids, or by codon optimization (C. P. Thompson et al., 2020). Our initial observations showed that using

the full-length Spike gene without removing the ER retention signal was ineffective for producing pseudotyped lentiviral particles, possibly due to poor membrane translocation of the Spike protein. However, the use of pCMV-SpikeΔ19 plasmid successfully yielded lentiviral particles that could infect 293FT-hACE2 cells. Our results align with previous reports where removing the ERRS sequence has been a commonly used approach for Spike-pseudotyped vector generation (Johnson et al., 2020; Ou et al., 2020). On the other hand, several other studies have also reported efficient pseudovirus generation with full-length Spike sequences (Nie et al., 2020b; Yang et al., 2020).

Taken together, our results indicate that it might be possible to generate low-titer pseudovirus particles using the full-length Spike protein and use it for neutralization assays after concentrating supernatants. Still, the deletion of ERRS has been shown to increase titers dramatically. In our hands, the use of SpikeΔ19 for pseudovirus packaging was efficient enough to render any need for supernatant concentration obsolete.

We also studied the use of the histone deacetylase inhibitor Sodium Butyrate (NaBut) to boost pseudovirus titers, as has been routinely reported in the literature for a variety of different pseudotypes (Gasmi et al., 1999; Olsen & Sechelski, 2008). NaBut has been shown to boost the potential of 293FT cells to produce retroviral and lentiviral vectors by activating the CMV enhancer and HIV-1 LTR promoter functions (Laughlin et al., 1995). Indeed, post-transfection addition of NaBut significantly boosted the number of Spike-pseudotyped lentiviral particles produced.

The reduction of the amount of FBS used during vector production may positively effect final titers because the stability of viral particles in serum-containing medium might be lower (Dautzenberg et al., 2020). However, this approach is also considered to be a "double-edged sword" as such reduction in FBS amounts may also negatively affect the viability of the producer cells, thereby decreasing the final titer (Gélinas et al., 2017). Similarly, lowered incubation temperatures during vector production can also increase titer due to enhanced stability of viral particles (S. G. Lee et al., 1996) or decrease the titer due to negative metabolic effects on the producer cells (Beer et al., 2003). To analyze whether fine-tuning of these parameters would significantly affect the production efficiency of Spike-pseudotyped lentiviral particles, we performed a series of experiments to determine if the amount of FBS in the collecting media or the incubation temperature had any influence on pseudovirus production. Our results indicated no change in

production efficiency under varying concentrations of FBS of different incubation temperatures, therefore all pseudovirus productions were carried at 37$^{o}$C by using the standard 10% FBS.

Although many studies focus solely on the use of S protein for pseudotyping, we have additionally considered the use of other structural proteins to enhance pseudovirus production. This approach additionally provides an opportunity to take into account any possible neutralizing antibodies against these antigens while neutralization tests are being run. In previous studies, Xu et al. demonstrated that expression of membrane protein (M) and small envelope protein (E) is required for the effective production and release of SARS-CoV-2 VLPs. M protein, like other coronaviridae members, is the most prevalent envelope protein that promotes other structural components into VLPs. Though E protein is useful in viral morphogenesis and release, its mechanism of action is unknown. N protein, which encapsulates the viral DNA into virions, does not seem to be essential in SARS-CoV-2 VLP assembly (R. Xu et al., 2020).

However, a poor viral yield was one of the challenges that we and others found during the development of pseudotyped virus containing SARS-CoV-2 spike protein alone. To test pseudovirus production efficiency in the presence of additional structural components, we attempted to produce pseudovirus by integrating the SARS-CoV-2 virus's M, N, and E proteins. To do this, we added plasmids encoding the M, N, and E proteins during the transfection of 293FT cells. We studied the formation of pseudovirus particles employing different amounts of M, N, and E expressing plasmids (0.25 μg or 1 μg) during transfection. Our results indicated that transfection with 0.25 μg plasmids encoding relevant proteins resulted in the greatest pseudovirus titer (approximately 1,7x105infectious particles per ml). By employing produced supernatants on 293FT cells expressing ACE2 or ACE2 plus TMPRSS2, we observed that the addition of M, N, and E proteins enhances pseudovirus titers by 3-4 fold.

As mentioned before, an important application of neutralization tests can be their use in analyzing the neutralizing activity against different SARS-CoV-2 variants of concern. For such an application, we tried to incorporate the D614G mutation into the Spike sequence of the pseudovirus particles to determine the impact of this alteration on pseudovirus generation, stability, and neutralization susceptibility. We found that using a D614G mutant Spike sequence boosted pseudovirus production and stability of viral

particles. These findings are in line with previous studies indicating that the D614G mutant exhibits higher stability and *in vitro* infectivity (Daniloski et al., 2021; Yurkovetskiy et al., n.d.; L. Zhang et al., 2020). Additionally, we noticed that the insertion of M protein into the particles has no effect on production efficiency but may somewhat decrease the pseudovirus's stability. This minor decrease instability was particularly noticeable in freeze/thaw assays, especially in the context of SpikeΔ19, as well as the particle stability at 37$^{o}$C, but was not significant when the more stable D614G mutant was used to produce pseudovirus. This observation puts further emphasis on the importance of D614G mutation in increasing the stability of SARS-CoV-2 particles.

We additionally showed that pseudovirus particles with the D614G mutation or M protein were equally susceptible to neutralization by soluble ACE2-IgG. In recent study, the N501Y mutation at the RBD was shown to be related with a higher ACE2/Spike affinity using a different molecular docking technique by Calcagnile et al. They also observed that SARS-CoV-2 Spike's calculated affinity for wild-type TMPRSS2 increased significantly after the D614G mutation was made (Calcagnile et al., 2021). For this reason, we investigated the stability and transduction effectiveness of Spike-pseudoviruses with various mutations. But we got results opposite to what they observed with docking. D614G mutation of spike enhances transduction efficiency and stability, particularly in ACE2-positive cells, but the N501Y mutation seems to have little impact. Additionally, overexpression of TMPRSS2 seems to significantly boost infection caused by the N501Y mutation while having little impact on the D614G variation.

We tested the neutralizing activity of CP samples from 16 COVID-19 survivors who applied for convalescent plasma donation and were selected according to the guidelines of the Turkish Ministry of Health. Some donors had strong neutralizing activity while others had little to no neutralization of the pseudovirus particles. Because even the lowest dilution of plasma used in the experiment was insufficient to neutralize half of the pseudovirus employed in the assay, we were unable to determine NT50 values for 7/16 donors (44%). We note that, identifying donors based on IgG positivity may not be the best way to predict the efficacy of convalescent plasma treatment. It has previously been reported that the extent of neutralizing activity in convalescent plasma samples correlates with the severity of COVID-19 experienced by the donor, where hospitalized patients presented with much higher neutralizing activity in their plasma samples upon recovery from the disease (Dogan et al., 2021; Robbiani et al., 2020a; Zhao et al., 2020).

Confirming this result, none of the donors in our cohort with low-activity plasma had been hospitalized with COVID-19, and the severity of symptoms upon diagnosis was typically greater in the group with high-activity CP.

Our findings also demonstrated donor-dependent variations in plasma neutralizing efficacy against various viral pseudotypes. The degree of neutralizing activity against the D614G mutant was decreased. While these findings suggest a distinct humoral response to the D614G mutant, we are unable to speculate more due to unknown viral genotype of the convalescent donors. As previously reported (Y. J. Hou et al., 2020; Weissman et al., n.d.), our findings can also be attributed to the D614G pseudovirus's enhanced titer and stability. The reaction to M protein-containing pseudovirus particles varied donor-dependently but had no influence on the NT50 values. Taken together, our findings demonstrate that the level of neutralizing activity in convalescent plasma samples is very variable and is dependent on the quality of humoral immune responses. If clinical effectiveness is to be enhanced, functional assessment of neutralizing activity using pseudovirus-based neutralization tests must be accepted as a crucial marker for selecting convalescent plasma donors.

Using a GFP-encoding lentiviral vector, we have established a feasible method under BSL-2 conditions for detection of neutralizing activity against SARS-CoV-2 with lentiviral particles pseudotyped with the Spike (S), Membrane (M), Envelope (E) and Nucleocapsid (N) proteins. Although such an approach is efficient in precisely detecting neutralizing activity, the use of flow cytometry-based data acquisition and analysis for GFP expression presents a bottleneck if a high number of samples are to be processed daily. Alternative approaches include pseudovirus particles encoding Luciferase which requires the use special bioluminescence reader equipment.

We aimed to increase the throughput of our method with colorimetric measurements using simple Optical Density readings. For this purpose, we produced lentiviral vector-based SARS-Cov-2 pseudovirus particles encoding Secreted Embryonic Alkaline Phosphatase (SEAP). This approach has been previously employed by Buck et al. to develop a high-throughput *in vitro* neutralization assay for papillomavirus (Buck et al., 2005).

Detection of SEAP activity in cell culture supernatants proved faster and easier than Flow Cytometry based analysis of GFP expressing cells. Optimized SEAP-based assays

showed the best correlation ($R^2$>0.95) to GFP-based pseudovirus at 90 minutes of incubation with supernatants from ACE2 expressing 293FT cells with the QuantiBlue substrate. Of note, a medium change at 24 hours following viral transduction was necessary for preventing SEAP overaccumulation, which may skew the results. For this reason, in our neutralization tests, lentiviral particles are also given as MOI=0.1-0.2 (the number of virions added per cell during infection of the target cells).

This SEAP-based method was used to examine the neutralizing activity of soluble ACE2-IgG, monoclonal anti-Spike antibody, and serum samples from vaccinated individuals. In addition to antibody levels, we looked at neutralizing activity in the sera of COVID-19 infected and vaccinated people by using SEAP-based method, and observed similar findings. While neutralizing activity was dramatically reduced 6 months after infection, people who received immunization after infection showed a considerable increase in neutralizing activity. Additionally, several studies observed a reduction in neutralization titer up to about one year following SARS-CoV-2 infection (Vacharathit et al., 2021). Similar to our findings, another research found that uninfected patients had no detectable antibodies or NAbs at baseline, but their NAb titers were over the positive criterion 7 days after receiving the second dose of vaccination (Favresse et al., 2021). Therefore vaccination should be considered to increase natural infection.

# 6. CONCLUSION

This thesis describes the step-by-step development of a pseudovirus-based neutralization test against SARS-CoV-2 and demonstrates its application to address different questions related to humoral immune response in COVID-19.

The strengths in our approach to neutralization tests can be summarized as follows:

- The target cells used ectopically express high levels of ACE2 and TMPRSS2 that dramatically increases the susceptibility to infection by pseudovirus, thereby enhancing the capacity to detect even a small amount of non-neutralized pseudovirus particles.
- The pseudovirus particles produced within this thesis incorporate not only the Spike protein of SARS-CoV-2 but also Membrane, Nucleocapsid and Envelope proteins. This approach increases the production efficiency and makes sure that the neutralization test accounts for neutralizing antibodies against these additional antigens.
- The use of SEAP based methods increases the throughput of neutralization assays by using simple optical density measurements since it becomes possible to acquire a whole plate of 96 samples within minutes as opposed to the hours it takes to run each sample individually through a flow cytometer to detect GFP expression.

We have applied this method to measure neutralizing activity in a variety of sample types and study humoral immune responses in COVID patients and vaccinated individuals. Our findings show that optimized SEAP-based methods can increase the availability of neutralizing assays by overcoming the need for advanced equipment and improving the processing speed of multiple samples in a given lab.

## REFERENCES


Adil, T., R, R., D, W., V, J., O, A.-T., F, R., A, M., & P, J. (2021). SARS-CoV-2 and the pandemic of COVID-19. *Postgraduate Medical Journal*, *97*(1144), 110–116. https://doi.org/10.1136/POSTGRADMEDJ-2020-138386

Ahmed, S. F., Quadeer, A. A., & McKay, M. R. (2020). Preliminary Identification of Potential Vaccine Targets for the COVID-19 Coronavirus (SARS-CoV-2) Based on SARS-CoV Immunological Studies. *Viruses 2020, Vol. 12, Page 254*, *12*(3), 254. https://doi.org/10.3390/V12030254

Ahn, J. Y., Sohn, Y., Lee, S. H., Cho, Y., Hyun, J. H., Baek, Y. J., Jeong, S. J., Kim, J. H., Ku, N. S., Yeom, J. S., Roh, J., Ahn, M. Y., Chin, B. S., Kim, Y. S., Lee, H., Yong, D., Kim, H. O., Kim, S., & Choi, J. Y. (2020). Use of Convalescent Plasma Therapy in Two COVID-19 Patients with Acute Respiratory Distress Syndrome in Korea. *Journal of Korean Medical Science*, *35*(14). https://doi.org/10.3346/JKMS.2020.35.E149

Al-Horani, R. A., & Kar, S. (2020). Potential Anti-SARS-CoV-2 Therapeutics That Target the Post-Entry Stages of the Viral Life Cycle: A Comprehensive Review. *Viruses*, *12*(10). https://doi.org/10.3390/V12101092

Amanat, F., Stadlbauer, D., Strohmeier, S., Nguyen, T. H. O., Chromikova, V., McMahon, M., Jiang, K., Arunkumar, G. A., Jurczyszak, D., Polanco, J., Bermudez-Gonzalez, M., Kleiner, G., Aydillo, T., Miorin, L., Fierer, D. S., Lugo, L. A., Kojic, E. M., Stoever, J., Liu, S. T. H., … Krammer, F. (2020). A serological assay to detect SARS-CoV-2 seroconversion in humans. *Nature Medicine 2020 26:7*, *26*(7), 1033–1036. https://doi.org/10.1038/s41591-020-0913-5

Antoine, R., Luiza, C. V. A., Marine, T., Ghizlane, M., Boris, B., Rémi, P., Joe, M., Sébastien, N., Mary, A.-A., Olivier, M., & Caroline, G. (2020). SARS-CoV-2 replication triggers an MDA-5-dependent interferon production which is unable to efficiently control replication. *BioRxiv*, 2020.10.28.358945. https://doi.org/10.1101/2020.10.28.358945

Appelberg, S., Gupta, S., Akusjärvi, S. S., Ambikan, A. T., Mikaeloff, F., Saccon, E., Végvári, Á., Benfeitas, R., Sperk, M., Ståhlberg, M., Krishnan, S., Singh, K., Penninger, J. M., Mirazimi, A., & Neogi, U. (2020). Dysregulation in Akt/mTOR/HIF-1 signaling identified by proteo-transcriptomics of SARS-CoV-2 infected cells. *Emerging Microbes and Infections*, 1748–1760. https://doi.org/10.1080/22221751.2020.1799723/SUPPL_FILE/TEMI_A_1799723_SM4659.XLSX

Arndt, A. L., Larson, B. J., & Hogue, B. G. (2010). A conserved domain in the coronavirus membrane protein tail is important for virus assembly. *Journal of Virology*, *84*(21), 11418–11428. https://doi.org/10.1128/JVI.01131-10

Bai, Z., Cao, Y., Liu, W., & Li, J. (2021). The SARS-CoV-2 Nucleocapsid Protein and Its Role in Viral Structure, Biological Functions, and a Potential Target for Drug or Vaccine Mitigation. *Viruses*, *13*(6). https://doi.org/10.3390/V13061115

Barnes, C. O., Jette, C. A., Abernathy, M. E., Dam, K.-M. A., Esswein, S. R., Gristick, H. B., Malyutin, A. G., Sharaf, N. G., Huey-Tubman, K. E., Lee, Y. E., Robbiani, D. F., Nussenzweig, M. C., West, A. P., & Bjorkman, P. J. (2020). Structural classification of neutralizing antibodies against the SARS-CoV-2 spike receptor-binding domain suggests vaccine and therapeutic strategies. *BioRxiv*, 2020.08.30.273920. https://doi.org/10.1101/2020.08.30.273920

Barone, P., & DeSimone, R. A. (2020). Convalescent plasma to treat coronavirus disease 2019 (COVID-19): considerations for clinical trial design. *Transfusion*, *60*(6), 1123–1127. https://doi.org/10.1111/TRF.15843

Barouch, D. H., Kik, S. V., Weverling, G. J., Dilan, R., King, S. L., Maxfield, L. F., Clark, S., Ng'ang'a, D., Brandariz, K. L., Abbink, P., Sinangil, F., de Bruyn, G., Gray, G. E., Roux, S., Bekker, L. G., Dilraj, A., Kibuuka, H., Robb, M. L., Michael, N. L., … Goudsmit, J. (2011). International seroepidemiology of adenovirus serotypes 5, 26, 35, and 48 in pediatric and adult populations. *Vaccine*, *29*(32), 5203–5209. https://doi.org/10.1016/J.VACCINE.2011.05.025

Barouch, D. H., Tomaka, F. L., Wegmann, F., Stieh, D. J., Alter, G., Robb, M. L., Michael, N. L., Peter, L., Nkolola, J. P., Borducchi, E. N., Chandrashekar, A., Jetton, D., Stephenson, K. E., Li, W., Korber, B., Tomaras, G. D., Montefiori, D. C., Gray, G., Frahm, N., … Schuitemaker, H. (2018). Evaluation of a mosaic HIV-1 vaccine in a multicentre, randomised, double-blind, placebo-controlled, phase 1/2a clinical trial (APPROACH) and in rhesus monkeys (NHP 13-19). *The Lancet*, *392*(10143), 232–243. https://doi.org/10.1016/S0140-6736(18)31364-3

Bastard, P., Rosen, L. B., Zhang, Q., Michailidis, E., Hoffmann, H. H., Zhang, Y., Dorgham, K., Philippot, Q., Rosain, J., Béziat, V., Manry, J., Shaw, E., Haljasmägi, L., Peterson, P., Lorenzo, L., Bizien, L., Trouillet-Assant, S., Dobbs, K., de Jesus, A. A., … Casanovaa, J. L. (2020). Autoantibodies against type I IFNs in patients with life-threatening COVID-19. *Science*, *370*(6515). https://doi.org/10.1126/SCIENCE.ABD4585/SUPPL_FILE/PAP.PDF

Beachboard, D. C., & Horner, S. M. (2016). Innate immune evasion strategies of DNA and RNA viruses. *Current Opinion in Microbiology*, *32*, 113–119. https://doi.org/10.1016/J.MIB.2016.05.015

Beer, C., Meyer, A., Müller, K., & Wirth, M. (2003). The temperature stability of mouse retroviruses depends on the cholesterol levels of viral lipid shell and cellular plasma membrane. *Virology*, *308*(1), 137–146. https://doi.org/10.1016/S0042-6822(02)00087-9

Beigel, J., KM, T., LE, D., AK, M., BS, Z., AC, K., E, H., HY, C., A, L., S, K., D, L. de C., RW, F., K, D., V, T., L, H., TF, P., R, P., DA, S., WR, S., … HC, L. (2020). Remdesivir for the Treatment of Covid-19 - Final Report. *The New England Journal of Medicine*, *383*(19), 1813–1826. https://doi.org/10.1056/NEJMOA2007764

Bello-López, J. M., Delgado-Balbuena, L., Rojas-Huidobro, D., & Rojo-Medina, J. (2018). Treatment of platelet concentrates and plasma with riboflavin and UV light: Impact in bacterial reduction. *Transfusion Clinique et Biologique*, *25*(3), 197–203. https://doi.org/10.1016/J.TRACLI.2018.03.004

Benjamin, R. J., & McLaughlin, L. S. (2012). Plasma components: properties, differences, and uses. *Transfusion*, *52*(SUPPL. 1), 9S-19S. https://doi.org/10.1111/J.1537-2995.2012.03622.X

Berthelot, J. M., & Lioté, F. (2020). COVID-19 as a STING disorder with delayed over-secretion of interferon-beta. *EBioMedicine*, *56*. https://doi.org/10.1016/J.EBIOM.2020.102801

Bestle, D., Heindl, M. R., Limburg, H., van Lam van, T., Pilgram, O., Moulton, H., Stein, D. A., Hardes, K., Eickmann, M., Dolnik, O., Rohde, C., Klenk, H. D., Garten, W., Steinmetzer, T., & Böttcher-Friebertshäuser, E. (2020). TMPRSS2 and furin are both essential for proteolytic activation of SARS-CoV-2 in human airway cells. *Life Science Alliance*, *3*(9). https://doi.org/10.26508/LSA.202000786

Bloch, E. M., Shoham, S., Casadevall, A., Sachais, B. S., Shaz, B., Winters, J. L., Van Buskirk, C., Grossman, B. J., Joyner, M., Henderson, J. P., Pekosz, A., Lau, B., Wesolowski, A., Katz, L., Shan, H., Auwaerter, P. G., Thomas, D., Sullivan, D. J., Paneth, N., … Tobian, A. A. R. (2020). Deployment of convalescent plasma for the prevention and treatment of COVID-19. *The Journal of Clinical Investigation*, *130*(6), 2757–2765. https://doi.org/10.1172/JCI138745

Boopathi, S., Poma, A. B., & Kolandaivel, P. (2020). Novel 2019 coronavirus structure, mechanism of action, antiviral drug promises and rule out against its treatment. *Journal of Biomolecular Structure and Dynamics*, 1–10. https://doi.org/10.1080/07391102.2020.1758788/SUPPL_FILE/TBSD_A_1758788_SM8253.DOCX

Bordi, L., E, N., L, S., A, D. C., MR, C., C, C., E, L., & None, O. B. O. I. C.-S. G. A. C. C. (2020). Differential diagnosis of illness in patients under investigation for the novel coronavirus (SARS-CoV-2), Italy, February 2020. *Euro Surveillance : Bulletin Europeen Sur Les Maladies Transmissibles = European Communicable Disease Bulletin*, *25*(8). https://doi.org/10.2807/1560-7917.ES.2020.25.8.2000170

Borges, L., Pithon-Curi, T. C., Curi, R., & Hatanaka, E. (2020). COVID-19 and Neutrophils: The relationship between hyperinflammation and neutrophil extracellular traps. *Mediators of Inflammation*, *2020*. https://doi.org/10.1155/2020/8829674

Boson, B., Legros, V., Zhou, B., Siret, E., Mathieu, C., Cosset, F. L., Lavillette, D., & Denolly, S. (2021). The SARS-CoV-2 envelope and membrane proteins modulate maturation and retention of the spike protein, allowing assembly of virus-like particles. *Journal of Biological Chemistry*, *296*, 100111. https://doi.org/10.1074/JBC.RA120.016175

Braciale, T. J., & Hahn, Y. S. (2013). Immunity to viruses. *Immunological Reviews*, *255*(1), 5–12. https://doi.org/10.1111/IMR.12109

Braun, J., Loyal, L., Frentsch, M., Wendisch, D., Georg, P., Kurth, F., Hippenstiel, S., Dingeldey, M., Kruse, B., Fauchere, F., Baysal, E., Mangold, M., Henze, L., Lauster, R., Mall, M. A., Beyer, K., Röhmel, J., Schmitz, J., Miltenyi, S., … Thiel, A. (2020). Presence of SARS-CoV-2-reactive T cells in COVID-19 patients and healthy donors. *MedRxiv*, 2020.04.17.20061440. https://doi.org/10.1101/2020.04.17.20061440

Brielle, E. S., Schneidman-Duhovny, D., & Linial, M. (2020). The SARS-CoV-2 Exerts a Distinctive Strategy for Interacting with the ACE2 Human Receptor. *Viruses 2020, Vol. 12, Page 497*, *12*(5), 497. https://doi.org/10.3390/V12050497

Brochot, E., Demey, B., Touzé, A., Belouzard, S., Dubuisson, J., Schmit, J. L., Duverlie, G., Francois, C., Castelain, S., & Helle, F. (2020). Anti-spike, Anti-nucleocapsid and Neutralizing Antibodies in SARS-CoV-2 Inpatients and Asymptomatic Individuals. *Frontiers in Microbiology*, *11*, 2468. https://doi.org/10.3389/FMICB.2020.584251/BIBTEX

Buck, C. B., Pastrana, D. V., Lowy, D. R., & Schiller, J. T. (2005). Generation of HPV pseudovirions using transfection and their use in neutralization assays. *Methods in Molecular Medicine*, *119*, 445–462. https://doi.org/10.1385/1-59259-982-6:445

Cai, Q., Yang, M., Liu, D., Chen, J., Shu, D., Xia, J., Liao, X., Gu, Y., Cai, Q., Yang, Y., Shen, C., Li, X., Peng, L., Huang, D., Zhang, J., Zhang, S., Wang, F., Liu, J., Chen, L., … Liu, L. (2020). Experimental Treatment with Favipiravir for COVID-19: An Open-Label Control Study. *Engineering*, *6*(10), 1192–1198. https://doi.org/10.1016/J.ENG.2020.03.007

Calcagnile, M., Forgez, P., Alifano, M., & Alifano, P. (2021). The lethal triad: SARS-CoV-2 Spike, ACE2 and TMPRSS2. Mutations in host and pathogen may affect the course of pandemic. *BioRxiv*, 2021.01.12.426365. https://doi.org/10.1101/2021.01.12.426365

Calisher, C. H., Childs, J. E., Field, H. E., Holmes, K. V., & Schountz, T. (2006). Bats: Important Reservoir Hosts of Emerging Viruses. *Clinical Microbiology Reviews*, *19*(3), 531–545. https://doi.org/10.1128/CMR.00017-06

Cao, X. (2020). COVID-19: immunopathology and its implications for therapy. *Nature Reviews. Immunology*, *20*(5), 269–270. https://doi.org/10.1038/S41577-020-0308-3

Cao, Y., Su, B., Guo, X., Sun, W., Deng, Y., Bao, L., Zhu, Q., Zhang, X., Zheng, Y., Geng, C., Chai, X., He, R., Li, X., Lv, Q., Zhu, H., Deng, W., Xu, Y., Wang, Y., Qiao, L., … Xie, X. S. (2020). Potent Neutralizing Antibodies against SARS-CoV-2 Identified by High-Throughput Single-Cell Sequencing of Convalescent Patients' B Cells. *Cell*, *182*(1), 73-84.e16. https://doi.org/10.1016/J.CELL.2020.05.025

Cascella, M., Rajnik, M., Cuomo, A., Dulebohn, S. C., & Di Napoli, R. (2021). Features, Evaluation, and Treatment of Coronavirus (COVID-19). *StatPearls*. https://www.ncbi.nlm.nih.gov/books/NBK554776/

Chakraborty, S., Mallajosyula, V., Tato, C. M., Tan, G. S., & Wang, T. T. (2021). SARS-CoV-2 vaccines in advanced clinical trials: Where do we stand? *Advanced Drug Delivery Reviews*, *172*, 314. https://doi.org/10.1016/J.ADDR.2021.01.014

Chan, J. F.-W., CC, Y., KK, T., TH, T., SC, W., KH, L., AY, F., AC, N., Z, Z., HW, T., GK, C., AR, T., VC, C., KH, C., OT, T., & KY, Y. (2020). Improved Molecular Diagnosis of COVID-19 by the Novel, Highly Sensitive and Specific COVID-19-RdRp/Hel Real-Time Reverse Transcription-PCR Assay Validated In Vitro and with Clinical Specimens. *Journal of Clinical Microbiology*, *58*(5). https://doi.org/10.1128/JCM.00310-20

Chan, J. F.-W., Yuan, S., Kok, K.-H., To, K. K.-W., Chu, H., Yang, J., Xing, F., Liu, J., Yip, C. C.-Y., Poon, R. W.-S., Tsoi, H.-W., Lo, S. K.-F., Chan, K.-H., Poon, V. K.-M., Chan, W.-M., Ip, J. D., Cai, J.-P., Cheng, V. C.-C., Chen, H., … Yuen, K.-Y. (2020). A familial cluster of pneumonia associated with the 2019 novel coronavirus indicating person-to-person transmission: a study of a family cluster. *The Lancet*, *395*(10223), 514–523. https://doi.org/10.1016/S0140-6736(20)30154-9

Chan, J. F. W., Kok, K. H., Zhu, Z., Chu, H., To, K. K. W., Yuan, S., & Yuen, K. Y. (2020). Genomic characterization of the 2019 novel human-pathogenic coronavirus isolated from a patient with atypical pneumonia after visiting Wuhan. *Https://Doi.Org/10.1080/22221751.2020.1719902*, *9*(1), 221–236. https://doi.org/10.1080/22221751.2020.1719902

Chang, C. K., Sue, S. C., Yu, T. H., Hsieh, C. M., Tsai, C. K., Chiang, Y. C., Lee, S. J., Hsiao, H. H., Wu, W. J., Chang, W. L., Lin, C. H., & Huang, T. H. (2006). Modular organization of SARS coronavirus nucleocapsid protein. *Journal of Biomedical Science*, *13*(1), 59–72. https://doi.org/10.1007/S11373-005-9035-9

Channappanavar, R., & Perlman, S. (2017). Pathogenic human coronavirus infections: causes and consequences of cytokine storm and immunopathology. *Seminars in Immunopathology*, *39*(5), 529–539. https://doi.org/10.1007/S00281-017-0629-X

Chen, N., Zhou, M., Dong, X., Qu, J., Gong, F., Han, Y., Qiu, Y., Wang, J., Liu, Y., Wei, Y., Xia, J., Yu, T., Zhang, X., & Zhang, L. (2020). Epidemiological and clinical characteristics of 99 cases of 2019 novel coronavirus pneumonia in Wuhan, China: a descriptive study. *The Lancet*, *395*(10223), 507–513. https://doi.org/10.1016/S0140-6736(20)30211-7

Chen, T., Wu, D., Chen, H., Yan, W., Yang, D., Chen, G., Ma, K., Xu, D., Yu, H., Wang, H., Wang, T., Guo, W., Chen, J., Ding, C., Zhang, X., Huang, J., Han, M., Li, S., Luo, X., … Ning, Q. (2020). Clinical characteristics of 113 deceased patients with coronavirus disease 2019: retrospective study. *BMJ*, *368*. https://doi.org/10.1136/BMJ.M1091

Chen, X., Li, R., Pan, Z., Qian, C., Yang, Y., You, R., Zhao, J., Liu, P., Gao, L., Li, Z., Huang, Q., Xu, L., Tang, J., Tian, Q., Yao, W., Hu, L., Yan, X., Zhou, X., Wu, Y., … Ye, L. (2020). Human monoclonal antibodies block the binding of SARS-CoV-2 spike protein to angiotensin converting enzyme 2 receptor. *Cellular & Molecular*

*Immunology*, *17*(6), 647–649. https://doi.org/10.1038/S41423-020-0426-7

Chen, Y., Yu, Z., Yi, H., Wei, Y., Han, X., Li, Q., Ji, C., Huang, J., Deng, Q., Liu, Y., Cai, M., He, S., Ma, C., & Zhang, G. (2019). The phosphorylation of the N protein could affect PRRSV virulence in vivo. *Veterinary Microbiology*, *231*, 226. https://doi.org/10.1016/J.VETMIC.2019.03.018

Choi, Y., & Chang, J. (2013). Viral vectors for vaccine applications. *Clinical and Experimental Vaccine Research*, *2*(2), 97–105. https://doi.org/10.7774/CEVR.2013.2.2.97

Chung, J. Y., Thone, M. N., & Kwon, Y. J. (2021). COVID-19 vaccines: The status and perspectives in delivery points of view. *Advanced Drug Delivery Reviews*, *170*, 1–25. https://doi.org/10.1016/J.ADDR.2020.12.011

Cong, Y., Ulasli, M., Schepers, H., Mauthe, M., V'kovski, P., Kriegenburg, F., Thiel, V., de Haan, C. A. M., & Reggiori, F. (2020). Nucleocapsid Protein Recruitment to Replication-Transcription Complexes Plays a Crucial Role in Coronaviral Life Cycle. *Journal of Virology*, *94*(4). https://doi.org/10.1128/JVI.01925-19

Cornillez-Ty, C. T., Liao, L., Yates, J. R., Kuhn, P., & Buchmeier, M. J. (2009). Severe Acute Respiratory Syndrome Coronavirus Nonstructural Protein 2 Interacts with a Host Protein Complex Involved in Mitochondrial Biogenesis and Intracellular Signaling. *Journal of Virology*, *83*(19), 10314–10318. https://doi.org/10.1128/JVI.00842-09/ASSET/F8AC21C4-4B6E-4B13-8BF3-F0757ECFB4C2/ASSETS/GRAPHIC/ZJV0190923890003.JPEG

Crawford, K. H. D., Eguia, R., Dingens, A. S., Loes, A. N., Malone, K. D., Wolf, C. R., Chu, H. Y., Tortorici, M. A., Veesler, D., Murphy, M., Pettie, D., King, N. P., Balazs, A. B., & Bloom, J. D. (2020). Protocol and Reagents for Pseudotyping Lentiviral Particles with SARS-CoV-2 Spike Protein for Neutralization Assays. *Viruses 2020, Vol. 12, Page 513*, *12*(5), 513. https://doi.org/10.3390/V12050513

Cunningham, A. C., Goh, H. P., & Koh, D. (2020). Treatment of COVID-19: old tricks for new challenges. *Critical Care 2020 24:1*, *24*(1), 1–2. https://doi.org/10.1186/S13054-020-2818-6

Dai, L., T, Z., K, X., Y, H., L, X., E, H., Y, A., Y, C., S, L., M, L., M, Y., Y, L., H, C., Y, Y., W, Z., C, K., G, W., J, Q., C, Q., … GF, G. (2020). A Universal Design of Betacoronavirus Vaccines against COVID-19, MERS, and SARS. *Cell*, *182*(3), 722-733.e11. https://doi.org/10.1016/J.CELL.2020.06.035

Daniloski, Z., Jordan, T. X., Ilmain, J. K., Guo, X., Bhabha, G., Tenoever, B. R., & Sanjana, N. E. (2021). The spike d614g mutation increases sars-cov-2 infection of multiple human cell types. *ELife*, *10*, 1–16. https://doi.org/10.7554/ELIFE.65365

Dautzenberg, I. J. C., Rabelink, M. J. W. E., & Hoeben, R. C. (2020). The stability of envelope-pseudotyped lentiviral vectors. *Gene Therapy 2020 28:1*, *28*(1), 89–104. https://doi.org/10.1038/s41434-020-00193-y

Davanzo, G. G., Codo, A. C., Brunetti, N. S., Boldrini, V., Knittel, T. L., Monterio, L. B., Moraes, D. de, Ferrari, A. J. R., Souza, G. F. de, Muraro, S. P., Profeta, G. S., Wassano, N. S., Santos, L. N., Carregari, V. C., Dias, A. H. S., Virgilio-da-Silva, J.

V., Castro, Í., Silva-Costa, L. C., Palma, A., … Farias, A. S. (2020). SARS-CoV-2 Uses CD4 to Infect T Helper Lymphocytes. *MedRxiv*, 2020.09.25.20200329. https://doi.org/10.1101/2020.09.25.20200329

de Haan, C. A. M., & Rottier, P. J. M. (2005). Molecular Interactions in the Assembly of Coronaviruses. *Advances in Virus Research*, *64*, 165–230. https://doi.org/10.1016/S0065-3527(05)64006-7

de Haan, C. A. M., Vennema, H., & Rottier, P. J. M. (2000). Assembly of the Coronavirus Envelope: Homotypic Interactions between the M Proteins. *Journal of Virology*, *74*(11), 4967–4978. https://doi.org/10.1128/JVI.74.11.4967-4978.2000/ASSET/490A1E46-32DC-4471-B6B9-6ECAFCC87515/ASSETS/GRAPHIC/JV1102234006.JPEG

DeDiego, M. L., Nieto-Torres, J. L., Regla-Nava, J. A., Jimenez-Guardeno, J. M., Fernandez-Delgado, R., Fett, C., Castano-Rodriguez, C., Perlman, S., & Enjuanes, L. (2014). Inhibition of NF- B-Mediated Inflammation in Severe Acute Respiratory Syndrome Coronavirus-Infected Mice Increases Survival. *Journal of Virology*, *88*(2), 913–924. https://doi.org/10.1128/JVI.02576-13/ASSET/FB10F834-7123-403B-BE46-58256E3A2D43/ASSETS/GRAPHIC/ZJV9990985340011.JPEG

Del Valle, D. M., Kim-Schulze, S., Huang, H. H., Beckmann, N. D., Nirenberg, S., Wang, B., Lavin, Y., Swartz, T. H., Madduri, D., Stock, A., Marron, T. U., Xie, H., Patel, M., Tuballes, K., Van Oekelen, O., Rahman, A., Kovatch, P., Aberg, J. A., Schadt, E., … Gnjatic, S. (2020). An inflammatory cytokine signature predicts COVID-19 severity and survival. *Nature Medicine 2020 26:10*, *26*(10), 1636–1643. https://doi.org/10.1038/s41591-020-1051-9

Deng, F. (2018). Advances and challenges in enveloped virus-like particle (VLP)-based vaccines. *Journal of Immunological Sciences*, *2*(2), 36–41. https://doi.org/10.29245/2578-3009/2018/2.1118

Deng, X., Garcia-Knight, M. A., Khalid, M. M., Servellita, V., Wang, C., Morris, M. K., Sotomayor-González, A., Glasner, D. R., Reyes, K. R., Gliwa, A. S., Reddy, N. P., Martin, C. S. S., Federman, S., Cheng, J., Balcerek, J., Taylor, J., Streithorst, J. A., Miller, S., Kumar, G. R., … Chiu, C. Y. (2021). Transmission, infectivity, and antibody neutralization of an emerging SARS-CoV-2 variant in California carrying a L452R spike protein mutation. *MedRxiv*, 2021.03.07.21252647. https://doi.org/10.1101/2021.03.07.21252647

Dhama, K., Patel, S., Sharun, K., … M. P.-T. medicine and, & 2020, U. (2020). SARS-CoV-2 jumping the species barrier: zoonotic lessons from SARS, MERS and recent advances to combat this pandemic virus. *Elsevier*. https://www.sciencedirect.com/science/article/pii/S1477893920303264

Dickerman, B. A., Gerlovin, H., Madenci, A. L., Kurgansky, K. E., Ferolito, B. R., Muñiz, M. J. F., Gagnon, D. R., Gaziano, J. M., Cho, K., Casas, J. P., & Hernán, M. A. (2021). Comparative Effectiveness of BNT162b2 and mRNA-1273 Vaccines in U.S. Veterans. *Https://Doi.Org/10.1056/NEJMoa2115463*. https://doi.org/10.1056/NEJMOA2115463

Dodd, R. Y., Crowder, L. A., Haynes, J. M., Notari, E. P., Stramer, S. L., & Steele, W. R. (2020). Screening Blood Donors for HIV, HCV, and HBV at the American Red

Cross: 10-Year Trends in Prevalence, Incidence, and Residual Risk, 2007 to 2016. *Transfusion Medicine Reviews*, *34*(2), 81–93. https://doi.org/10.1016/J.TMRV.2020.02.001

Dogan, M., Kozhaya, L., Placek, L., Gunter, C., Yigit, M., Hardy, R., Plassmeyer, M., Coatney, P., Lillard, K., Bukhari, Z., Kleinberg, M., Hayes, C., Arditi, M., Klapper, E., Merin, N., Liang, B. T. T., Gupta, R., Alpan, O., & Unutmaz, D. (2021). SARS-CoV-2 specific antibody and neutralization assays reveal the wide range of the humoral immune response to virus. *Communications Biology 2021 4:1*, *4*(1), 1–13. https://doi.org/10.1038/s42003-021-01649-6

Donaldson, B., Lateef, Z., Walker, G. F., Young, S. L., & Ward, V. K. (2018). Virus-like particle vaccines: immunology and formulation for clinical translation. *Https://Doi.Org/10.1080/14760584.2018.1516552*, *17*(9), 833–849. https://doi.org/10.1080/14760584.2018.1516552

Dong, L., Tian, J., He, S., Zhu, C., Wang, J., Liu, C., & Yang, J. (2020). Possible Vertical Transmission of SARS-CoV-2 From an Infected Mother to Her Newborn. *JAMA*, *323*(18), 1846–1848. https://doi.org/10.1001/JAMA.2020.4621

Dong, Y., X, M., Y, H., X, Q., F, J., Z, J., & S, T. (2020). Epidemiology of COVID-19 Among Children in China. *Pediatrics*, *145*(6). https://doi.org/10.1542/PEDS.2020-0702

Drexler, J. F., Corman, V. M., & Drosten, C. (2014). Ecology, evolution and classification of bat coronaviruses in the aftermath of SARS. *Antiviral Research*, *101*(1), 45–56. https://doi.org/10.1016/J.ANTIVIRAL.2013.10.013

Du, L., He, Y., Zhou, Y., Liu, S., Zheng, B. J., & Jiang, S. (2009). The spike protein of SARS-CoV — a target for vaccine and therapeutic development. *Nature Reviews Microbiology 2009 7:3*, *7*(3), 226–236. https://doi.org/10.1038/nrmicro2090

Du, R.-H., Liang, L.-R., Yang, C.-Q., Wang, W., Cao, T.-Z., Li, M., Guo, G.-Y., Du, J., Zheng, C.-L., Zhu, Q., Hu, M., Li, X.-Y., Peng, P., & Shi, H.-Z. (2020). Predictors of mortality for patients with COVID-19 pneumonia caused by SARS-CoV-2: a prospective cohort study. *European Respiratory Journal*, *55*(5). https://doi.org/10.1183/13993003.00524-2020

Duan, K, B, L., C, L., H, Z., T, Y., J, Q., M, Z., L, C., S, M., Y, H., C, P., M, Y., J, H., Z, W., J, Y., X, G., D, W., X, Y., L, L., … X, Y. (2020). Effectiveness of convalescent plasma therapy in severe COVID-19 patients. *Proceedings of the National Academy of Sciences of the United States of America*, *117*(17), 9490–9496. https://doi.org/10.1073/PNAS.2004168117

Duan, Kai, Liu, B., Li, C., Zhang, H., Yu, T., Qu, J., Zhou, M., Chen, L., Meng, S., Hu, Y., Peng, C., Yuan, M., Huang, J., Wang, Z., Yu, J., Gao, X., Wang, D., Yu, X., Li, L., … Yang, X. (2020a). Effectiveness of convalescent plasma therapy in severe COVID-19 patients. *Proceedings of the National Academy of Sciences of the United States of America*, *117*(17), 9490–9496. https://doi.org/10.1073/PNAS.2004168117/-/DCSUPPLEMENTAL

Duan, Kai, Liu, B., Li, C., Zhang, H., Yu, T., Qu, J., Zhou, M., Chen, L., Meng, S., Hu, Y., Peng, C., Yuan, M., Huang, J., Wang, Z., Yu, J., Gao, X., Wang, D., Yu, X., Li,

L., … Yang, X. (2020b). Effectiveness of convalescent plasma therapy in severe COVID-19 patients. *Proceedings of the National Academy of Sciences of the United States of America*, *117*(17), 9490–9496. https://doi.org/10.1073/PNAS.2004168117/-/DCSUPPLEMENTAL

Dutta, N. K., Mazumdar, K., & Gordy, J. T. (2020). The Nucleocapsid Protein of SARS–CoV-2: a Target for Vaccine Development. *Journal of Virology*, *94*(13). https://doi.org/10.1128/JVI.00647-20

ECDC. (2021). *EUROPEAN COMMISSION DIRECTORATE-GENERAL FOR HEALTH AND FOOD SAFETY Directorate B-Health systems, medical products and innovation B4-Medical products: quality, safety, innovation An EU programme of COVID-19 convalescent plasma collection and transfusion Gu*.

Egloff, C., Vauloup-Fellous, C., Picone, O., Mandelbrot, L., & Roques, P. (2020). Evidence and possible mechanisms of rare maternal-fetal transmission of SARS-CoV-2. *Journal of Clinical Virology*, *128*, 104447. https://doi.org/10.1016/J.JCV.2020.104447

Espeseth, A., PJ, C., MP, C., D, W., DJ, D., C, C., GO, D., JD, G., R, S., S, T., Z, W., J, A., L, Z., JA, F., KS, C., DC, F., KA, V., K, B., AH, L., … AJ, B. (2020). Modified mRNA/lipid nanoparticle-based vaccines expressing respiratory syncytial virus F protein variants are immunogenic and protective in rodent models of RSV infection. *NPJ Vaccines*, *5*(1). https://doi.org/10.1038/S41541-020-0163-Z

Fang, Y., Zhang, H., Xu, Y., Xie, J., Pang, P., & Ji, W. (2020). CT Manifestations of Two Cases of 2019 Novel Coronavirus (2019-nCoV) Pneumonia. *Https://Doi.Org/10.1148/Radiol.2020200280*, *295*(1), 208–209. https://doi.org/10.1148/RADIOL.2020200280

Favresse, J., Gillot, C., Di Chiaro, L., Eucher, C., Elsen, M., Van Eeckhoudt, S., David, C., Morimont, L., Dogné, J. M., & Douxfils, J. (2021). Neutralizing antibodies in covid-19 patients and vaccine recipients after two doses of bnt162b2. *Viruses*, *13*(7). https://doi.org/10.3390/V13071364/S1

FDA. (2020). *Recommendations for Investigational COVID-19 Convalescent Plasma | FDA*. https://www.fda.gov/vaccines-blood-biologics/investigational-new-drug-applications-inds-cber-regulated-products/recommendations-investigational-covid-19-convalescent-plasma

Fehr, A. R., Channappanavar, R., Jankevicius, G., Fett, C., Zhao, J., Athmer, J., Meyerholz, D. K., Ahel, I., & Perlman, S. (2016). The Conserved Coronavirus Macrodomain Promotes Virulence and Suppresses the Innate Immune Response during Severe Acute Respiratory Syndrome Coronavirus Infection. *MBio*, *7*(6). https://doi.org/10.1128/MBIO.01721-16

Fehr, A. R., & Perlman, S. (2015). Coronaviruses: An Overview of Their Replication and Pathogenesis. *Coronaviruses: Methods and Protocols*, *1282*, 1–23. https://doi.org/10.1007/978-1-4939-2438-7_1

Feng, L., Chen, G., & Peng, J. (2018). An ontology-based cognitive model for faults diagnosis of hazardous chemical storage devices. *International Journal of Cognitive Informatics and Natural Intelligence*, *12*(4), 101–114.

https://doi.org/10.4018/IJCINI.2018100106

Feng, Z., Diao, B., Wang, R., Wang, G., Wang, C., Tan, Y., Liu, L., Wang, C., Liu, Y., Liu, Y., Yuan, Z., Ren, L., Wu, Y., & Chen, Y. (2020). The Novel Severe Acute Respiratory Syndrome Coronavirus 2 (SARS-CoV-2) Directly Decimates Human Spleens and Lymph Nodes. *MedRxiv*, 2020.03.27.20045427. https://doi.org/10.1101/2020.03.27.20045427

Focosi, D., Anderson, A. O., Tang, J. W., & Tuccori, M. (2020). Convalescent Plasma Therapy for COVID-19: State of the Art. *Clinical Microbiology Reviews*, *33*(4), 1–17. https://doi.org/10.1128/CMR.00072-20

Focosi, D., Maggi, F., Mazzetti, P., & Pistello, M. (2021). Viral infection neutralization tests: A focus on severe acute respiratory syndrome-coronavirus-2 with implications for convalescent plasma therapy. *Reviews in Medical Virology*, *31*(2). https://doi.org/10.1002/RMV.2170

Folegatti, P. M., Bittaye, M., Flaxman, A., Lopez, F. R., Bellamy, D., Kupke, A., Mair, C., Makinson, R., Sheridan, J., Rohde, C., Halwe, S., Jeong, Y., Park, Y. S., Kim, J. O., Song, M., Boyd, A., Tran, N., Silman, D., Poulton, I., … Gilbert, S. (2020). Safety and immunogenicity of a candidate Middle East respiratory syndrome coronavirus viral-vectored vaccine: a dose-escalation, open-label, non-randomised, uncontrolled, phase 1 trial. *The Lancet Infectious Diseases*, *20*(7), 816–826. https://doi.org/10.1016/S1473-3099(20)30160-2

Frampton, D., Rampling, T., Cross, A., Bailey, H., Heaney, J., Byott, M., Scott, R., Sconza, R., Price, J., Margaritis, M., Bergstrom, M., Spyer, M. J., Miralhes, P. B., Grant, P., Kirk, S., Valerio, C., Mangera, Z., Prabhahar, T., Moreno-Cuesta, J., … Nastouli, E. (2021). Genomic characteristics and clinical effect of the emergent SARS-CoV-2 B.1.1.7 lineage in London, UK: a whole-genome sequencing and hospital-based cohort study. *The Lancet Infectious Diseases*, *21*(9), 1246–1256. https://doi.org/10.1016/S1473-3099(21)00170-5/ATTACHMENT/B17274F6-4A28-4388-9F1C-597F26B1C61B/MMC1.PDF

Franz, K. M., Neidermyer, W. J., Tan, Y. J., Whelan, S. P. J., & Kagan, J. C. (2018). STING-dependent translation inhibition restricts RNA virus replication. *Proceedings of the National Academy of Sciences of the United States of America*, *115*(9), E2058–E2067. https://doi.org/10.1073/PNAS.1716937115

Freer, G., & Matteucci, D. (2009). Influence of Dendritic Cells on Viral Pathogenicity. *PLOS Pathogens*, *5*(7), e1000384. https://doi.org/10.1371/JOURNAL.PPAT.1000384

Fukushi, S., Mizutani, T., Saijo, M., Matsuyama, S., Miyajima, N., Taguchi, F., Itamura, S., Kurane, I., & Morikawa, S. (2005). Vesicular stomatitis virus pseudotyped with severe acute respiratory syndrome coronavirus spike protein. *The Journal of General Virology*, *86*(Pt 8), 2269–2274. https://doi.org/10.1099/VIR.0.80955-0

Garcia-Beltran, W. F., Lam, E. C., St. Denis, K., Nitido, A. D., Garcia, Z. H., Hauser, B. M., Feldman, J., Pavlovic, M. N., Gregory, D. J., Poznansky, M. C., Sigal, A., Schmidt, A. G., Iafrate, A. J., Naranbhai, V., & Balazs, A. B. (2021). Multiple SARS-CoV-2 variants escape neutralization by vaccine-induced humoral immunity. *Cell*, *184*(9), 2372. https://doi.org/10.1016/J.CELL.2021.03.013

Garcia, V., Krishnan, R., Davis, C., Batenchuk, C., Boeuf, F. Le, Abdelbary, H., & Diallo, J. S. (2014). High-throughput titration of luciferase-expressing recombinant viruses. *Journal of Visualized Experiments : JoVE*, *91*. https://doi.org/10.3791/51890

Garraud, O., Heshmati, F., Pozzetto, B., Lefrere, F., Girot, R., Saillol, A., & Laperche, S. (2016). Plasma therapy against infectious pathogens, as of yesterday, today and tomorrow. *Transfusion Clinique et Biologique*, *23*(1), 39–44. https://doi.org/10.1016/J.TRACLI.2015.12.003

Gasmi, M., Glynn, J., Jin, M.-J., Jolly, D. J., Yee, J.-K., & Chen, S.-T. (1999). Requirements for Efficient Production and Transduction of Human Immunodeficiency Virus Type 1-Based Vectors. *Journal of Virology*, *73*(3), 1828–1834. https://doi.org/10.1128/JVI.73.3.1828-1834.1999/ASSET/F4730950-599F-4860-920C-DC17AF700B45/ASSETS/GRAPHIC/JV0391457004.JPEG

Ge, X. Y., Hu, B., & Shi, Z. L. (2015). Bat Coronaviruses. *Bats and Viruses: A New Frontier of Emerging Infectious Diseases*, 127–155. https://doi.org/10.1002/9781118818824.CH5

Gélinas, J.-F., Davies, L. A., Gill, D. R., & Hyde, S. C. (2017). *Assessment of selected media supplements to improve F/HN lentiviral vector production yields*. https://doi.org/10.1038/s41598-017-07893-3

Gerasimenko, J. V., Tepikin, A. V., Petersen, O. H., & Gerasimenko, O. V. (1998). Calcium uptake via endocytosis with rapid release from acidifying endosomes. *Current Biology*, *8*(24), 1335–1338. https://doi.org/10.1016/S0960-9822(07)00565-9

Gorbalenya, A. E., Baker, S. C., Baric, R. S., de Groot, R. J., Drosten, C., Gulyaeva, A. A., Haagmans, B. L., Lauber, C., Leontovich, A. M., Neuman, B. W., Penzar, D., Perlman, S., Poon, L. L. M., Samborskiy, D., Sidorov, I. A., Sola, I., & Ziebuhr, J. (2020). Severe acute respiratory syndrome-related coronavirus: The species and its viruses – a statement of the Coronavirus Study Group. *BioRxiv*. https://doi.org/10.1101/2020.02.07.937862

Grant, R. A., Morales-Nebreda, L., Markov, N. S., Swaminathan, S., Guzman, E. R., Abbott, D. A., Donnelly, H. K., Donayre, A., Goldberg, I. A., Klug, Z. M., Borkowski, N., Lu, Z., Kihshen, H., Politanska, Y., Sichizya, L., Kang, M., Shilatifard, A., Qi, C., Argento, A. C., … Investigators, for T. N. S. S. (2020). Alveolitis in severe SARS-CoV-2 pneumonia is driven by self-sustaining circuits between infected alveolar macrophages and T cells. *BioRxiv*, 2020.08.05.238188. https://doi.org/10.1101/2020.08.05.238188

Greaney, A. J., Starr, T. N., Gilchuk, P., Zost, S. J., Binshtein, E., Loes, A. N., Hilton, S. K., Huddleston, J., Eguia, R., Crawford, K. H. D., Dingens, A. S., Nargi, R. S., Sutton, R. E., Suryadevara, N., Rothlauf, P. W., Liu, Z., Whelan, S. P. J., Carnahan, R. H., Crowe, J. E., & Bloom, J. D. (2021). Complete Mapping of Mutations to the SARS-CoV-2 Spike Receptor-Binding Domain that Escape Antibody Recognition. *Cell Host & Microbe*, *29*(1), 44-57.e9. https://doi.org/10.1016/J.CHOM.2020.11.007

Grehan, K., Ferrara, F., & Temperton, N. (2015). An optimised method for the production of MERS-CoV spike expressing viral pseudotypes. *MethodsX*, *2*, 379–384.

https://doi.org/10.1016/J.MEX.2015.09.003

Grifoni, A., D, W., SI, R., J, M., JM, D., CR, M., SA, R., A, S., L, P., RS, J., D, M., AM, de S., A, F., AF, C., JA, G., B, P., F, K., DM, S., S, C., & A, S. (2020). Targets of T Cell Responses to SARS-CoV-2 Coronavirus in Humans with COVID-19 Disease and Unexposed Individuals. *Cell*, *181*(7), 1489-1501.e15. https://doi.org/10.1016/J.CELL.2020.05.015

Gu, H., Chen, Q., Yang, G., He, L., Fan, H., Deng, Y. Q., Wang, Y., Teng, Y., Zhao, Z., Cui, Y., Li, Y., Li, X. F., Li, J., Zhang, N. N., Yang, X., Chen, S., Guo, Y., Zhao, G., Wang, X., … Zhou, Y. (2020). Adaptation of SARS-CoV-2 in BALB/c mice for testing vaccine efficacy. *Science (New York, N.Y.)*, *369*(6511). https://doi.org/10.1126/SCIENCE.ABC4730

Guan, W., Ni, Z., Hu, Y., Liang, W., Ou, C., He, J., Liu, L., Shan, H., Lei, C., Hui, D. S. C., Du, B., Li, L., Zeng, G., Yuen, K.-Y., Chen, R., Tang, C., Wang, T., Chen, P., Xiang, J., … Zhong, N. (2020). Clinical Characteristics of Coronavirus Disease 2019 in China. *Https://Doi.Org/10.1056/NEJMoa2002032*, *382*(18), 1708–1720. https://doi.org/10.1056/NEJMOA2002032

Guo, Y. R., Cao, Q. D., Hong, Z. S., Tan, Y. Y., Chen, S. D., Jin, H. J., Tan, K. Sen, Wang, D. Y., & Yan, Y. (2020). The origin, transmission and clinical therapies on coronavirus disease 2019 (COVID-19) outbreak- A n update on the status. *Military Medical Research*, *7*(1), 1–10. https://doi.org/10.1186/S40779-020-00240-0/TABLES/1

Gupta, M. K., Vemula, S., Donde, R., Gouda, G., Behera, L., & Vadde, R. (2021). In-silico approaches to detect inhibitors of the human severe acute respiratory syndrome coronavirus envelope protein ion channel. *Journal of Biomolecular Structure and Dynamics*, *39*(7), 2617–2627. https://doi.org/10.1080/07391102.2020.1751300/SUPPL_FILE/TBSD_A_1751300_SM4751.XLSX

Habel, J. R., Nguyen, T. H. O., van de Sandt, C. E., Juno, J. A., Chaurasia, P., Wragg, K., Koutsakos, M., Hensen, L., Jia, X., Chua, B., Zhang, W., Tan, H. X., Flanagan, K. L., Doolan, D. L., Torresi, J., Chen, W., Wakim, L. M., Cheng, A. C., Doherty, P. C., … Kedzierska, K. (2020). Suboptimal SARS-CoV-2-specific CD8 + T cell response associated with the prominent HLA-A*02:01 phenotype. *Proceedings of the National Academy of Sciences of the United States of America*, *117*(39), 24384–24391. https://doi.org/10.1073/PNAS.2015486117

Hasson, S. S. A. A., Al-Busaidi, J. K. Z., & Sallam, T. A. (2015). The past, current and future trends in DNA vaccine immunisations. *Asian Pacific Journal of Tropical Biomedicine*, *5*(5), 344–353. https://doi.org/10.1016/S2221-1691(15)30366-X

Heald-Sargent, T., & Gallagher, T. (2012). Ready, Set, Fuse! The Coronavirus Spike Protein and Acquisition of Fusion Competence. *Viruses 2012, Vol. 4, Pages 557-580*, *4*(4), 557–580. https://doi.org/10.3390/V4040557

Hobernik, D., & Bros, M. (2018). DNA Vaccines—How Far From Clinical Use? *International Journal of Molecular Sciences 2018, Vol. 19, Page 3605*, *19*(11), 3605. https://doi.org/10.3390/IJMS19113605

Hoepel, W., Chen, H.-J., Allahverdiyeva, S., Manz, X., Aman, J., Biobank, A. U. C.-19, Bonta, P., Brouwer, P., Taeye, S. de, Caniels, T., Straten, K. van der, Golebski, K., Griffith, G., Jonkers, R., Larsen, M., Linty, F., Neele, A., Nouta, J., Baarle, F. van, … Dunnen, J. den. (2020). Anti-SARS-CoV-2 IgG from severely ill COVID-19 patients promotes macrophage hyper-inflammatory responses. *BioRxiv*, 2020.07.13.190140. https://doi.org/10.1101/2020.07.13.190140

Hoffmann, M, H, K.-W., S, S., N, K., T, H., S, E., TS, S., G, H., NH, W., A, N., MA, M., C, D., & S, P. (2020). SARS-CoV-2 Cell Entry Depends on ACE2 and TMPRSS2 and Is Blocked by a Clinically Proven Protease Inhibitor. *Cell*, *181*(2), 271-280.e8. https://doi.org/10.1016/J.CELL.2020.02.052

Hoffmann, Markus, Kleine-Weber, H., Schroeder, S., Krüger, N., Herrler, T., Erichsen, S., Schiergens, T. S., Herrler, G., Wu, N. H., Nitsche, A., Müller, M. A., Drosten, C., & Pöhlmann, S. (2020a). SARS-CoV-2 Cell Entry Depends on ACE2 and TMPRSS2 and Is Blocked by a Clinically Proven Protease Inhibitor. *Cell*, *181*(2), 271-280.e8. https://doi.org/10.1016/J.CELL.2020.02.052

Hoffmann, Markus, Kleine-Weber, H., Schroeder, S., Krüger, N., Herrler, T., Erichsen, S., Schiergens, T. S., Herrler, G., Wu, N. H., Nitsche, A., Müller, M. A., Drosten, C., & Pöhlmann, S. (2020b). SARS-CoV-2 Cell Entry Depends on ACE2 and TMPRSS2 and Is Blocked by a Clinically Proven Protease Inhibitor. *Cell*, *181*(2), 271-280.e8. https://doi.org/10.1016/J.CELL.2020.02.052

Holm, C. K., Rahbek, S. H., Gad, H. H., Bak, R. O., Jakobsen, M. R., Jiang, Z., Hansen, A. L., Jensen, S. K., Sun, C., Thomsen, M. K., Laustsen, A., Nielsen, C. G., Severinsen, K., Xiong, Y., Burdette, D. L., Hornung, V., Lebbink, R. J., Duch, M., Fitzgerald, K. A., … Paludan, S. R. (2016). Influenza A virus targets a cGAS-independent STING pathway that controls enveloped RNA viruses. *Nature Communications*, *7*. https://doi.org/10.1038/NCOMMS10680

Hou, Y. J., Chiba, S., Halfmann, P., Ehre, C., Kuroda, M., Dinnon, K. H., Leist, S. R., Schäfer, A., Nakajima, N., Takahashi, K., Lee, R. E., Mascenik, T. M., Graham, R., Edwards, C. E., Tse, L. V., Okuda, K., Markmann, A. J., Bartelt, L., Silva, A. De, … Baric, R. S. (2020). SARS-CoV-2 D614G variant exhibits efficient replication ex vivo and transmission in vivo. *Science*, *370*(6523), 1464–1468. https://doi.org/10.1126/SCIENCE.ABE8499/SUPPL_FILE/PAP.PDF

Hou, Y., Meulia, T., Gao, X., Saif, L. J., & Wang, Q. (2018). Deletion of both the Tyrosine-Based Endocytosis Signal and the Endoplasmic Reticulum Retrieval Signal in the Cytoplasmic Tail of Spike Protein Attenuates Porcine Epidemic Diarrhea Virus in Pigs. *Journal of Virology*, *93*(2). https://doi.org/10.1128/JVI.01758-18

Hsieh, P.-K., Chang, S. C., Huang, C.-C., Lee, T.-T., Hsiao, C.-W., Kou, Y.-H., Chen, I.-Y., Chang, C.-K., Huang, T.-H., & Chang, M.-F. (2005). Assembly of Severe Acute Respiratory Syndrome Coronavirus RNA Packaging Signal into Virus-Like Particles Is Nucleocapsid Dependent. *Journal of Virology*, *79*(22), 13848–13855. https://doi.org/10.1128/JVI.79.22.13848-13855.2005/ASSET/2EA04F7A-F672-4625-A835-CDC726F5D45C/ASSETS/GRAPHIC/ZJV0220570150007.JPEG

Hu, B., Guo, H., Zhou, P., & Shi, Z.-L. (2020). Characteristics of SARS-CoV-2 and

COVID-19. *Nature Reviews Microbiology 2020 19:3*, *19*(3), 141–154. https://doi.org/10.1038/s41579-020-00459-7

Hu, J. J., Liu, X., Xia, S., Zhang, Z., Zhang, Y., Zhao, J., Ruan, J., Luo, X., Lou, X., Bai, Y., Wang, J., Hollingsworth, L. R., Magupalli, V. G., Zhao, L., Luo, H. R., Kim, J., Lieberman, J., & Wu, H. (2020). FDA-approved disulfiram inhibits pyroptosis by blocking gasdermin D pore formation. *Nature Immunology*, *21*(7), 736–745. https://doi.org/10.1038/S41590-020-0669-6

Hu, Y., Wen, J., Tang, L., Zhang, H., Zhang, X., Li, Y., Wang, J., Han, Y., Li, G., Shi, J., Tian, X., Jiang, F., Zhao, X., Wang, J., Liu, S., Zeng, C., Wang, J., & Yang, H. (2003). The M Protein of SARS-CoV: Basic Structural and Immunological Properties. *Genomics, Proteomics & Bioinformatics*, *1*(2), 118. https://doi.org/10.1016/S1672-0229(03)01016-7

Huang, C., Wang, Y., Li, X., Ren, L., Zhao, J., Hu, Y., Zhang, L., Fan, G., Xu, J., Gu, X., Cheng, Z., Yu, T., Xia, J., Wei, Y., Wu, W., Xie, X., Yin, W., Li, H., Liu, M., … Cao, B. (2020). Clinical features of patients infected with 2019 novel coronavirus in Wuhan, China. *The Lancet*, *395*(10223), 497–506. https://doi.org/10.1016/S0140-6736(20)30183-5

Humphreys, I. R., & Sebastian, S. (2018). Novel viral vectors in infectious diseases. *Immunology*, *153*(1), 1–9. https://doi.org/10.1111/IMM.12829

Hung, I. F. N., To, K. K. W., Lee, C. K., Lee, K. L., Chan, K., Yan, W. W., Liu, R., Watt, C. L., Chan, W. M., Lai, K. Y., Koo, C. K., Buckley, T., Chow, F. L., Wong, K. K., Chan, H. S., Ching, C. K., Tang, B. S. F., Lau, C. C. Y., Li, I. W. S., … Yuen, K. Y. (2011). Convalescent Plasma Treatment Reduced Mortality in Patients With Severe Pandemic Influenza A (H1N1) 2009 Virus Infection. *Clinical Infectious Diseases*, *52*(4), 447–456. https://doi.org/10.1093/CID/CIQ106

Hwang, S. S., Lim, J., Yu, Z., Kong, P., Sefik, E., Xu, H., Harman, C. C. D., Kim, L. K., Lee, G. R., Li, H. B., & Flavell, R. A. (2020). Cryo-EM structure of the 2019-nCoV spike in the prefusion conformation. *Science (New York, N.Y.)*, *367*(6483), 1255–1260. https://doi.org/10.1126/SCIENCE.ABB2507

Jackson, L. A., Anderson, E. J., Rouphael, N. G., Roberts, P. C., Makhene, M., Coler, R. N., McCullough, M. P., Chappell, J. D., Denison, M. R., Stevens, L. J., Pruijssers, A. J., McDermott, A., Flach, B., Doria-Rose, N. A., Corbett, K. S., Morabito, K. M., O'Dell, S., Schmidt, S. D., II, P. A. S., … Beigel, J. H. (2020). An mRNA Vaccine against SARS-CoV-2 — Preliminary Report. *Https://Doi.Org/10.1056/NEJMoa2022483*, *383*(20), 1920–1931. https://doi.org/10.1056/NEJMOA2022483

Jang, K. J., Jeong, S., Kang, D. Y., Sp, N., Yang, Y. M., & Kim, D. E. (2020). A high ATP concentration enhances the cooperative translocation of the SARS coronavirus helicase nsP13 in the unwinding of duplex RNA. *Scientific Reports 2020 10:1*, *10*(1), 1–13. https://doi.org/10.1038/s41598-020-61432-1

Ji, W., Wang, W., Zhao, X., Zai, J., & Li, X. (2020). Cross-species transmission of the newly identified coronavirus 2019-nCoV. *Journal of Medical Virology*, *92*(4), 433–440. https://doi.org/10.1002/JMV.25682

Jiang, H. wei, Zhang, H. nan, Meng, Q. feng, Xie, J., Li, Y., Chen, H., Zheng, Y. xiao, Wang, X. ning, Qi, H., Zhang, J., Wang, P. H., Han, Z. G., & Tao, S. ce. (2020). SARS-CoV-2 Orf9b suppresses type I interferon responses by targeting TOM70. *Cellular & Molecular Immunology 2020 17:9*, *17*(9), 998–1000. https://doi.org/10.1038/s41423-020-0514-8

Jiang, S., Hillyer, C., & Du, L. (2020). Neutralizing Antibodies against SARS-CoV-2 and Other Human Coronaviruses. *Trends in Immunology*, *41*(5), 355–359. https://doi.org/10.1016/J.IT.2020.03.007

Jiang, S., Zhang, X., & Du, L. (2020). Therapeutic antibodies and fusion inhibitors targeting the spike protein of SARS-CoV-2. *Https://Doi.Org/10.1080/14728222.2020.1820482*, *25*(6), 415–421. https://doi.org/10.1080/14728222.2020.1820482

Johnson, M. C., Lyddon, T. D., Suarez, R., Salcedo, B., LePique, M., Graham, M., Ricana, C., Robinson, C., & Ritter, D. G. (2020). Optimized Pseudotyping Conditions for the SARS-COV-2 Spike Glycoprotein. *Journal of Virology*, *94*(21). https://doi.org/10.1128/JVI.01062-20

Jones, B. A., Grace, D., Kock, R., Alonso, S., Rushton, J., Said, M. Y., McKeever, D., Mutua, F., Young, J., McDermott, J., & Pfeiffer, D. U. (2013). Zoonosis emergence linked to agricultural intensification and environmental change. *Proceedings of the National Academy of Sciences of the United States of America*, *110*(21), 8399–8404. https://doi.org/10.1073/PNAS.1208059110/-/DCSUPPLEMENTAL

Joung, J., Ladha, A., Saito, M., Kim, N.-G., Woolley, A. E., Segel, M., Barretto, R. P. J., Ranu, A., Macrae, R. K., Faure, G., Ioannidi, E. I., Krajeski, R. N., Bruneau, R., Huang, M.-L. W., Yu, X. G., Li, J. Z., Walker, B. D., Hung, D. T., Greninger, A. L., … Zhang, F. (2020). Detection of SARS-CoV-2 with SHERLOCK One-Pot Testing. *Https://Doi.Org/10.1056/NEJMc2026172*, *383*(15), 1492–1494. https://doi.org/10.1056/NEJMC2026172

Ju, B., Zhang, Q., Ge, J., Wang, R., Sun, J., Ge, X., Yu, J., Shan, S., Zhou, B., Song, S., Tang, X., Yu, J., Lan, J., Yuan, J., Wang, H., Zhao, J., Zhang, S., Wang, Y., Shi, X., … Zhang, L. (2020). Human neutralizing antibodies elicited by SARS-CoV-2 infection. *Nature 2020 584:7819*, *584*(7819), 115–119. https://doi.org/10.1038/s41586-020-2380-z

Kanne, J. (2020). Chest CT Findings in 2019 Novel Coronavirus (2019-nCoV) Infections from Wuhan, China: Key Points for the Radiologist. *Radiology*, *295*(1), 16–17. https://doi.org/10.1148/RADIOL.2020200241

Karikó, K., Muramatsu, H., Welsh, F. A., Ludwig, J., Kato, H., Akira, S., & Weissman, D. (2008). Incorporation of Pseudouridine Into mRNA Yields Superior Nonimmunogenic Vector With Increased Translational Capacity and Biological Stability. *Molecular Therapy*, *16*(11), 1833–1840. https://doi.org/10.1038/MT.2008.200

Kauffman, K. J., Webber, M. J., & Anderson, D. G. (2016). Materials for non-viral intracellular delivery of messenger RNA therapeutics. *Journal of Controlled Release*, *240*, 227–234. https://doi.org/10.1016/J.JCONREL.2015.12.032

Kawasaki, T., & Kawai, T. (2014). Toll-like receptor signaling pathways. *Frontiers in Immunology*, *5*(SEP). https://doi.org/10.3389/FIMMU.2014.00461

Kellner, M. J., Koob, J. G., Gootenberg, J. S., Abudayyeh, O. O., & Zhang, F. (2019). SHERLOCK: nucleic acid detection with CRISPR nucleases. *Nature Protocols 2019 14:10*, *14*(10), 2986–3012. https://doi.org/10.1038/s41596-019-0210-2

Khailany, R. A., Safdar, M., & Ozaslan, M. (2020). Genomic characterization of a novel SARS-CoV-2. *Gene Reports*, *19*, 100682. https://doi.org/10.1016/J.GENREP.2020.100682

Kirtipal, N., Bharadwaj, S., & Kang, S. G. (2020). From SARS to SARS-CoV-2, insights on structure, pathogenicity and immunity aspects of pandemic human coronaviruses. *Infection, Genetics and Evolution*, *85*, 104502. https://doi.org/10.1016/J.MEEGID.2020.104502

Korber, B., Fischer, W. M., Gnanakaran, S., Yoon, H., Theiler, J., Abfalterer, W., Hengartner, N., Giorgi, E. E., Bhattacharya, T., Foley, B., Hastie, K. M., Parker, M. D., Partridge, D. G., Evans, C. M., Freeman, T. M., de Silva, T. I., Angyal, A., Brown, R. L., Carrilero, L., … Montefiori, D. C. (2020). Tracking Changes in SARS-CoV-2 Spike: Evidence that D614G Increases Infectivity of the COVID-19 Virus. *Cell*, *182*(4), 812-827.e19. https://doi.org/10.1016/J.CELL.2020.06.043

Kumar, S., Thambiraja, T. S., Karuppanan, K., & Subramaniam, | Gunasekaran. (2021). Omicron and Delta variant of SARS-CoV-2: A comparative computational study of spike protein. *Journal of Medical Virology*, 1–9. https://doi.org/10.1002/JMV.27526

Kutzler, M. A., & Weiner, D. B. (2008). DNA vaccines: ready for prime time? *Nature Reviews Genetics 2008 9:10*, *9*(10), 776–788. https://doi.org/10.1038/nrg2432

Lamers, M. M., Beumer, J., Vaart, J. Van Der, Knoops, K., Puschhof, J., Breugem, T. I., Ravelli, R. B. G., Schayck, J. P. Van, Mykytyn, A. Z., Duimel, H. Q., Donselaar, E. Van, Riesebosch, S., Kuijpers, H. J. H., Schipper, D., Wetering, W. J. V. De, Graaf, M. De, Koopmans, M., Cuppen, E., Peters, P. J., … Clevers, H. (2020). SARS-CoV-2 productively infects human gut enterocytes. *Science*, *369*(6499), 50–54. https://doi.org/10.1126/SCIENCE.ABC1669

Lau, S. K. P., Woo, P. C. Y., Li, K. S. M., Huang, Y., Tsoi, H. W., Wong, B. H. L., Wong, S. S. Y., Leung, S. Y., Chan, K. H., & Yuen, K. Y. (2005). Severe acute respiratory syndrome coronavirus-like virus in Chinese horseshoe bats. *Proceedings of the National Academy of Sciences*, *102*(39), 14040–14045. https://doi.org/10.1073/PNAS.0506735102

Laughlin, M. A., Chang, G. Y., Oakes, J. W., Gonzalez-Scarano, F., & Pomerantz, R. J. (1995). Sodium butyrate stimulation of HIV-1 gene expression: a novel mechanism of induction independent of NF-kappa B. *Journal of Acquired Immune Deficiency Syndromes and Human Retrovirology : Official Publication of the International Retrovirology Association*, *9*(4), 332–339. https://doi.org/10.1097/00042560-199508000-00002

Lauring, A. S., Jones, J. O., & Andino, R. (2010). Rationalizing the development of live attenuated virus vaccines. *Nature Biotechnology 2010 28:6*, *28*(6), 573–579. https://doi.org/10.1038/nbt.1635

Law, H. K. W., Chung, Y. C., Hoi, Y. N., Sin, F. S., Yuk, O. C., Luk, W., Nicholls, J. M., Peiris, J. S. M., & Lau, Y. L. (2005). Chemokine up-regulation in SARS-coronavirus–infected, monocyte-derived human dendritic cells. *Blood*, *106*(7), 2366–2374. https://doi.org/10.1182/BLOOD-2004-10-4166

Ledgerwood, J. E., Costner, P., Desai, N., Holman, L., Enama, M. E., Yamshchikov, G., Mulangu, S., Hu, Z., Andrews, C. A., Sheets, R. A., Koup, R. A., Roederer, M., Bailer, R., Mascola, J. R., Pau, M. G., Sullivan, N. J., Goudsmit, J., Nabel, G. J., & Graham, B. S. (2010). A replication defective recombinant Ad5 vaccine expressing Ebola virus GP is safe and immunogenic in healthy adults. *Vaccine*, *29*(2), 304–313. https://doi.org/10.1016/J.VACCINE.2010.10.037

Lee, C. (2019). Griffithsin, a Highly Potent Broad-Spectrum Antiviral Lectin from Red Algae: From Discovery to Clinical Application. *Marine Drugs 2019, Vol. 17, Page 567*, *17*(10), 567. https://doi.org/10.3390/MD17100567

Lee, S. G., Kim, S., Robbins, P. D., & Kim, B. G. (1996). Optimization of environmental factors for the production and handling of recombinant retrovirus. *Applied Microbiology and Biotechnology 1996 45:4*, *45*(4), 477–483. https://doi.org/10.1007/BF00578459

Leroy, E. M., Kumulungui, B., Pourrut, X., Rouquet, P., Hassanin, A., Yaba, P., Délicat, A., Paweska, J. T., Gonzalez, J. P., & Swanepoel, R. (2005). Fruit bats as reservoirs of Ebola virus. *Nature 2005 438:7068*, *438*(7068), 575–576. https://doi.org/10.1038/438575a

Letko, M., Marzi, A., & Munster, V. (2020a). Functional assessment of cell entry and receptor usage for SARS-CoV-2 and other lineage B betacoronaviruses. *Nature Microbiology*, *5*(4), 562–569. https://doi.org/10.1038/S41564-020-0688-Y

Letko, M., Marzi, A., & Munster, V. (2020b). Functional assessment of cell entry and receptor usage for SARS-CoV-2 and other lineage B betacoronaviruses. *Nature Microbiology*, *5*(4), 562–569. https://doi.org/10.1038/S41564-020-0688-Y

Li, C. K., Wu, H., Yan, H., Ma, S., Wang, L., Zhang, M., Tang, X., Temperton, N. J., Weiss, R. A., Brenchley, J. M., Douek, D. C., Mongkolsapaya, J., Tran, B.-H., Lin, C. S., Screaton, G. R., Hou, J., McMichael, A. J., & Xu, X.-N. (2008). T cell responses to whole SARS coronavirus in humans. *Journal of Immunology (Baltimore, Md. : 1950)*, *181*(8), 5490–5500. https://doi.org/10.4049/JIMMUNOL.181.8.5490

Li, C., Yang, Y., & Ren, L. (2020). Genetic evolution analysis of 2019 novel coronavirus and coronavirus from other species. *Infection, Genetics and Evolution : Journal of Molecular Epidemiology and Evolutionary Genetics in Infectious Diseases*, *82*. https://doi.org/10.1016/J.MEEGID.2020.104285

Li, F. (2016). Structure, Function, and Evolution of Coronavirus Spike Proteins. *Http://Dx.Doi.Org/10.1146/Annurev-Virology-110615-042301*, *3*, 237–261. https://doi.org/10.1146/ANNUREV-VIROLOGY-110615-042301

Li, G., Fan, Y., Lai, Y., Han, T., Li, Z., Zhou, P., Pan, P., Wang, W., Hu, D., Liu, X., Zhang, Q., & Wu, J. (2020). Coronavirus infections and immune responses. *Journal of Medical Virology*, *92*(4), 424–432. https://doi.org/10.1002/JMV.25685

Li, S. W., Wang, C. Y., Jou, Y. J., Huang, S. H., Hsiao, L. H., Wan, L., Lin, Y. J., Kung, S. H., & Lin, C. W. (2016). SARS Coronavirus Papain-Like Protease Inhibits the TLR7 Signaling Pathway through Removing Lys63-Linked Polyubiquitination of TRAF3 and TRAF6. *International Journal of Molecular Sciences 2016, Vol. 17, Page 678*, *17*(5), 678. https://doi.org/10.3390/IJMS17050678

Li, Y.-C., WZ, B., & T, H. (2020). The neuroinvasive potential of SARS-CoV2 may play a role in the respiratory failure of COVID-19 patients. *Journal of Medical Virology*, *92*(6), 552–555. https://doi.org/10.1002/JMV.25728

Lian, N., H, X., S, L., J, H., J, Z., & Q, L. (2020). Umifenovir treatment is not associated with improved outcomes in patients with coronavirus disease 2019: a retrospective study. *Clinical Microbiology and Infection : The Official Publication of the European Society of Clinical Microbiology and Infectious Diseases*, *26*(7), 917–921. https://doi.org/10.1016/J.CMI.2020.04.026

Lighter, J., M, P., S, H., S, S., D, J., F, F., & A, S. (2020). Obesity in Patients Younger Than 60 Years Is a Risk Factor for COVID-19 Hospital Admission. *Clinical Infectious Diseases : An Official Publication of the Infectious Diseases Society of America*, *71*(15), 896–897. https://doi.org/10.1093/CID/CIAA415

Liu, L., Wang, P., Nair, M. S., Yu, J., Rapp, M., Wang, Q., Luo, Y., Chan, J. F.-W., Sahi, V., Figueroa, A., Guo, X. V., Cerutti, G., Bimela, J., Gorman, J., Zhou, T., Chen, Z., Yuen, K.-Y., Kwong, P. D., Sodroski, J. G., … Ho, D. D. (2020). Potent neutralizing antibodies against multiple epitopes on SARS-CoV-2 spike. *Nature 2020 584:7821*, *584*(7821), 450–456. https://doi.org/10.1038/s41586-020-2571-7

Liu, M. (2019). A Comparison of Plasmid DNA and mRNA as Vaccine Technologies. *Vaccines*, *7*(2). https://doi.org/10.3390/VACCINES7020037

Liu, P., W, C., & JP, C. (2019). Viral Metagenomics Revealed Sendai Virus and Coronavirus Infection of Malayan Pangolins ( Manis javanica). *Viruses*, *11*(11). https://doi.org/10.3390/V11110979

Liu, Y., Mao, B., Liang, S., Yang, J.-W., Lu, H.-W., Chai, Y.-H., Wang, L., Zhang, L., Li, Q.-H., Zhao, L., He, Y., Gu, X.-L., Ji, X.-B., Li, L., Jie, Z.-J., Li, Q., Li, X.-Y., Lu, H.-Z., Zhang, W.-H., … Xu, J.-F. (2020). Association between age and clinical characteristics and outcomes of COVID-19. *European Respiratory Journal*, *55*(5). https://doi.org/10.1183/13993003.01112-2020

Logunov, D. Y., Dolzhikova, I. V., Shcheblyakov, D. V., Tukhvatulin, A. I., Zubkova, O. V., Dzharullaeva, A. S., Kovyrshina, A. V., Lubenets, N. L., Grousova, D. M., Erokhova, A. S., Botikov, A. G., Izhaeva, F. M., Popova, O., Ozharovskaya, T. A., Esmagambetov, I. B., Favorskaya, I. A., Zrelkin, D. I., Voronina, D. V., Shcherbinin, D. N., … Gintsburg, A. L. (2021). Safety and efficacy of an rAd26 and rAd5 vector-based heterologous prime-boost COVID-19 vaccine: an interim analysis of a randomised controlled phase 3 trial in Russia. *The Lancet*, *397*(10275), 671–681. https://doi.org/10.1016/S0140-6736(21)00234-8/ATTACHMENT/5B392723-A191-4FD1-B36A-F0B5603CA1DD/MMC1.PDF

Lopes, A., G, V., & V, P. (2019). Cancer DNA vaccines: current preclinical and clinical developments and future perspectives. *Journal of Experimental & Clinical Cancer Research : CR*, *38*(1). https://doi.org/10.1186/S13046-019-1154-7

Lu, H. (2020). Drug treatment options for the 2019-new coronavirus (2019-nCoV). *BioScience Trends*, *14*(1), 69–71. https://doi.org/10.5582/BST.2020.01020

Lu, R., Zhao, X., Li, J., Niu, P., Yang, B., Wu, H., Wang, W., Song, H., Huang, B., Zhu, N., Bi, Y., Ma, X., Zhan, F., Wang, L., Hu, T., Zhou, H., Hu, Z., Zhou, W., Zhao, L., … Tan, W. (2020). Genomic characterisation and epidemiology of 2019 novel coronavirus: implications for virus origins and receptor binding. *The Lancet*, *395*(10224), 565–574. https://doi.org/10.1016/S0140-6736(20)30251-8

Lu, X., Zhang, L., Du, H., Zhang, J., Li, Y. Y., Qu, J., Zhang, W., Wang, Y., Bao, S., Li, Y., Wu, C., Liu, H., Liu, D., Shao, J., Peng, X., Yang, Y., Liu, Z., Xiang, Y., Zhang, F., … Wong, G. W. K. (2020). SARS-CoV-2 Infection in Children. *Https://Doi.Org/10.1056/NEJMc2005073*, *382*(17), 1663–1665. https://doi.org/10.1056/NEJMC2005073

Lurie, N., Saville, M., Hatchett, R., & Halton, J. (2020). Developing Covid-19 Vaccines at Pandemic Speed. *Https://Doi.Org/10.1056/NEJMp2005630*, *382*(21), 1969–1973. https://doi.org/10.1056/NEJMP2005630

Malik, Y. S., Sircar, S., Bhat, S., Sharun, K., Dhama, K., Dadar, M., Tiwari, R., & Chaicumpa, W. (2020). Emerging novel coronavirus (2019-nCoV)—current scenario, evolutionary perspective based on genome analysis and recent developments. *Veterinary Quarterly*, *40*(1), 68–76. https://doi.org/10.1080/01652176.2020.1727993/SUPPL_FILE/TVEQ_A_1727993_SM0882.ZIP

Mantlo, E., N, B., J, M., S, P., & C, H. (2020). Antiviral activities of type I interferons to SARS-CoV-2 infection. *Antiviral Research*, *179*. https://doi.org/10.1016/J.ANTIVIRAL.2020.104811

Marano, G., Vaglio, S., Pupella, S., Facco, G., Catalano, L., Liumbruno, G. M., & Grazzini, G. (2016). Convalescent plasma: New evidence for an old therapeutic tool? *Blood Transfusion*, *14*(2), 152–157. https://doi.org/10.2450/2015.0131-15

Masters, P. S. (2006). The Molecular Biology of Coronaviruses. *Advances in Virus Research*, *66*, 193–292. https://doi.org/10.1016/S0065-3527(06)66005-3

McBride, R., van Zyl, M., & Fielding, B. C. (2014). The Coronavirus Nucleocapsid Is a Multifunctional Protein. *Viruses 2014, Vol. 6, Pages 2991-3018*, *6*(8), 2991–3018. https://doi.org/10.3390/V6082991

McCallum, M., Marco, A. De, Lempp, F., Tortorici, M. A., Pinto, D., Walls, A. C., Beltramello, M., Chen, A., Liu, Z., Zatta, F., Zepeda, S., di Iulio, J., Bowen, J. E., Montiel-Ruiz, M., Zhou, J., Rosen, L. E., Bianchi, S., Guarino, B., Fregni, C. S., … Veesler, D. (2021). N-terminal domain antigenic mapping reveals a site of vulnerability for SARS-CoV-2. *BioRxiv : The Preprint Server for Biology*. https://doi.org/10.1101/2021.01.14.426475

McCarthy, K. R., Rennick, L. J., Nambulli, S., Robinson-McCarthy, L. R., Bain, W. G., Haidar, G., & Paul Duprex, W. (2021). Recurrent deletions in the SARS-CoV-2 spike glycoprotein drive antibody escape. *Science (New York, N.Y.)*, *371*(6534), 1139–1142. https://doi.org/10.1126/SCIENCE.ABF6950

McGill, A. R., Kahlil, R., Dutta, R., Green, R., Howell, M., Mohapatra, S., & Mohapatra, S. S. (2021). SARS–CoV-2 Immuno-Pathogenesis and Potential for Diverse Vaccines and Therapies: Opportunities and Challenges. *Infectious Disease Reports 2021, Vol. 13, Pages 102-125*, *13*(1), 102–125. https://doi.org/10.3390/IDR13010013

Mcguire, L. W., & Redden, W. R. (1919). TREATMENT OF INFLUENZAL PNEUMONIA BY THE USE OF CONVALESCENT HUMAN SERUM: SECOND REPORT. *Journal of the American Medical Association*, *72*(10), 709–713. https://doi.org/10.1001/JAMA.1919.02610100017007

Mehta, P., DF, M., M, B., E, S., RS, T., & JJ, M. (2020). COVID-19: consider cytokine storm syndromes and immunosuppression. *Lancet (London, England)*, *395*(10229), 1033–1034. https://doi.org/10.1016/S0140-6736(20)30628-0

Mendoza, E. J., Manguiat, K., Wood, H., & Drebot, M. (2020). Two Detailed Plaque Assay Protocols for the Quantification of Infectious SARS-CoV-2. *Current Protocols in Microbiology*, *57*(1). https://doi.org/10.1002/CPMC.105

Meng, B., Kemp, S. A., Papa, G., Datir, R., Ferreira, I. A. T. M., Marelli, S., Harvey, W. T., Lytras, S., Mohamed, A., Gallo, G., Thakur, N., Collier, D. A., Mlcochova, P., Robson, S. C., Loman, N. J., Connor, T. R., Golubchik, T., Martinez Nunez, R. T., Ludden, C., … Gupta, R. K. (2021). Recurrent emergence of SARS-CoV-2 spike deletion H69/V70 and its role in the Alpha variant B.1.1.7. *Cell Reports*, *35*(13). https://doi.org/10.1016/J.CELREP.2021.109292

Mercado, N. B., Zahn, R., Wegmann, F., Loos, C., Chandrashekar, A., Yu, J., Liu, J., Peter, L., McMahan, K., Tostanoski, L. H., He, X., Martinez, D. R., Rutten, L., Bos, R., van Manen, D., Vellinga, J., Custers, J., Langedijk, J. P., Kwaks, T., … Barouch, D. H. (2020). Single-shot Ad26 vaccine protects against SARS-CoV-2 in rhesus macaques. *Nature 2020 586:7830*, *586*(7830), 583–588. https://doi.org/10.1038/s41586-020-2607-z

Meselson, M. (2020). Droplets and Aerosols in the Transmission of SARS-CoV-2. *Https://Doi.Org/10.1056/NEJMc2009324*, *382*(21), 2063–2063. https://doi.org/10.1056/NEJMC2009324

Millet, J., & Whittaker, G. (2016). Murine Leukemia Virus (MLV)-based Coronavirus Spike-pseudotyped Particle Production and Infection. *Bio-Protocol*, *6*(23). https://doi.org/10.21769/BIOPROTOC.2035

Mistry, P., Barmania, F., Mellet, J., Peta, K., Strydom, A., Viljoen, I. M., James, W., Gordon, S., & Pepper, M. S. (2022). SARS-CoV-2 Variants, Vaccines, and Host Immunity. *Frontiers in Immunology*, *12*. https://doi.org/10.3389/FIMMU.2021.809244

Miyakawa, K., Jeremiah, S. S., Ohtake, N., Matsunaga, S., Yamaoka, Y., Nishi, M., Morita, T., Saji, R., Nishii, M., Kimura, H., Hasegawa, H., Takeuchi, I., & Ryo, A. (2020). Rapid quantitative screening assay for SARS-CoV-2 neutralizing antibodies using HiBiT-tagged virus-like particles. *Journal of Molecular Cell Biology*, *12*(12), 987–990. https://doi.org/10.1093/JMCB/MJAA047

Monteil, V., H, K., P, P., A, H., RA, W., M, S., A, L., E, G., C, H. D. P., F, P., JP, R., G,

W., H, Z., AS, S., R, C., N, M., A, M., & JM, P. (2020). Inhibition of SARS-CoV-2 Infections in Engineered Human Tissues Using Clinical-Grade Soluble Human ACE2. *Cell*, *181*(4), 905-913.e7. https://doi.org/10.1016/J.CELL.2020.04.004

Moxley, G., Posthuma, D., Carlson, P., Estrada, E., Han, J., Benson, L. L., & Neale, M. C. (2002). Sexual Dimorphism in Innate Immunity. *ARTHRITIS & RHEUMATISM*, *46*(1), 250–258. https://doi.org/10.1002/1529-0131

Mu, J., Fang, Y., Yang, Q., Shu, T., Wang, A., Huang, M., Jin, L., Deng, F., Qiu, Y., & Zhou, X. (2020). SARS-CoV-2 N protein antagonizes type I interferon signaling by suppressing phosphorylation and nuclear translocation of STAT1 and STAT2. *Cell Discovery 2020 6:1*, *6*(1), 1–4. https://doi.org/10.1038/s41421-020-00208-3

Müller, M. A., Corman, V. M., Jores, J., Meyer, B., Younan, M., Liljander, A., Bosch, B. J., Lattwein, E., Hilali, M., Musa, B. E., Bornstein, S., & Drosten, C. (2014). MERS Coronavirus Neutralizing Antibodies in Camels, Eastern Africa, 1983–1997. *Emerging Infectious Diseases*, *20*(12), 2093. https://doi.org/10.3201/EID2012.141026

Munnink, B. B. O., Sikkema, R. S., Nieuwenhuijse, D. F., Molenaar, R. J., Munger, E., Molenkamp, R., Van Der Spek, A., Tolsma, P., Rietveld, A., Brouwer, M., Bouwmeester-Vincken, N., Harders, F., Der Honing, R. H. Van, Wegdam-Blans, M. C. A., Bouwstra, R. J., GeurtsvanKessel, C., Van Der Eijk, A. A., Velkers, F. C., Smit, L. A. M., … Koopmans, M. P. G. (2021). Transmission of SARS-CoV-2 on mink farms between humans and mink and back to humans. *Science (New York, N.Y.)*, *371*(6525), 172–177. https://doi.org/10.1126/SCIENCE.ABE5901

Muruato, A. E., Fontes-Garfias, C. R., Ren, P., Garcia-Blanco, M. A., Menachery, V. D., Xie, X., & Shi, P. Y. (2020). A high-throughput neutralizing antibody assay for COVID-19 diagnosis and vaccine evaluation. *Nature Communications*, *11*(1). https://doi.org/10.1038/S41467-020-17892-0

Naqvi, A. A. T., Fatima, K., Mohammad, T., Fatima, U., Singh, I. K., Singh, A., Atif, S. M., Hariprasad, G., Hasan, G. M., & Hassan, M. I. (2020). Insights into SARS-CoV-2 genome, structure, evolution, pathogenesis and therapies: Structural genomics approach. *Biochimica et Biophysica Acta. Molecular Basis of Disease*, *1866*(10), 165878. https://doi.org/10.1016/J.BBADIS.2020.165878

National Center for Immunization and Respiratory Diseases (NCIRD), D. of V. D. (2021). Science Brief: Omicron (B.1.1.529) Variant. *CDC COVID-19 Science Briefs*. https://www.ncbi.nlm.nih.gov/books/NBK575856/

Neufeldt, C. J., Cerikan, B., Cortese, M., Frankish, J., Lee, J.-Y., Plociennikowska, A., Heigwer, F., Joecks, S., Burkart, S. S., Zander, D. Y., Gendarme, M., Debs, B. El, Halama, N., Merle, U., Boutros, M., Binder, M., & Bartenschlager, R. (2020). SARS-CoV-2 infection induces a pro-inflammatory cytokine response through cGAS-STING and NF-κB. *BioRxiv*, 2020.07.21.212639. https://doi.org/10.1101/2020.07.21.212639

Neuman, B. W., Kiss, G., Kunding, A. H., Bhella, D., Baksh, M. F., Connelly, S., Droese, B., Klaus, J. P., Makino, S., Sawicki, S. G., Siddell, S. G., Stamou, D. G., Wilson, I. A., Kuhn, P., & Buchmeier, M. J. (2011). A structural analysis of M protein in coronavirus assembly and morphology. *Journal of Structural Biology*, *174*(1), 11–

22. https://doi.org/10.1016/J.JSB.2010.11.021

Ni, G., Ma, Z., & Damania, B. (2018). cGAS and STING: At the intersection of DNA and RNA virus-sensing networks. *PLoS Pathogens*, *14*(8). https://doi.org/10.1371/JOURNAL.PPAT.1007148

Ni, L., Ye, F., Cheng, M. L., Feng, Y., Deng, Y. Q., Zhao, H., Wei, P., Ge, J., Gou, M., Li, X., Sun, L., Cao, T., Wang, P., Zhou, C., Zhang, R., Liang, P., Guo, H., Wang, X., Qin, C. F., … Dong, C. (2020). Detection of SARS-CoV-2-Specific Humoral and Cellular Immunity in COVID-19 Convalescent Individuals. *Immunity*, *52*(6), 971-977.e3. https://doi.org/10.1016/J.IMMUNI.2020.04.023

Niazi, S. K., Bhatti, F. A., Salamat, N., Ghani, E., & Tayyab, M. (2015). Impact of nucleic acid amplification test on screening of blood donors in Northern Pakistan. *Transfusion*, *55*(7), 1803–1811. https://doi.org/10.1111/TRF.13017

Nie, J., Li, Q., Wu, J., Zhao, C., Hao, H., Liu, H., Zhang, L., Nie, L., Qin, H., Wang, M., Lu, Q., Li, X., Sun, Q., Liu, J., Fan, C., Huang, W., Xu, M., & Wang, Y. (2020a). Establishment and validation of a pseudovirus neutralization assay for SARS-CoV-2. *Emerging Microbes & Infections*, *9*(1), 680–686. https://doi.org/10.1080/22221751.2020.1743767

Nie, J., Li, Q., Wu, J., Zhao, C., Hao, H., Liu, H., Zhang, L., Nie, L., Qin, H., Wang, M., Lu, Q., Li, X., Sun, Q., Liu, J., Fan, C., Huang, W., Xu, M., & Wang, Y. (2020b). Establishment and validation of a pseudovirus neutralization assay for SARS-CoV-2. *Emerging Microbes & Infections*, *9*(1), 680–686. https://doi.org/10.1080/22221751.2020.1743767

Nie, J., Li, Q., Wu, J., Zhao, C., Hao, H., Liu, H., Zhang, L., Nie, L., Qin, H., Wang, M., Lu, Q., Li, X., Sun, Q., Liu, J., Fan, C., Huang, W., Xu, M., & Wang, Y. (2020c). Quantification of SARS-CoV-2 neutralizing antibody by a pseudotyped virus-based assay. *Nature Protocols 2020 15:11*, *15*(11), 3699–3715. https://doi.org/10.1038/s41596-020-0394-5

Nieto-Torres, J. L., DeDiego, M. L., Álvarez, E., Jiménez-Guardeño, J. M., Regla-Nava, J. A., Llorente, M., Kremer, L., Shuo, S., & Enjuanes, L. (2011). Subcellular location and topology of severe acute respiratory syndrome coronavirus envelope protein. *Virology*, *415*(2), 69–82. https://doi.org/10.1016/J.VIROL.2011.03.029

Noval, M. G., Kaczmarek, M. E., Koide, A., Rodriguez-Rodriguez, B. A., Louie, P., Tada, T., Hattori, T., Panchenko, T., Romero, L. A., Teng, K. W., Bazley, A., Vries, M. de, Samanovic, M. I., Weiser, J. N., Aifantis, I., Cangiarella, J., Mulligan, M. J., Desvignes, L., Dittmann, M., … Stapleford, K. A. (2020). High titers of multiple antibody isotypes against the SARS-CoV-2 spike receptor-binding domain and nucleoprotein associate with better neutralization. *BioRxiv*, 2020.08.15.252353. https://doi.org/10.1101/2020.08.15.252353

Nunnally, B. K., Turula, V. E., & Sitrin, R. D. (2015). Vaccine analysis: Strategies, principles, and control. *Vaccine Analysis: Strategies, Principles, and Control*, 1–665. https://doi.org/10.1007/978-3-662-45024-6

Olsen, J. C., & Sechelski, J. (2008). Use of Sodium Butyrate to Enhance Production of Retroviral Vectors Expressing CFTR cDNA. *Https://Home.Liebertpub.Com/Hum*,

*6*(9), 1195–1202. https://doi.org/10.1089/HUM.1995.6.9-1195

Oostra, M., Hagemeijer, M. C., van Gent, M., Bekker, C. P. J., te Lintelo, E. G., Rottier, P. J. M., & de Haan, C. A. M. (2008). Topology and Membrane Anchoring of the Coronavirus Replication Complex: Not All Hydrophobic Domains of nsp3 and nsp6 Are Membrane Spanning. *Journal of Virology*, *82*(24), 12392–12405. https://doi.org/10.1128/JVI.01219-08/SUPPL_FILE/TABLE_1.DOC

Otsuka, R., & Seino, K. I. (2020). Macrophage activation syndrome and COVID-19. *Inflammation and Regeneration*, *40*(1). https://doi.org/10.1186/S41232-020-00131-W

Ou, X., Liu, Y., Lei, X., Li, P., Mi, D., Ren, L., Guo, L., Guo, R., Chen, T., Hu, J., Xiang, Z., Mu, Z., Chen, X., Chen, J., Hu, K., Jin, Q., Wang, J., & Qian, Z. (2020). Characterization of spike glycoprotein of SARS-CoV-2 on virus entry and its immune cross-reactivity with SARS-CoV. *Nature Communications 2020 11:1*, *11*(1), 1–12. https://doi.org/10.1038/s41467-020-15562-9

Pachetti, M., Marini, B., Benedetti, F., Giudici, F., Mauro, E., Storici, P., Masciovecchio, C., Angeletti, S., Ciccozzi, M., Gallo, R. C., Zella, D., & Ippodrino, R. (2020). Emerging SARS-CoV-2 mutation hot spots include a novel RNA-dependent-RNA polymerase variant. *Journal of Translational Medicine*, *18*(1), 1–9. https://doi.org/10.1186/S12967-020-02344-6/FIGURES/4

Palacios, R., Batista, A. P., Santos, C., Albuquerque, N., Patiño, E. G., Do, J., Santos, P., Reis, M. T., Conde, P., De Oliveira Piorelli, R., Carlos, L., Júnior, P., Raboni, S. M., Ramos, F., Adolfo, G., Romero, S., Fábio, 15, Leal, E., Fernando, L., … Leal De Oliveira, D. B. (2021). *Title Efficacy and safety of a COVID-19 inactivated vaccine in healthcare 2 professionals in Brazil: The PROFISCOV study 3 4*. https://ssrn.com/abstract=3822780

Pamukcu, C., Celik, E., Ergun, E. Z., Karahan, Z. S., Turkoz, G., Aras, M., Eren, C., Sili, U., Bilgin, H., Suder, I., Mandaci, B. C., Dingiloglu, B., Tatli, O., Doganay, G. D., Baris, S., Ozoren, N., & Sutlu, T. (2020). Lentiviral vector-based SARS-CoV-2 pseudovirus enables analysis of neutralizing activity in COVID-19 convalescent plasma. *BioRxiv*, 2020.12.28.424590. https://doi.org/10.1101/2020.12.28.424590

Pan, Y., D, Z., P, Y., LLM, P., & Q, W. (2020). Viral load of SARS-CoV-2 in clinical samples. *The Lancet. Infectious Diseases*, *20*(4), 411–412. https://doi.org/10.1016/S1473-3099(20)30113-4

Pardi, N., Hogan, M. J., Porter, F. W., & Weissman, D. (2018). mRNA vaccines — a new era in vaccinology. *Nature Reviews Drug Discovery 2018 17:4*, *17*(4), 261–279. https://doi.org/10.1038/nrd.2017.243

Park, A., & A, I. (2020). Type I and Type III Interferons - Induction, Signaling, Evasion, and Application to Combat COVID-19. *Cell Host & Microbe*, *27*(6), 870–878. https://doi.org/10.1016/J.CHOM.2020.05.008

Park, J. G., Oladunni, F. S., Chiem, K., Ye, C., Pipenbrink, M., Moran, T., Walter, M. R., Kobie, J., & Martinez-Sobrido, L. (2021). Rapid in vitro assays for screening neutralizing antibodies and antivirals against SARS-CoV-2. *Journal of Virological Methods*, *287*, 113995. https://doi.org/10.1016/J.JVIROMET.2020.113995

Park, S. E. (2020). Epidemiology, virology, and clinical features of severe acute respiratory syndrome -coronavirus-2 (SARS-CoV-2; Coronavirus Disease-19). *Clinical and Experimental Pediatrics*, *63*(4), 119–124. https://doi.org/10.3345/CEP.2020.00493

Petsch, B., Schnee, M., Vogel, A. B., Lange, E., Hoffmann, B., Voss, D., Schlake, T., Thess, A., Kallen, K.-J., Stitz, L., & Kramps, T. (2012). Protective efficacy of in vitro synthesized, specific mRNA vaccines against influenza A virus infection. *Nature Biotechnology 2012 30:12*, *30*(12), 1210–1216. https://doi.org/10.1038/nbt.2436

Pinto, D., Park, Y. J., Beltramello, M., Walls, A. C., Tortorici, M. A., Bianchi, S., Jaconi, S., Culap, K., Zatta, F., De Marco, A., Peter, A., Guarino, B., Spreafico, R., Cameroni, E., Case, J. B., Chen, R. E., Havenar-Daughton, C., Snell, G., Telenti, A., … Corti, D. (2020). Cross-neutralization of SARS-CoV-2 by a human monoclonal SARS-CoV antibody. *Nature 2020 583:7815*, *583*(7815), 290–295. https://doi.org/10.1038/s41586-020-2349-y

Plante, J. A., Liu, Y., Liu, J., Xia, H., Johnson, B. A., Lokugamage, K. G., Zhang, X., Muruato, A. E., Zou, J., Fontes-Garfias, C. R., Mirchandani, D., Scharton, D., Bilello, J. P., Ku, Z., An, Z., Kalveram, B., Freiberg, A. N., Menachery, V. D., Xie, X., … Shi, P. Y. (2020). Spike mutation D614G alters SARS-CoV-2 fitness. *Nature 2020 592:7852*, *592*(7852), 116–121. https://doi.org/10.1038/s41586-020-2895-3

Plante, J. A., Mitchell, B. M., Plante, K. S., Debbink, K., Weaver, S. C., & Menachery, V. D. (2021). The variant gambit: COVID-19's next move. *Cell Host & Microbe*, *29*(4), 508–515. https://doi.org/10.1016/J.CHOM.2021.02.020

Plotkin, S. (2014). History of vaccination. *Proceedings of the National Academy of Sciences*, *111*(34), 12283–12287. https://doi.org/10.1073/PNAS.1400472111

Polack, F. P., Thomas, S. J., Kitchin, N., Absalon, J., Gurtman, A., Lockhart, S., Perez, J. L., Marc, G. P., Moreira, E. D., Zerbini, C., Bailey, R., Swanson, K. A., Roychoudhury, S., Koury, K., Li, P., Kalina, W. V., Cooper, D., Robert W. Frenck, J., Hammitt, L. L., … Gruber, W. C. (2020). Safety and Efficacy of the BNT162b2 mRNA Covid-19 Vaccine. *Https://Doi.Org/10.1056/NEJMoa2034577*, *383*(27), 2603–2615. https://doi.org/10.1056/NEJMOA2034577

Posthuma, C. C., te Velthuis, A. J. W., & Snijder, E. J. (2017). Nidovirus RNA polymerases: Complex enzymes handling exceptional RNA genomes. *Virus Research*, *234*, 58–73. https://doi.org/10.1016/J.VIRUSRES.2017.01.023

Prasad, A., Muthamilarasan, M., & Prasad, M. (2020). Synergistic antiviral effects against SARS-CoV-2 by plant-based molecules. *Plant Cell Reports 2020 39:9*, *39*(9), 1109–1114. https://doi.org/10.1007/S00299-020-02560-W

Qiang, G., Bao, L., Mao, H., Wang, L., Xu, K., Yang, M., Li, Y., Zhu, L., Wang, N., Lv, Z., Gao, H., Ge, X., Kan, B., Hu, Y., Liu, J., Cai, F., Jiang, D., Yin, Y., Qin, C., … Qin, C. (2020). Development of an inactivated vaccine candidate for SARS-CoV-2. *Science*, *369*(6499), 77–81. https://doi.org/10.1126/SCIENCE.ABC1932

Qin, C., Zhou, L., Hu, Z., Zhang, S., Yang, S., Tao, Y., Xie, C., Ma, K., Shang, K., Wang, W., & Tian, D. S. (2020). Dysregulation of Immune Response in Patients With

Coronavirus 2019 (COVID-19) in Wuhan, China. *Clinical Infectious Diseases : An Official Publication of the Infectious Diseases Society of America*, *71*(15), 762–768. https://doi.org/10.1093/CID/CIAA248

Quinlan, B. D., Mou, H., Zhang, L., Guo, Y., He, W., Ojha, A., Parcells, M. S., Luo, G., Li, W., Zhong, G., Choe, H., & Farzan, M. (2020). The SARS-CoV-2 Receptor-Binding Domain Elicits a Potent Neutralizing Response Without Antibody-Dependent Enhancement. *SSRN Electronic Journal*. https://doi.org/10.2139/SSRN.3575134

Rajendran, K., Krishnasamy, N., Rangarajan, J., Rathinam, J., Natarajan, M., & Ramachandran, A. (2020). Convalescent plasma transfusion for the treatment of COVID-19: Systematic review. *Journal of Medical Virology*, *92*(9), 1475–1483. https://doi.org/10.1002/JMV.25961

Ranard, L., JA, F., M, A., DE, A., RC, G., D, K., SK, K., K, T., D, K., LE, R., G, S., AJ, K., MB, L., A, S., N, U., & A, M. (2020). Approach to Acute Cardiovascular Complications in COVID-19 Infection. *Circulation. Heart Failure*, *13*(7), 167–176. https://doi.org/10.1161/CIRCHEARTFAILURE.120.007220

RECOVERY, T. (2020). Dexamethasone in Hospitalized Patients with Covid-19. *Https://Doi.Org/10.1056/NEJMoa2021436*, *384*(8), 693–704. https://doi.org/10.1056/NEJMOA2021436

*Report of the WHO-China Joint Mission on Coronavirus Disease 2019 (COVID-19)*. (n.d.). Retrieved October 6, 2021, from https://www.who.int/publications/i/item/report-of-the-who-China-joint-mission-on-coronavirus-disease-2019-(COVID-19)

Robbiani, D. F., Gaebler, C., Muecksch, F., Lorenzi, J. C. C., Wang, Z., Cho, A., Agudelo, M., Barnes, C. O., Gazumyan, A., Finkin, S., Hägglöf, T., Oliveira, T. Y., Viant, C., Hurley, A., Hoffmann, H. H., Millard, K. G., Kost, R. G., Cipolla, M., Gordon, K., … Nussenzweig, M. C. (2020a). Convergent antibody responses to SARS-CoV-2 in convalescent individuals. *Nature 2020 584:7821*, *584*(7821), 437–442. https://doi.org/10.1038/s41586-020-2456-9

Robbiani, D. F., Gaebler, C., Muecksch, F., Lorenzi, J. C. C., Wang, Z., Cho, A., Agudelo, M., Barnes, C. O., Gazumyan, A., Finkin, S., Hägglöf, T., Oliveira, T. Y., Viant, C., Hurley, A., Hoffmann, H. H., Millard, K. G., Kost, R. G., Cipolla, M., Gordon, K., … Nussenzweig, M. C. (2020b). Convergent antibody responses to SARS-CoV-2 in convalescent individuals. *Nature*, *584*(7821), 437–442. https://doi.org/10.1038/S41586-020-2456-9

Rojas, M., Rodríguez, Y., Monsalve, D. M., Acosta-Ampudia, Y., Camacho, B., Gallo, J. E., Rojas-Villarraga, A., Ramírez-Santana, C., Díaz-Coronado, J. C., Manrique, R., Mantilla, R. D., Shoenfeld, Y., & Anaya, J. M. (2020). Convalescent plasma in Covid-19: Possible mechanisms of action. *Autoimmunity Reviews*, *19*(7). https://doi.org/10.1016/J.AUTREV.2020.102554

Rossi, M., & Young, J. W. (2005). Human dendritic cells: potent antigen-presenting cells at the crossroads of innate and adaptive immunity. *Journal of Immunology (Baltimore, Md. : 1950)*, *175*(3), 1373–1381. https://doi.org/10.4049/JIMMUNOL.175.3.1373

Rothan, H. A., & Byrareddy, S. N. (2020). *The epidemiology and pathogenesis of coronavirus disease (COVID-19) outbreak*. https://doi.org/10.1016/j.jaut.2020.102433

Rowe, T., Abernathy, R. A., Hu-Primmer, J., Thompson, W. W., Lu, X., Lim, W., Fukuda, K., Cox, N. J., & Katz, J. M. (1999). Detection of antibody to avian influenza A (H5N1) virus in human serum by using a combination of serologic assays. *Journal of Clinical Microbiology*, *37*(4), 937–943. https://doi.org/10.1128/JCM.37.4.937-943.1999

Sabino, E. C., Buss, L. F., Carvalho, M. P. S., Prete, C. A., Crispim, M. A. E., Fraiji, N. A., Pereira, R. H. M., Parag, K. V., da Silva Peixoto, P., Kraemer, M. U. G., Oikawa, M. K., Salomon, T., Cucunuba, Z. M., Castro, M. C., de Souza Santos, A. A., Nascimento, V. H., Pereira, H. S., Ferguson, N. M., Pybus, O. G., … Faria, N. R. (2021). Resurgence of COVID-19 in Manaus, Brazil, despite high seroprevalence. *Lancet (London, England)*, *397*(10273), 452–455. https://doi.org/10.1016/S0140-6736(21)00183-5

Sakai, Y., Kawachi, K., Terada, Y., Omori, H., Matsuura, Y., & Kamitani, W. (2017). Two-amino acids change in the nsp4 of SARS coronavirus abolishes viral replication. *Virology*, *510*, 165–174. https://doi.org/10.1016/J.VIROL.2017.07.019

Sakr, M. M., Elsayed, N. S., & El-Housseiny, G. S. (2021). Latest updates on SARS-CoV-2 genomic characterization, drug, and vaccine development; a comprehensive bioinformatics review. *Microbial Pathogenesis*, *154*. https://doi.org/10.1016/J.MICPATH.2021.104809

Sallard, E., FX, L., Y, Y., F, M., & N, P.-S. (2020). Type 1 interferons as a potential treatment against COVID-19. *Antiviral Research*, *178*. https://doi.org/10.1016/J.ANTIVIRAL.2020.104791

Sarkar, R., Lo, M., Saha, R., Dutta, S., & Chawla-Sarkar, M. (2021). S glycoprotein diversity of the Omicron Variant. *MedRxiv*, 2021.12.04.21267284. https://doi.org/10.1101/2021.12.04.21267284

Schmidt, F., Weisblum, Y., Muecksch, F., Hoffmann, H. H., Michailidis, E., Lorenzi, J. C. C., Mendoza, P., Rutkowska, M., Bednarski, E., Gaebler, C., Agudelo, M., Cho, A., Wang, Z., Gazumyan, A., Cipolla, M., Caskey, M., Robbiani, D. F., Nussenzweig, M. C., Rice, C. M., … Bieniasz, P. D. (2020). Measuring SARS-CoV-2 neutralizing antibody activity using pseudotyped and chimeric viruses. *The Journal of Experimental Medicine*, *217*(11). https://doi.org/10.1084/JEM.20201181

Schoeman, D., & Fielding, B. C. (2019). Coronavirus envelope protein: current knowledge. *Virology Journal 2019 16:1*, *16*(1), 1–22. https://doi.org/10.1186/S12985-019-1182-0

Shahani, L., Singh, S., & Khardori, N. M. (2012). Immunotherapy in Clinical Medicine: Historical Perspective and Current Status. *Medical Clinics of North America*, *96*(3), 421–431. https://doi.org/10.1016/J.MCNA.2012.04.001

Shang, J., Wan, Y., Luo, C., Ye, G., Geng, Q., Auerbach, A., & Li, F. (2020). Cell entry mechanisms of SARS-CoV-2. *Proceedings of the National Academy of Sciences of the United States of America*, *117*(21). https://doi.org/10.1073/PNAS.2003138117

Shanker, A. K., Bhanu, D., Alluri, A., & Gupta, S. (2020). Whole-genome sequence analysis and homology modelling of the main protease and non-structural protein 3 of SARS-CoV-2 reveal an aza-peptide and a lead inhibitor with possible antiviral properties. *New Journal of Chemistry*, *44*(22), 9202–9212. https://doi.org/10.1039/D0NJ00974A

Shanmugaraj, B., Siriwattananon, K., Wangkanont, K., & Phoolcharoen, W. (n.d.). *Allergy and Immunology Perspectives on monoclonal antibody therapy as potential therapeutic intervention for Coronavirus disease-19 (COVID-19)*. https://doi.org/10.12932/AP-200220-0773

Shen, C., Wang, Z., Zhao, F., Yang, Y., Li, J., Yuan, J., Wang, F., Li, D., Yang, M., Xing, L., Wei, J., Xiao, H., Yang, Y., Qu, J., Qing, L., Chen, L., Xu, Z., Peng, L., Li, Y., … Liu, L. (2020). Treatment of 5 Critically Ill Patients With COVID-19 With Convalescent Plasma. *JAMA*, *323*(16), 1582–1589. https://doi.org/10.1001/JAMA.2020.4783

Shen, X., Tang, H., McDanal, C., Wagh, K., Fischer, W., Theiler, J., Yoon, H., Li, D., Haynes, B. F., Sanders, K. O., Gnanakaran, S., Hengartner, N., Pajon, R., Smith, G., Glenn, G. M., Korber, B., & Montefiori, D. C. (2021). SARS-CoV-2 variant B.1.1.7 is susceptible to neutralizing antibodies elicited by ancestral spike vaccines. *Cell Host & Microbe*, *29*(4), 529-539.e3. https://doi.org/10.1016/J.CHOM.2021.03.002

Sherer, Y., Levy, Y., & Shoenfeld, Y. (2005). IVIG in autoimmunity and cancer – efficacy versus safety. *Http://Dx.Doi.Org/10.1517/14740338.1.2.153*, *1*(2), 153–158. https://doi.org/10.1517/14740338.1.2.153

Shi, C.-S., Qi, H.-Y., Boularan, C., Huang, N.-N., Abu-Asab, M., Shelhamer, J. H., & Kehrl, J. H. (2014). SARS-Coronavirus Open Reading Frame-9b Suppresses Innate Immunity by Targeting Mitochondria and the MAVS/TRAF3/TRAF6 Signalosome. *The Journal of Immunology*, *193*(6), 3080–3089. https://doi.org/10.4049/JIMMUNOL.1303196/-/DCSUPPLEMENTAL

Shi, C. S., Nabar, N. R., Huang, N. N., & Kehrl, J. H. (2019). SARS-Coronavirus Open Reading Frame-8b triggers intracellular stress pathways and activates NLRP3 inflammasomes. *Cell Death Discovery 2019 5:1*, *5*(1), 1–12. https://doi.org/10.1038/s41420-019-0181-7

Shi, J., Z, W., G, Z., H, Y., C, W., B, H., R, L., X, H., L, S., Z, S., Y, Z., P, L., L, L., P, C., J, W., X, Z., Y, G., W, T., G, W., … Z, B. (2020). Susceptibility of ferrets, cats, dogs, and other domesticated animals to SARS-coronavirus 2. *Science (New York, N.Y.)*, *368*(6494), 1016–1020. https://doi.org/10.1126/SCIENCE.ABB7015

Shin, D., Mukherjee, R., Grewe, D., Bojkova, D., Baek, K., Bhattacharya, A., Schulz, L., Widera, M., Mehdipour, A. R., Tascher, G., Geurink, P. P., Wilhelm, A., van der Heden van Noort, G. J., Ovaa, H., Müller, S., Knobeloch, K. P., Rajalingam, K., Schulman, B. A., Cinatl, J., … Dikic, I. (2020). Papain-like protease regulates SARS-CoV-2 viral spread and innate immunity. *Nature 2020 587:7835*, *587*(7835), 657–662. https://doi.org/10.1038/s41586-020-2601-5

Sia, S. F., Yan, L.-M., Chin, A. W. H., Fung, K., Choy, K.-T., Wong, A. Y. L., Kaewpreedee, P., Perera, R. A. P. M., Poon, L. L. M., Nicholls, J. M., Peiris, M., & Yen, H.-L. (2020). Pathogenesis and transmission of SARS-CoV-2 in golden

hamsters. *Nature 2020 583:7818*, *583*(7818), 834–838. https://doi.org/10.1038/s41586-020-2342-5

Siddell, S. G., Walker, P. J., Lefkowitz, E. J., Mushegian, A. R., Adams, M. J., Dutilh, B. E., Gorbalenya, A. E., Harrach, B., Harrison, R. L., Junglen, S., Knowles, N. J., Kropinski, A. M., Krupovic, M., Kuhn, J. H., Nibert, M., Rubino, L., Sabanadzovic, S., Sanfaçon, H., Simmonds, P., … Davison, A. J. (2019). Additional changes to taxonomy ratified in a special vote by the International Committee on Taxonomy of Viruses (October 2018). *Archives of Virology*, *164*(3), 943–946. https://doi.org/10.1007/S00705-018-04136-2/TABLES/1

Siu, Y. L., Teoh, K. T., Lo, J., Chan, C. M., Kien, F., Escriou, N., Tsao, S. W., Nicholls, J. M., Altmeyer, R., Peiris, J. S. M., Bruzzone, R., & Nal, B. (2008). The M, E, and N Structural Proteins of the Severe Acute Respiratory Syndrome Coronavirus Are Required for Efficient Assembly, Trafficking, and Release of Virus-Like Particles. *Journal of Virology*, *82*(22), 11318–11330. https://doi.org/10.1128/JVI.01052-08/SUPPL_FILE/SUPPL_DATA.ZIP

Smith, E. C., & Denison, M. R. (2013). Coronaviruses as DNA Wannabes: A New Model for the Regulation of RNA Virus Replication Fidelity. *PLoS Pathogens*, *9*(12), 1–4. https://doi.org/10.1371/JOURNAL.PPAT.1003760

Snijder, E. J., Decroly, E., & Ziebuhr, J. (2016). The Nonstructural Proteins Directing Coronavirus RNA Synthesis and Processing. *Advances in Virus Research*, *96*, 59–126. https://doi.org/10.1016/BS.AIVIR.2016.08.008

Sommer, I. E., & Roberto Bakker, P. (2020). *What can psychiatrists learn from SARS and MERS outbreaks?* https://doi.org/10.1038/s41380-020-0704-x

Starr, T. N., Greaney, A. J., Hilton, S. K., Ellis, D., Crawford, K. H. D., Dingens, A. S., Navarro, M. J., Bowen, J. E., Tortorici, M. A., Walls, A. C., King, N. P., Veesler, D., & Bloom, J. D. (2020). Deep Mutational Scanning of SARS-CoV-2 Receptor Binding Domain Reveals Constraints on Folding and ACE2 Binding. *Cell*, *182*(5), 1295. https://doi.org/10.1016/J.CELL.2020.08.012

Steffen, T. L., Stone, E. T., Hassert, M., Geerling, E., Grimberg, B. T., Espino, A. M., Pantoja, P., Climent, C., Hoft, D. F., George, S. L., Sariol, C. A., Pinto, A. K., & Brien, J. D. (2020). The receptor binding domain of SARS-CoV-2 spike is the key target of neutralizing antibody in human polyclonal sera. *BioRxiv*, 2020.08.21.261727. https://doi.org/10.1101/2020.08.21.261727

Stockman, L., R, B., & P, G. (2006). SARS: systematic review of treatment effects. *PLoS Medicine*, *3*(9), 1525–1531. https://doi.org/10.1371/JOURNAL.PMED.0030343

Stone, E. T., Geerling, E., Steffen, T. L., Hassert, M., Dickson, A., Spencer, J. F., Toth, K., DiPaolo, R. J., Brien, J. D., & Pinto, A. K. (2020). Characterization of cells susceptible to SARS-COV-2 and methods for detection of neutralizing antibody by focus forming assay. *BioRxiv*, 2020.08.20.259838. https://doi.org/10.1101/2020.08.20.259838

Su, S., Wong, G., Shi, W., Liu, J., Lai, A. C. K., Zhou, J., Liu, W., Bi, Y., & Gao, G. F. (2016). Epidemiology, Genetic Recombination, and Pathogenesis of Coronaviruses. *Trends in Microbiology*, *24*(6), 490–502.

https://doi.org/10.1016/J.TIM.2016.03.003

Sun, J., Zhu, A., Li, H., Zheng, K., Zhuang, Z., Chen, Z., Shi, Y., Zhang, Z., Chen, S., Liu, X., Dai, J., Li, X., Huang, S., Huang, X., Luo, L., Wen, L., Zhuo, J., Li, Y., Wang, Y., … Li, Y. (2020). Isolation of infectious SARS-CoV-2 from urine of a COVID-19 patient. *Https://Doi.Org/10.1080/22221751.2020.1760144*, *9*(1), 991–993. https://doi.org/10.1080/22221751.2020.1760144

Sun, L., Xing, Y., Chen, X., Zheng, Y., Yang, Y., Nichols, D. B., Clementz, M. A., Banach, B. S., Li, K., Baker, S. C., & Chen, Z. (2012). Coronavirus papain-like proteases negatively regulate antiviral innate immune response through disruption of STING-mediated signaling. *PloS One*, *7*(2). https://doi.org/10.1371/JOURNAL.PONE.0030802

Sun, P., Lu, X., Xu, C., Sun, W., & Pan, B. (2020). Understanding of COVID-19 based on current evidence. In *Journal of Medical Virology* (Vol. 92, Issue 6, pp. 548–551). John Wiley and Sons Inc. https://doi.org/10.1002/jmv.25722

Sun, S., Gu, H., Cao, L., Chen, Q., Ye, Q., Yang, G., Li, R.-T., Fan, H., Deng, Y.-Q., Song, X., Qi, Y., Li, M., Lan, J., Feng, R., Guo, Y., Zhu, N., Qin, S., Wang, L., Zhang, Y.-F., … Qin, C.-F. (2021). Characterization and structural basis of a lethal mouse-adapted SARS-CoV-2. *BioRxiv*, 2020.11.10.377333. https://doi.org/10.1101/2020.11.10.377333

Suschak, J. J., Williams, J. A., & Schmaljohn, C. S. (2017). Advancements in DNA vaccine vectors, non-mechanical delivery methods, and molecular adjuvants to increase immunogenicity. *Https://Doi.Org/10.1080/21645515.2017.1330236*, *13*(12), 2837–2848. https://doi.org/10.1080/21645515.2017.1330236

Swain, S. L., McKinstry, K. K., & Strutt, T. M. (2012). Expanding roles for $CD4^+$ T cells in immunity to viruses. *Nature Reviews. Immunology*, *12*(2), 136–148. https://doi.org/10.1038/NRI3152

Tahir Ul Qamar, M., SM, A., MA, A., & LL, C. (2020). Structural basis of SARS-CoV-2 3CL pro and anti-COVID-19 drug discovery from medicinal plants. *Journal of Pharmaceutical Analysis*, *10*(4), 313–319. https://doi.org/10.1016/J.JPHA.2020.03.009

Tai, W., He, L., Zhang, X., Pu, J., Voronin, D., Jiang, S., Zhou, Y., & Du, L. (2020). Characterization of the receptor-binding domain (RBD) of 2019 novel coronavirus: implication for development of RBD protein as a viral attachment inhibitor and vaccine. *Cellular & Molecular Immunology 2020 17:6*, *17*(6), 613–620. https://doi.org/10.1038/s41423-020-0400-4

Tandon, R., Mitra, D., Sharma, P., Stray, S. S., Bates, J. T., & Marshall, G. D. (2020). Effective Screening of SARS-CoV-2 Neutralizing Antibodies in Patient Serum using Lentivirus Particles Pseudotyped with SARS-CoV-2 Spike Glycoprotein. *MedRxiv*, 2020.05.21.20108951. https://doi.org/10.1101/2020.05.21.20108951

Tang, X., Wu, C., Li, X., Song, Y., Yao, X., Wu, X., Duan, Y., Zhang, H., Wang, Y., Qian, Z., Cui, J., & Lu, J. (2020). On the origin and continuing evolution of SARS-CoV-2. *National Science Review*, *7*(6), 1012–1023. https://doi.org/10.1093/NSR/NWAA036

Tani, H., Kimura, M., Tan, L., Yoshida, Y., Ozawa, T., Kishi, H., Fukushi, S., Saijo, M., Sano, K., Suzuki, T., Kawasuji, H., Ueno, A., Miyajima, Y., Fukui, Y., Sakamaki, I., Yamamoto, Y., & Morinaga, Y. (2021). Evaluation of SARS-CoV-2 neutralizing antibodies using a vesicular stomatitis virus possessing SARS-CoV-2 spike protein. *Virology Journal*, *18*(1), 1–10. https://doi.org/10.1186/S12985-021-01490-7/TABLES/2

Tanriover, M. D., Doğanay, H. L., Akova, M., Güner, H. R., Azap, A., Akhan, S., Köse, Ş., Erdinç, F. Ş., Akalın, E. H., Tabak, Ö. F., Pullukçu, H., Batum, Ö., Şimşek Yavuz, S., Turhan, Ö., Yıldırmak, M. T., Köksal, İ., Taşova, Y., Korten, V., Yılmaz, G., … Aksu, K. (2021). Efficacy and safety of an inactivated whole-virion SARS-CoV-2 vaccine (CoronaVac): interim results of a double-blind, randomised, placebo-controlled, phase 3 trial in Turkey. *Lancet (London, England)*, *398*(10296), 213. https://doi.org/10.1016/S0140-6736(21)01429-X

Tegally, H., Wilkinson, E., Giovanetti, M., Iranzadeh, A., Fonseca, V., Giandhari, J., Doolabh, D., Pillay, S., San, E. J., Msomi, N., Mlisana, K., Gottberg, A. von, Walaza, S., Allam, M., Ismail, A., Mohale, T., Glass, A. J., Engelbrecht, S., Zyl, G. Van, … Oliveira, T. de. (2020). Emergence and rapid spread of a new severe acute respiratory syndrome-related coronavirus 2 (SARS-CoV-2) lineage with multiple spike mutations in South Africa. *MedRxiv*, 2020.12.21.20248640. https://doi.org/10.1101/2020.12.21.20248640

Temperton, N. J., Chan, P. K., Simmons, G., Zambon, M. C., Tedder, R. S., Takeuchi, Y., & Weiss, R. A. (2005). Longitudinally profiling neutralizing antibody response to SARS coronavirus with pseudotypes. *Emerging Infectious Diseases*, *11*(3), 411–416. https://doi.org/10.3201/EID1103.040906

The U.S. Food and Drug Administration. (2021). *FDA authorizes REGEN-COV monoclonal antibody therapy for post-exposure prophylaxis (prevention) for COVID-19 | FDA*. https://www.fda.gov/drugs/drug-safety-and-availability/fda-authorizes-regen-cov-monoclonal-antibody-therapy-post-exposure-prophylaxis-prevention-covid-19

Thomas, S. (2020). *The Structure of the Membrane Protein of SARS-CoV-2 Resembles the Sugar Transporter semiSWEET*. https://doi.org/10.20944/PREPRINTS202004.0512.V1

Thompson, C. P., Grayson, N. E., Paton, R. S., Bolton, J. S., Lourenço, J., Penman, B. S., Lee, L. N., Odon, V., Mongkolsapaya, J., Chinnakannan, S., Dejnirattisai, W., Edmans, M., Fyfe, A., Imlach, C., Kooblall, K., Lim, N., Liu, C., López-Camacho, C., McInally, C., … Young, P. (2020). Detection of neutralising antibodies to SARS-CoV-2 to determine population exposure in Scottish blood donors between March and May 2020. *Eurosurveillance*, *25*(42), 2000685. https://doi.org/10.2807/1560-7917.ES.2020.25.42.2000685/CITE/PLAINTEXT

Thompson, M. R., Kaminski, J. J., Kurt-Jones, E. A., & Fitzgerald, K. A. (2011). Pattern recognition receptors and the innate immune response to viral infection. *Viruses*, *3*(6), 920–940. https://doi.org/10.3390/V3060920

Tian, X., Li, C., Huang, A., Xia, S., Lu, S., Shi, Z., Lu, L., Jiang, S., Yang, Z., Wu, Y., & Ying, T. (2020). Potent binding of 2019 novel coronavirus spike protein by a SARS

coronavirus-specific human monoclonal antibody. *Emerging Microbes and Infections*, *9*(1), 382–385. https://doi.org/10.1080/22221751.2020.1729069/SUPPL_FILE/TEMI_A_1729069_SM0688.DOCX

Tiberghien, P., de Lamballerie, X., Morel, P., Gallian, P., Lacombe, K., & Yazdanpanah, Y. (2020). Collecting and evaluating convalescent plasma for COVID-19 treatment: why and how? *Vox Sanguinis*, *115*(6), 488–494. https://doi.org/10.1111/VOX.12926

Tighe, P. J., Urbanowicz, R. A., Fairclough, C. L., McClure, C. P., Thomson, B. J., Gomez, N., Chappell, J. G., Tsoleridis, T., Loose, M., Carlile, M., Moore, C., Holmes, N., Sang, F., Hrushikesh, D., Clark, G., Temperton, N., Brooks, T., Ball, J. K., Irving, W. L., & Tarr, A. W. (2020). Potent anti-SARS-CoV-2 Antibody Responses are Associated with Better Prognosis in Hospital Inpatient COVID-19 Disease. *MedRxiv*, 2020.08.22.20176834. https://doi.org/10.1101/2020.08.22.20176834

To, K., OT, T., WS, L., AR, T., TC, W., DC, L., CC, Y., JP, C., JM, C., TS, C., DP, L., CY, C., LL, C., WM, C., KH, C., JD, I., AC, N., RW, P., CT, L., … KY, Y. (2020). Temporal profiles of viral load in posterior oropharyngeal saliva samples and serum antibody responses during infection by SARS-CoV-2: an observational cohort study. *The Lancet. Infectious Diseases*, *20*(5), 565–574. https://doi.org/10.1016/S1473-3099(20)30196-1

Totura, A. L., & Baric, R. S. (2012). SARS coronavirus pathogenesis: host innate immune responses and viral antagonism of interferon. *Current Opinion in Virology*, *2*(3), 264–275. https://doi.org/10.1016/J.COVIRO.2012.04.004

Tu, Y. F., Chien, C. S., Yarmishyn, A. A., Lin, Y. Y., Luo, Y. H., Lin, Y. T., Lai, W. Y., Yang, D. M., Chou, S. J., Yang, Y. P., Wang, M. L., & Chiou, S. H. (2020). A Review of SARS-CoV-2 and the Ongoing Clinical Trials. *International Journal of Molecular Sciences 2020, Vol. 21, Page 2657*, *21*(7), 2657. https://doi.org/10.3390/IJMS21072657

Ura, T., Okuda, K., & Shimada, M. (2014). Developments in Viral Vector-Based Vaccines. *Vaccines 2014, Vol. 2, Pages 624-641*, *2*(3), 624–641. https://doi.org/10.3390/VACCINES2030624

Vacharathit, V., Srichatrapimuk, S., Manopwisedjaroen, S., Kirdlarp, S., Srisaowakarn, C., Setthaudom, C., Inrueangsri, N., Pisitkun, P., Kunakorn, M., Hongeng, S., Sungkanuparph, S., & Thitithanyanont, A. (2021). SARS-CoV-2 neutralizing antibodies decline over one year and patients with severe COVID-19 pneumonia display a unique cytokine profile. *International Journal of Infectious Diseases : IJID : Official Publication of the International Society for Infectious Diseases*, *112*, 227–234. https://doi.org/10.1016/J.IJID.2021.09.021

van Boheemen, S., de Graaf, M., Lauber, C., Bestebroer, T. M., Raj, V. S., Zaki, A. M., Osterhaus, A. D. M. E., Haagmans, B. L., Gorbalenya, A. E., Snijder, E. J., & Fouchier, R. A. M. (2012). Genomic characterization of a newly discovered coronavirus associated with acute respiratory distress syndrome in humans. *MBio*, *3*(6). https://doi.org/10.1128/MBIO.00473-12

Veras, F. P., Pontelli, M. C., Silva, C. M., Toller-Kawahisa, J. E., de Lima, M., Nascimento, D. C., Schneider, A. H., Caetité, D., Tavares, L. A., Paiva, I. M., Rosales, R., Colón, D., Martins, R., Castro, I. A., Almeida, G. M., Lopes, M. I. F., Benatti, M. N., Bonjorno, L. P., Giannini, M. C., … Cunha, F. Q. (2020). SARS-CoV-2-triggered neutrophil extracellular traps mediate COVID-19 pathology. *Journal of Experimental Medicine*, *217*(12). https://doi.org/10.1084/JEM.20201129/152086

Waehler, R., Russell, S. J., & Curiel, D. T. (2007). Engineering targeted viral vectors for gene therapy. *Nature Reviews Genetics 2007 8:8*, *8*(8), 573–587. https://doi.org/10.1038/nrg2141

Wang, Changtai, Liu, Z., Chen, Z., Huang, X., Xu, M., He, T., & Zhang, Z. (2020). The establishment of reference sequence for SARS-CoV-2 and variation analysis. *Journal of Medical Virology*, *92*(6), 667–674. https://doi.org/10.1002/JMV.25762

Wang, Chunyan, Li, W., Drabek, D., Okba, N. M. A., van Haperen, R., Osterhaus, A. D. M. E., van Kuppeveld, F. J. M., Haagmans, B. L., Grosveld, F., & Bosch, B.-J. (2020). A human monoclonal antibody blocking SARS-CoV-2 infection. *Nature Communications 2020 11:1*, *11*(1), 1–6. https://doi.org/10.1038/s41467-020-16256-y

Wang, H., Yang, P., Liu, K., Guo, F., Zhang, Y., Zhang, G., & Jiang, C. (2008). SARS coronavirus entry into host cells through a novel clathrin- and caveolae-independent endocytic pathway. *Cell Research 2008 18:2*, *18*(2), 290–301. https://doi.org/10.1038/cr.2008.15

Wang, J., & Zhang, H. (2013). Nontrivial independent sets of bipartite graphs and cross-intersecting families. *Journal of Combinatorial Theory, Series A*, *120*(1), 129–141. https://doi.org/10.1016/J.JCTA.2012.07.005

Wang, L. F., Shi, Z., Zhang, S., Field, H., Daszak, P., & Eaton, B. T. (2006). Review of Bats and SARS - Volume 12, Number 12—December 2006 - Emerging Infectious Diseases journal - CDC. *Emerging Infectious Diseases*, *12*(12), 1834–1840. https://doi.org/10.3201/EID1212.060401

Wang, M., R, C., L, Z., X, Y., J, L., M, X., Z, S., Z, H., W, Z., & G, X. (2020). Remdesivir and chloroquine effectively inhibit the recently emerged novel coronavirus (2019-nCoV) in vitro. *Cell Research*, *30*(3), 269–271. https://doi.org/10.1038/S41422-020-0282-0

Wang, M. Y., Zhao, R., Gao, L. J., Gao, X. F., Wang, D. P., & Cao, J. M. (2020a). SARS-CoV-2: Structure, Biology, and Structure-Based Therapeutics Development. In *Frontiers in Cellular and Infection Microbiology* (Vol. 10). Frontiers Media S.A. https://doi.org/10.3389/fcimb.2020.587269

Wang, M. Y., Zhao, R., Gao, L. J., Gao, X. F., Wang, D. P., & Cao, J. M. (2020b). SARS-CoV-2: Structure, Biology, and Structure-Based Therapeutics Development. In *Frontiers in Cellular and Infection Microbiology* (Vol. 10). Frontiers Media S.A. https://doi.org/10.3389/fcimb.2020.587269

Wang, P., Liu, L., Iketani, S., Luo, Y., Guo, Y., Wang, M., Yu, J., Zhang, B., Kwong, P. D., Graham, B. S., Mascola, J. R., Chang, J. Y., Yin, M. T., Sobieszczyk, M.,

Kyratsous, C. A., Shapiro, L., Sheng, Z., Nair, M. S., Huang, Y., & Ho, D. D. (2021). Increased Resistance of SARS-CoV-2 Variants B.1.351 and B.1.1.7 to Antibody Neutralization. *Research Square*. https://doi.org/10.21203/RS.3.RS-155394/V1

Wang, Qidi, Zhang, L., Kuwahara, K., Li, L., Liu, Z., Li, T., Zhu, H., Liu, J., Xu, Y., Xie, J., Morioka, H., Sakaguchi, N., Qin, C., & Liu, G. (2020). Correction: Immunodominant SARS Coronavirus Epitopes in Humans Elicited Both Enhancing and Neutralizing Effects on Infection in Non-human Primates. *ACS Infectious Diseases*, *2016*(5), 2021. https://doi.org/10.1021/ACSINFECDIS.0C00148

Wang, Qihui, Zhang, Y., Wu, L., Niu, S., Song, C., Zhang, Z., Lu, G., Qiao, C., Hu, Y., Yuen, K. Y., Wang, Q., Zhou, H., Yan, J., & Qi, J. (2020). Structural and Functional Basis of SARS-CoV-2 Entry by Using Human ACE2. *Cell*, *181*(4), 894-904.e9. https://doi.org/10.1016/J.CELL.2020.03.045/ATTACHMENT/9E7684DA-BAEE-487B-9D65-478D87F0C2BB/MMC1.PDF

Wang, Qiong, Qiu, Y., Li, J. Y., Zhou, Z. J., Liao, C. H., & Ge, X. Y. (2020). A Unique Protease Cleavage Site Predicted in the Spike Protein of the Novel Pneumonia Coronavirus (2019-nCoV) Potentially Related to Viral Transmissibility. *Virologica Sinica*, *35*(3), 337. https://doi.org/10.1007/S12250-020-00212-7

Wang, W., Y, X., R, G., R, L., K, H., G, W., & W, T. (2020). Detection of SARS-CoV-2 in Different Types of Clinical Specimens. *JAMA*, *323*(18), 1843–1844. https://doi.org/10.1001/JAMA.2020.3786

Wang, X., Guo, X., Xin, Q., Pan, Y., Hu, Y., Li, J., Chu, Y., Feng, Y., & Wang, Q. (2020). Neutralizing Antibody Responses to Severe Acute Respiratory Syndrome Coronavirus 2 in Coronavirus Disease 2019 Inpatients and Convalescent Patients. *Clinical Infectious Diseases : An Official Publication of the Infectious Diseases Society of America*, *71*(10), 2688–2694. https://doi.org/10.1093/CID/CIAA721

Watanabe, Y., Allen, J. D., Wrapp, D., McLellan, J. S., & Crispin, M. (2020). Site-specific glycan analysis of the SARS-CoV-2 spike. *Science*, *369*(6501), 330–333. https://doi.org/10.1126/SCIENCE.ABB9983

Weisblum, Y., Schmidt, F., Zhang, F., DaSilva, J., Poston, D., Lorenzi, J. C. C., Muecksch, F., Rutkowska, M., Hoffmann, H. H., Michailidis, E., Gaebler, C., Agudelo, M., Cho, A., Wang, Z., Gazumyan, A., Cipolla, M., Luchsinger, L., Hillyer, C. D., Caskey, M., … Bieniasz, P. D. (2020). Escape from neutralizing antibodies by SARS-CoV-2 spike protein variants. *ELife*, *9*, 1. https://doi.org/10.7554/ELIFE.61312

Weissman, D., Alameh, M., Silva, T. de, … P. C.-C. host &, & 2021, undefined. (n.d.). D614G spike mutation increases SARS CoV-2 susceptibility to neutralization. *Elsevier*. Retrieved November 29, 2021, from https://www.sciencedirect.com/science/article/pii/S193131282030634X

Wells, J. M., Li, L. H., Sen, A., Jahreis, G. P., & Hui, S. W. (2000). Electroporation-enhanced gene delivery in mammary tumors. *Gene Therapy 2000 7:7*, *7*(7), 541–547. https://doi.org/10.1038/sj.gt.3301141

wenzhong, liu, & hualan, L. (2020). *COVID-19:Attacks the 1-Beta Chain of Hemoglobin and Captures the Porphyrin to Inhibit Human Heme Metabolism*.

https://doi.org/10.26434/CHEMRXIV.11938173.V9

Wilkie, M., Satti, I., Minhinnick, A., Harris, S., Riste, M., Ramon, R. L., Sheehan, S., Thomas, Z. R. M., Wright, D., Stockdale, L., Hamidi, A., O'Shea, M. K., Dwivedi, K., Behrens, H. M., Davenne, T., Morton, J., Vermaak, S., Lawrie, A., Moss, P., & McShane, H. (2020). A phase I trial evaluating the safety and immunogenicity of a candidate tuberculosis vaccination regimen, ChAdOx1 85A prime – MVA85A boost in healthy UK adults. *Vaccine*, *38*(4), 779–789. https://doi.org/10.1016/J.VACCINE.2019.10.102

Wong, S. S. Y., & Yuen, K. Y. (2008). The management of coronavirus infections with particular reference to SARS. *Journal of Antimicrobial Chemotherapy*, *62*(3), 437–441. https://doi.org/10.1093/JAC/DKN243

Woo, P. C. Y., Lau, S. K. P., Lam, C. S. F., Lau, C. C. Y., Tsang, A. K. L., Lau, J. H. N., Bai, R., Teng, J. L. L., Tsang, C. C. C., Wang, M., Zheng, B.-J., Chan, K.-H., & Yuen, K.-Y. (2012). Discovery of seven novel Mammalian and avian coronaviruses in the genus deltacoronavirus supports bat coronaviruses as the gene source of alphacoronavirus and betacoronavirus and avian coronaviruses as the gene source of gammacoronavirus and deltacoronavirus. *Journal of Virology*, *86*(7), 3995–4008. https://doi.org/10.1128/JVI.06540-11

Wu, A., Peng, Y., Huang, B., Ding, X., Wang, X., Niu, P., Meng, J., Zhu, Z., Zhang, Z., Wang, J., Sheng, J., Quan, L., Xia, Z., Tan, W., Cheng, G., & Jiang, T. (2020). Genome Composition and Divergence of the Novel Coronavirus (2019-nCoV) Originating in China. *Cell Host and Microbe*, *27*(3), 325–328. https://doi.org/10.1016/J.CHOM.2020.02.001/ATTACHMENT/7C271FA1-5188-4CC6-8C72-4DA7ADC5C964/MMC2.XLSX

Wu, F., Wang, A., Liu, M., Wang, Q., Chen, J., Xia, S., Ling, Y., Zhang, Y., Xun, J., Lu, L., Jiang, S., Lu, H., Wen, Y., & Huang, J. (2020). Neutralizing Antibody Responses to SARS-CoV-2 in a COVID-19 Recovered Patient Cohort and Their Implications. *SSRN Electronic Journal*. https://doi.org/10.2139/SSRN.3566211

Wu, F., Zhao, S., Yu, B., Chen, Y. M., Wang, W., Song, Z. G., Hu, Y., Tao, Z. W., Tian, J. H., Pei, Y. Y., Yuan, M. L., Zhang, Y. L., Dai, F. H., Liu, Y., Wang, Q. M., Zheng, J. J., Xu, L., Holmes, E. C., & Zhang, Y. Z. (2020). A new coronavirus associated with human respiratory disease in China. *Nature 2020 579:7798*, *579*(7798), 265–269. https://doi.org/10.1038/s41586-020-2008-3

Wu, Z., & McGoogan, J. M. (2020). Characteristics of and Important Lessons From the Coronavirus Disease 2019 (COVID-19) Outbreak in China: Summary of a Report of 72 314 Cases From the Chinese Center for Disease Control and Prevention. *JAMA*, *323*(13), 1239–1242. https://doi.org/10.1001/JAMA.2020.2648

Wuertz, K. M. G., Treuting, P. M., Hemann, E. A., Esser-Nobis, K., Snyder, A. G., Graham, J. B., Daniels, B. P., Wilkins, C., Snyder, J. M., Voss, K. M., Oberst, A., Lund, J., & Gale, M. (2019). STING is required for host defense against neuropathological West Nile virus infection. *PLOS Pathogens*, *15*(8), e1007899. https://doi.org/10.1371/JOURNAL.PPAT.1007899

Xie, Xuelei, Z, Z., W, Z., C, Z., F, W., & J, L. (2020). Chest CT for Typical Coronavirus Disease 2019 (COVID-19) Pneumonia: Relationship to Negative RT-PCR Testing.

*Radiology*, *296*(2), E41–E45. https://doi.org/10.1148/RADIOL.2020200343

Xie, Xuping, Liu, Y., Liu, J., Zhang, X., Zou, J., Fontes-Garfias, C. R., Xia, H., Swanson, K. A., Cutler, M., Cooper, D., Menachery, V. D., Weaver, S. C., Dormitzer, P. R., & Shi, P. Y. (2021). Neutralization of SARS-CoV-2 spike 69/70 deletion, E484K and N501Y variants by BNT162b2 vaccine-elicited sera. *Nature Medicine 2021 27:4*, *27*(4), 620–621. https://doi.org/10.1038/s41591-021-01270-4

Xie, Xuping, Muruato, A. E., Zhang, X., Lokugamage, K. G., Fontes-Garfias, C. R., Zou, J., Liu, J., Ren, P., Balakrishnan, M., Cihlar, T., Tseng, C. T. K., Makino, S., Menachery, V. D., Bilello, J. P., & Shi, P. Y. (2020). A nanoluciferase SARS-CoV-2 for rapid neutralization testing and screening of anti-infective drugs for COVID-19. *Nature Communications 2020 11:1*, *11*(1), 1–11. https://doi.org/10.1038/s41467-020-19055-7

Xie, Xuping, Muruato, A., Lokugamage, K. G., Narayanan, K., Zhang, X., Zou, J., Liu, J., Schindewolf, C., Bopp, N. E., Aguilar, P. V., Plante, K. S., Weaver, S. C., Makino, S., LeDuc, J. W., Menachery, V. D., & Shi, P. Y. (2020). An Infectious cDNA Clone of SARS-CoV-2. *Cell Host & Microbe*, *27*(5), 841-848.e3. https://doi.org/10.1016/J.CHOM.2020.04.004

Xie, Y., Cao, S., Dong, H., Li, Q., Chen, E., … W. Z.-T. J. of, & 2020, U. (2020). Effect of regular intravenous immunoglobulin therapy on prognosis of severe pneumonia in patients with COVID-19. *Ncbi.Nlm.Nih.Gov*. https://www.ncbi.nlm.nih.gov/pmc/articles/pmc7151471/

Xiong, H. L., Wu, Y. T., Cao, J. L., Yang, R., Liu, Y. X., Ma, J., Qiao, X. Y., Yao, X. Y., Zhang, B. H., Zhang, Y. L., Hou, W. H., Shi, Y., Xu, J. J., Zhang, L., Wang, S. J., Fu, B. R., Yang, T., Ge, S. X., Zhang, J., … Xia, N. S. (2020). Robust neutralization assay based on SARS-CoV-2 S-protein-bearing vesicular stomatitis virus (VSV) pseudovirus and ACE2-overexpressing BHK21 cells. *Emerging Microbes & Infections*, *9*(1), 2105–2113. https://doi.org/10.1080/22221751.2020.1815589

Xu, R., Shi, M., Li, J., Song, P., & Li, N. (2020). Construction of SARS-CoV-2 Virus-Like Particles by Mammalian Expression System. *Frontiers in Bioengineering and Biotechnology*, *8*, 862. https://doi.org/10.3389/FBIOE.2020.00862/BIBTEX

Xu, Z., Shi, L., Wang, Y., Zhang, J., Huang, L., Zhang, C., Liu, S., Zhao, P., Liu, H., Zhu, L., Tai, Y., Bai, C., Gao, T., Song, J., Xia, P., Dong, J., Zhao, J., & Wang, F. S. (2020). Pathological findings of COVID-19 associated with acute respiratory distress syndrome. *The Lancet Respiratory Medicine*, *8*(4), 420–422. https://doi.org/10.1016/S2213-2600(20)30076-X

Yang, R., Huang, B., A, R., Li, W., Wang, W., Deng, Y., & Tan, W. (2020). Development and effectiveness of pseudotyped SARS-CoV-2 system as determined by neutralizing efficiency and entry inhibition test in vitro. *Biosafety and Health*, *2*(4), 226–231. https://doi.org/10.1016/J.BSHEAL.2020.08.004

Yap, J. K. Y., Moriyama, M., & Iwasaki, A. (2020). Inflammasomes and Pyroptosis as Therapeutic Targets for COVID-19. *The Journal of Immunology*, *205*(2), 307–312. https://doi.org/10.4049/JIMMUNOL.2000513

Yongchen, Z., Shen, H., Wang, X., Shi, X., Li, Y., Yan, J., Chen, Y., & Gu, B. (2020).

Different longitudinal patterns of nucleic acid and serology testing results based on disease severity of COVID-19 patients. *Https://Doi.Org/10.1080/22221751.2020.1756699*, *9*(1), 833–836. https://doi.org/10.1080/22221751.2020.1756699

Yost, C. C., Schwertz, H., Cody, M. J., Wallace, J. A., Campbell, R. A., Vieira-De-Abreu, A., Araujo, C. V., Schubert, S., Harris, E. S., Rowley, J. W., Rondina, M. T., Fulcher, J. M., Koening, C. L., Weyrich, A. S., & Zimmerman, G. A. (2016). Neonatal NET-inhibitory factor and related peptides inhibit neutrophil extracellular trap formation. *The Journal of Clinical Investigation*, *126*(10), 3783–3798. https://doi.org/10.1172/JCI83873

Yurkovetskiy, L., Pascal, K. E., Tomkins-Tinch, C., Nyalile, T., Wang, Y., Baum, A., Diehl, W. E., Dauphin, A., Carbone, C., Veinotte, K., Egri, S. B., Schaffner, S. F., Lemieux, J. E., Munro, J., Sabeti, P. C., Kyratsous, C. A., Shen, K., & Luban, J. (n.d.). *SARS-CoV-2 Spike protein variant D614G increases infectivity and retains sensitivity to antibodies that target the receptor binding domain*. https://doi.org/10.1101/2020.07.04.187757

Yurkovetskiy, L., Wang, X., Pascal, K. E., Tomkins-Tinch, C., Nyalile, T. P., Wang, Y., Baum, A., Diehl, W. E., Dauphin, A., Carbone, C., Veinotte, K., Egri, S. B., Schaffner, S. F., Lemieux, J. E., Munro, J. B., Rafique, A., Barve, A., Sabeti, P. C., Kyratsous, C. A., … Luban, J. (2020). Structural and Functional Analysis of the D614G SARS-CoV-2 Spike Protein Variant. *Cell*, *183*(3), 739-751.e8. https://doi.org/10.1016/J.CELL.2020.09.032

Z, X., L, S., Y, W., J, Z., L, H., C, Z., S, L., P, Z., H, L., L, Z., Y, T., C, B., T, G., J, S., P, X., J, D., J, Z., & FS, W. (2020). Pathological findings of COVID-19 associated with acute respiratory distress syndrome. *The Lancet. Respiratory Medicine*, *8*(4), 420–422. https://doi.org/10.1016/S2213-2600(20)30076-X

Zeng, Chunxi, Hou, X., Yan, J., Zhang, C., Li, W., Zhao, W., Du, S., & Dong, Y. (2020). Leveraging mRNA Sequences and Nanoparticles to Deliver SARS-CoV-2 Antigens In Vivo. *Advanced Materials*, *32*(40), 2004452. https://doi.org/10.1002/ADMA.202004452

Zeng, Cong, Evans, J. P., Pearson, R., Qu, P., Zheng, Y.-M., Robinson, R. T., Hall-Stoodley, L., Yount, J., Pannu, S., Mallampalli, R. K., Saif, L., Oltz, E., Lozanski, G., & Liu, S.-L. (2020). Neutralizing antibody against SARS-CoV-2 spike in COVID-19 patients, health care workers and convalescent plasma donors: a cohort study using a rapid and sensitive high-throughput neutralization assay. *MedRxiv*, 2020.08.02.20166819. https://doi.org/10.1101/2020.08.02.20166819

Zhang, J. S., Chen, J. T., Liu, Y. X., Zhang, Z. S., Gao, H., Liu, Y., Wang, X., Ning, Y., Liu, Y. F., Gao, Q., Xu, J. G., Qin, C., Dong, X. P., & Yin, W. D. (2005). A serological survey on neutralizing antibody titer of SARS convalescent sera. *Journal of Medical Virology*, *77*(2), 147–150. https://doi.org/10.1002/JMV.20431

Zhang, L., Jackson, C. B., Mou, H., Ojha, A., Rangarajan, E. S., Izard, T., Farzan, M., & Choe, H. (2020). The D614G mutation in the SARS-CoV-2 spike protein reduces S1 shedding and increases infectivity. *BioRxiv*. https://doi.org/10.1101/2020.06.12.148726

Zhang, T., Wu, Q., & Zhang, Z. (2020). Probable Pangolin Origin of SARS-CoV-2 Associated with the COVID-19 Outbreak. *Current Biology*, *30*(7), 1346-1351.e2. https://doi.org/10.1016/j.cub.2020.03.022

Zhang, W., RH, D., B, L., XS, Z., XL, Y., B, H., YY, W., GF, X., B, Y., ZL, S., & P, Z. (2020). Molecular and serological investigation of 2019-nCoV infected patients: implication of multiple shedding routes. *Emerging Microbes & Infections*, *9*(1), 386–389. https://doi.org/10.1080/22221751.2020.1729071

Zhang, Yali, Wang, S., Wu, Y., Hou, W., Yuan, L., Sheng, C., Wang, J., Ye, J., Zheng, Q., Ma, J., Xu, J., Wei, M., Li, Z., Nian, S., Xiong, H., Zhang, L., Shi, Y., Fu, B., Cao, J., … Xia, N. (2020). Virus-free and live-cell visualizing SARS-CoV-2 cell entry for studies of neutralizing antibodies and compound inhibitors. *BioRxiv*, 2020.07.22.215236. https://doi.org/10.1101/2020.07.22.215236

Zhang, Yan, M, X., S, Z., P, X., W, C., W, J., H, C., X, D., H, Z., H, Z., C, W., J, Z., X, S., R, T., W, W., D, W., J, M., Y, C., D, Z., … S, Z. (2020). Coagulopathy and Antiphospholipid Antibodies in Patients with Covid-19. *The New England Journal of Medicine*, *382*(17), e38. https://doi.org/10.1056/NEJMC2007575

Zhang, Yulin, Gao, Y., Qiao, L., Wang, W., & Chen, D. (2020). Inflammatory Response Cells During Acute Respiratory Distress Syndrome in Patients With Coronavirus Disease 2019 (COVID-19). *Https://Doi.Org/10.7326/L20-0227*, *173*(5), 402–404. https://doi.org/10.7326/L20-0227

Zhao, J., Yuan, Q., Wang, H., Liu, W., Liao, X., Su, Y., Wang, X., Yuan, J., Li, T., Li, J., Qian, S., Hong, C., Wang, F., Liu, Y., Wang, Z., He, Q., Li, Z., He, B., Zhang, T., … Zhang, Z. (2020). Antibody Responses to SARS-CoV-2 in Patients With Novel Coronavirus Disease 2019. *Clinical Infectious Diseases*, *71*(16), 2027–2034. https://doi.org/10.1093/CID/CIAA344

Zheng, Y.-Y., YT, M., JY, Z., & X, X. (2020). COVID-19 and the cardiovascular system. *Nature Reviews. Cardiology*, *17*(5), 259–260. https://doi.org/10.1038/S41569-020-0360-5

Zheng, Yi, Zhuang, M. W., Han, L., Zhang, J., Nan, M. L., Zhan, P., Kang, D., Liu, X., Gao, C., & Wang, P. H. (2020). Severe acute respiratory syndrome coronavirus 2 (SARS-CoV-2) membrane (M) protein inhibits type I and III interferon production by targeting RIG-I/MDA-5 signaling. *Signal Transduction and Targeted Therapy*, *5*(1). https://doi.org/10.1038/S41392-020-00438-7

Zheng, Yue, Larragoite, E. T., Williams, E. S. C. P., Lama, J., Cisneros, I., Delgado, J. C., Slev, P., Rychert, J., Innis, E. A., Coiras, M., Rondina, M. T., Spivak, A. M., & Planelles, V. (2021). Neutralization assay with SARS-CoV-1 and SARS-CoV-2 spike pseudotyped murine leukemia virions. *Virology Journal*, *18*(1), 1–6. https://doi.org/10.1186/S12985-020-01472-1/FIGURES/5

Zhou, P., Yang, X.-L., Wang, X.-G., Hu, B., Zhang, L., Zhang, W., Si, H.-R., Zhu, Y., Li, B., Huang, C.-L., Chen, H.-D., Chen, J., Luo, Y., Guo, H., Jiang, R.-D., Liu, M.-Q., Chen, Y., Shen, X.-R., Wang, X., … Shi, Z.-L. (2020). A pneumonia outbreak associated with a new coronavirus of probable bat origin. *Nature 2020 579:7798*, *579*(7798), 270–273. https://doi.org/10.1038/s41586-020-2012-7

Zhou, Y, P, V., K, L., J, A., R, C., JW, N., D, B., S, P., JH, M., AR, R., & G, S. (2015). Protease inhibitors targeting coronavirus and filovirus entry. *Antiviral Research*, *116*, 76–84. https://doi.org/10.1016/J.ANTIVIRAL.2015.01.011

Zhou, Yonggang, Fu, B., Zheng, X., Wang, D., Zhao, C., Qi, Y., Sun, R., Tian, Z., Xu, X., & Wei, H. (2020). Pathogenic T-cells and inflammatory monocytes incite inflammatory storms in severe COVID-19 patients. *National Science Review*, *7*(6), 998–1002. https://doi.org/10.1093/NSR/NWAA041

Zhu, F. C., Guan, X. H., Li, Y. H., Huang, J. Y., Jiang, T., Hou, L. H., Li, J. X., Yang, B. F., Wang, L., Wang, W. J., Wu, S. P., Wang, Z., Wu, X. H., Xu, J. J., Zhang, Z., Jia, S. Y., Wang, B. Sen, Hu, Y., Liu, J. J., … Chen, W. (2020). Immunogenicity and safety of a recombinant adenovirus type-5-vectored COVID-19 vaccine in healthy adults aged 18 years or older: a randomised, double-blind, placebo-controlled, phase 2 trial. *The Lancet*, *396*(10249), 479–488. https://doi.org/10.1016/S0140-6736(20)31605-6

Zhu, F. C., Li, Y. H., Guan, X. H., Hou, L. H., Wang, W. J., Li, J. X., Wu, S. P., Wang, B. Sen, Wang, Z., Wang, L., Jia, S. Y., Jiang, H. D., Wang, L., Jiang, T., Hu, Y., Gou, J. B., Xu, S. B., Xu, J. J., Wang, X. W., … Chen, W. (2020). Safety, tolerability, and immunogenicity of a recombinant adenovirus type-5 vectored COVID-19 vaccine: a dose-escalation, open-label, non-randomised, first-in-human trial. *The Lancet*, *395*(10240), 1845–1854. https://doi.org/10.1016/S0140-6736(20)31208-3

Zhu, N., Zhang, D., Wang, W., Li, X., Yang, B., Song, J., Zhao, X., Huang, B., Shi, W., Lu, R., Niu, P., Zhan, F., Ma, X., Wang, D., Xu, W., Wu, G., Gao, G. F., & Tan, W. (2020a). A Novel Coronavirus from Patients with Pneumonia in China, 2019. *New England Journal of Medicine*, *382*(8), 727–733. https://doi.org/10.1056/NEJMOA2001017/SUPPL_FILE/NEJMOA2001017_DISCLOSURES.PDF

Zhu, N., Zhang, D., Wang, W., Li, X., Yang, B., Song, J., Zhao, X., Huang, B., Shi, W., Lu, R., Niu, P., Zhan, F., Ma, X., Wang, D., Xu, W., Wu, G., Gao, G. F., & Tan, W. (2020b). A Novel Coronavirus from Patients with Pneumonia in China, 2019. *The New England Journal of Medicine*, *382*(8), 727–733. https://doi.org/10.1056/NEJMOA2001017

Zhu, Z., Z, L., T, X., C, C., G, Y., T, Z., J, L., & Y, X. (2020). Arbidol monotherapy is superior to lopinavir/ritonavir in treating COVID-19. *The Journal of Infection*, *81*(1), e21–e23. https://doi.org/10.1016/J.JINF.2020.03.060

Zost, S. J., Gilchuk, P., Case, J. B., Binshtein, E., Chen, R. E., Nkolola, J. P., Schäfer, A., Reidy, J. X., Trivette, A., Nargi, R. S., Sutton, R. E., Suryadevara, N., Martinez, D. R., Williamson, L. E., Chen, E. C., Jones, T., Day, S., Myers, L., Hassan, A. O., … Crowe, J. E. (2020). Potently neutralizing and protective human antibodies against SARS-CoV-2. *Nature 2020 584:7821*, *584*(7821), 443–449. https://doi.org/10.1038/s41586-020-2548-6

Zou, L., F, R., M, H., L, L., H, H., Z, H., J, Y., M, K., Y, S., J, X., Q, G., T, S., J, H., HL, Y., M, P., & J, W. (2020). SARS-CoV-2 Viral Load in Upper Respiratory Specimens of Infected Patients. *The New England Journal of Medicine*, *382*(12), 1177–1179. https://doi.org/10.1056/NEJMC2001737

# APPENDIX

## APPENDIX A: Chemicals

| Chemicals and Media Components | Company |
|---|---|
| Agarose | Sigma, Germany |
| Ampicillin Sodium Salt | CellGro, USA |
| Distilled Water | Merck Millipore, USA |
| DMEM | Lonza, Swiss |
| DMSO | Sigma, Germany |
| DNA Gel Loading Dye, 6X | NEB, USA |
| DPBS | Sigma, Germany |
| Ethanol | Sigma, Germany |
| Ethidium Bromide | Sigma, Germany |
| Fetal Bovine Serum | Thermo Scientific, USA |
| HEPES Solution, 1 M | Sigma, Germany |
| LB Agar | BD, USA |
| LB Broth | BD, USA |
| L-glutamine, 200 mM | Sigma, Germany |
| MEM Vitamin Solution, 100X | Sigma, Germany |
| MEM Non-essential Amino Acid Solution | Sigma, Germany |
| 2-Mercaptoethanol | Sigma, Germany |
| PIPES | Sigma, Germany |
| Sodium Pyruvate | Sigma, Germany |

## APPENDIX B: Equipments

| Equipment | Company |
|---|---|
| Autoclave | ASTELL SWIFTCLAVE, UK |
| Balance | Precisa BJ210C, |
| Centrifuge | Beckman Coulter, Allegra X-12 , USA |
| | Beckman Coulter, Allegra X-30 R, USA |
| CO2 incubator | Steri Cycle i60, Thermo Fisher Scientific, USA |
| Deepfreeze | -150$^{o}$C, Thermo Fisher Scientific ,USA |
| -80$^{o}$C, Binder, USA | |
| -20$^{o}$C, Bosch, Turkey | |
| Electrophoresis Apparatus | Thermo Fisher Scientific, EC1000_90 PowerSuply, USA |
| | Thermo Fisher Scientific, MIDICELL PRIMO, USA |
| Filters (0.22μm and 0.45μm) | Molgen, Turkey |
| Flow cytometer | SONY BIOTECHNOLOGY, SH800 Cell Sorter, USA |
| | BD FACSCalibur Flow Cytometer, USA |
| | BD Accuri™ Flow Cytometer, USA |
| Gel Documentation | BIO-RAD, USA |
| Heater/ Stirrer | Yellow Line, USA |
| Hemocytometer | ISOLAB, Germany |
| Ice Machine | Scotsman Inc., USA |
| Incubator | BINDER , USA |
| Laminar Flow | Thermo Fisher Scientific SDFE2020, USA |
| Liquid Nitrogen Tank | Taylor-Wharton, 3000RS, USA |
| Microliter Pipettes | Axygen, USA |
| Microscope | Zeiss, Primo Vert, Germany |
| | TCSSP 5 II Leica Micro System, Germany |
| Microcentifuge | Beckman Coulter Microfuge 16, USA |
| | GILSON GmCLab Capsulfuge PMC-880, Mikro200R, Hetich, Germany |
| Microwave Oven | Beko,Turkey |
| Microplate Reader | Molecular Devices VersaMax™ Tunable, |
| pH meter | Hanna HI 2020 Edge®, USA |
| rtPCR | Pikoreal Thermo Fisher Scientific, USA |
| Refrigerator | Bosch, Turkey |
| | Arçelik, Turkey |
| Shaker Incubator | New Brunswick Sci., Innova 4330, USA |
| Spectrophotometer | Beckman Coulter DU730, USA |
| Thermocycler | Eppendorf, Mastercycler Gradient, Germany |
| | BIO-RAD, T100 , USA |
| Thermoshaker | Thermal Shake Lite VWR, USA |
| Vortex | Clifton™ Cyclone Vortex Mixers, USA |
| Waterbath | Memmert Water Bath , Germany |

## APPENDIX C: Plasmid Maps

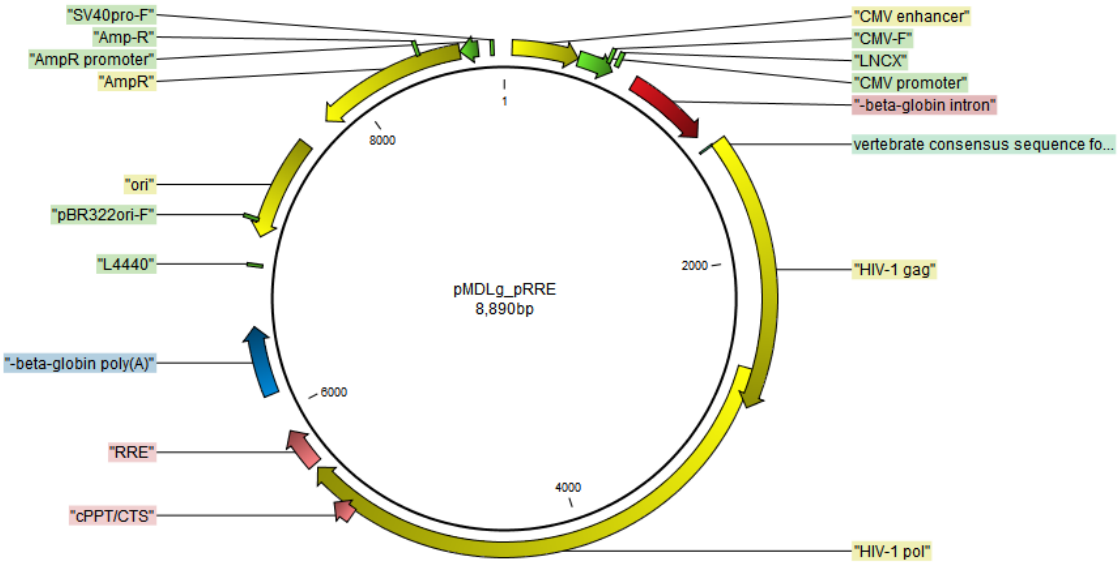


**Figure C1.** The vector map of pMDLg/pRRE

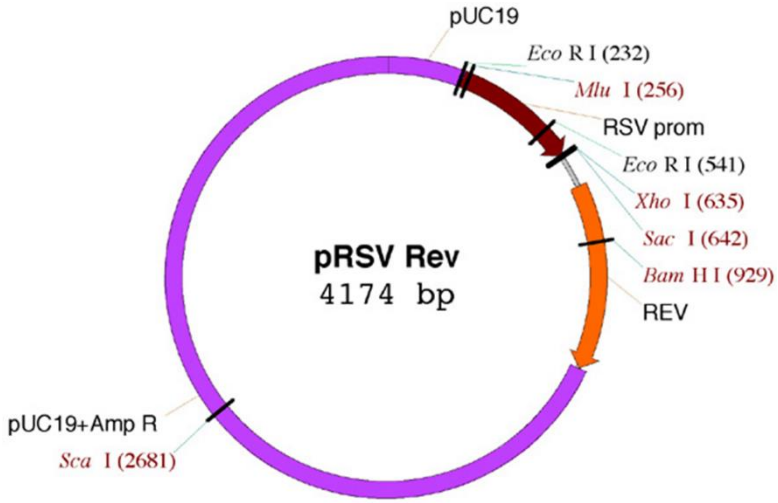


**Figure C2.** The vector map of pRSV-REV

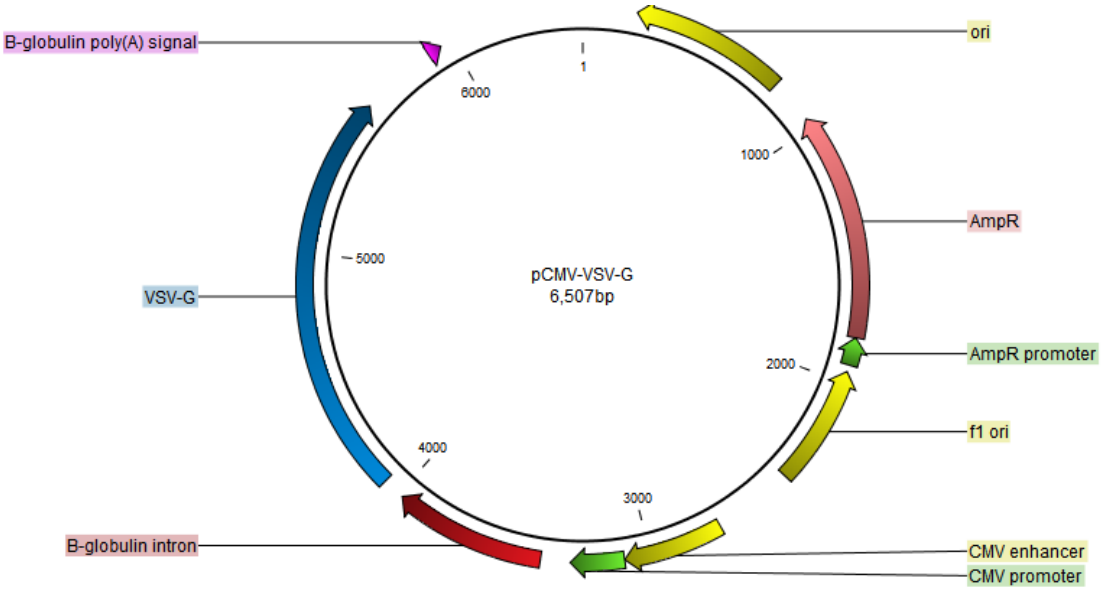


**Figure C3.** The vector map of pCMV-VSV-G

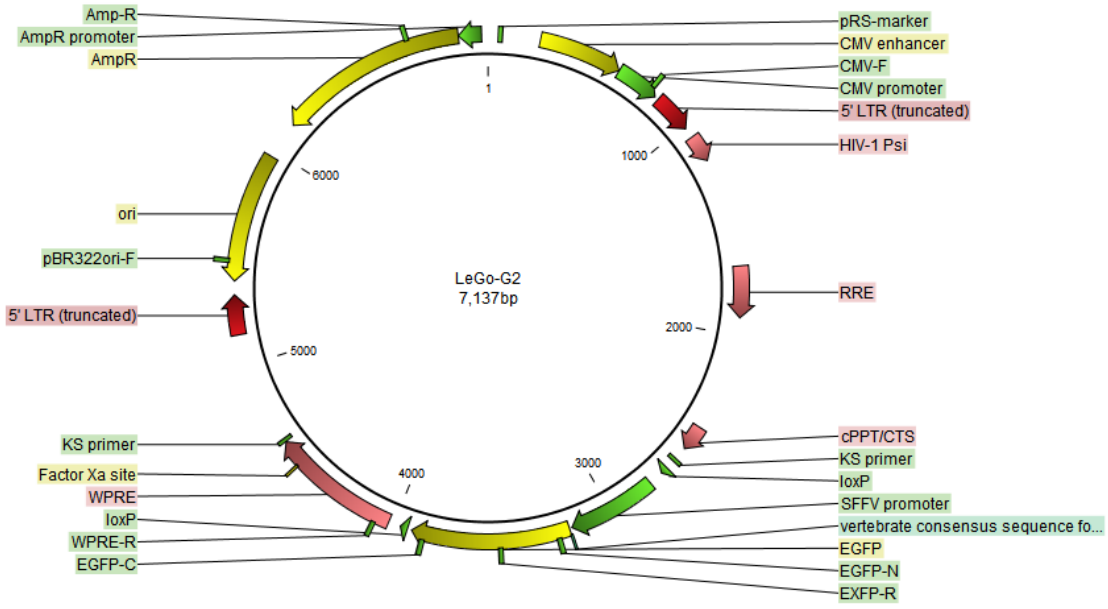


**Figure C4.** The vector map of LeGO-G2

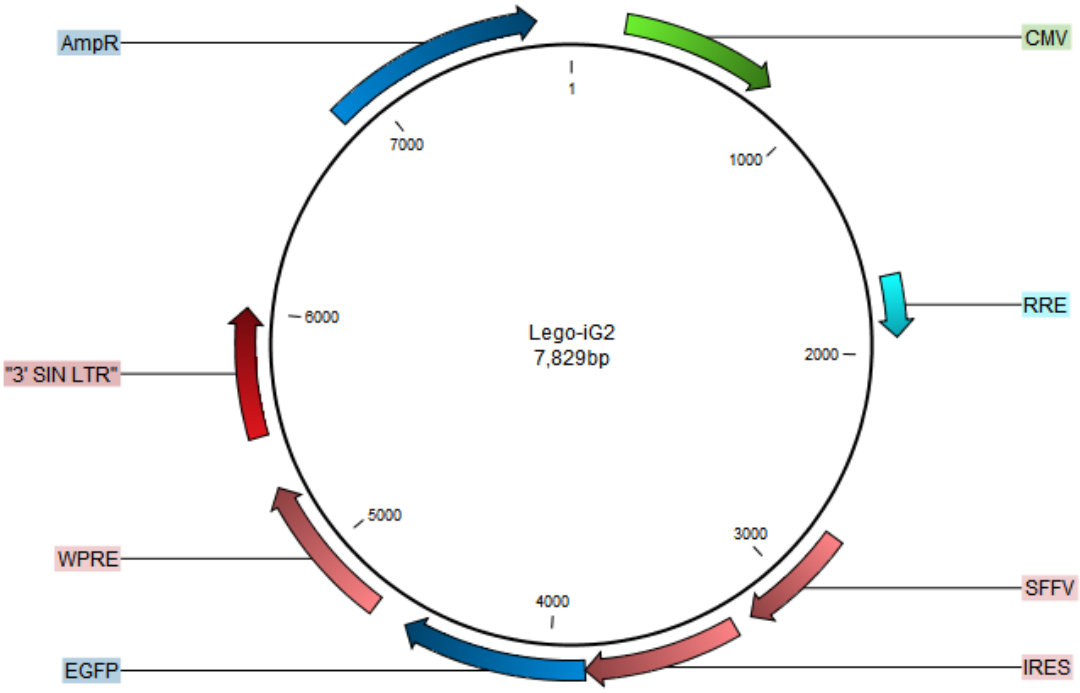


**Figure C5.** The vector map of LeGO-iG2

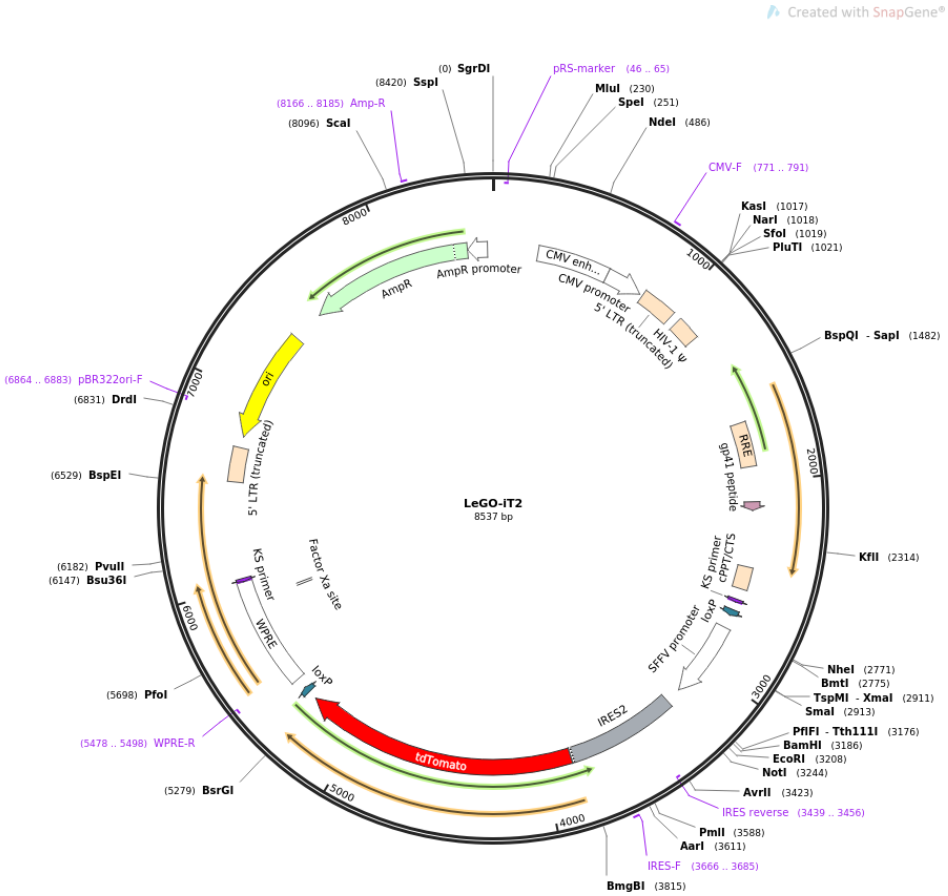


**Figure C6.** The vector map of LeGO-iT2

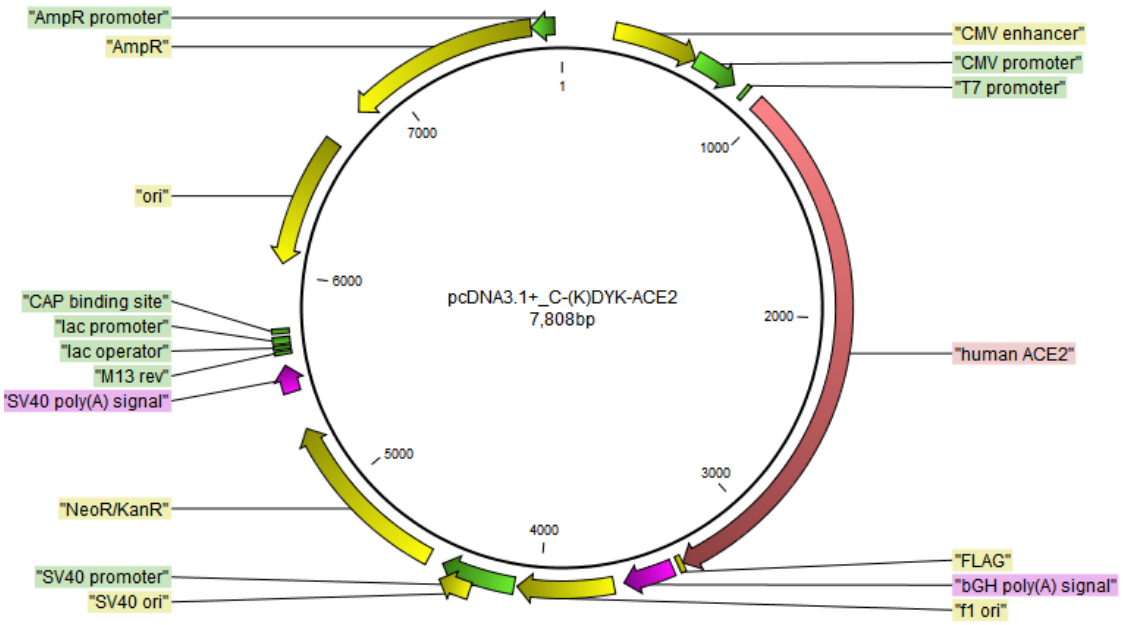


**Figure C7.** The vector map of pcDNA3.1+C-(K)DYK-ACE2

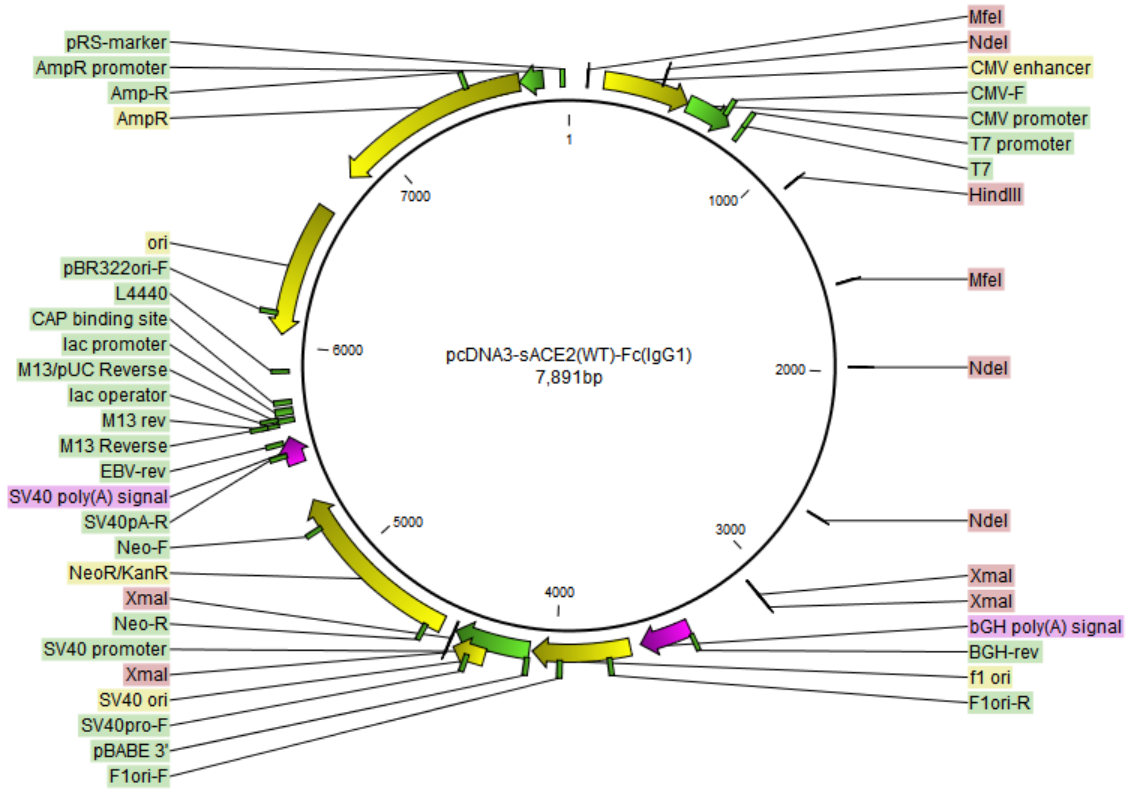


**Figure C8.** The vector map of pcDNA3-sACE2(WT)-Fc(IgG1)

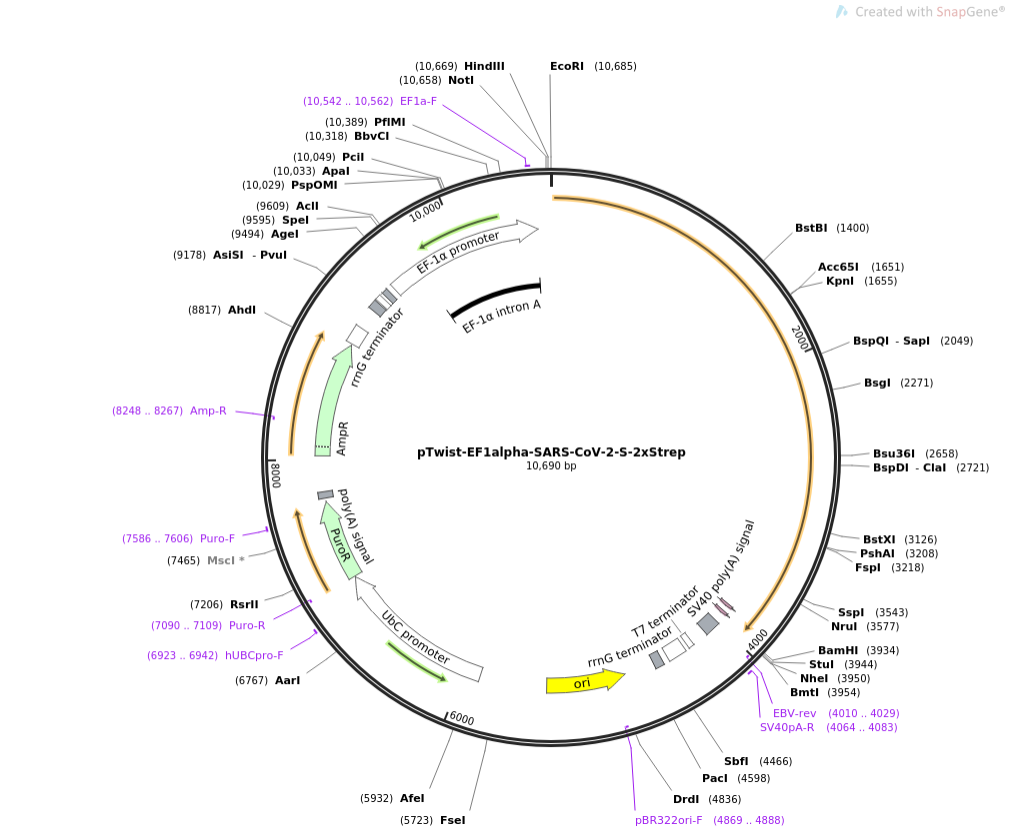


**Figure C9.** The vector map of pTwist-EF1alpha-SARS-CoV-2-S-2xStrep

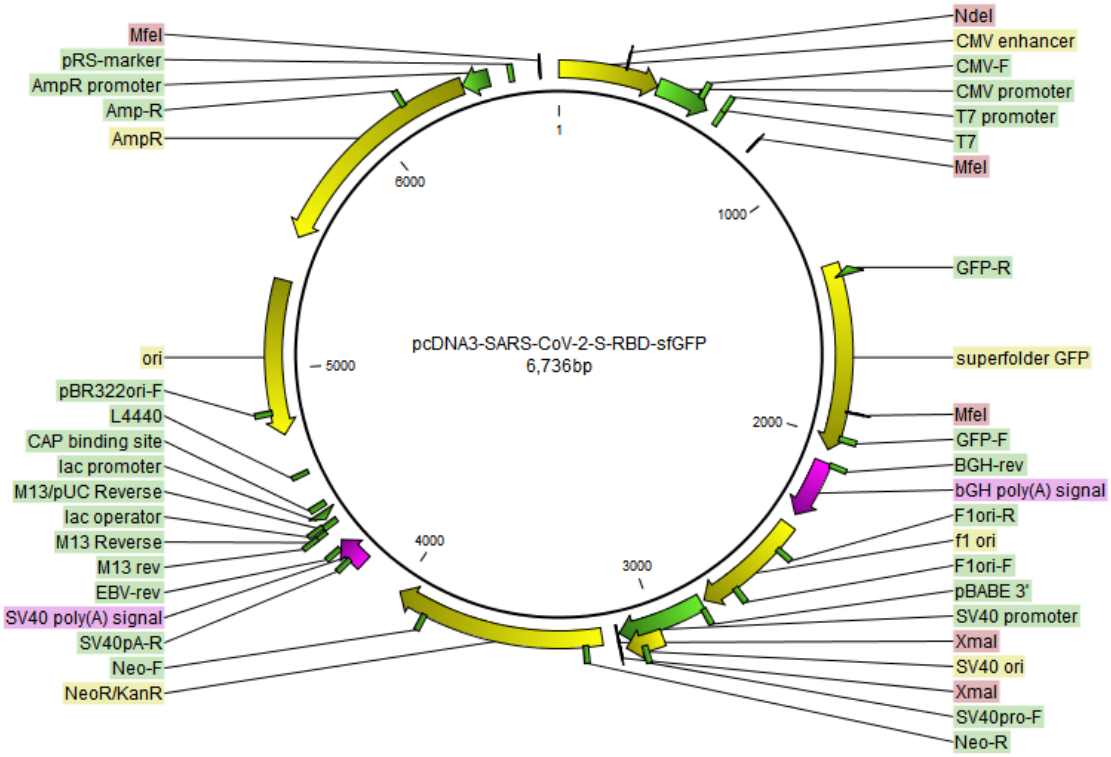


**Figure C10.** The vector map of pcDNA3-SARS-CoV-2-S-RBD-sfGFP

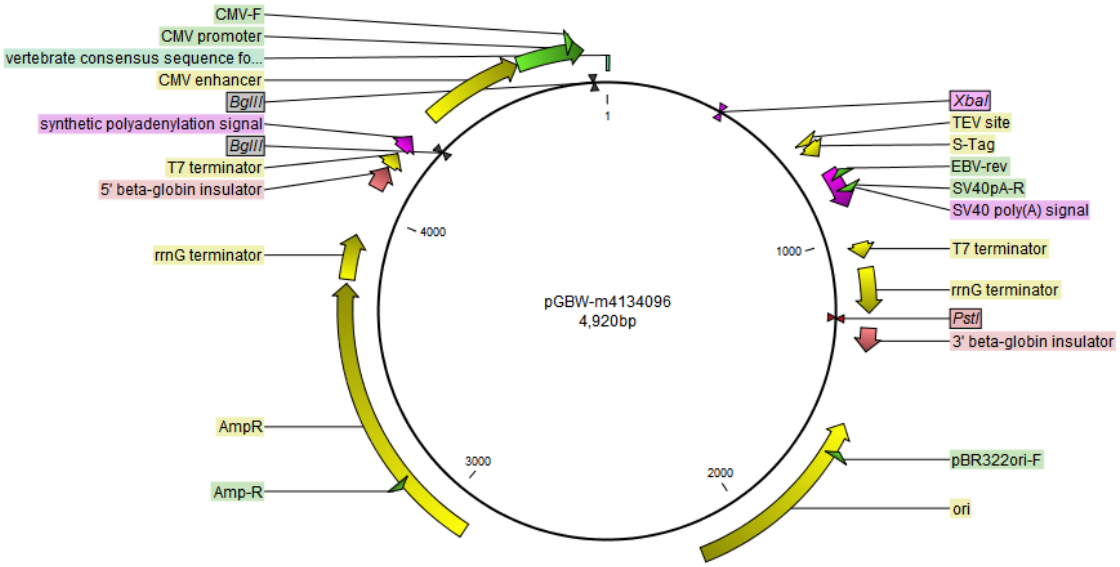


**Figure C11.** The vector map of pGBW-m4134096

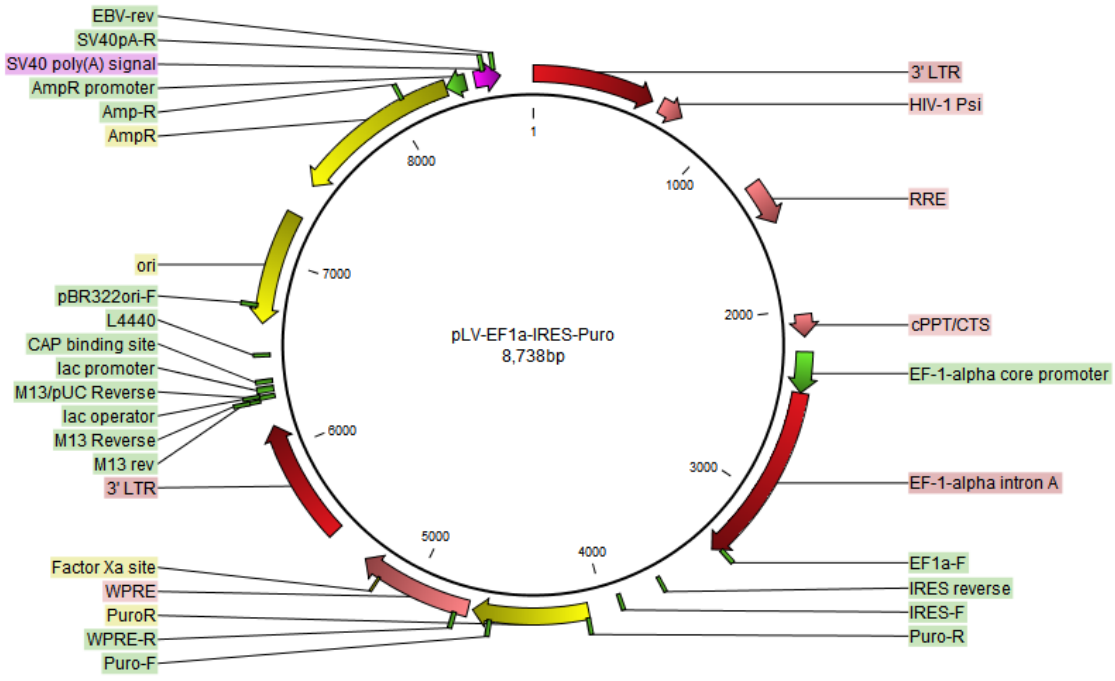


**Figure C12.** The vector map of pLV-EF1a-IRES-Puro

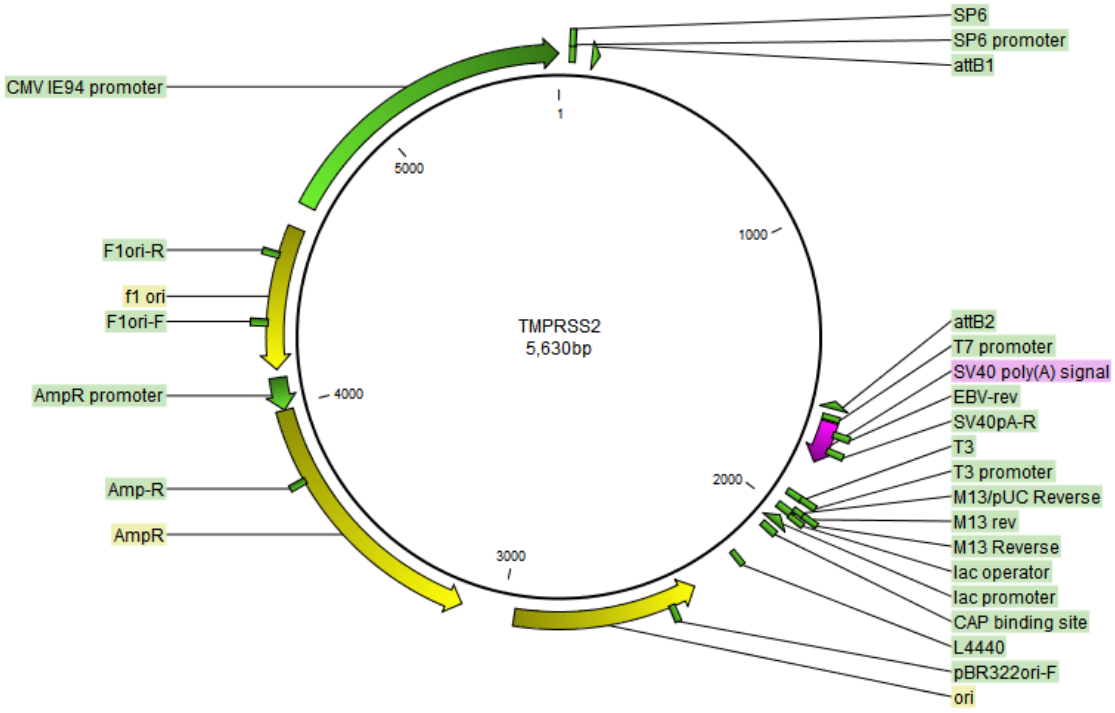


**Figure C13.** The vector map of TMPRSS2

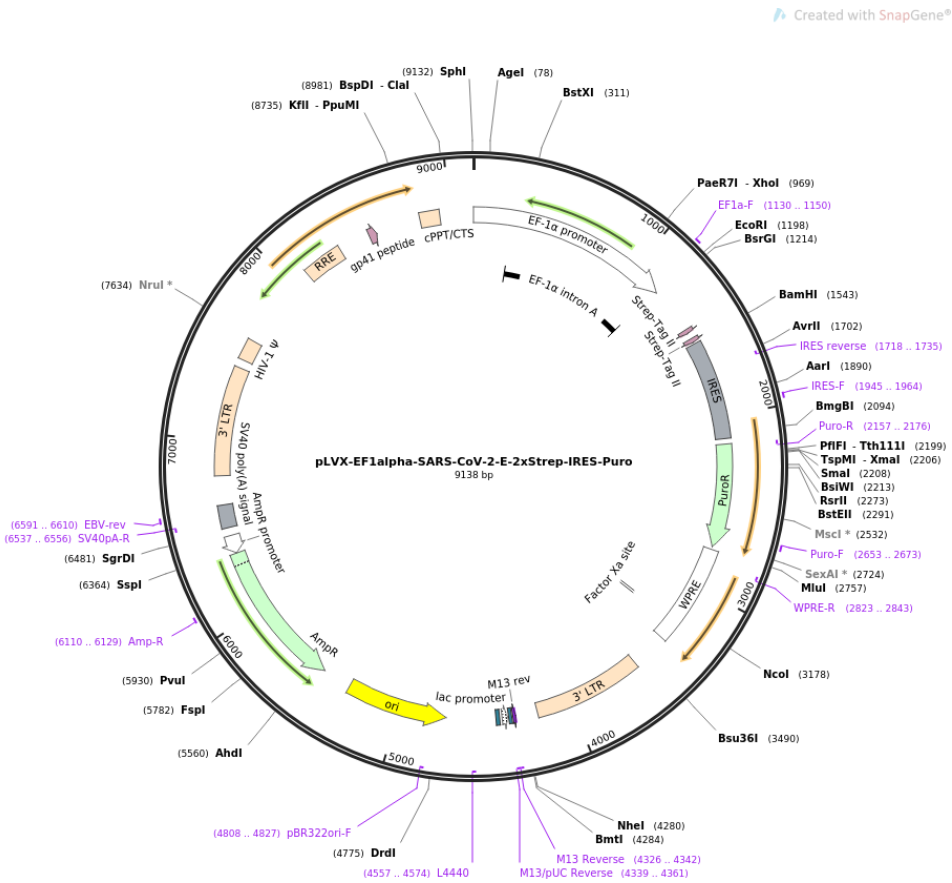


**Figure C14.** The vector map of pLVX-EF1alpha-SARS-CoV-2-E-2xStrep-IRES-Puro

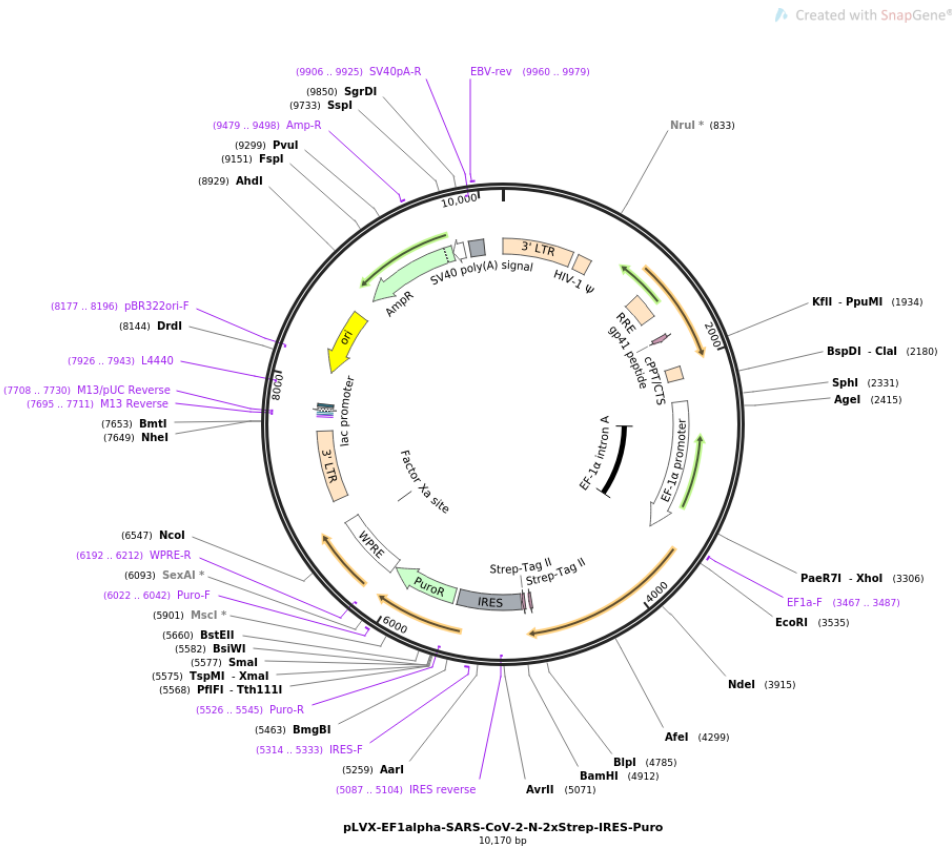


**Figure C15.** The vector map of pLVX-EF1alpha-SARS-CoV-2-N-2xStrep-IRES-Puro

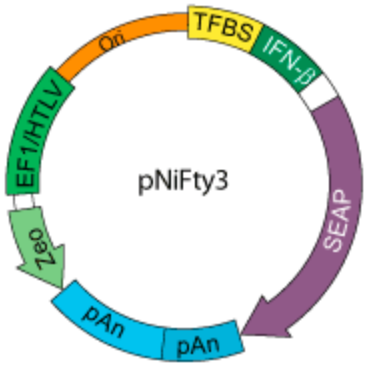


**Figure C16.** The vector map of pNiFty3-N-SEAP

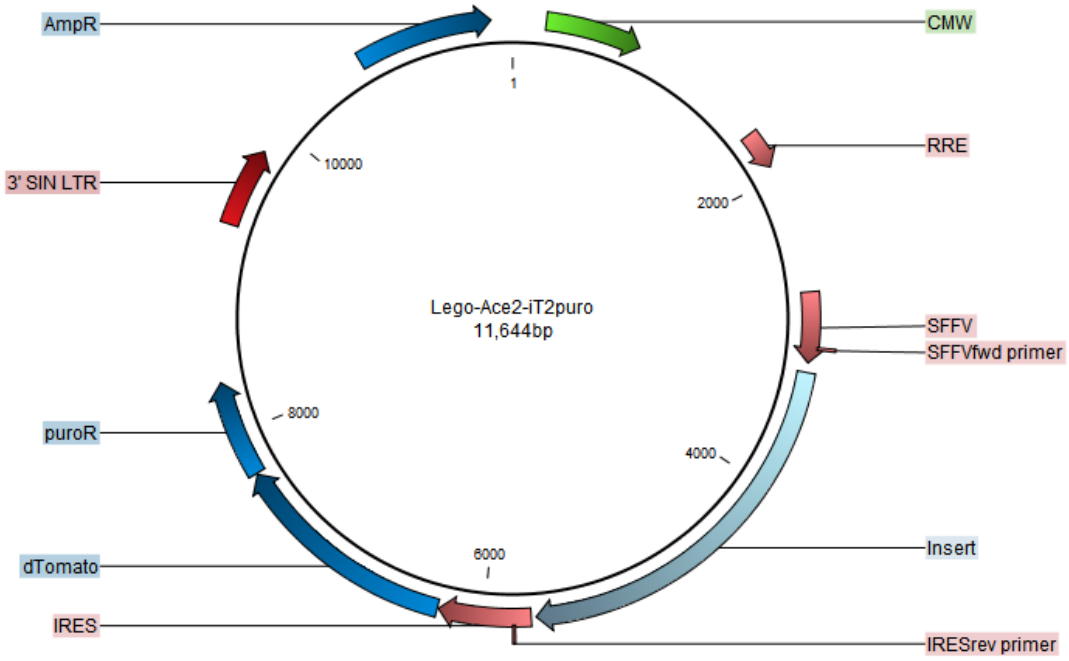


**Figure C17.** The vector map of LeGo-ACE2-iT2puro

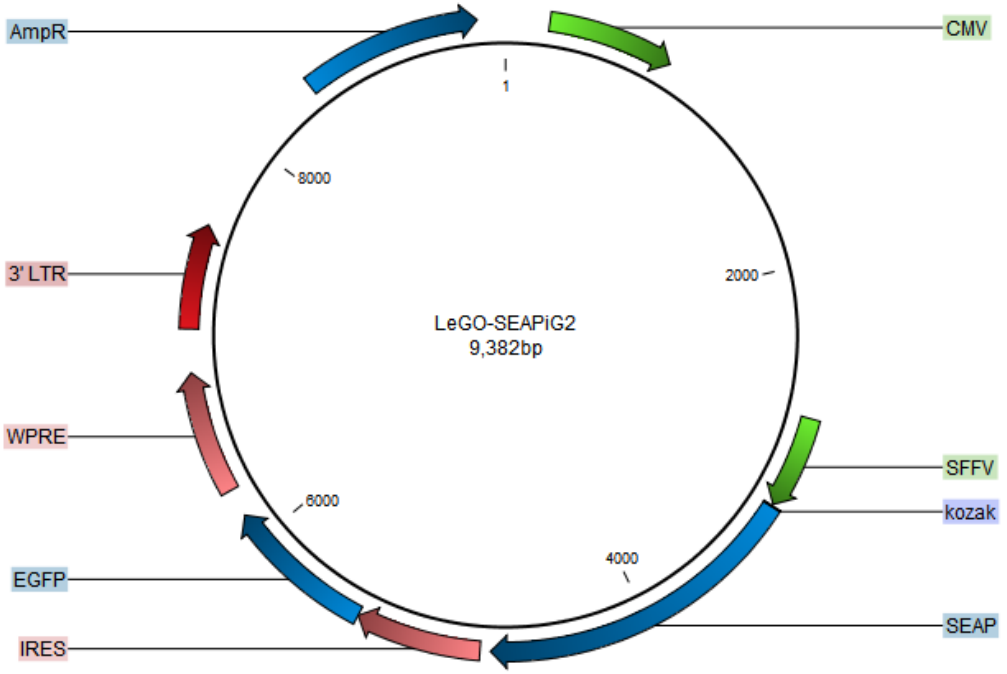


**Figure C18.** The vector map of LeGo-SEAP-iG2

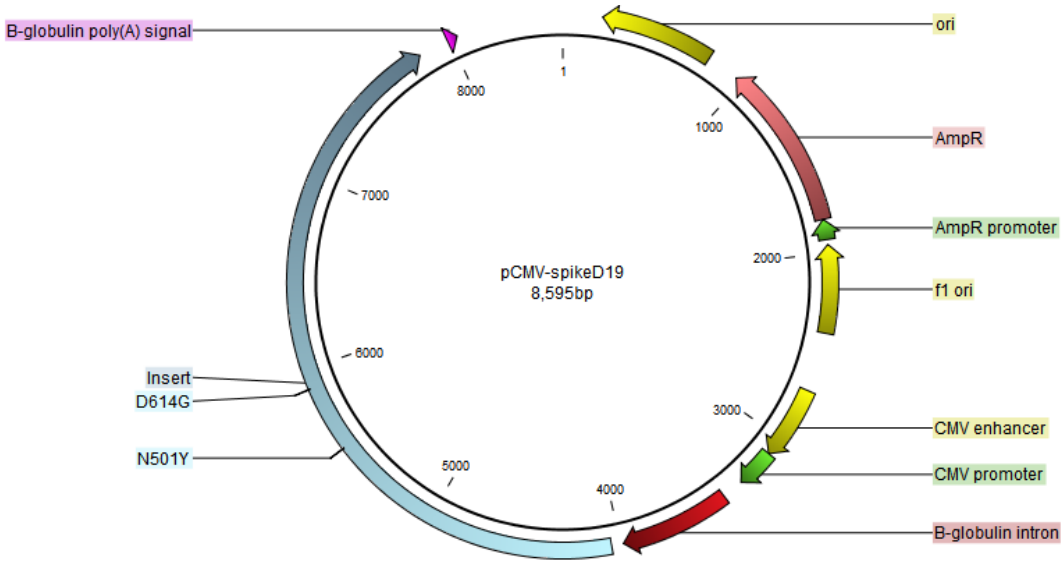


**Figure C19.** The vector map of pCMV-SpikeΔ19

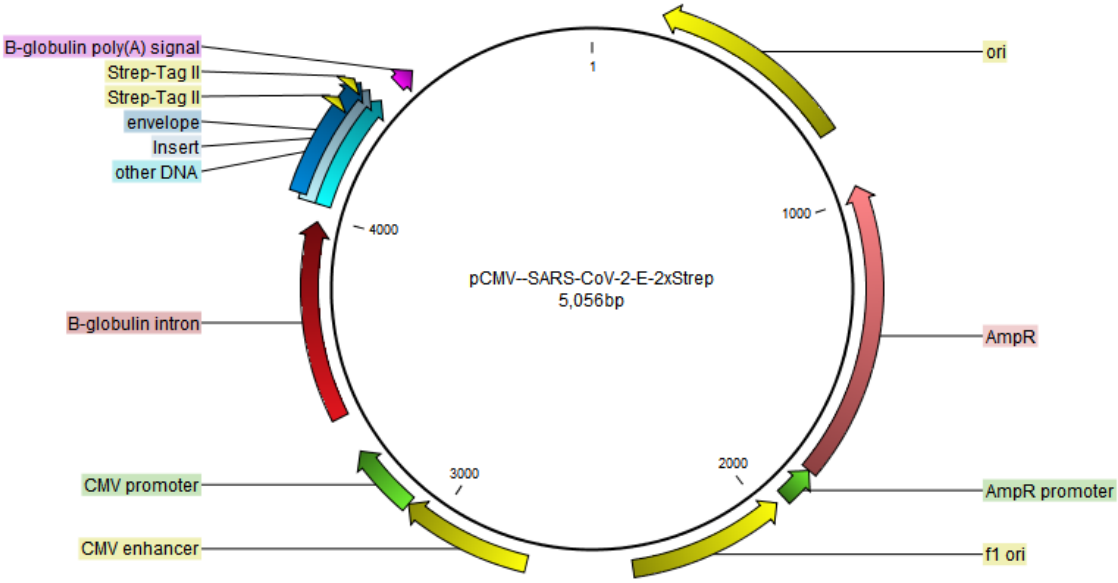


**Figure C20.** The vector map of pCMV-SARS-CoV-2-E-2xStrep

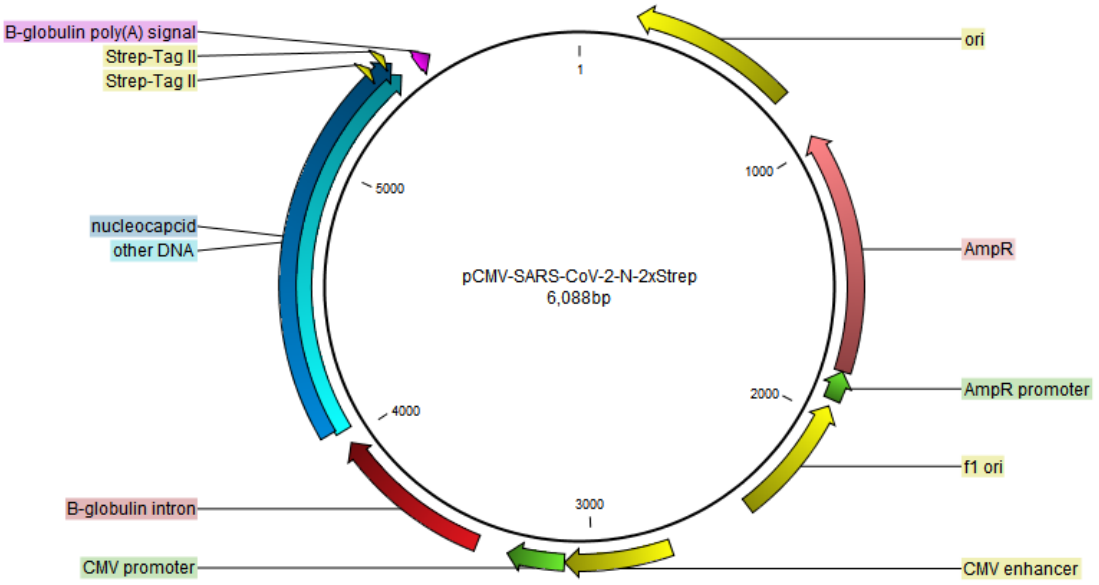


**Figure C21.** The vector map of pCMV-SARS-CoV-2-N-2xStrep

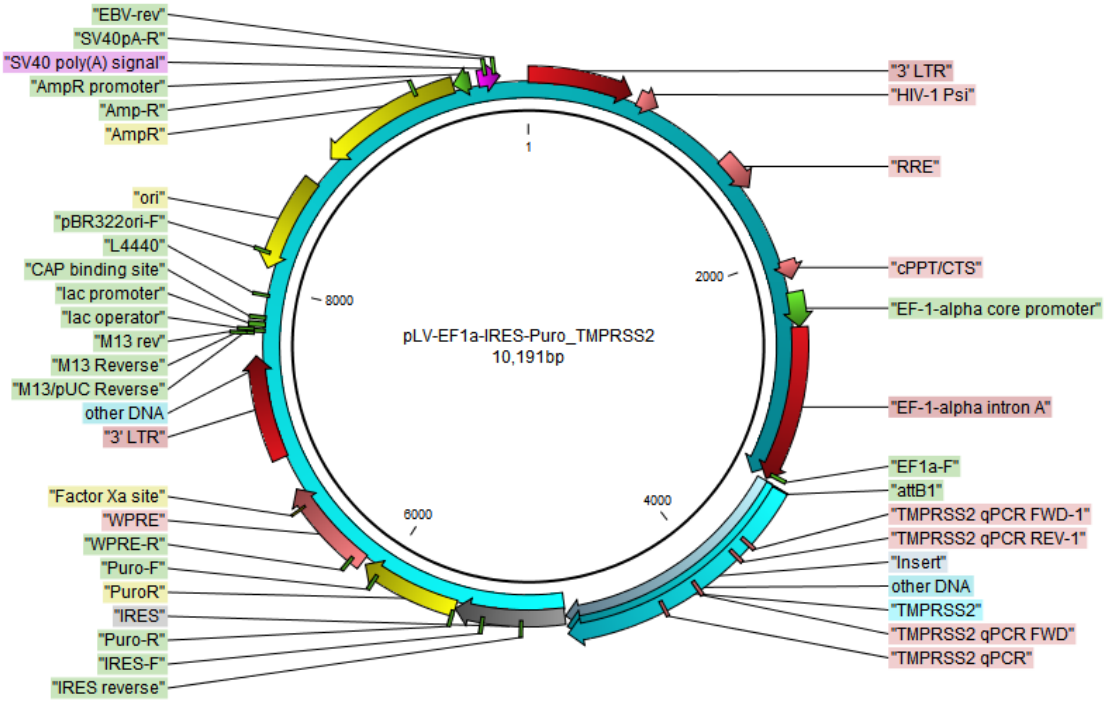


**Figure C22.** The vector map of pLV-EF1a-TMPRSS2iPuro

# APPENDIX D: Sequencing Results

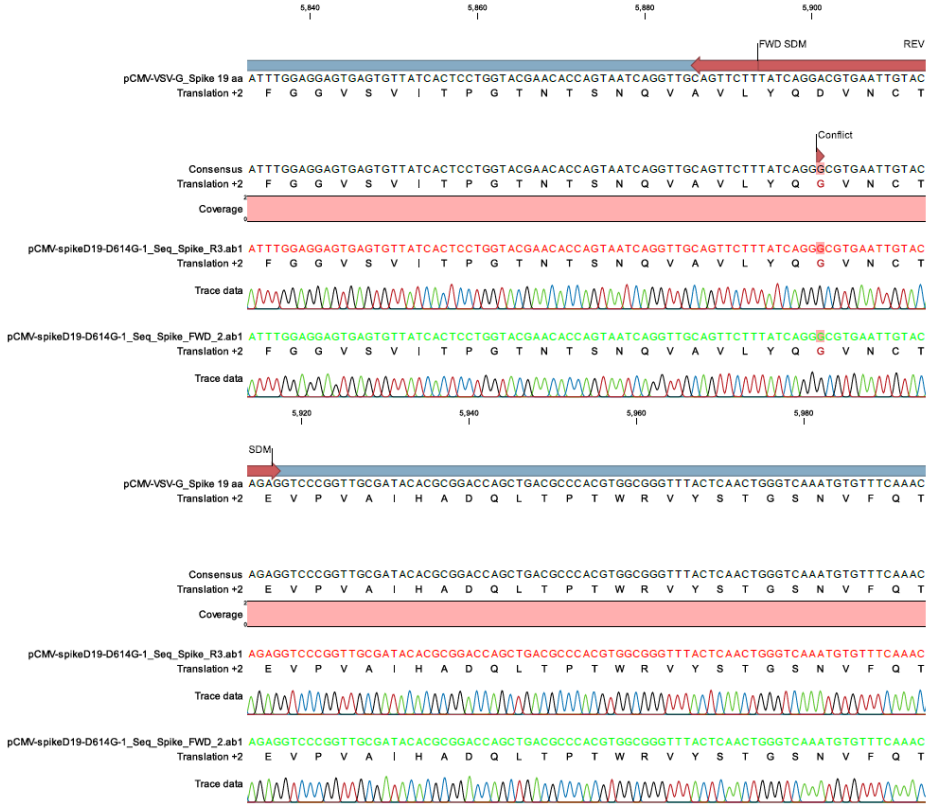


**Figure D1.** Sequencing result of pCMV-SpikeΔ19(D614G) construct

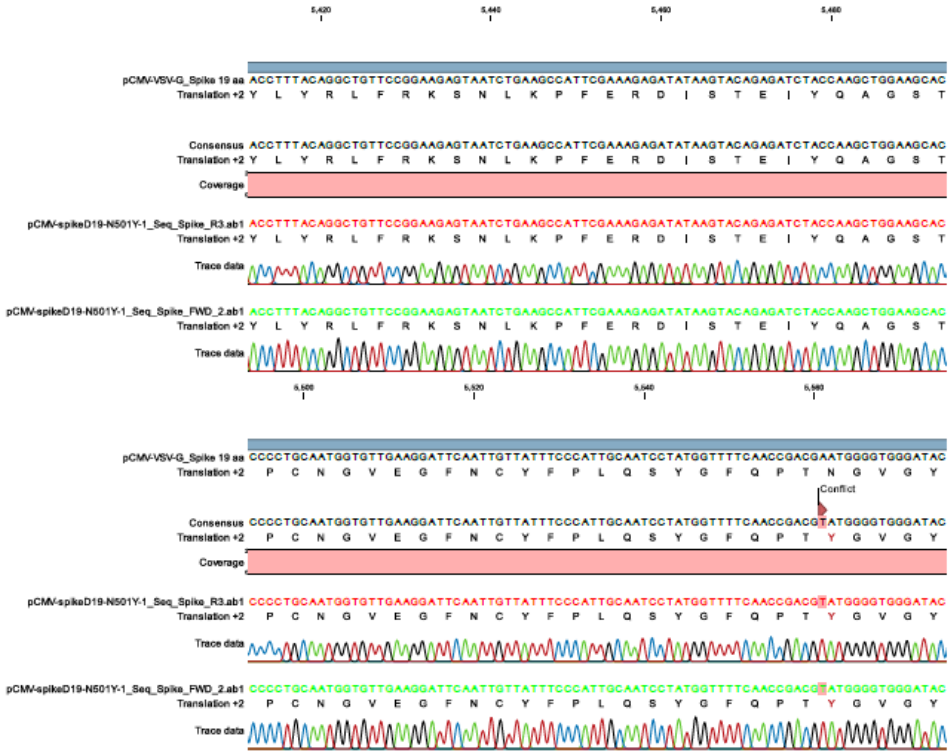


**Figure D2.** Sequencing result of pCMV-SpikeΔ19(N501Y) construct